

**UNIVERSIDADE DE LISBOA**  
**FACULDADE DE FARMÁCIA**  
**DEPARTAMENTO DE FARMÁCIA GALÉNICA E TECNOLOGIA**  
**FARMACÊUTICA**



**New polyurethane nail lacquers for the delivery of  
antifungal drugs**

**Bárbara Susana Gregorí Valdés**

**Orientadores: Prof. Doutora Helena Margarida de Oliveira Marques Ribeiro**

**Prof. Doutor João Moura Bordado**

**Tese especialmente elaborada para a obtenção do grau de Doutor em Farmácia,  
especialidade de Tecnologia Farmacêutica.**

**2017**



**UNIVERSIDADE DE LISBOA**  
**FACULDADE DE FARMÁCIA**  
**DEPARTAMENTO DE FARMÁCIA GALÉNICA E TECNOLOGIA**  
**FARMACÊUTICA**



**New polyurethane nail lacquers for the delivery of antifungal drugs**

**Bárbara Susana Gregorí Valdés**

Orientadores: Prof. Doutora Helena Margarida de Oliveira Marques Ribeiro  
Prof. Doutor João Moura Bordado

Tese especialmente elaborada para a obtenção do grau de Doutor em Farmácia, especialidade  
de Tecnologia Farmacêutica.

**Júri:**

Presidente:

Doutora Matilde da Luz dos Santos Duque da Fonseca e Castro, Professora  
Catedrática e Diretora da Faculdade de Farmácia da Universidade de Lisboa.

Vogais:

- Doutor Francisco Javier Otero Espinar, *Titular de Universidad Facultad de Farmacia da Universidade Santiago de Compostela*, Espanha;
- Doutora Maria Eugénia Soares Rodrigues Tavares de Pina, Professora Associada com Agregação Faculdade de Farmácia da Universidade de Coimbra;
- Doutora Ana Paula Rocha Duarte, Professora Auxiliar Convidada Universidade Atlântica;
- Doutor Rui Miguel Galhano dos Santos Lopes, Bolseiro de Pós-Doutoramento Instituto Superior Técnico da Universidade de Lisboa;
- Doutora Helena Margarida de Oliveira Marques Ribeiro, Professora Associada Faculdade de Farmácia da Universidade de Lisboa, Orientadora;
- Doutora Joana Marques Marto, Professora Auxiliar Convidada Faculdade de Farmácia da Universidade de Lisboa.

Fundação para a Ciência e a Tecnologia. Grant (SFRH/BD/78962/2011)



To my daughter



“Competition breeds excellence  
and whoever says otherwise,  
is still hurting from a loss in the past.  
Victory is around the corner if you keep competing.”

— Patrick Bet-David



# Table of Contents

<i>Acknowledgements</i> .....	<i>xvi</i>
<i>Abstract</i> .....	<i>xviii</i>
<i>Resumo</i> .....	<i>xx</i>
<i>List of figures</i> .....	<i>xxv</i>
<i>List of Tables</i> .....	<i>xxix</i>
<i>Abbreviations &amp; Symbols</i> .....	<i>xxxii</i>
<i>Chapter 1: General Introduction</i> .....	<i>1</i>
<i>1. Onychomycosis</i> .....	<i>5</i>
1.1 Epidemiology .....	<i>5</i>
1.2 Risk factors.....	<i>6</i>
1.3 Clinical classification .....	<i>7</i>
<i>2. Transungual delivery</i> .....	<i>9</i>
2.1 Nail structure and transungual permeation.....	<i>9</i>
2.2 Mathematical description of nail permeability.....	<i>12</i>
<i>3. Onychomycosis topical therapy</i> .....	<i>13</i>
3.1 Drug delivery enhancers.....	<i>14</i>
3.2 Examples of antifungal drugs.....	<i>20</i>
3.3 Examples of topical pharmaceutical forms .....	<i>25</i>
<i>4. Nail Lacquer in onychomycosis therapy</i> .....	<i>32</i>
<i>5. Polyurethane a potential excipient in therapeutic nail lacquer</i> .....	<i>42</i>
5.1 Synthesis of Polyurethane .....	<i>42</i>
5.2 Monomers for the synthesis of polyurethanes.....	<i>43</i>
5.3 Methods for synthesis of polyurethanes .....	<i>47</i>

5.4 Synthesis of polyurethanes from carbohydrates.....	48
5.5 Application of polyurethane in Biomedical Industry .....	49
5.6 Application of polyurethane in drug delivery system. ....	50
6. <i>References</i> .....	53
<i>Chapter 2: Synthesis and characterization of polyurethanes employing carbohydrates.....</i>	<i>69</i>
<i>1. Introduction.....</i>	<i>71</i>
<i>2. Materials and methods.....</i>	<i>72</i>
2.1 Materials.....	72
2.2 Methods.....	72
2.2.1 Synthesis of the polyurethane quasi-prepolymers.....	72
2.2.2 Synthesis of polyurethanes.....	73
2.3 Characterization of polyurethane quasi-prepolymers .....	74
2.3.1 Determination of viscosity .....	74
2.3.2 Free isocyanate content .....	74
2.3.3 FTIR .....	74
2.4 Polyurethane characterization .....	74
2.4.1 Solubility studies for polyurethanes .....	74
2.4.2 FTIR .....	74
2.4.3 NMR.....	74
2.4.4 Thermoanalytical measurements.....	75
2.4.5 Cytotoxicity assay .....	75
2.4.5.1 Preparation of sample.....	75
2.4.5.2 Direct contact assay.....	75
<i>3. Results and discussion.....</i>	<i>76</i>
3.1 Syntheses of polyurethane quasi-prepolymers .....	76

3.2 Viscosity and NCO content of polyurethane quasi-prepolymers.....	76
3.3 FTIR analysis of polyurethane quasi pre-polymers .....	77
3.4 Synthesis and characterization of polyurethanes .....	79
3.4.1 Solubility of PU.....	79
3.4.2 FTIR analysis of polyurethanes.....	80
3.4.3 NMR analysis of polyurethane.....	81
3.4.3.1 <sup>1</sup> HNMR of polyurethane .....	81
3.4.3.2 <sup>13</sup> C NMR of polyurethanes.....	86
3.5 DSC analysis of polyurethanes .....	86
3.6 Results of cytotoxicity assay .....	87
4. Conclusions.....	89
5. References .....	90
 <i>Chapter 3: Synthesis of biocompatible polyurethanes. Characterization by Techniques Spectroscopy, GPC and MALDI-TOF .....</i>	
<i>95</i>	
1. Introduction.....	97
2. Material and Methods.....	98
2.1 Materials.....	98
2.2 Methods.....	98
2.2.1 Synthesis of quasi-prepolymers .....	98
2.2.2 Synthesis of Polyurethanes.....	99
2.2.3 Determination of viscosity .....	99
2.2.4 Determination of free isocyanate .....	99
2.2.5 FTIR Characterization.....	99
2.2.6 NMR Characterization .....	100
2.2.7 DOSY .....	100

2.2.8 Hydrodynamic radii (rh).....	102
2.2.9 Gel Permeation Chromatographic .....	102
2.2.10 MALDI-TOF.....	103
2.2.11 In vitro cytotoxicity assay .....	104
2.2.11.1 Preparation of samples .....	104
<i>3. Results and discussion.....</i>	<i>105</i>
3.1 Viscosity and free isocyanate of quasi-prepolymers.....	105
3.2 FTIR Characterization.....	106
3.2.1 Characterization of quasi-prepolymers polyurethanes .....	106
3.2.2 Characterization of Polyurethanes .....	107
3.3 <sup>1</sup> H NMR Characterization .....	110
3.3.1 Characterization of some monomer by <sup>1</sup> H NMR spectroscopy .....	110
3.3.1. 1 Characterization of IPDI .....	110
3.3.1. 2 Characterization of PPG by <sup>1</sup> H NMR .....	112
3.3.1. 3 Characterization of Isosorbide by <sup>1</sup> H-NMR.....	113
3.3.2 Analysis of PUs synthesized of by NMR spectroscopy .....	115
3.3.2.1 Analysis of polyurethanes by <sup>1</sup> H-NMR spectroscopy.....	117
3.3.2.2 Analysis of polyurethanes by <sup>13</sup> C-NMR spectroscopy .....	121
3.5 DOSY of Polyurethanes .....	125
3.6 Hydrodynamic radii.....	128
3.7 Result of the analyzis of polyurethanes by GPC.....	128
3.8 MALDI-TOF.....	129
3.9 Cytotoxicity assay .....	131
<i>4. Conclusions.....</i>	<i>133</i>
<i>5. References .....</i>	<i>134</i>

<i>Chapter 4: New polyurethane nail lacquers for the delivery terbinafine – formulation and antifungal activity evaluation.....</i>	<i>139</i>
<i>1.Introduction.....</i>	<i>143</i>
<i>2.Materials and methods.....</i>	<i>144</i>
2.1 Materials.....	144
2.2 Methods.....	144
2.2.1 Preparation of the PU based nail lacquers.....	144
2.2.2 <i>In vitro</i> cytotoxicity assay.....	145
2.2.3 Determination of wettability by measurement of contact angle.....	146
2.2.4 PALS.....	146
2.2.5 SEM.....	147
2.2.6 Adhesion test.....	147
2.2.7 Viscosity measurement.....	148
2.2.8 <i>In vitro</i> release of terbinafine hydrochloride from therapeutic nail lacquers.....	148
2.2.9 <i>In vitro</i> antifungal activity.....	149
<i>3. Results and Discussion.....</i>	<i>149</i>
3.1 <i>In vitro</i> cytotoxicity.....	149
3.2 Wettability.....	151
3.3 PALS determination of free volume in films.....	151
3.4 SEM.....	154
3.5 <i>In vitro</i> adhesion test.....	155
3.7 <i>In vitro</i> release of terbinafine from Formulations A PU 19-10%, B PU 20-10% and C PU 21-10%.....	156
3.8 Antifungal activity.....	157
<i>4. Conclusions.....</i>	<i>159</i>
<i>5.References.....</i>	<i>160</i>

<i>Chapter 5: Formulation optimization of PU based Nail Lacquers containing Terbinafine hydrochloride and Ciclopirox Olamine</i> .....	165
<i>1. Introduction</i> .....	167
<i>2. Material and methods</i> .....	168
2.1 Materials.....	168
2.2 Methods.....	168
2.2.1 Preparation of Nail lacquers .....	168
2.2.2 Direct contact cytotoxicity assay for Nail lacquer .....	169
2.2.3 Determination of wettability by contact angle measurement.....	169
2.2.4 SEM.....	169
2.2.5 Adhesion test.....	170
2.2.6 Drying time for nail lacquer therapeutics.....	170
2.2.7 Viscosity determination.....	170
2.2.8 <i>In vitro</i> release of terbinafine from nail lacquers containing different concentrations of PU.....	170
2.2.9. <i>In vitro</i> antifungal activity.....	171
2.2.10. Final formulations - Permeation studies.....	171
2.2.11 Porosity measurement .....	173
<i>3. Results and discussion</i> .....	173
3.1 Direct contact assay.....	173
3.2 Wettability.....	175
3.3 SEM.....	176
3.4 Adhesion test results.....	177
3.5 Nail lacquer's drying time.....	179
3.6 Viscosity values.....	179

3.7 Preliminary test for select formulation with better condition to release the terbinafine	180
3.8 Antifungal activity.....	181
3.9 Permeation Test.....	182
3.10 Porosity study.....	184
4. <i>Conclusions</i> .....	187
5. <i>References</i> .....	188
<i>Chapter 6: Conclusions and Final Remarks</i> .....	193
Annex 1. Spectrum <sup>1</sup> H NMR PEG 1 500.....	201
Annex 2. Spectrum <sup>1</sup> H NMR pMDI.....	202
Annex 3. Spectrum <sup>1</sup> H NMR Sucrose.....	203
Annex 4. MALDI-TOF mass spectra of PU19.....	204
Annex 5. MALDI-TOF mass spectra of PU20.....	205
Annex 6. MALDI-TOF mass spectra of PU21.....	206
Annex 7. MALDI-TOF mass spectra of PU22.....	207

## Acknowledgements

I would like to express my special appreciation to my advisors. To Professors Helena Margarida Ribeiro and João Moura Bordado, a special thanks for the opportunity to work in two excellent group (CERENA and NanoBB). The relentless support and availability, were crucial for the completion of this work and allowed me to grow as a research.

Also, a special acknowledgement is due to Professors Pedro Manuel Teixeira Gomes, Jose Ascenço and Paulo Gordo as critical thinking and scientific discussions were crucial for the completion of this work. To Professor Francisco Javier Otero Espinar for all the support and trust, as well as for welcoming me into his research group of University Santiago de Compostela and to Elena Coutrin for all the help with some scientific issues and time dedicated. To Professor Ana Paula Serro, PhD's Auguste Rodrigues Fernandes and Clara Gomes, Centro de Química Estrutural (CQE), Instituto Superior Técnico. Without, your collaboration a significant part of this work would not be possible.

Furthermore, I would like to mention, my gratitude to PhD. Lídia Gonçalves, for support in compatibility test. To Professor Humberto Ferreira for the time employ in characterization of polyurethanes. To Professors Andreia Ascenso and Sandra Simões for the help in validation process and works in the laboratory. To PhD's Rui Santos, Margarida Mateus, Susete Fernandes and Luz Fernandez for the help in chemical characterization and unconditional support. To MSc. Inês Casais for the graphic desing of some imagen of the text. To PhD Joana Marto for the precious help in antifungal test. To MSc. Ana Salgado for the help in developing the HPLC methods.

Thanks so much to Maria Helena Gil for the restless support and friendship.

To the company DS Produtos Químicos Lda., Especially to Mr. Óscar Brás, for the availability of several raw materials.

To all my colleagues from the former Nanomedicine and Drug Delivery Systems group for all the help and constant support. In particular, to Inês Ferreira, Maria Paisana, Paulo Roque Lino, Sara Raposo, Carla Eleutério, Diogo Baltazar, Diana Gaspar and João Quintas.

An acknowledgement is also due to the Faculdade de Farmácia, Universidade de Lisboa, in particular the “Departamento de Farmácia Galénica e Tecnologia Farmacêutica”, the Research Institute for Medicines (iMed.Ulisboa), the Microbiological Department and the Chemistry Department of Instituto Superior Técnico of Universidade de Lisboa for the infrastructures and conditions that allowed me to develop my PhD work.

To Noel, Susan, my mother and my father for the unconditional love, encourage to finish the research and support in all the difficult situations.

To the Portuguese government (Fundação para a Ciência e a Tecnologia) for the grant (SFRH/BD/78962/2011).

## Abstract

Nail fungal infections frequently addressed as onychomycosis present a considerable prevalence on the global population.

Despite not being a life-threatening disease, this infection causes several social problems to the infected patients. Unfortunately, the topical therapy available, does not include one of the most effectively drugs and oral therapy comprises several problems.

Nail lacquers are solutions of film forming polymers, which leave a film on the nail plate after solvent evaporation. This polymer film can be water resistant or water soluble and can act as a drug reservoir, allowing a drug to permeate through the nail plate. The nail lacquers water resistant are occlusive and adhesive to the nail. They present advantages regarding nail hydration, permanence on the nail plate and patient compliance, when compared to creams, gels and solutions.

The development of polyurethane based nail lacquers for the delivery drugs to treat onychomycosis is still a challenge. Nowadays there are drugs with pharmacological activity (antifungal) for treatment of onychomycosis (i.e. terbinafine hydrochloride), but there is no nail lacquer formulation in the market capable of delivering them into the nail with success.

Polyurethanes are being used for sustained and controlled delivery of various drugs. The development of a new polyurethane based on carbohydrates for the delivery of antifungal (terbinafine hydrochloride and ciclopirox olamine) to treat onychomycosis, is the main aim of this thesis.

The thesis is divided in two main topics:

The first part presents the synthesis of polyurethanes from carbohydrates and derivatives. The biocompatible polyurethanes were successfully synthesized employing carbohydrates and aliphatic isocyanates. The polyurethanes were synthesized by pre-polymerization method. This process allows maintain better control the structure and properties of the final polymer,

through a simple change of chain extender. It was possible to obtain polyurethanes with different properties from the same pre-polymer, that are typically liquids, which facilitates handling on an industrial scale, when compared with monomeric isocyanate systems. The polyurethanes were characterized by FTIR, NMR, GPC and MALDI-TOF. The biocompatibility of these materials was also assessed using keratinocytes cell.

In the second part of our work, four polymers were used to prepare nail lacquers containing terbinafine hydrochloride as a model drug. The results obtained from the structural/characterization analysis of these PU based nail lacquers, comprising all the data and information that allowed the selection of the best of them to optimize the final formulations.

At this stage, only one of the tested PU was selected to the complete physical, chemical and microbiological studies with two drug models: terbinafine hydrochloride and ciclopirox olamine. PU based nail lacquers with different amounts of the polyurethane selected previous were prepared. Cytotoxicity, wettability, SEM, adhesion test, viscosity, *in vitro* release and permeation studies as well as the antifungal activity were performed.

**Keywords:** Onychomycosis, nail lacquer; polyurethanes; adhesion to keratin, transungual drug delivery.

## Resumo

As três últimas décadas foram marcadas por significativas alterações nos padrões das infecções fúngicas. Este fato, aliado ao aumento da população de risco, como doentes com Síndrome de Imunodeficiência Adquirida (SIDA), transplantados, com patologias hematológicas ou com outros comprometimentos imunitários, como terapêuticas imunossupressoras, fez com que estas infecções assumissem uma maior importância no contexto de saúde pública.

A onicomicose é uma infecção fúngica da lâmina ungueal (unha) que representa entre 15 a 40% de todas as onicopatias. Pode ser provocada por dermatófitos, fungos filamentosos, não dermatófitos ou leveduras, principalmente as do gênero *Candida*. Apesar de estar associada a diferentes agentes etiológicos, em 90% dos casos os responsáveis são dermatófitos, principalmente *Trichophyton rubrum*.

A prevalência das onicomicoses na população em geral tem sido estimada entre 14% e 23%, sendo que estes números têm aumentado consideravelmente nas últimas décadas e estão relacionados com a diabetes, doença arterial periférica, psoríase, imunodepressão e envelhecimento. Em estados avançados, esta patologia pode causar dor, desconforto, limitações físicas e ocupacionais, condições estas que interferem com a qualidade de vida do doente.

Os antifúngicos são largamente prescritos na prática clínica para o tratamento de infecções fúngicas na unha. Os antifúngicos podem ser administrados por via sistêmica ou tópica. A escolha da terapêutica é feita tendo em conta factores como o grau de infecção da unha e potenciais interações e contraindicações. No entanto, a administração tópica apresenta maior conforto para o doente.

Para tratamento das onicomicoses (tratamento de iniciais e bem delimitadas), têm sido usados com muita aceitação desde 1990, sistemas de libertação transungueal baseados em vernizes medicamentosos. Os vernizes medicamentosos são soluções ungueais, onde se incluem polímeros, solventes voláteis, promotores da permeação e fármacos. Depois de aplicado na unha, os solventes voláteis evaporam e os polímeros deixam um sistema matricial

(filme) onde o fármaco pode estar incluído. Este sistema é formado por cadeias de uma ou de várias substâncias químicas polimerizadas, que funcionam como agentes moduladores da permeação. A partir desta matriz o fármaco difunde-se até à estrutura da unha e exerce ação fungicida. A penetração e o transporte de um fármaco na unha é um requisito para que o mesmo desempenhe a sua atividade terapêutica. A maioria dos fármacos não consegue permear a unha, pelo que é necessário um veículo para promover a sua libertação no local de ação.

Os vernizes medicamentosos preparados a partir de polímeros hidrófobos possuem vantagens sobre outras formulações. Estes sistemas não são solúveis em água deixando uma camada de polímero com maior durabilidade na unha, o que permite manter a sua ação por um maior período de tempo. O tratamento é simples e indolor, o progresso é visível e permite a remoção da zona infectada da unha.

Os antifúngicos selecionados nesta tese, como moléculas modelos, foram o cloridrato de terbinafina (TH) e o ciclopirox olamina (CPX).

O cloridrato de terbinafina, composto sintético derivado da alilamina ( $C_3H_5NH_2$ ), tem como mecanismo de ação a inibição da esqualeno epoxidase, uma enzima crucial no processo de síntese do ergosterol, o que origina a acumulação de esqualeno, levando à disrupção da membrana com consequente morte da célula fúngica. O cloridrato de terbinafina apresenta concentrações mínimas inibitórias para o *T. rubrum* de 0.004–0.06  $\mu\text{g/mL}$ , *C. Albicans* 0.06–16  $\mu\text{g/mL}$  e *A. fumigatus* 1.4  $\mu\text{g/mL}$ . O seu peso molecular é 291.43 g/mol. Trata-se de uma molécula lipofílica, que possui elevada eficácia no tratamento das onicomicoses por se difundir muito bem no leito ungueal. Esta molécula ainda não se encontra no mercado em vernizes medicamentosos.

O ciclopirox olamina é um agente antimicótico sintético da família das piridonas. Possui amplo espectro com atividade inibitória contra dermatófitos, *C.Candida*, *M. furfur*, entre outros fungos. O mecanismo de ação estudado para a *Candida albicans* indica que este inibe a captação de precursores da síntese macromolecular que ocorre em duas etapas: i) inibindo a entrada de iões metálicos, dos iões fosfatos e do potássio; ii) atuando sobre a cadeia

respiratória da célula fúngica devido às propriedades quelantes. O ciclopirox olamina apresenta uma concentração mínima inibitória para o *T. rubrum* de 0.031–0.5 µg/mL, *C. Albicans* 0.06-0.5 µg/mL e para o *A. fumigatus* 0.42 µg/mL e um peso molecular 207.03 g/mol. A sua eficácia está relacionada com o fato desta molécula se difundir na epiderme e nos folículos pilossebáceos, com destaque para a impregnação das camadas superficiais do estrato córneo. Possui a capacidade de penetrar e atravessar a queratina das unhas. Encontrase disponível em verniz medicamentoso e foi utilizado nesta tese como fármaco modelo e para avaliar a capacidade da utilização de poliuretanos como polímeros de vernizes medicamentosos.

As formulações de vernizes medicamentosos desenvolvidas nesta fase incluíam solventes voláteis: etanol, acetato de etilo e butilo. Esta seleção foi realizada de acordo com a pesquisa efectuada essencialmente em patentes.

Os poliuretanos (PU) são polímeros de grande aplicação industrial, pois apresentam propriedades físicas e químicas diferentes de acordo com a estrutura dos monómeros que dá origem ao polímero final. Otto Bayer e colaboradores pela Ferbenindustri na Alemanha, em 1937 foram os primeiros a sintetiza-los. É um material notável por sua alta performance devido à excelente resistência química, a solventes, à abrasão e à hidrólise, além de possuir resistência antifúngica, e por apresentar dureza e tenacidade combinada com flexibilidade à baixa temperatura. A ligação uretana (–NH–COO–) é um resultado da reação entre um grupo isocianato (–NCO) do diisocianato e um grupo hidroxilo (–OH) do polioliol.

Os poliuretanos têm sido aplicados nas indústrias médica e farmacêutica desde 1970 em próteses e microesferas para regeneração óssea. No entanto, o uso de PU como um excipiente para a veiculação de farmacos na unha ainda não foi objeto de estudo.

A presente tese está dividida em dois grandes tópicos:

1 – Síntese e caracterização de poliuretanos a partir de carboidratos.

Esta síntese tem como objetivo a obtenção de polímeros biocompatíveis. Deste modo, os polímeros foram sintetizados a partir de polipropileno glicol, polietileno glicol, metil difenil

diisocianato polimérico, diisocianato de isoforona e de uma fonte renovável, representada pelos carboidratos e seus derivados (sacarose e D-isossorbida). Os poliuretanos sintetizados a partir de sacarose, polietileno glicol e metil difenil diisocianato polimérico deram origem a polímeros insolúveis em solventes polares, com uma estrutura extremamente entrecruzada e não apresentaram biocompatibilidade. A dissolução do polietileno glicol com dimetilsulfoxido a baixa temperatura de reação contribuí para elevados tempos de síntese e com a presença do solvente no processo de produção. A proposta para eliminar estes problemas consistiu em substituir o diisocianato aromático por diisocianatos alifáticos, em substituir os poliglicólicos (sacarose) com glicólicos de 2 OH (D-isossorbida) e em substituir o polietileno glicol por polipropileno glicol.

A síntese de poliuretano a partir de moléculas hidrofílicas com dos hidroxilos livres, permitiu obter poliuretanos lineares e com solubilidade em solventes polares. A solubilização do polímero é muito importante porque deste modo é garantido a solubilidade do fármaco na matriz polimérica. Por outro lado, a síntese de polímeros pouco reticulados permitire obter uma matriz com um volume livre que permitirá depois a libertação do fármaco. Foram efetuadas sínteses de poliuretanos a partir de dois isocianatos alifáticos o diisocianato de isoforona (IPDI) e 4,4'-diciclo-hexil-metileno (HMDI). O resultado destas sínteses, permitiram obter os poliuretanos obtidos a partir de IPDI mais biocompatíveis quando comparados com os poliuretanos obtidos a partir de HMDI. Todos os poliuretanos foram caracterizados por FTIR e RMN para confirmar a sua estrutura. Foram ainda efetuados estudos dos coeficientes de difusão e volume hidrodinâmico, confirmando-se que à medida que aumenta o peso molecular e a viscosidade, diminui o raio hidrodinâmico e o polímero difunde menos no solvente onde foi solubilizado previamente. Foram determinados os pesos moleculares por duas técnicas diferentes, Cromatografia de Permeação em Gel e Ionização por Dessorção a Laser Assistida por Matriz Tempo de Vôo. Ambas técnicas permitiram concluir que existe uma relação entre peso molecular e relação estequiométrica entre monómeros que formam parte da estrutura do polímero.

Uma vez sintetizados os poliuretanos com as características ideais, estes foram selecionados como excipientes de vernizes medicamentosos.

## 2- Preparação de vernizes medicamentosos

O desafio desta fase do trabalho consistiu em obter formulações de vernizes medicamentosos empregando quatro poliuretanos como excipientes biocompatíveis, seguros, eficazes e com adesividade a unha como forma farmacêutica com actividade antifúngica.

Para avaliar o melhor polímero, foram preparadas e avaliadas várias formulações de vernizes medicamentosos contendo cloridrato de terbinafina. Estudos de biocompatibilidade celular (queratinócitos), determinação do ângulo de contacto entre a unha e os vernizes, o volume livre das formulações, a morfologia dos filmes bem como a adesão dos vernizes à queratina e sua viscosidade foram efectuados. Para além destes, foram realizados estudos *in vitro* de libertação e de eficácia antifúngica. A selecção do poliuretano foi realizada com base nestes estudos.

Numa ultima fase, e com o objetivo de otimizar a formulação do verniz medicamentoso, foi estudado a influência da concentração polímero nos vernizes e a inclusão de ciclopirox olamina como segundo fármaco modelo.

As formulações desenvolvidas foram caracterizadas avaliadas através de estudos de biocompatibilidade, de molhabilidade, de microscopia, de adesividade, de viscosidade e de ensaios *in vitro* de libertação e de permeação das substâncias ativas bem como de avaliação da eficácia antifúngica.

**Palavras-chave:** Onicomioses, verniz medicamentoso; poliuretanos; adesão à queratina, sistemas para libertação transungual, ação antifúngica.

## List of figures

### Chapter 1

Figure 1. 1. Scanning electron micrograph of nail plate a) no affecting by fungal infection and b) nail affected by a fungal infection. ....	5
Figure 1. 2. Types of onychomycosis according to the mode and site of invasion of the pathogen. ....	7
Figure 1. 3. Representation of nail structure. ....	10
Figure 1. 4. Factors that affect nail permeation of topically applied formulations. Adapted from (35). ....	12
Figure 1. 5. Colloidal carriers for drug delivery. Adapted from (113). ....	30
Figure 1. 6. Scheme of synthesis of polyurethane adapted from (141). ....	42
Figure 1. 7. Architecture of the chain of polyurethane. Adapted from (142) ....	43
Figure 1. 8. Biomedical application of polyurethanes. ....	50
Figure 1. 9. Release of nanoparticles from polyurethane matrix. Adapted from (162) ....	51

### Chapter 2

Figure 2. 1. Scheme of the quasi-prepolymer reaction. ....	76
Figure 2. 2. FTIR in ATR mode spectra of the Pre-6, Pre-8, Pre10 and Pre-12. ....	78
Figure 2. 3. FTIR in ATR mode spectra of the Pre-14, PEG 1500, DMSO and pMDI. ....	78
Figure 2. 4. Ideal structure for polyurethanes: a) PUS, b) PUF, c) PUG. ....	79
Figure 2. 5. Structure of polyurethanes obtained, a) PUS, b) PUF, c) PUG. ....	80
Figure 2. 6. FTIR in ATR mode spectra of polyurethanes prepared with Pre-14. ....	81
Figure 2. 7. Structure of PEG. ....	82
Figure 2. 8. Structure of pMDI. ....	82
Figure 2. 9. Structure of Sucrose. ....	83

Figure 2. 10. Spectrum $^1\text{H}$ -NMR of PUS 14/4.....	85
Figure 2. 11. Spectrum $^{13}\text{C}$ -NMR of PUS 14/4.....	86
Figure 2. 12. DSC thermograms of polyurethane PUS 14/4, PUS 14/6, PUS 14/8. ....	87
Figure 2. 13. HaCaT cells after 72h of proliferation under contact with polyurethane. A) glass slide (control), B) PUS 14/4.....	88

### Chapter 3

Figure 3. 1. Two step procedure for the synthesis of isosorbide from D-glucose adapted from (13). ....	97
Figure 3. 2. Typical spectrum DOSY ( $D$ ( $\text{m}^2\text{s}^{-1}$ ) vs $\delta$ (ppm)). ....	101
Figure 3. 3. Synthetic route of polyurethane PU19, PU20, PU21, and PU22.....	105
Figure 3. 4. Spectra of quasi-prepolymer polyurethanes. ....	106
Figure 3. 5. FTIR spectra of Isosorbide, PPG, IPDI and PUs.....	107
Figure 3. 6. FTIR of PU, C=O, C–H and C–O–C stretching bands of PUs.....	108
Figure 3. 7. FTIR spectrum of PU22.....	109
Figure 3. 8. The structure of IPDI. ....	110
Figure 3. 9. $^1\text{H}$ NMR spectrum of the IPDI (500 MHz, in $\text{CDCl}_3$ at room temperature). ....	111
Figure 3. 10. The structure of PPG.....	112
Figure 3. 11. $^1\text{H}$ NMR spectrum of the PPG (500 MHz, in $\text{CDCl}_3$ at room temperature).....	113
Figure 3. 12. The structure of Isosorbide. ....	114
Figure 3. 13. $^1\text{H}$ NMR spectrum of the Isosorbide (500 MHz, in $\text{CDCl}_3$ at room temperature). .....	114
Figure 3. 14. Segment of polyurethane with monomers IPDI and PPG (A). Segment of a chain of polyurethane with monomers IPDI and D-isosorbide (B). ....	116

Figure 3. 15. Segment of a chain of polyurethane with monomers HMDI and PPG (A). Segment of a chain of polyurethane with monomers HMDI and D-isosorbide (B). .....	117
Figure 3. 16. <sup>1</sup> H NMR spectra of PUs (500 MHz, in DMSO-d <sub>6</sub> at room temperature). .....	118
Figure 3. 17. <sup>1</sup> H NMR spectrum of PU22 in DMSO-d <sub>6</sub> . Bruker 500 MHz spectrometer.....	120
Figure 3. 18. <sup>13</sup> C NMR spectra of the polyurethanes (500 MHz, in DMSO-d <sub>6</sub> at room temperature). .....	122
Figure 3. 19. <sup>13</sup> C NMR spectrum of the PU 22 (500 MHz, in DMSO-d <sub>6</sub> at room temperature). .....	124
Figure 3. 20. DOSY spectra of polyurethanes ( <sup>1</sup> H 500 MHz, in DMSO-d <sub>6</sub> at room temperature, 0.348 mg/mL).....	126
Figure 3. 21. Diffusion coefficient vs concentration for PU19–PU22 in DMSO-d <sub>6</sub> , measured at T = 30 °C. ....	127
Figure 3. 22. MALDI-TOF mass spectra of polyurethane after deisotoping procedure. ....	130
Figure 3. 23. HaCaT cells after 72h of proliferation a) glass slide (control) , b) PU19. ....	132
Figure 3. 24. HaCaT cell viability by MTT after proliferation under different polymers material. Control (glass slide), (mean ± SD, n = 6). ....	132

#### Chapter 4

Figure 4. 1. HaCaT cell viability by MTT after proliferation under different nail lacquer formulations. Control (glass slide) (mean±SD, n = 6). .....	150
Figure 4. 2. Scan Electron Micrograph with 1000x magnification. A) dorsal surface of nail plate B) film of Formulation A PU 19-10%, C) film of Formulation B PU20-10%, D) film of Formulation C PU21-10%.....	154
Figure 4. 3. Release profile of terbinafine from PU based nail lacquer for 24 h in aqueous solution of 0.5% Tagat® CH 60 at 32°C (mean ±SD, n = 3). .....	156

## Chapter 5

Figure 5.1. Micrograph with 400x magnification of HaCaT cells after 72h of proliferation under contact with different therapeutic nail lacquer: A) glass slide, B) Formulation A PU19-10% TH, C) Formulation D PU19-15% TH, D) Formulation E PU19-20% TH, E) Formulation F PU19-25% TH and F) PU19. ....	174
Figure 5. 2. HaCaT cell viability by MTT after proliferation under different nail lacquers. Control (glass slide), (mean $\pm$ SD, n = 6).....	174
Figure 5.3. Water contact angle of PU terbinafine nail lacquers (mean $\pm$ SD, n= 3). ....	176
Figure 5.4. Scan Electron Micrograph with 1000x magnification. A) dorsal surface of nail plate B) film of Formulation A PU 19-10% TH, C) film of Formulation D PU19-15% TH, D) film of Formulation E PU19-20% TH, E) film of Formulation F PU19-25% TH, F) film of Formulation G PU19-10% CPX and G) Ony-Tec <sup>®</sup> . ....	177
Figure 5.5. Nail lacquer adhesion test to keratin of cow horn. ....	178
Figure 5.6. Release of TH from different formulations at 32 °C (mean $\pm$ SD, n = 6).....	180
Figure 5.7. Amount of drug determined in nail plate after 11 days of experiments. One-way ANOVA and Tukey's multiple comparison tests indicates significant differences between Ony-Tec <sup>®</sup> and PU based nail lacquer formulations. ....	184
Figure 5.8. Cumulative curves of porosity obtained by MIP for treated and untreated nail and PoreXpert models of the microstructure of a) untreated nail, b) Ony-Tec <sup>®</sup> treated nails and c) Formulation A PU19-10% TH treated nails. Cubes represent the pores and cilindrs the conection between pores. ....	185

## List of Tables

### Chapter 1

Table 1. 1. Overview of the most referenced transungual permeation enhancers. ....	18
Table 1. 2. Antifungal drug properties that influences permeation. Measurement conditions, e.g. base/salt used, medium/solvent composition, pH, ionic strength, and temperature are provided in parentheses when available. Adapted from (37).....	21
Table 1. 3. Minimum inhibitory concentration for antifungals used in onychomycosis. (Values displayed in $\mu\text{g}/\text{mL}$ , *MIC range). ....	23
Table 1. 4. Topical formulation of antifungal. ....	25
Table 1. 5. Vehicles composition of CPX nail formulations. Adapted from (115). ....	31
Table 1. 6. Nail lacquer formulations.....	35
Table 1. 7. Polyglycols employing in synthesis of polyurethanes. ....	44
Table 1. 8. Name, toxicity and chemical structure of diisocyanates.....	44
Table 1. 9. Carbohydrates employed as chain extender in the synthesis of polyurethanes. ....	45
Table 1. 10. The most common catalyst in synthesis of polyurethane.....	46

### Chapter 2

Table 2. 1. Relation of monomers for synthesis of quasi-prepolymers.....	73
Table 2. 2. Relation of monomers for synthesis of polyurethane. ....	73
Table 2. 3. Formulation, isocyanate content and viscosity of the polyurethane quasi pre-polymers. (mean $\pm$ SD, n=3). ....	77
Table 2. 4. Chemical shifts of PEG 1500.....	82
Table 2. 5. Chemical shifts of pMDI.....	83
Table 2. 6. Chemical shifts of Sucrose.....	84

### Chapter 3

Table 3. 1. Molar ratios employed in the synthesis of the quasi-prepolymers.....	99
Table 3. 2. Molar ratios employed in the synthesis of the PU. ....	99
Table 3. 3. Values of viscosity and free isocyanate of quasi-prepolymers, (n=3). ....	106
Table 3. 4. Assignments of <sup>1</sup> H NMR and chemical shifts of IPDI .....	111
Table 3. 5. Assignments of <sup>1</sup> H-NMR and chemical shifts of PPG.....	113
Table 3. 6. Assignments of <sup>1</sup> H NMR and chemical shifts of Isosorbide.....	115
Table 3. 7. Assignments of <sup>1</sup> H-NMR and chemical shifts of PU 19, PU 20 and PU21.....	119
Table 3. 8. Assignments of <sup>1</sup> H-NMR and chemical shifts of PU 22.....	121
Table 3. 9. Assignments of <sup>13</sup> C NMR chemical shifts for PU19, PU20 and PU21.....	123
Table 3. 10. Assignments of <sup>13</sup> C NMR and chemical shifts for PU22. ....	125
Table 3. 11. Values of D for PU19- PU22, measured at T=30°C, DMSO-d <sub>6</sub> . ....	127
Table 3. 12. Values of r <sub>h</sub> for PU19-PU22, measured at T=30 °C, DMSO.d <sub>6</sub> .....	128
Table 3. 13. Average Molecular weight by GPC. ....	128
Table 3. 14. Higher mass identified by MALDI -TOF and mass calculated according to molar ratios. ....	131

### Chapter 4

Table 4. 1. PU, terbinafine based nail lacquers composition. ....	145
Table 4. 2. PALS parameters (lifetime and intensity components), hole radius (R) and free volume cavity associated with the o-Ps lifetime for PU, terbinafine based nail lacquers.....	153
Table 4. 3 Antifungal activity of different formulations with terbinafine against <i>Trycophyton rubrum</i> , <i>Candida albicans</i> and <i>Aspergillus brasiliensis</i> . ....	158

## Chapter 5

Table 5. 1. Nail lacquers composition.....	169
Table 5. 2. Nail lacquer's drying time (mean±SD, n= 3).....	179
Table 5. 3. Viscosity values of therapeutic nail lacquers (mean±SD, n= 3).....	180
Table 5. 4. Inhibition zone (mm) of all formulations in plate dish for <i>Candida albicans</i> , and <i>Aspergillus brasiliensis</i> (mean±SD, n=2). ....	181
Table 5. 5. Permeation profiles of formulations and Ony-Tec® trough the nail. (mean±SD, n=3). ....	183
Table 5. 6. Main parameters of the models obtained from porosity data using PoreXpert....	186

## Abbreviations & Symbols

<sup>13</sup>C-NMR- Carbon Nuclear Magnetic Resonance

<sup>1</sup>H-NMR- Proton Nuclear Magnetic Resonance

ATCC- American type culture collection

BS- Base

DOSY- Diffusion-ordered NMR spectroscopy

DO- Optical density

CPX- Ciclopirox

CS- HCl salt

DABCO 1,4- Diazobicyclo[2.2.2]- octane

DMDEE -Dimorpholino- diethylether

DMSO- Dimethylsulfoxide

DSC- Differential scanning calorimetry

e.g- Exemple

EW- Hydroethanolic solution.

FTIR -Fourier Transform Infrared Spectroscopy

FWHM- Full width at half maximum

GPC- Gel Permeation Chromatographic

h- hours

HDI- Hexamethylene diisocyanate

HMDI- 4,4' methylene bis (cyclohexyl isocyanate)

HPLC-High Performance Liquid Chromatography

IPDI- Isophorone diisocyanate

ISO- International Standard Organisation

KC- KCl solution

LD<sub>50</sub>- Dosis Letal 50%

LDI- L-lysine ethyl ester diisocyanate

MALDI-TOF- Matrix Assisted Laser Desorption Ionization Time Of Flight

MDI- Methylene diphenyl diisocyanate

MIC- Minimum inhibitory concentration

MIP- Mercury Intrusion Porosimetry

MTT 3-(4,5-dimethylthiazol-2-yl)-2,5-diphenyltetrazolium bromide

Mw- Molecular weight

NC- NaCl solution

NMR -Nuclear Magnetic Resonance

NS- Nitrate salt

OS-Olamine salt

PALS-Positron Annihilation Lifetime Spectroscopy

PBS- phosphate buffer solution

PEG- Poly ethylene glycol

PPG- Poly propylene glycol

ppm- parts per million

PU- Polyurethane

PUF- Polyurethane from fructose

PUG- Polyurethane from glucose

PUS- Polyurethane from sucrose

$r_h$  - Hydrodynamic radius

RSD- Relative Standard Deviation

RT - Room temperature

SEM -Scanning electron microscopy

SEPA®- 2-n-nonyl-1,3-dioxolane

SIF/P- Simulated intestinal fluid

TB- Tris buffer

TH- Terbinafine hydrochloride

THF-Tetrahydrofuran

UB- Unspecified buffer

UHP- Urea hydrogen peroxide

USP- United States Pharmacopeia

W- Water



## **Chapter 1: General Introduction**



This heading section was adapted from a chapter of the book:

Barbara S. Gregorí Valdés, Carolina de Carvalho Moore Vilela, Andreia Ascenso, João Moura Bordado, Helena M. Ribeiro. Topical Formulations for Onychomycosis. A Review, in Andreia Ascenso, Helena Ribeiro, Sandra Simões (eds). Carrier-Mediated Dermal Delivery: Applications. in: the Prevention and Treatment of Skin Disorders. Pan Stanford Publishing. 2016. 503-553.



## 1. Onychomycosis

Onychomycosis is a fungal infection of the nail that causes a great concern because of the disfiguring appearance of the nails (1). The nail problem is caused by different types of fungi that can easily attack the nails due to their keratinolytic enzyme (2). In the Figure 1.1 is showed the aspect of the microorganism and the debased structure of keratin of the nail.

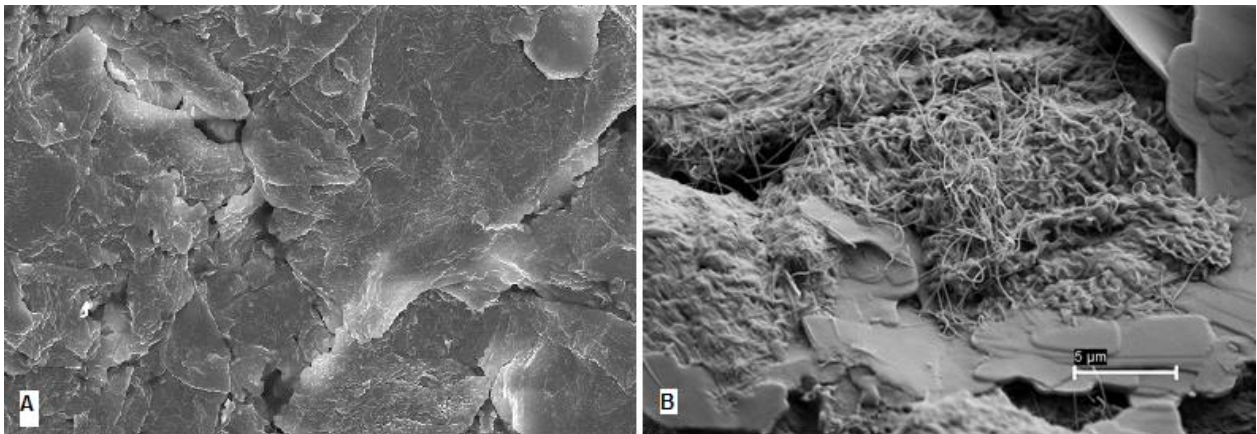


Figure 1. 1. Scanning electron micrograph of nail plate a) no affecting by fungal infection and b) nail affected by a fungal infection.

### 1.1 Epidemiology

Onychomycosis prevalence has been reported to occur from 3 to 26% in the general population (1,3–6).

Onychomycosis cases have been increasing in the past decades, from a prevalence of 1-2% to 14-15% in a 20 year time window (4). According to several large studies, it is expected that onychomycosis prevalence will increase to 20% or more in the next decade (4).

Onychomycosis is a serious public health problem leading to detrimental physical and psychological effects. There are specific population groups affected by this disease. About 50% of all psoriasis patients (1-8% of general population) report nail psoriasis and 40 to 60% are affected by onychomycosis (5,7,8). Onychomycosis also affects about 1/3 of diabetes patients since they are more prone to suffer foot complications that can lead to dermatophyte infections, ulceration, osteomyelitis, cellulitis and tissue necrosis that may result at worst in amputation (9).

Onychomycosis greatly affects the patients' quality of life even not being a life threatening condition. Approximately half of the patients with onychomycosis report some discomfort due to this condition: pain, difficulty on wearing footwear and walking, emotional embarrassment and work related difficulties.

## 1.2 Risk factors

Onychomycosis is an ailment that has several different risk factors. With regard to **age**, it is reported that onychomycosis is more prevalent at an older age, being the elderly the most affected population with an age/infection correlation of 20% and up to 50% of subjects over 60 and 70 years old, respectively (1,10,11). This correlation is often attributed to poor peripheral circulation, sedentary lifestyle, weaker immune system, diabetes, nail trauma, difficulty in performing foot hygiene and slower growing nails (2,10,12,13). Children are rarely affected by onychomycosis, with an incidence of just about 0.4%, since this group has smaller nail surface, faster nail growth, fewer nail injuries and lower tinea pedis incidence rate besides less contact with infected surfaces (5,14–16).

**Gender** is also considered a risk factor being males more often affected by this type of nail infection (2,11,17). Several authors postulated that this may be due to hormone differences between sexes, leading to a difference in the capacity to inhibit the growth of dermatophytes (18). It is also considered that the use of occlusive footwear and nail injuries may contribute to a higher incidence in males (2).

Recent studies had stated that onychomycosis may have a **genetic** basis, with an autosomal dominant pattern of inheritance related to *T. rubrum* infection, and increased susceptibility when at least one parent had onychomycosis (5,8,17,19–22).

The **environment** plays a major role in contracting a fungal infection. The societal factor cannot be disregarded. Those who regularly does not wear shoes tend to show a lower infection rate (2,15). On the contrary, athletes display an increased infection rate due to occlusive footwear which allows a dark and moist environment for onychomycosis to develop. Also, athletes contact more with moist infected surfaces, like swimming pools, communal shower rooms and public toilets (23). Nail trauma, synthetic clothing (which

retains sweat) and tinea pedis are also associated with sports and the incidence of this disease (2,5,13,21,23–26).

**Immunodeficiency** in HIV-infected individuals and transplant recipients also consists a risk factor for onychomycosis. Such persons whose T-lymphocyte count is as low as  $400/\text{mm}^3$  tend to have a more widespread infection affecting both toe and fingernails (1,5,11,23,25–29).

**Diabetic** individuals are three times more likely to have onychomycosis than the general population, being 34% with onychomycosis. Diabetic people have decreased peripheral circulation, neuropathy, impaired wound healing and increased difficulty on foot checkups due to obesity, retinopathy or cataracts. Therefore, injuries in toenails may be unnoticed due to neuropathy and act as entryways for bacteria, fungi, and other pathogens, leading to serious complications (4,5,11,21,24,30).

### 1.3 Clinical classification

There are five types of onychomycosis established according to the mode and site of invasion by the pathogen: distal and lateral subungual onychomycosis, white superficial onychomycosis, proximal subungual onychomycosis, total dystrophic onychomycosis (Figure 1.2) and endonyx onychomycosis (1,2,5,29,31–33).

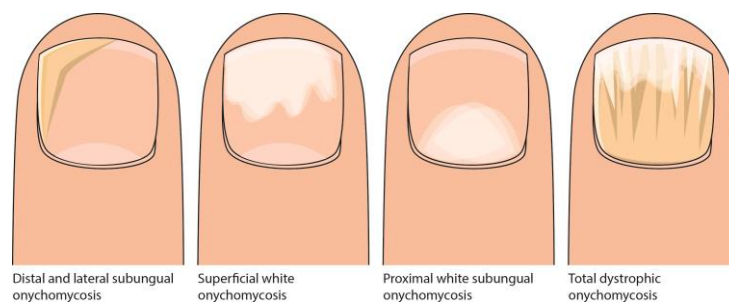


Figure 1. 2. Types of onychomycosis according to the mode and site of invasion of the pathogen.

#### *Distal and lateral subungual onychomycosis (DLSO)*

DLSO is the most common type of onychomycosis (1,2). The fungal infection progresses in the nail from the distal to the proximal edge, via the distal-lateral margins or through the lateral nail plate groove, originating from the hyponychium. This type of infection is mainly

caused by *Trichophyton* spp. and sometimes by *Scytalidium* spp. and *Candida* spp (5). It is frequent to find paronychia in these individuals, leading to subungual hyperkeratosis, nail thickening and onycholysis (nail detachment from the nail bed). The subungual space can be colonized by infectious bacteria and fungi, causing discoloration of the nail plate (1,2,5).

#### *Proximal subungual onychomycosis (PSO)*

In this type of onychomycosis, fungi invade the area under the nail cuticle and induce the infection of the proximal nail plate. Then, it progresses distally along the nail plate. This clinical manifestation of onychomycosis is mainly prevalent in immunocompromised individuals, being especially common in AIDS patients where it is considered an early HIV infection clinical marker. The fungi responsible for PSO are *T. rubrum*, *C. albicans*, *Fusarium* spp., *Aspergillus* spp. and *Scopulariopsis brevicaulis* (5, 25).

#### *Superficial white onychomycosis (SWO)*

SWO presents itself as opaque white patches on the dorsal surface of the nail plate. The upper layers of nail keratin are infected mainly by *Trichophyton mentagrophytes* and *T. rubrum*. Other pathogens responsible for this infection are non-dermatophyte molds such as *Fusarium* spp., *Acremonium* spp. and *Aspergillus* spp (28).

#### *Endonyx onychomycosis (EM)*

EM is the most recently described form of onychomycosis, being reported as an infection of both superficial and deeper layers of the nail plate. EM does not usually cause nail thickening, detachment, and inflammatory processes, but it leads to lamellar splitting, coarse pitting and milky white patches within affected nail plates (4). Usual pathogens are *T. soudanense* and *T. violaceum* (29, 30).

#### *Total dystrophic onychomycosis (TDO)*

TDO is usually considered the end stage of any other type of onychomycosis. It can also exist on its own - primary total dystrophic onychomycosis - occurring mostly in patients with chronic mucocutaneous candidiasis. It is described as the nearly complete destruction of the nail plate.

Diagnosing onychomycosis is important in order to guarantee the best possible treatment and with less side effects. Nowadays, the diagnosis is based on a clinical evaluation in which nail samples are collected and analyzed by microscopy and fungal culture (1,15,23,25). Onychomycosis should be differentiated from other similar conditions, such as psoriasis of

the nail, eczema, bacterial infections, contact dermatitis, traumatic onycho-dystrophies, chronic onycholysis, lichen planus, chronic paronychia, hemorrhage or trauma, onychogryphosis, median canalicular dystrophy, pincer nail, yellow nail syndrome, subungual malignant melanoma and subungual squamous cell carcinoma (4,15). Among these disorders, it is especially difficult to differentiate onychomycosis from nail psoriasis, since they tend to share similar nail morphological changes (34).

## **2. Transungual delivery**

All drugs must reach their target location to be more effective. Particularly, the nail unit has different characteristics from the rest of body surface, and consequently, topical formulations may not deliver enough drug amounts to the nail bed. Therefore, it is quite important to clearly understand the nail biology for the development of a more active topical formulations.

### **2.1 Nail structure and transungual permeation**

The nail plate is the main obstacle in the nail unit for drug permeation. It is hard, thin (0.25-1 mm), slightly elastic, translucent, convex shaped, and consists of 80-90 layers of dead, keratinized, flattened cells tightly bound to each other via intercellular links (35,36). The nail is constituted by nail plate, lateral fold, proximal fold, matrix, nail bed and distal groove as showed in Figure 1.3 (37). The nail plate can be divided into three macroscopic layers - dorsal, intermediate and ventral layers - being the dorsal layer the hardest one (37). Regarding its chemical composition, the nail is composed of fibrous proteins, keratins (80% “hard” keratin, remaining “soft” keratin), water and a low amount of lipids (0.1-1%) in contrast to the stratum corneum (~10%). Under normal conditions, the nail plate can contain 7-12% of water, but this content can rise to 35% (35–37).

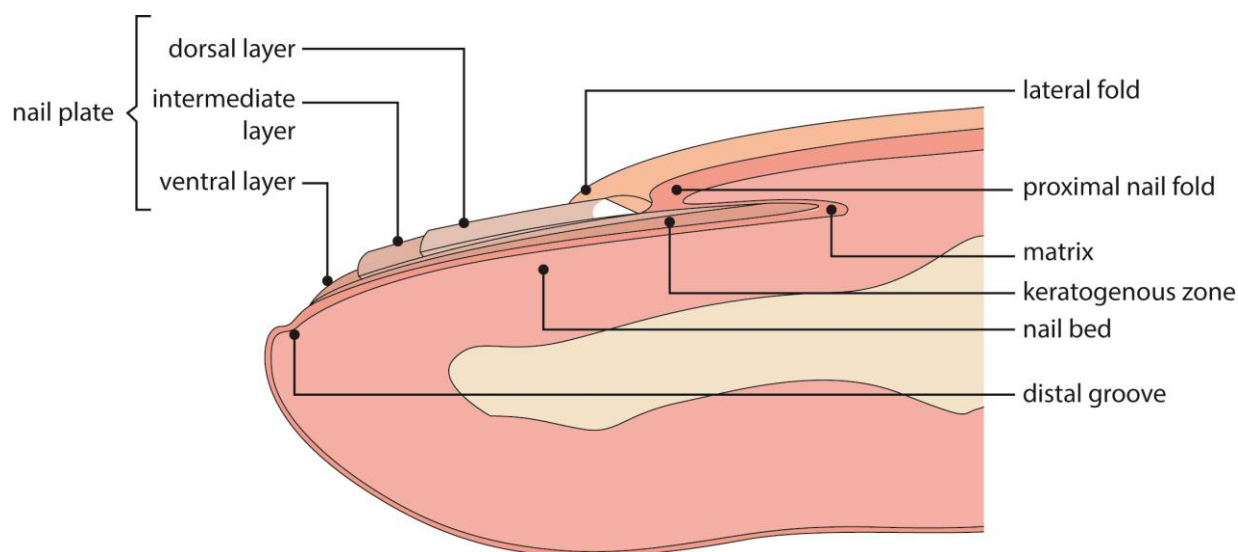


Figure 1. 3. Representation of nail structure.

Transungual permeation is dependent on drug properties (molecular weight, log P, charge, pKa, etc.), formulation characteristics (pH, water content, etc.), nail plate properties (diseased state, hydration, thickness and keratin content) and drug-keratin interactions.

Accordingly, the most significant properties of the permeant drug are:

**Molecular weight** – it shows an inverse relationship with the drug permeation into the nail plate. Heavier molecules have a higher time permeation through the keratin network on the nail plate (35). Drugs below  $300 \text{ gmol}^{-1}$  Mw have enhanced transungual permeation rate (37). Indeed, the molecular weight is considered to be the most significant property affecting the nail permeation.

**Log P** – permeation rate was found to decrease with an increase in carbon chain length or lipophilicity attributed to the hydrophilic nature of the nail plate (37-40).

**Charge** – non-ionic drugs were found to have about 10-fold greater permeability as compared to their ionic counterparts (38). However, Elsayed *et al.* (37) stated that these results did not take into account the molecular weight of the permeant drug, and regarding other studies, drug ionization can have a permeation enhancement effect due to an increase of aqueous solubility maximizing the transungual flux.

**pKa and other physicochemical properties** – in general, soluble molecules have good permeation across the nail plate. Weak acidic drugs are well permeated at higher pH, while weak basic drugs exhibit better permeation at lower pH values. Ionization can also contribute

to increasing drug solubility. Conversely, if the molecule is sublimable at body temperature, it will be advantageous for permeating through the diseased nail plate, since it can overcome air cavities by being sublimed and reach the other side of the cavity (36).

On the other hand, the formulation composition also plays an important role on drug transungual permeation, as follows:

**pH** – nail keratin has an isoelectric point of 5.0, turning to a net negative charge at pH 7.4 and net positive charge at pH 2.0. Therefore, some molecules might be repelled due to charging depending on pH. Some studies have stated that antifungal drugs have lower activity in acidic environments (39).

**Water content** – water enhances the diffusion through the nail plate. As water hydrates the nail plate, its volume increases, and this swelling causes larger pores, facilitating the permeation of bigger molecules. (35)

Finally, the nail plate properties influence the drug transungual permeation as well (35,40):

**Diseased nail plate** – this state has an enormous influence in permeation as diseased nail plates have uneven thickness, fungi concentration, and onycholysis, which can lead to a detached nail surrounded by non-detached areas. In some cases, this can be beneficial since some formulations can be applied to the detached space (41).

**Hydration** – it increases the unguinal permeability of polar compounds, as discussed before.

**Drug binding to keratin** – it can lead to disappointing results since it reduces the availability of the permeant drug and weakens its concentration gradient. Although this interaction highly influences antifungal activity, it is not frequently considered in many studies (42).

In summary, all factors that affect the drug transungual permeation are outlined in Figure 1.4.

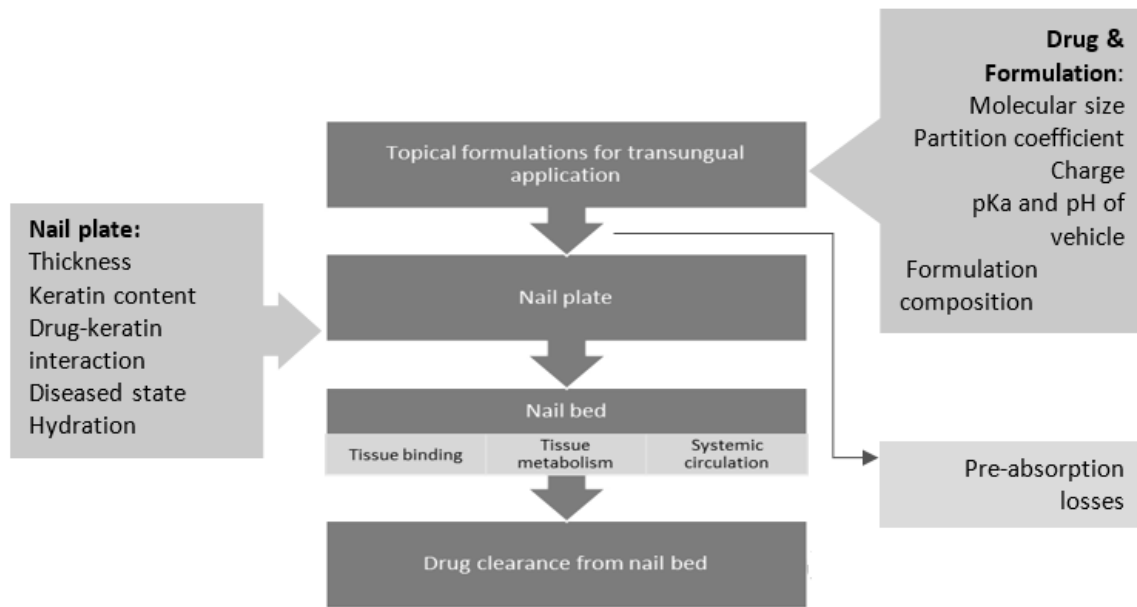


Figure 1. 4. Factors that affect nail permeation of topically applied formulations. Adapted from (35).

## 2.2 Mathematical description of nail permeability

Fick's adapted laws of permeability can be used for studying permeation through the nail plate.

Flux ( $J$ ) occurs when an amount of permeant ( $Q$  in mol or g) moves across a membrane with a certain area ( $A$  in  $m^2$ ) during time ( $t$  in s) (equation A). **Fick's first law** describes the flux where  $D$  is the permeant diffusion coefficient ( $m^2s^{-1}$ ) and  $\frac{\partial C}{\partial x}$  is the permeant concentration gradient. The negative sign indicates that the flux is in direction of decreasing concentration (equation B).

$$(A) \quad J = \frac{Q}{At} \qquad (B) \quad J = -D \frac{\partial C}{\partial x}$$

The permeability coefficient ( $P$ ) is given by equation C:

$$(C) \quad P = \frac{DK}{h}$$

In which  $K$  is the distribution equilibrium (distribution constant), and  $h$  is the membrane thickness (in m) (37,43).

According to Kobayashi *et al.* (44), the functional dependence of  $D$  on  $M_w$  of the molecule can be described by equation D:

$$(D) \quad D = D^0(-\beta.Mw)$$

Here  $D^0$  represents the diffusivity of a hypothetical molecule having zero molecular weight and  $\beta$  is a constant.

Nail permeability was found to be independent of the drug lipophilicity according to equation E (44):

$$(E) \quad \log P = \log\left(\frac{D^0}{h}\right) - \beta'.Mw \quad , \text{ where } \beta' = \beta/2.303$$

As human nails are not always available for studies, it is important to establish a viable *in vitro* model. Animal hooves have been used as a human nail model in the last decades. There are reports of bovine, porcine and equine hoof use (35). Saner *et al.* (35) described, the relationship between permeability coefficients through human nail plates and hoof membranes can be portrayed by the equation F:

$$(F) \quad \log P_N = 3.723 + 1.751 \log P_H$$

In which  $P_N$  is the human nail plate permeability coefficient and  $P_H$  is the permeability coefficient through bovine hoof membrane obtained experimentally. Recently researchers have used keratin films made from human hair as a model for human nails (36,45,46). Other models used to study nail permeability included wax blocks, nail clippings, cadaver nail plates and excised cadaver toes (37).

### 3. Onychomycosis topical therapy

There are several therapeutic options to treat this fungal nail infection: oral, topical and combined therapy (5,10,15,27,29,47–51). Adhesive patches have also been studied but displayed very low drug permeation. Thus, these pharmaceutical forms have a low representativity in the market (52).

Despite being more effective, oral therapy presents several risks for patients, including adverse reactions and possible drug interactions (10,53–57). This is especially relevant in the elderly (the most affected age group) who are polymedicated, and therefore, more susceptible to these reactions (10,12). Thus, it would be expected a higher investment on topical therapy. Currently, most common topical formulations present a low drug delivery to the infection site

mainly due to the nail plate characteristics, and the cure rate is lower than oral and combined therapy. Topical formulations are also bothersome to apply if there are several affected nails, reducing patient compliance (58,59). Nonetheless, there are several topical formulations available on the market used in mono or combined therapy. Firstly, it will be reviewed different drug delivery enhancers, antifungal drugs, and finally, several pharmaceutical forms employed in the topical treatment of onychomycosis.

### 3.1 Drug delivery enhancers

The nail plate is a great barrier to drug permeation, as stated before. Thus, it is important to enhance the permeation to guarantee effective drug delivery.

There are several **physical enhancement methods** such as nail plate abrasion, etching of the nail surface with acid, ablation of the nail with pulsed lasers, microporation of the nail plate, application of low frequency ultrasound and electric current through the nail (38). Although these methods are effective, reduce patient compliance and need the presence of a specialized technician to perform them.

**Chemical enhancement** of unguis drug delivery can also be useful. This type of enhancement is cheaper, easier to apply, and can be conducted by the patient before or concomitantly with drug application. It focuses on breaking chemical and physical bonds that maintain the integrity of the nail plate keratin. Targets for unguis chemical penetration enhancers are disulfide, peptide, hydrogen and polar bonds. Chemical enhancers are classified according to the targeted bond and respective mechanism (40).

The nail plate is cohesive due to S-S bonds, and these are great targets for enhancers. Enhancers targeting this bond will reduce the disulfide linkage, engaging in nucleophilic attacks as follows:



In this way, enhancers with thiol or ammonia groups with lone pairs of electrons will offer an advantage in breaking keratin bonding (43).

## Disulfide bond cleaving by reducing agents

### *Thiols*

Thiols are compounds containing sulfhydryl groups (–SH groups) that reduce the disulfide linkage in the keratin matrix of the nail (60). Examples of thiols used as permeation enhancers include N-acetylcysteine, mercaptoethanol, N-(2-mercaptopropionyl) glycine, pyrithione and thioglycolic acid. Once disulfide bonds are cleaved, they are unlikely to be reformed. Thus these alterations is permanent.

### *Sulfites*

Sodium sulfite is known to cleave disulfide bonds when incubated with proteins and peptides, producing thiols and thiosulfates. It was then found to enhance transungual permeation both on pretreatment and co-application (61).

### *Disulfide bond cleaving by oxidizing agents*

In this category of enhancers, hydrogen peroxide has been used alone or in combination. Pretreatment of nails with hydrogen peroxide has shown to increase mannitol permeation 3-fold (62). MedNail® technology consists of the pretreating nail with reducing agent TGA, followed by this oxidizing agent UHP. Treatment with this technology increased terbinafine drug flux 18-fold (63).

## Enhancement by solvents

### *Water*

The effect of water is recognized in the literature as a key enhancer. As nail hydration increases permeability by a mechanism that is thought to be related to swelling and formation of larger pores through the keratin matrix, the water content in formulations becomes necessary to guarantee maximum drug unguinal flux. Gunt *et al.* (64) reported a several fold increase related to nail hydration. Kobayashi *et al.*(44) also reported the enhancement of nail permeation by nail hydration. Notwithstanding, in some cases, nail hydration caused by formulation does not seem to improve unguinal permeation (38).

### *DMSO*

DMSO is a transdermal enhancer that interacts with the lipid domains of the stratum corneum, increasing fluidity and promoting partitioning of drugs into the skin. Stüttgen and Bauer (65) reported that DMSO had enhanced the delivery of econazole. However, DMSO has irritating properties at high concentrations.

### *Keratolytic agents*

Keratolytic agents disrupt the tertiary structure and hydrogen bonds present in the keratin matrix, 'unfolding' keratin and allowing larger molecules to pass through the nail pores (63). Urea and salicylic acid soften and hydrate the nail plate, enhancing drug permeation. This type of agents weakens and damages the nail plate (38). Nevertheless, urea cannot induce enhanced flux on its own, but it rather acts by synergizing with other enhancers to increase permeability. For example, urea combined with N-acetylcysteine increased the unguinal concentration of itraconazole by 94-, 20- and 49-fold compared with control (no enhancer), only urea and only N-acetylcysteine, respectively (38). It was also reported an increase in permeation for the concomitant use of urea and MPG. This synergy may be explained by easier access of other permeation enhancers during the keratin unfolding by urea.

Urea has also been used to chemically avulse infected nail at higher concentrations around 40% (66,67). It has also been included in nail lacquers (68).

### *Enzymes*

Keratinolytic enzymes hydrolyze the keratin matrix of the nail plate, altering its barrier properties and facilitating permeation. Studies have shown that keratinase enzyme markedly enhances nail permeation (61). This enzyme affects the surface of the human nail, causing corneocytes to detach and lift off the plate corroding the surface.

Papain is an endopeptidase containing a highly reactive sulfhydryl group and has shown promising results as a transungual enhancer (35).

### *Other enhancers*

SEPA®), a skin penetration enhancer, has been reported by Hui *et al.*(69) to increase the unguinal permeation of econazole. These findings suggest that adding SEPA® to an econazole lacquer can increase drug permeation up to 6 times, exceeding the MIC necessary to inhibit fungal growth.

Some formulations contain etching agents which are surface modifiers used to disrupt the dorsal surface of the nail to enhance permeation and promote adhesion of films. Phosphoric acid and tartaric acid are two etching agents commonly used as enhancers of transungual permeation (63). Polyethylene glycols and hydrophobins are other two types of permeation enhancers (70,71). Curiously, methanol has also shown some advantages in drug permeation (63).

All the enhancer are summarized in Table 1.1.

Table 1. 1. Overview of the most referenced transungual permeation enhancers.

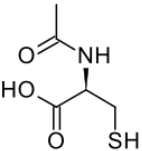
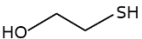
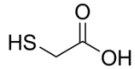
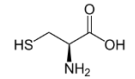
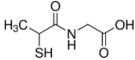
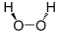
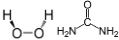
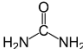
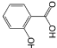
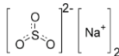
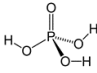
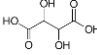
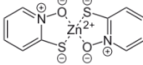
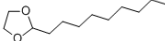
Enhancer	Structure	Increase in unguinal permeation	Experiment setup; permeant (Ref)
Thiols/Mercaptans			
N-acetylcysteine (5%)		49 x increase in nail drug content	Nails immersed in drug solution; Itraconazole
N-acetylcysteine (15%)		2x increase in mean drug uptake, but not statistically significant. Mean residence time in nail plate increased from 4.2 weeks to 5.5 weeks	Drug was applied twice daily on nail plates of humans for 6 weeks; Oxiconazole
N-acetylcysteine (3%)		13 x increase in flux from an aqueous formulation; 7x increase from lipidic formulation	Diffusion cells; 5-fluoruracilo
N-acetylcysteine (3%)		Drug measurable in presence but not in the absence of enhancer	Diffusion cells; tolnaftate
Mercaptoethanol		16 x increase in flux from an aqueous formulation; 8 x increase in flux from lipidic formulation	Diffusion cells; 5- fluoruracilo
		Drug measurable in presence but not in the absence of enhancer	Diffusion cells; tolnaftate
Thioglycolic acid		3.8x increase in flux	Diffusion cells; caffeine
Thioglycolic acid		2 x increase in mannitol concentration in receptor medium	Diffusion cells; mannitol
Cysteine		1.7 x increase in mannitol concentration in receptor medium	Diffusion cells; mannitol
N-(2-mercaptopropionyl) glycine		2.5 x increase in flux	Diffusion cells; water

Table 1.1. Continued.

Enhancer	Structure	Increase in unguinal permeation	Experiment setup; permeant (Ref)
Keratolytic agents			
Hydrogen peroxide		3.2 x increase in mannitol concentration in receptor medium	Diffusion cells; mannitol
Urea hydrogen peroxide		18 x increase in flux	Diffusion cells; terbinafine
Urea		-	Human nail; Fluconazole (68)
Salicylic acid		-	(72)
Sulfites			
Sodium sulfite		2 x increase in permeation through nail clipping	Diffusion cells; 5,6-carboxyfluorescein
Enzymes/Proteins			
Keratinase		2.3 x increase in flux	Diffusion cells; Metformin (61)
Hydrophobins		Up to 3.5x enhancement	Diffusion cells; terbinafine (70)
Etching agents			
Phosphoric acid		Increase in nail roughness score	Human nail (73)
Tartaric acid		Increase in nail roughness score	Human nail (73)
Other			
Pyrithione		Up to 2.5x increase in flux	Diffusion cells; water (60)
2-n-nonyl-1,3-dioxolane (SEPA®)		7x increase in concentration, 1.3x increase in deeper layer flux	Diffusion cell; econazole (69)

### 3.2 Examples of antifungal drugs

Table 1.2 represents several antifungal drugs and their main physicochemical characteristics that affect the transungual permeation. It should be noted that permeation coefficient and flux values were not included as reported in the literature considering that there are different methods and protocols to determine them (37). Since these coefficients are dependent on many factors, it is more appropriate to understand their values in the literature context.

The capability of inhibiting fungal proliferation is usually measured by assessing the MIC of the drug (74,75). MIC values for antifungal drugs are summarized in Table 1.3. Although these values do not take into account some characteristics (keratin binding, pH influence), they can serve as guidance (37).

Table 1. 2. Antifungal drug properties that influences permeation. Measurement conditions, e.g. base/salt used, medium/solvent composition, pH, ionic strength, and temperature are provided in parentheses when available. Adapted from (37).

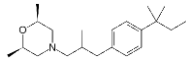
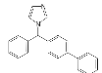
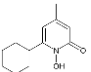
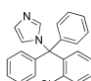
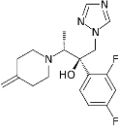
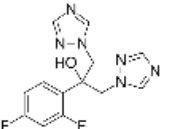
Antifungal Drugs	Chemical Structure	Mw (g/mol)	Aqueous solubility (mg/ml)	Log P	log n-octanol/aqueous medium distribution constant	pKa	Ref
Amorolfine		317.5	9.320 (CS, W, T20) 9.995 (CS, W, T32) $8.8 \times 10^{-3}$ (CS, pH 7.4 PB, T32)	5.7	0.33 (CS, W, T20)	6.6	(37,76)
Bifonazole		310.4	$0.13 \times 10^{-3}$ (BS, pH 7.4 PBS, T32) $0.51 \times 10^{-3}$ (BS, pH 8–10 0.1 M NC, T25) 0.345 (BS, I = 0.02 M pH 7.0 UB, T25)	4.8	4.77 5.2 (BS, 10 mM pH 7.4 PB, RT)	5.85 (I = 0.01 M UB, T25) 5.72 (0.1 M NC, T25)	(37,76)
Ciclopirox		207.3	12.4 (OS, W, RT) 8.590 (OS, W, T32) 1.47 (OS, 5 mM pH 7.0 TB, RT) 1.020 (OS, pH 7.4 PB, T32) 0.22 (OS, 0.1 M HCl, RT)	2	0.53 (OS, 5 mM pH 7.0 TB, RT)	7.2 $8.07 \pm 0.05$ (42% v/v EW, T32)	(37,76)
Clotrimazole		344.8	$2.7 \times 10^{-3}$ (BS, pH 7.4 PB, T32) $0.39 \times 10^{-3}$ (BS, W, T25)	5	4.9 (BS, 10 mM pH 7.4 PBS, RT)	$6.02 \pm 0.05$ (0.15 M KC, T25) $4.74 \pm 0.04$ (42% v/v EW, T32)	(37,76)
Efinaconazole		348.4	Predicted: 0.61	2	-	Predicted: 7.45–12.7	(37,76)
Fluconazole		306.3	5 (BS, W, T23) 14 (BS, 0.1 M HCl, T23)	0.4	0.5 (BS, 100 mM pH 7.4 PBS)	$1.76 \pm 0.10$ (0.1 M NC, T24)	(37,76)

Table 1.2. (continued).

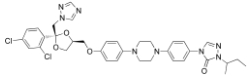
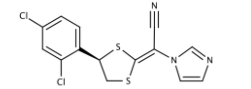
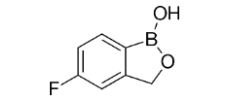
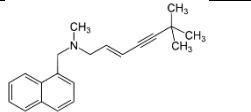
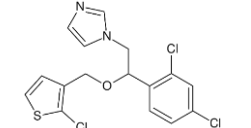
Antifungal Drugs	Chemical Structure	Mw (g/mol)	Aqueous solubility (mg/ml)	Log P	log n-octanol/aqueous medium distribution constant	pKa	Ref
Itraconazole		705.63	0.00964	5.7	-	3.70	(37,76)
Luliconazole		354.3	0.00062 (BS, W)	4	4.34 (pH 7.16 UB, T20) 3.78 (pH 4.00 UB, T20)	4.65	(37,76)
Tavaborole		151.9	~ 1.0	1.24	-	-	(37,76–78)
Terbinafine		291.43	2.92 (CS, pH 3 UB, T25) 1.57 (CS, pH 3 W, T25) 1.12 (CS, pH 5 W, T25) 0.101 (CS, pH 5 UB, T25) 0.02 (CS, pH 6.8 SIF/P, T37) 1.5 × 10 <sup>-3</sup> (CS, pH 9 UB, T25)	5.6	6.0 ± 0.1 (neutral form, 0.15 M KC, T37) [50] 2.3 ± 0.1 (ionized form, 0.15 M KC, T37) 5.5 ± 0.1 (calculated for pH 6.8 from the two above-mentioned values, T37)	7.05 (0.15 M KC, T37)	(37,70,76)
Tioconazole		387.7	0.0165	5.3	4.4	6.77	(76)

Table 1. 3. Minimum inhibitory concentration for antifungals used in onychomycosis. (Values displayed in µg/mL, \*MIC range).

MIC (µg/mL)	Amorolfine	Bifonazole	Butenafine	Ciclopirox	Efinaconazole	Itraconazole	Ketoconazole	Tavaborole	Terbinafine
<i>T. rubrum</i>	0.004-0.015*	≤0.12-1*	0.015-0.12*	0.031-0.5*	≤0.001–0.015*	≤0.015-0.125*	0.06-0.5*	1-2	0.004-0.06*
<i>T. mentagrophytes</i>	0.004-0.06*	0.5-4*	0.06-0.12*	0.031-0.5*	≤0.001–0.03*	≤0.015-0.5*	0.5-2*	2	0.004-0.5*
<i>T. tonsurans</i>	0.25	0.5-2*	0.12	0.25	0.016	0.06-0.25*	0.5-2*		0.015-0.06*
<i>T. verrucosum</i>	0.12	0.25	0.12	0.13	0.0039	0.12	0.12		0.015
<i>M. canis</i>	0.06-0.25*	1-2*	0.12	0.25	0.13-0.25*	≤0.015-0.03*	0.25-0.5*		0.008-0.03*
<i>M. gypseum</i>	0.063-0.25*	≤0.12-8*	0.06-0.12*	0.31	0.010	0.031-0.25*	0.5-4*		0.004-0.06*
<i>E. floccosum</i>	0.13-0.25*	0.25-0.5*	0.06	0.31	0.005	0.03-0.5*	0.25-0.5*	1	0.015-0.06*
<i>T. interdigitale</i>									0.017
<i>Geo. candidum</i>	1-2*	>64	>0.5			1	2-4*		0.12-0.25*
<i>Scopulariopsis brevicaulis</i>	0.09	2-4	0.5	0.59	0.25	>4	2-4*		0.12
<i>Aspergillus fumigatus</i>	>4	2-4*	>0.5	0.42	0.089	0.5-1*	8	0.25	1.4
<i>Fusarium oxysporum</i>	>4	>64	>0.5	1	1	>4	>8		>2.5
<i>Fusarium solani</i>	4	>64	>0.5	>4	0.5	>4	>8	2	4
<b>References</b>	(79,80)	(79)	(79)	(80,81)	(80)	(79,80)	(79)	(77,78)	(79,80,82)

Table 1.3. (Continued).

MIC (µg/mL)	Amorolfine	Bifonazole	Butenafine	Ciclopirox	Efinaconazole	Itraconazole	Ketoconazole	Tavaborole	Terbinafine
<i>Fusarium verticillioides</i>	>64	>64	>0.5			2	2		>0.5
<i>Acremonium potronii</i>	0.26			0.25	0.31	2.5			0.25
<i>Acremonium sclerotigenum</i>	1			1.4	0.18	4			0.09
<i>Aspergillus flavus</i>	4			3.4	0.11	0.18			0.11
<i>Aspergillus niger</i>	4			0.63	0.2	0.63			0.16
<i>Aspergillus sydowii</i>	4			0.59	0.037	0.3			0.076
<i>Aspergillus terreus</i>	4			0.5	0.09	0.21			0.13
<i>Aspergillus nidulans</i>	4			1	0.0078	0.089			0.063
<i>C. albicans</i>	0.03-0.5*			0.06-0.5*	0.0005-0.25*	0.004-2*		0.5	0.06-16*
<i>C. glabrata</i>	4.9			0.13	0.026	0.74			8
<i>C. krusei</i>	0.27			0.21	0.024	0.38			8
<i>C.parapsilosis</i>	0.56			0.22	0.0046	0.13			0.28
<i>C. ropicalis</i>	4			0.5	0.014	0.31			8
<i>C.guilliermondii</i>	0.25			0.25	0.016	0.13			1
<i>C. kefyi</i>	0.063			0.13	0.002	0.031			2
<i>C. lusitaniae</i>	0.5			0.25	0.0039	0.13			4
<b>References</b>	(79,80)	(79)	(79)	(80,81)	(80)	(79,80)	(79)	(77,78)	(79,80,82)

### 3.3 Examples of Topical Pharmaceutical Forms

Antifungal drugs are formulated in several topical pharmaceutical forms, such as creams, solutions, gels and lacquers (Table 1.4).

Table 1. 4. Topical formulation of antifungal.

Antifungal	Chemical Group	Commercial name	Approved in	Fungals	Formulation	Posology	Effectiveness	Reference
Amorolfine	Morpholine	Loceryl, Locetar, Sinibal, Unglyfol, Curanail	UK (1991), Switzerland (1991), France (1992), and more than 50 other countries Not approved in USA and Canada	<i>Candida sp</i> , <i>Trichophyton sp</i> , <i>Microsporum sp</i> , <i>Epidermophyton</i>	5% lacquer	1-2 weekly, 6-12 months after removal of affected area	50% mycological cure in cases of distal fingernail and toenail onychomycosis	(37,83–91)
Bifonazole (+40% urea)	Imidazole	Canespor, Canesten, Mycospor, Amypor (Onyster, Canespro)	Australia, Portugal, other countries	<i>T. rubrum</i> , <i>T. mentagrophytes</i> , <i>T. tonsurans</i> , <i>T. verrucosum</i> , <i>M. canis</i> , <i>M. gypseum</i> , <i>E. floccosum</i> , <i>Scopulariopsis brevicaulis</i> , <i>Aspergillus fumigatus</i>	1% cream (40% urea)	After ablation of the nail with 40% urea cream, application once daily for 4 weeks	33.6% overall cure rates	(37,66,67,77,88–90)

Table 1.4. (Continued)

Antifungal	Chemical Group	Commercial name	Approved in	Fungals	Formulation	Posology	Effectiveness	Reference
Ciclopirox	Hydroxypyridone derivative	Mycoster, Niogermos, Batrafen, Kitonail, Ony-Tec, Stieprox, Loprox, Penlac, Ciclopoli, RejuveNail	France (1991), Germany (1992/2008), Austria (1999), Canada	Trichophyton sp, S. brevicialis, Candida sp, Malassezia furfur, Aspergillus sp, Fusarium solan	8% lacquer	Once daily, 48 weeks	34-46% mycological cure 29-36% overall cure	(37,77,83,88–90,92–94)
Efinaconazole	Triazole	Jublia	Canada (2013), USA (2014)	<i>T. rubrum</i> , <i>T. mentagrophytes</i> , <i>Aspergillus sp</i> , <i>Candida albicans</i>	10% topical solution	Once daily for 48 weeks	53-55% mycological cure rate, 15-18% complete cure	(37,87–90,95)
Tavaborole	Oxaborole antifungal	Kerydin	USA (2014)	<i>T. rubrum</i> , <i>T. mentagrophytes</i> , <i>Aspergillus sp</i> , <i>Fusarium sp</i> , <i>Candida albicans</i>	5% topical solution	Once daily for 48 weeks	31-36% mycological cure, 6.5-9.5% complete cure	(37,77,87–90,96,97)
Tioconazole	Imidazole	Trosyl, Trosyd	Portugal, UK, France and 30 more countries	<i>T. rubrum</i> , <i>T. mentagrophytes</i>	28% solution	Daily, 3-12 months	22% of patients mycological cure	(3,37,83,88–90,98)

### *Cream*

Creams are semi-solid topical preparations used for delivery of one or more active substances, or for their emollient or protective action. The base may consist of natural or synthetic substances, being a multiphase preparation with lipophilic and aqueous phases. Lipophilic creams have the lipophilic phase as the continuous one, containing water-in-oil emulsifying agents at a higher percentage. The opposite is observed in hydrophilic creams. Creams may also contain other suitable excipients, such as preservatives, antioxidants, stabilizers, emulsifiers, thickeners and penetration enhancers (99–101).

As reported by Tietz *et al.* (67), a 1% bifonazole cream used after nail ablation by 40% urea paste (Canespor®, Canespro®) was effective in the treatment of onychomycosis. Bifonazole is an imidazole antifungal drug, acting by blocking the conversion of 24-methylendihydrolanosterol to desmethylsterol in fungi as well as inhibiting HMG-CoA (3-hydroxy-3-methylglutaryl-coenzyme A) and compromising the cell membrane. It is active against most dermatophytes, some non-dermatophytes, and molds. This bifonazole cream also contained benzylic alcohol, cetostearyl alcohol, cetyl palmitate, octyldodecanol, polysorbate 60, sorbitan monostearate and purified water (102). The urea paste was applied daily with an impermeable bandage until the ablation of the nail was achieved, and then 1% bifonazole cream was applied once daily for 4 weeks. At the end, 33.6% of patients were cured (55,66,67,79,88–90).

Lahfa *et al.* (66) studied the efficacy of using bifonazole and urea in the same formulation (Amycor Onychoset®).

Other cream formulations in the European market include Selergo®, Loprox®, Ertaczo®, Avage®, Mycoster®, Locetar® and Fougera® (35,88,89).

### *Solution*

Topical solutions are liquid preparations used for the delivery of one or more active substances that are solubilized in a suitable vehicle. These formulations are transparent and free of visible particles. They may also contain preservatives, antioxidants, stabilizers and buffers (99–101).

Solutions have some advantages compared to other topical formulations (41,42,103). As a liquid solution, the formula can be applied to the stratum corneum and subungual space as well as on the nail plate surface, and it does not require the patient to posteriorly remove the film as necessary for a nail lacquer (103).

In the USA market (42,96,104–107), a 10% efinaconazole solution has been recently available. This formulation contains 100 mg of efinaconazole per gram and its inactive ingredients are alcohol, anhydrous citric acid, butylated hydroxytoluene, C12-15 alkyl lactate (co-solvent), cyclomethicone (wetting agent), diisopropyl adipate (co-solvent), disodium edetate and purified water. This formulation should be applied once daily for 48 weeks. Overall cure rates were reported in 15-18% of patients, being mycological cure rates between 53-56% of patients studied. Efinaconazole acts by inhibiting the conversion of lanosterol to ergosterol in the ergosterol synthesis pathway. It possesses a broad spectrum of activity against dermatophytes, non-dermatophytes and yeasts (16,23,37,77,80,83,87,108,109).

5% Tavaborole solution (Kerydin®) is also available in the United States of American market, and it contains ethanol USP, propylene glycol USP and edetate calcium disodium USP (41,77). This solution should be applied once daily for 48 weeks. In conducted clinical trials, 31-36% mycological cure and 6.5-9.5% complete cure was achieved in patients treated with this drug. It shows activity against yeasts, molds, dermatophytes and filamentous fungi. It was specially developed for onychomycosis treatment (96,97).

There is a 28% tioconazole topical solution in the European market (Trosyd®, Trosyl®) formulated with undecylenic acid and ethyl acetate (110). It is applied daily for 3-12 months. The average overall cure rate is 22%. Nowadays, its use is in decline as other more effective antifungal drugs appear on the market (83).

Naumann *et al.* (111) describe several formulations, including a topical solution for the use of EV-086K, a new antifungal with a high lipophilicity which is not beneficial to transungual delivery (111). This solution was formulated by dissolving 5.7% of EV-086K in 30% ethanol and 63.75% water, besides the presence of Transcutol®P as solubilizer, 0.05% each of citric acid and sodium phosphatemonobasic for pH adjustment and 0.1% of butylated hydroxytoluene and, EDTA for chemical stability. The study showed that this formulation provided high permeability at the beginning of the penetration process (test in equine hoof), but the maximum drug concentration stabilized at 35% in the acceptor phase after 24h. These results were not significant compared to other formulations.

Other topical solutions available in the market are Canespor®, Mycooster®, and Lamisil® among others (88).

### *Gel*

Gels are formed by suitable gelling agents and can be classified as lipophilic gels or hydrophilic gels. Lipophilic gels (oleogels) usually consist of liquid paraffin with polyethylene or fatty oils gelled with colloidal silica, aluminum or zinc soaps. Hydrogels (hydrophilic gels) are prepared with water, glycerol or propylene glycol gelled with gelling agents such as starch, cellulose derivatives, carbomers and magnesium-aluminium silicates (100).

Although there are some gel formulations in the market (e.g. Lamisil®, a terbinafine formulation), they are mostly used for skin fungal infections instead of onychomycosis.

Along with the cream formulation previously referred, Naumann *et al.* (111) also studied a gel formulation for EV-086K delivery. Hydroxyethyl cellulose gel was formulated with the following excipients: 10% of EV-086K, 1.5% glycerol, 1% Tylose and 87.5% water. Among other tested formulations, the hydrogel had the less promising results in equine and bovine hoof penetration test (only 22% and 15% of applied dose was recovered, respectively), and thus it was not evaluated in the human nail.

Kerai *et al.* (53) have recently investigated the use of UV-curable gels (currently used in cosmetics) for the treatment of onychomycosis. The formulated gels contained diurethane dimethacrylate, ethyl methacrylate, 2-hydroxy-2-methylpropiophenone, an antifungal drug (amorolfine HCl or terbinafine HCl) and an organic liquid (ethanol or 1-Methyl-2-pyrrolidone) as drug solvent. Amorolfine was released to a greater extent than terbinafine, and even not reaching concentrations as high as the comparative nail lacquer, the concentrations were well above the MIC for *T.rubrum*, the main pathogen for onychomycosis. In addition, cured gel formulation could maintain the drug release for longer periods, being a promising candidate for future onychomycosis treatment.

## **Advances in Nail Formulations**

### *Colloidal Carriers*

The literature reports the success of some colloidal carriers for onychomycosis treatment since the drug easily diffuses along the skin tissue to the nail bed. Therefore, application to the skin surrounding the nail could be an effective area to treat for onychomycosis (112–114).

Colloidal carriers or colloidal drug delivery systems are particulates or vesicular dosage forms, having a size range from 1 nm to 0.5  $\mu\text{m}$  (Figure 1.5). They are essential for successful drug transport and delivery by protecting and maintaining the loaded drug until the site of action is reached.

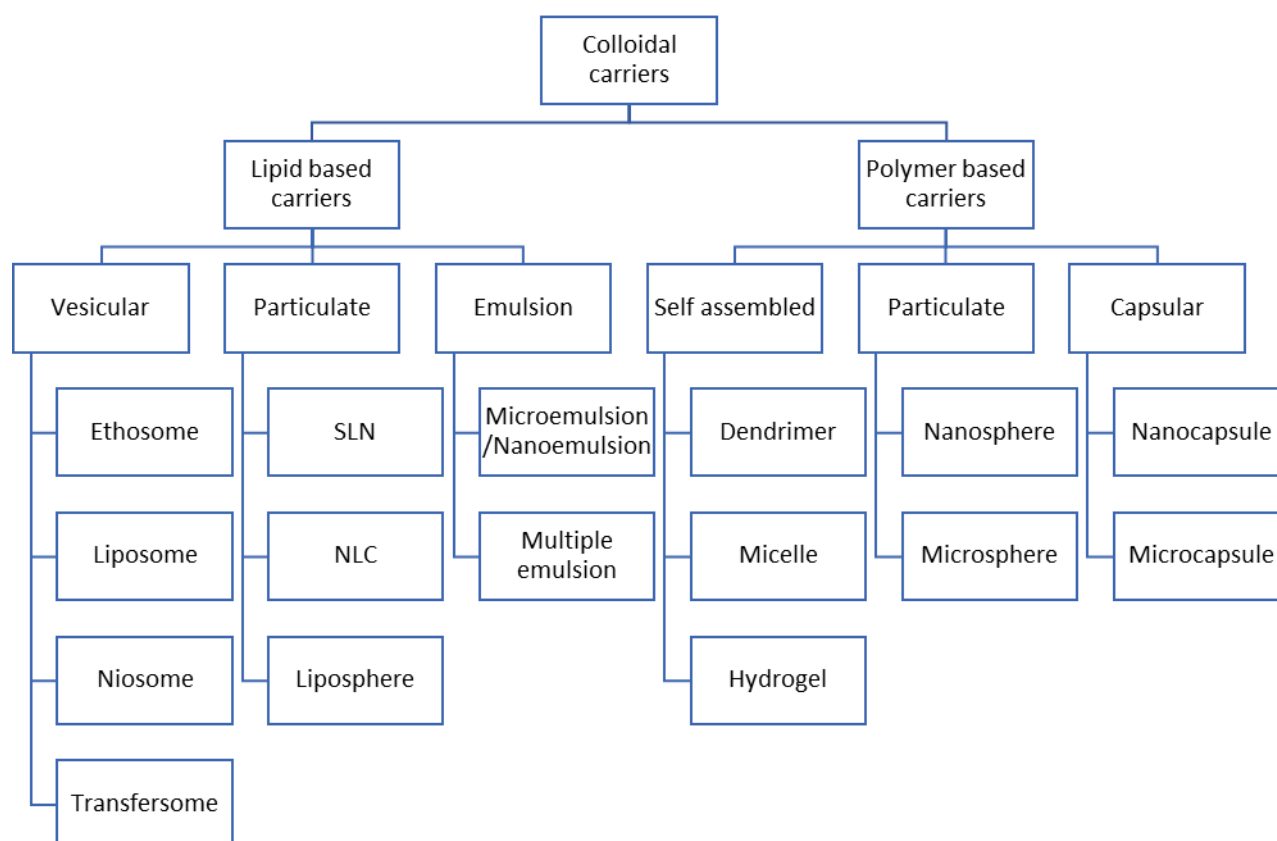


Figure 1. 5. Colloidal carriers for drug delivery. Adapted from (113).

Along with gel and solution formulations, Naumann also studied a colloidal carrier formulation for the delivery of **EV-086K**, containing water, propylene glycol, emulsifiers (Tagat®O2V and Synperonic™PE/L 101) and an oil component (Pelemol® BIP). This colloidal carrier system contributed to recovering  $7.25 \pm 0.30\%$  drug from the nail slices. These results were comparable to those obtained with a tested solution and nail lacquer (111). Nogueiras-Nieto *et al.* (115) developed in 2013 an aqueous formulation based on polypseudorotaxanes of Pluronic® F-127 and **ciclopirox** complexed with partially **methylated  $\beta$ -cyclodextrin**. The obtainment of *in situ* gelling thermosensitive hydrogels was due to the presence of the poloxamer Pluronic ®F127 (PF127), which facilitated drug solubilization via micelle creation forming a gel upon nail application. Partially m $\beta$ -CD was

also added to further improve drug solubilization. In addition, a penetration enhancer (N-acetyl-l-cysteine) alone or in combination with urea was also added to the formulations. Ciclopirox was incorporated into three different vehicles—simple aqueous solutions, thermosensitive hydrogels, and polypseudorotaxanes thermosensitive hydrogels. The composition of these vehicles is presented in Table 1.5.

Table 1. 5. Vehicles composition of CPX nail formulations. Adapted from (115).

Name	Solvent	AC (%)	PF127 (%)	Mβ-CD (%)
CPX–N-acetylcysteine solution (CPX–AC)	Water	10	–	–
CPX–thermosensitive hydrogel (CPX–TH)	Water	10	20	–
CPX–polypseudorotaxanes thermosensitive hydrogel (CPO–PPR)	Water	10	20	10

Recently Yang *et al.* (113) have developed a **gel with transfersomes containing terbinafine** prepared by ethanol injection method. The final formulation contained terbinafine, phospholipids, polysorbate 80, sodium cholesteryl sulfate, anhydrous ethanol, sodium benzoate, sodium pyrosulfate and phosphate buffer (pH 5.0). After 12h, it was obtained  $88.52 \pm 4.06 \text{ mg.cm}^{-2}$  and  $94.38 \pm 5.26 \text{ mg.cm}^{-2}$  of permeated and penetrated drug, respectively.

Vaghasiya *et al.* (116) studied another formulation composed of **solid lipid nanoparticles** for sustained release and skin targeting of **terbinafine** for the treatment of onychomycosis. The terbinafine loaded solid lipid nanoparticles formulation consisted of Compritol® 888 ATO as lipid matrix, Pluronic® F-127 as a stabilizer and distilled water as a dispersion medium, and prepared by the solvent injection technique. It was observed  $40.57 \pm 1.76\%$  of the applied drug retained in the skin after 8h (116).

**Terbinafine in transfersome 067** is a carrier -based liquid spray that has been developed for the delivery of terbinafine to the nail bed to treat onychomycosis. A 2011 study demonstrated that Terbinafine in transfersome 067 had greater antifungal activity against onychomycosis caused by dermatophytes compared to the free form vehiculated in an oral formulation (117). This formulation has also been tested in clinical trials (118).

There is another study with **terbinafine -loaded liposomes** formulation composed of bioadhesive polymers, pullulan, and Eudragit®L100, and prepared by thin film hydration method. This formulation also showed interesting results (119).

Barot *et al.* (120) studied a **microemulsion-based gel containing terbinafine**, oleic acid, Labrasol, Transcutol, water and Carbomer 934P. This formulation was developed to be applied between the nail bed and nail plate generated by onycholysis. It was obtained  $49.3\% \pm 4.12\%$  drug retention in the skin, and the total amount of terbinafine permeated after 12h was  $244.65 \pm 18.43 \mu\text{g}\cdot\text{cm}^{-2}$ . In 2012, Barot also described a microemulsion based antifungal gel incorporating itraconazole (120).

Barot *et al.* (121) developed a gel **microemulsion containing itraconazole** for the topical treatment of onychomycosis. The microemulsion contained benzyl alcohol, isopropyl myristate, Pluronic F68 (surfactant), ethanol, double distilled water and itraconazole. The microemulsion was incorporated into a gel by adding Carbomer 934P. Nail permeation enhancers like urea and salicylic acid were also used to increase drug penetration through the nail plate. The optimized formulation showed promising results: 92.75% drug entrapment efficacy and a complete drug release in 60 min with a highest nail uptake of  $0.386\%/\text{mm}^2$  (39 mg drug) (72).

Angamuthu (122) described the study of poly (lactide-co-glycolide) microspheres for the controlled release of **terbinafine** administered by intralesion injection. These microspheres were developed using O/W emulsification and modified solvent extraction/evaporation technique with methylene chloride, and methanol. This formulation achieved controlled release through 30 days and proper deposition onto the nail bed and plate.

Another **microemulsion-based gel** was studied by Kumar *et al.* (123). This gel contained **fluconazole** (against *Aspergillus niger*), oleic acid, polysorbate 80, propylene glycol and water. It exhibited an *in vitro* drug release of 72.23% in 7h.

#### 4. Nail Lacquer in onychomycosis therapy

Nail lacquers have been used for a long time in cosmetics, with both protective and decorative purposes. In the 1990's decade, nail lacquers started being used to administer drugs to the nail unit. Nail lacquers are **solutions of film-forming polymers** which leave a polymer film on the nail plate after solvent evaporation. This polymer film can be water resistant or water

soluble and acts as a drug reservoir, allowing it to permeate through the nail plate. Depending on the formulation and drug, the lacquer can be removed either mechanically or with organic solvents after a certain time, and it should be reapplied to reestablish the drug pool. Thus, the duration of the film residence in the nail constitutes an important property of a lacquer formulation (124). Although these formulations are commonly applied with a brush, there are also other types of applicators such as spatulas and sponge tips.

Being occlusive and adhesive to the nail, nail lacquers' films have **advantages** regarding nail hydration, permanence on the nail plate and patient compliance (when compared to creams, gels, and solutions).

These preparations usually contain the intended drug, a polymer, a volatile solvent and suspension agents (56,91,125).

The **drug** should present the following properties: a) low MIC for pathogens causing the disease (dermatophytes, yeasts, etc.), being effective at low concentrations; b) low molecular weight and volume to better permeate through the keratin matrix pores; c) water soluble, since water easily permeates through the matrix vehiculating the drug; and d) affordable and easily obtainable, so that the nail lacquer can be easily produced and obtained by patients (61).

The **polymer** choice can also influence the nail lacquer quality. Hydrophilic polymers have advantages regarding permeation and adhesion to the nail plate, having a soft, flexible and matte finish, which can improve patient compliance. However, these polymers allow more drug loss and are less occlusive. Hydrophobic polymers have a more durable, harder and glossier finish. This contributes for a more occlusive lacquer which can compromise the cumulative amount of permeated drug. Employing both types of polymers seems to be a good approach since it will combine both excellent permeation characteristics and higher resistance to environmental drug loss (126).

Effective formulations usually include **permeation enhancers** such as thiols/mercaptans, keratolytic agents, keratinases, etc. Other excipients can also be critical to allow better permeation conditions, including hydration, pH, and solubility. This can be achieved by using plasticizers, humectants, solvents, solubilizers, etc (127).

Colorless and non-glossy medicated nail lacquers are more acceptable by male patients (39). Despite male patient compliance, it could be considered advantageous for female patients to formulate a colored medicated nail lacquer for the treatment of onychomycosis since this disease alters the normal appearance of the nail.

After screening for the most suitable formulation components, it is important to check their compatibility and progressively adjust the quantities through pre-formulation studies.

There are several parameters to be evaluated in nail lacquer formulations to assess a higher **quality**, such as drug content, drug permeation studies (permeation coefficient, flow, the cumulative amount of permeated drug); gloss; flow; film adhesivity; viscosity; pH; drying time; non-volatile content, etc. According to this quality control, nail lacquers must present the final properties: a) be physically and chemically stable; b) release therapeutic levels of drug onto the nail; c) have a suitable viscosity to freely flow into all the edges and grooves of the nail for easy application; d) dry quickly (3-5 minutes) and form an even film once applied; e) adhere to the nail plate to not come off or flake during daily activities, but at the same time, be easily removed with an enamel remover and f) be cosmetically pleasant and well tolerated (38).

Several examples of nail lacquer formulations for onychomycosis treatment are presented in Table 1.6. However, only nail lacquers containing amorolfine and ciclopirox are currently commercialized (39).

**Amorolfine** is a morpholine antifungal agent approved for the treatment of onychomycosis in 1981 (128). It is usually presented as a nail lacquer containing 5% amorolfine. This active substance inhibits delta14 reductase and delta7-delta8 isomerase, causing ergosterol depletion and ergosterol accumulation in the cytoplasmic membrane of the fungus cell. Amorolfine is effective against dermatophytes (*Trichophyton spp.*, *Microsporum spp.*, *Epidermophyton spp.*), yeasts (*Candida spp.*, *Cryptococcus spp.*, *Malassezia spp.*) and some molds (*Alternaria spp.*, *Hendersonula spp.*, *Scopulariopsis spp.*). Amorolfine can be present in the nail up to 27% from the nail lacquer formulation after 2 weeks treatment, being this concentration enough to inhibit most fungi. This formulation should be applied once or twice weekly for 6 months. Studies report mycological cures in 52-60% of the patients, and complete cures (both clinical and mycological) up to 44% of patients (54,77). Even after apparent cure, some authors recommend the use of amorolfine as prophylaxis (129). Amorolfine is available in Europe (e.g. Loceryl®, Locetar®, Curanail®), but not in USA (77,89–91,130).

Table 1. 6. Nail lacquer formulations.

Drug	Commercial name	Polymer	Solvents & other excipients	Ref.
Econazole		Butyl methacrylate, dimethylaminoethyl methacrylate, methyl methacrylate polymer	2-n-nonyl-1,3-dioxolane Ethanol	(69)
		Hydroxypropyl chitosan (HPCH)	Cetostearyl alcohol Ethyl alcohol (95°) Ethyl acetate Purified water	(131)
	Ciclopoli®		Ethyl acetate	
Ciclopirox		Hydroxypropyl chitosan (HPCH)	Ethanol 96% Cetostearyl alcohol Water	(126)
		Pluronic F127	Partially methylated $\beta$ -cyclodextrin N-acetyl-L-cysteine	(115)
	Mycoster®		Ethyl acetate	
		Methylvinyl ether	Isopropanol Maleic acid monobutylester	(128)
			Glycerol triacetate Docusate sodium	
Fluconazole		Polyvinylpyrrolidone K25	Urea Ethanol Demineralized water	(68)
		Poly (vinyl methyl ether alt maleic acid monobutylester)	Ethanol	
		Poly (2-hydroxyethyl methacrylate)	Ethanol	
Tavaborole			Dibutyl sebacate Water	(78)
		Poly (vinylacetate)	Ethanol Ethyl acetate Dibutyl sebacate	

Table 1.6. (Continued)

Drug	Commercial name	Polymer	Solvents & other excipients	Ref
Terbinafine		HPMC E-15	Ethanol	(132)
		PEG 400	Purified water	
		Poly (4-vinyl phenol)	Ethyl acetate	(57)
		Cellulose acetate	Dibutyl phthalate	
Ketoconazole		Ethyl cellulose	Triethyl citrate	(133)
		Propylene glycol	Hydroxypropyl- $\beta$ -cyclodextrin	
		PEG 400	Isopropyl alcohol	(134)
		Acrylates copolymer	Acetone	
Miconazole			Glycerin	(135)
			Urea hydrogen peroxide	
			Ethanol	(111)
			Salicylic acid	
Amorolfine	Loceryl®		Ethanol	(110)
			Thioglycolic acid	
			Ethanol	(134)
			Panthenol	
EV-086K			Tocopheryl acetate	(135)
			Phytantriol	
			Butylene glycol	(110)
			Benzophenone-3	
Amorolfine	Loceryl®		Calcium chloride	(110)
			Fragrance	
			Urea hydrogen peroxide	(135)
			Salicylic acid	
Amorolfine	Loceryl®		Ethanol	(111)
			Transcutol® P	
			Ethanol	(110)
			Glycerol triacetate	
Amorolfine	Loceryl®		Butyl acetate	(110)
			Ethyl acetate	
			Ethanol	(110)
			Ethanol	

**Ciclopiroxamine** belongs to the group of hydroxyl-pyridone derivatives, and it has been used as a nail lacquer to treat onychomycosis since 1990. It exerts its antifungal activity by chelating trivalent cations, like  $\text{Fe}^{3+}$  and  $\text{Al}^{3+}$ , compromising fungal metal-dependent enzymes and reducing the fungus nutrient intake. Ciclopirox is active against dermatophytes (*Trichophyton spp.*, *Microsporum spp.*, *Epidermophyton floccosum*), yeasts (*Candida spp.*, *Malassezia furfur*, *Cryptococcus neoformans*, *Sacchromyces cerevisiae*), molds (*Aspergillus spp.*, *Scopulariopsis brevicaulis*, *Fusarium solani*) and some bacteria, which is advantageous in cases of mixed infection. It is also reported to have some anti-inflammatory activity by inhibiting the local production of prostaglandins and leukotrienes. The nail lacquer available in the market has a concentration of 8% ciclopirox, which increases to 35% after application and evaporation of the volatile solvents. Studies show that it can exceed MIC for the three most important onychomycosis pathogens—*T.rubrum*, *T. mentagrophytes*, and *Candida albicans*. Common posology is once daily application for 6-12 months over the clean nail plate and slightly over the surrounding skin. However, there are trials stating that once the weekly application is effective. Clinical trials have reported complete cure in 29-36% of patients. Ciclopirox is available in both Europe and United States of America: MycoSter®<sup>®</sup>, Niogermos®<sup>®</sup>, Batrafen®<sup>®</sup>, Kitonail®<sup>®</sup>, Onytec®<sup>®</sup>, Stieprox®<sup>®</sup>, Loprox®<sup>®</sup>, Penlac®<sup>®</sup>, Ciclopoli®<sup>®</sup> and RejuveNail®<sup>®</sup> (77,83,88–94).

Besides these main drugs, others have been recently studied as well as specific excipients as follows.

Monti *et al.* (131) purposed to evaluate the water-soluble film forming agent hydroxypropyl chitosan included in an experimental nail lacquer (P-3051) containing **ciclopirox**. Hydroxypropyl chitosan is a water-soluble derivative of chitosan. Chitosans are polysaccharides derived from chitin and natural components of the exoskeleton of crustaceans being widely employed in medicine for their wound healing, bacteriostatic, skin moisturizing, and protecting properties. In particular, hydroxypropyl chitosan was chosen considering its favorable properties, such as high water solubility; high plasticity; affinity to keratin; wound-healing activity; high compatibility with human tissues, etc. P-3051 was composed by 1% hydroxypropyl chitosan, 1% cetostearyl alcohol, 73% ethyl alcohol (95°), 4% ethyl acetate and 13% purified water. This formulation was compared with a commercial brand (Penlac™) constituted by 8% ciclopirox, ethyl acetate, isopropyl alcohol, butyl monoester of poly (methylvinyl ether/maleic acid) in isopropyl alcohol. Bovine hoof membranes were used as

the human nail plate model. Drug concentrations were determined by HPLC (high-performance liquid chromatography). Regarding lag times, the respective values obtained were  $3.36 \pm 0.46$  h for P-3051 vs.  $12.48 \pm 1.31$  for Penlac™. The percent of permeated drug (Q%30h) was also significantly different for the two formulations: 2.58% for P-3051 vs. 1.06% for Penlac™. In fact, a faster drug penetration time might allow the drug to permeate the nail before the hydro soluble film is degraded. Greater efficiency of P-3051 could be attributed to a affinity of hydroxypropyl chitosan to the nail matrix, resulting in an intimate contact and strong adhesion of the lacquer to keratin substrate (131).

An *in vitro* study with the formulation previously developed by Monti *et al* (131) reported an achievement of 13% complete cure rate, which was quite low. It was concluded that ciclopirox formulated in the new hydrolacquer technology is more active and better tolerated than the reference ciclopirox nail lacquer for the long-term treatment of onychomycosis. In addition, it is much easier to apply without needing any bothersome removal procedures (136).

In 2009, Monti *et al.* compared the transungual permeation of **ciclopirox** with **amorolfine** vehiculated in the same **hydroxypropyl chitosan-based lacquer** and a **water insoluble reference** (Loceryl® containing Eudragit® RL100, triacetine, butyl acetate, ethyl acetate, ethyl alcohol and drug). The study was performed on bovine hoof slices, and drug concentration was determined by HPLC. Amorolfine experimental lacquer showed higher permeation than the commercial water-insoluble option. Also, ciclopirox lacquers showed a better performance than amorolfine lacquers (114).

Later in 2012, a **clinical trial** with these formulations was conducted (56). The results supported *in vitro* data except from day 15 to day 25 in which the nail concentration of these drugs decreased. The authors hypothesized that the steady state had not been reached yet. Moreover, *in vitro* studies do not take into account all the environmental interactions that occur under *in vivo* conditions where both fingers and toenails are constantly exposed to tissues, liquids, and blood circulation, resulting in some drug loss. This may be a disadvantage for water soluble formulations since the contact with water can lead to a loss of medication; however, it can be countered by a more frequent application (56).

Chouhan *et al.* (57) studied the influence of a permeation enhancer **hydroxypropyl- $\beta$ -cyclodextrin** in a **terbinafine** nail lacquer formulation. This formulation was composed of cellulose acetate and ethyl cellulose as film forming polymers, triethyl citrate as a plasticizer,

and isopropyl alcohol and acetone as solvents. Formulations containing this enhancer demonstrated a higher flux than the control formulation in *in vitro* studies. The lacquer containing 10% (w/v) hydroxypropyl- $\beta$ -cyclodextrin showed maximum flux of  $4.586 \pm 0.08 \mu\text{g/mL/cm}^2$  as compared to the control flux of  $0.868 \pm 0.06 \mu\text{g/mL/cm}^2$ , demonstrating its ability to enhance the transungual permeation of poorly soluble drugs (57).

A **ketoconazole** nail lacquer for onychomycosis treatment was also described by Kiran *et al.* in 2010 (122). The studied formulations contained ketoconazole, propylene glycol, glycerin, ethanol, polyethylene glycol 400, thioglycolic acid and urea solution in  $\text{H}_2\text{O}_2$ . Several factors were evaluated including non-volatile content, drying time, smoothness of flow, gloss and permeation studies in human nail plates. Urea hydrogen peroxide enhanced hydration state and thioglycolic acid cleaved keratin bonds, allowing better penetration results which could be promising upon formulation optimization (133).

In 2011, a novel lacquer formulation for the transungual delivery of **ketoconazole** was reported by Hafeez *et al.* The vehicle used had an anhydrous/alcohol composition with a dual acrylate-silicone hybrid copolymer system that offered film forming and occlusion properties due to synergistic plasticizing components (134). It contained ethanol, polysilicone-8, panthenol, acrylates copolymer, tocopheryl acetate, phytantriol, butylene glycol, benzophenone-3, calcium chloride and fragrance, as well as radiolabeled [ $1\text{-}^{14}\text{C}$ ]-Ketoconazole. This test formulation was compared with a commercial ketoconazole cream. The study was conducted on human nails placed in a diffusion cell simulating physiological conditions. The formulations were then administered once daily for 7 days. Sampling was made by drilling and radioactivity was measured from the samples obtained. Following the 7-day exposure, the ketoconazole content measured in the ventral/intermediate layers was  $0.81 \pm 0.39 \mu\text{g/mg}$  or  $535 \pm 260 \mu\text{g/cm}^3$  for the lacquer formulation and  $0.09 \pm 0.05 \mu\text{g/mg}$  or  $53 \pm 29 \mu\text{g/cm}^3$  for the control formulation. The drug concentration attained in the nail was approximately 2,140 times higher than the MIC for common dermatophytes, exceeding the MIC for most common onychomycosis pathogens. According to these results, this lacquer formulation can be a potential effective topical treatment for onychomycosis (134).

Hui *et al.* (69) assessed the enhancing properties of **2-n-nonyl-1,3-dioxolane** in a lacquer formulation (EcoNail™) to increase the permeation of **econazole**. The test formulation contained 5% (w/w) econazole, Eudragit® RL/PO, ethanol and 18% (w/w) 2-n-nonyl-1,3-dioxolane. The assay was performed on healthy human nail plates collected from cadavers

and using a diffusion cell. An aliquot of all tested formulations was applied on the nails twice daily for 14 days, washing the nail plates between applications. After incubation, nail samples were obtained with a drill and radioactivity of labeled compounds was measured. The concentration and flux of econazole into the deep layer of the human nail in the test group was about 6.3-fold and 7.5-fold higher than the control group, respectively. Econazole concentration was about 15,000 times the MIC for most dermatophytes species and 150 times that for most molds. On the contrary, dioxolane did not penetrate to deeper layers of the nail. These authors hypothesized that besides facilitating diffusion of the drug, dioxolane also functioned as an adhesion promoter and plasticizer for the film-forming polymer, softening the Eudragit film in the lacquer. These results suggest that 2-n-nonyl-1,3-dioxolane-enhanced econazole lacquer has the potential to be an effective topical treatment for onychomycosis (69).

The same author performed another study (78) in which reported the nail penetration of **tavaborole** (AN2690) from different vehicles and compared with ciclopirox. Four formulations, all containing 10% (w/w) AN2690 were compared for their ability to deliver AN2690 to the deep layers of the nail plate and into the nail bed. The composition (w/w) of these different vehicles was: *formulation A*: 70% ethanol and 20% poly (vinyl methyl ether alt maleic acid monobutylester), a polymer that forms a water insoluble film, very durable and resistant to damage; *formulation B*: 56% ethanol, 14% water, 15% poly (2-hydroxyethyl methacrylate) and 5% dibutyl sebacate, forming a water soluble film; *formulation C*: 55% ethanol, 15% ethyl acetate, 15% poly (vinylacetate) and 5% dibutyl sebacate, forming a water insoluble film that can be removed by peeling or scratching the surface; *formulation D*: 20% propylene glycol and 70% ethanol (only solvents). Aliquots of those formulations were applied on human nail plates once daily for 14 days. The ventral/intermediate nail samples were collected at the end of the 14<sup>th</sup> day dose period, stored at 4°C and analyzed for drug by LC/MS/MS. Considering that any formulation showed a distinct advantage over the others, the simplest formulation (D) was chosen for further development (78).

Baran *et al.* (68) evaluated the efficacy of a **fluconazole-urea** nail lacquer in onychomycosis treatment of 13 patients. The lacquer was composed of 1% fluconazole, 20% urea, polyvinylpyrrolidone k25, glycerol triacetate, docusate sodium, ethanol and demineralized water. After 12-18 months' treatment, about 90% of patients had positive results regarding clinical and mycological cure (68).

A **terbinafine bilayered nail lacquer** for onychomycosis was developed by Shivakumar *et al.* in 2010. Since aqueous-based nail lacquers promote nail hydration and drug diffusion through the nail but lack durability, the authors studied an underlying drug-loaded hydrophilic lacquer with an overlying water resistant film. The hydrophilic nail lacquer was composed of 5% (w/v) terbinafine, 6% (w/v) hydroxypropyl chitosan E-15 (water soluble polymer), 10% (v/v) PEG 400 (penetration enhancer, plasticizer and humectant), 60% (v/v) ethanol and 19% purified water. Formulation controls as a hydrophilic nail lacquer of E-15 containing terbinafine but devoid of PEG 400 and a placebo (formulation without the active drug) hydrophilic lacquer of hydroxypropyl chitosan E-15 containing PEG 400 were similarly prepared for comparison. Briefly, terbinafine was dissolved in a mixture of water and ethanol (pH 3.0) by a bath sonicator. Hydroxypropyl chitosan E-15 was soaked overnight in the hydroalcoholic mixture (pH 3.0) and sonicated to ensure complete polymer dissolution. The two hydroalcoholic solutions were mixed and stirred to obtain a clear homogeneous solution to which PEG 400 was added. The hydrophobic nail lacquer was prepared by dissolving poly (4-vinyl phenol) in ethyl acetate at 10% (w/v). Dibutyl phthalate was used as a plasticizer in the lacquer at 4% (v/v). The pH, viscosity and drying time of the hydrophilic nail lacquers were found to be around 4.0, 500 cps, and  $300 \pm 75$ s, respectively. *In vitro* drug permeation studies were performed with cadaver nails. Although therapeutic concentration values were reached in *in vitro* studies, a clinical study on infected patients should be performed to ascertain clear results (132).

Vipin *et al.* (135) presented in 2014 a **miconazole** nail lacquer. This formulation included a film former (nitrocellulose), permeation enhancers (urea in hydrogen peroxide and propylene glycol), a keratolytic agent (salicylic acid) and an antifungal agent (miconazole nitrate) in ethanol. Several formulations were tested regarding nonvolatile content, gloss, smoothness to flow, drug release (bovine hoof model), drug content (UV spectrophotometry) and antifungal activity. Among ten formulations, the nail lacquer prepared with 2% drug, 3% nitrocellulose, 0.5% ethyl cellulose, 20% salicylic acid, 5% propylene glycol and 5% urea in H<sub>2</sub>O<sub>2</sub> exhibited the best results, being a promising formulation for the treatment of *Candida albicans* (135).

Naumann *et al.* (111) studied the controlled delivery of **EV-086K** nail lacquer through the nail plate. 5% Eudragit® E100, dimethylaminoethyl methacrylate, butyl methacrylate and methyl methacrylate were mixed with 85% ethanol and stirred until the polymer was completely dissolved. 5% EV-086K and 5% Transcutol® P were stirred in a separate amber

glass until a clear solution was obtained. Then, the polymer–ethanol mixture was added. Bovine hoof slices, equine hood slices, and human nails were employed for delivery studies. This nail lacquer penetrated into the nail at higher concentrations than other studied formulations. However, it did not reach the acceptor compartment (111).

## 5. Polyurethane a potential excipient in therapeutic nail lacquer

The polyurethanes (PU) are among one of the most important class of specialty polymers (137)). They are obtained by the reaction between isocyanate and hydroxyl compounds (138). The polyurethane production was developed by Otto Bayer and co-workers in 1937 (139) for the polyaddition reaction. Since then the polyurethanes have found many different applications and the polyurethanes market has been growing uninterruptedly (140). Polyurethanes are polymers containing urethane linkages ( $-\text{NHCOO}-$ ) in the main polymer chain. They can be classified into the following major groups: flexible foams, rigid foams, elastomers, fibers, molding compositions, surface coatings and adhesives (137).

### 5.1 Synthesis of polyurethane

Polyurethanes are synthesized from three components, namely a polyol (polyglycol), a diisocyanate and a chain extender (diol) as shown in Figure 1.6.

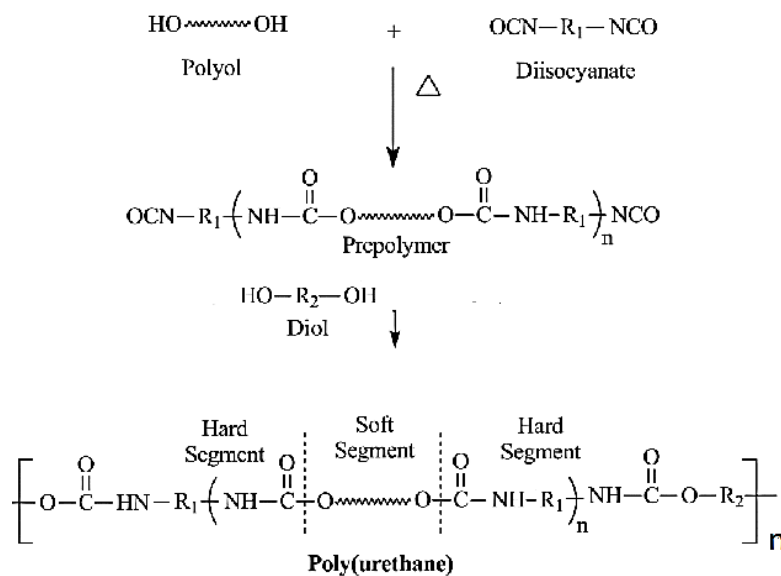


Figure 1. 6. Scheme of Synthesis of polyurethane adapted from (141).

They present a segmented architecture, where in the diisocyanate and the chain extender (diol of low molecular weight) form the hard segments of the polymer chain and the polyol of high molecular weight (interception sections) form the soft segments as represent the Figure 1.7.

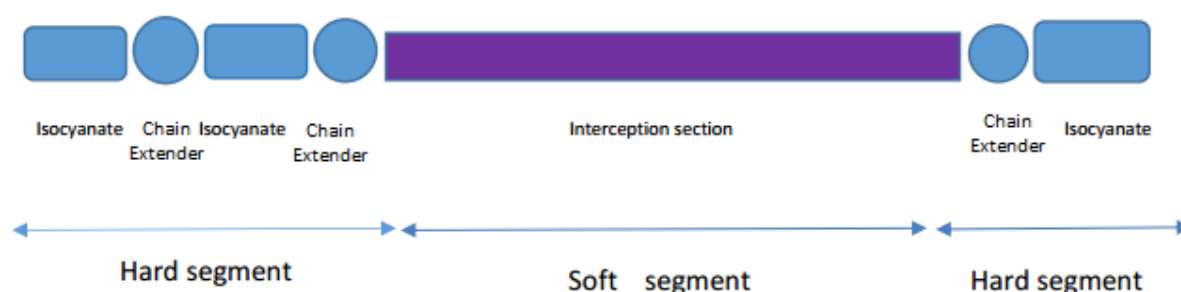


Figure 1. 7. Architecture of the chain of polyurethane. Adapted from (142)

The hard and soft segments of the polyurethane are responsible for the wide range of elastomeric properties presented by this polymer. The soft segments, owing to their low glass transition temperatures are responsible for the elasticity of the polyurethane. However, the hard segments make the polymer stiffer due to the presence of inter-chain hydrogen bonds between the hard segment in the polymer. The hydrogen bonding causes the hard segments to pack themselves into crystalline domains which function as physical crosslinks between the polymer chains.

For the producing a material with a broad range of mechanical properties which is both elastic and strong, the architecture of the polymer is modulated by variations such as:

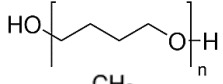
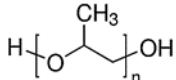
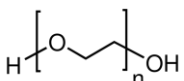
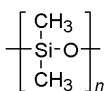
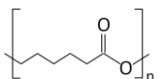
- The ratio of the hard segment to the diol.
- The choice of the hard segment and soft segment components (139).

## 5.2 Monomers for the synthesis of polyurethanes

### *Polyglycols of high molecular weight*

Convenient long chain polyglycols such as polyethylene oxide diols, linear or ramified, and polyester diols are used as monomers for the synthesis of PU (137,138,139) (Table 1.7).

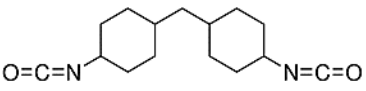
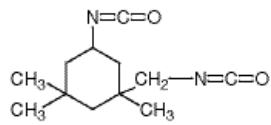
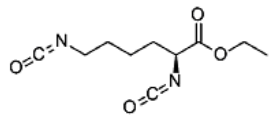
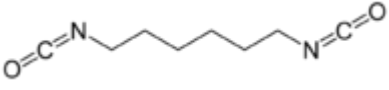
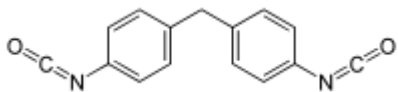
Table 1. 7. Polyglycols employing in synthesis of polyurethanes.

Polyglycols	Chemical structure
Poly (tetramethylene oxide)	
Poly (propylene glycol)	
Poly (ethylene glycol)	
Poly (dimethyl siloxane)	
Poly ε-caprolactone	

*Diisocyanates*

In order to obtain non-toxic polyurethanes, the diisocyanates (138,139), employing are representing in Table 1.8.

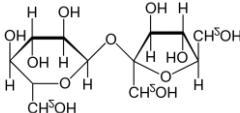
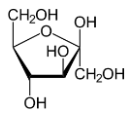
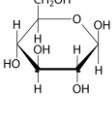
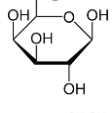
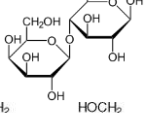
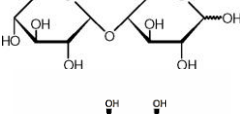
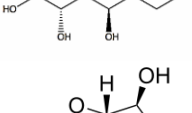
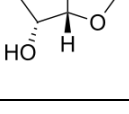
Table 1. 8. Name, toxicity and chemical structure of diisocyanates.

Diisocyanates	LD <sub>50</sub> (mg/Kg)	Chemical structure
HMDI	9 900	
IPDI	1000	
LDI	Value no relevant	
HDI	Value no relevant	
MDI	2 200	

*Chain extenders*

Carbohydrates are frequently employed as chain extenders in the architecture of the polymer. Some examples of the synthesis of polyurethanes from a renewable source (143) are shown in Table 1.9.

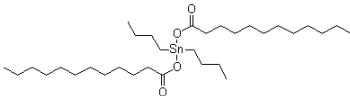
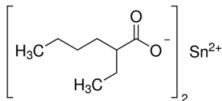
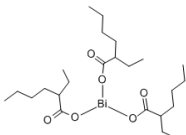
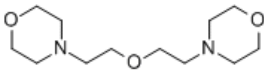
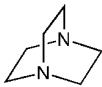
Table 1. 9. Carbohydrates employed as chain extender in the synthesis of polyurethanes.

Chain extender	Chemical structure
Sucrose	
Fructose	
Glucose	
Galactose	
Lactose	
Maltose	
Sorbitol	
Isosorbide	

*Catalysts*

Currently, the flexible polyurethanes are made with the aid of at least one catalyst (139). They ensure the completion of the reaction in the polyurethane. Catalysts controlling the reaction time and for defining polymer architecture that influences the ultimate mechanical properties. Specifically, it is the catalyst's activity and selectivity towards each of the many reactions occurring in the formation of polyurethanes that determine the structure of the resulting material. The amine and organometallic are among the most used catalysts employing in the synthesis of polyurethane, which showed in Table 1.10.

Table 1. 10. The most common catalyst in synthesis of polyurethane.

Catalyst	Structure	Class
Dibutyltin dilaurate		Organometallic
Tin(II) 2-ethylhexanoate Sn		Organometallic
Bismuth 2-ethylhexanoate Bi		Organometallic
DMDEE		amine
DABCO		Amine

### 5.3 Methods for synthesis of polyurethanes

The polyurethanes are synthesized by three methods:

- the one-shot method,
- the prepolymer method,
- the quasi-prepolymer method (144).

The prepolymer method and the quasi-prepolymer method correspond to processes known as 'two-step methods' or 'two-step polymerization'.

The **one-shot method** is a process that takes place in one step. All the ingredients are mixed simultaneously, and the resulting mixture is allowed polymerize.

In the **prepolymer method**, the macroglycol is pre-reacted with an excess of poly-isocyanate. This prepolymer is then mixed with the rest of the ingredients during processing.

In the **quasi-prepolymer method**, a part of the diol is mixed with the isocyanate and the rest of the polymer and the other constituents are mixed as a second phase.

In the pre-polymer process, the free content of isocyanate result of the reaction between the diisocyanate and polyol is about 1-12%. On the other hand the quasi-prepolymer present generally more that 25% of free isocyanate, in this process the NCO/OH ratio is 4:1, to yield a low viscosity system consisting of a pre-polymer dissolved in excess of isocyanate (137).

#### *Advantages of quasi-prepolymer.*

- Allows maintain better control the structure and properties of the final polymer. Through a simple change of chain extender, it is possible to obtain polyurethanes with different properties from the same pre- polymer.
- The pre- polymers are typically liquids, which facilitates handling on an industrial scale.
- When compared with monomeric isocyanate systems, the prepolymers have a lower vapor pressure and consequently lower toxicity.
- The viscosity of the prepolymers is higher than that of the monomeric isocyanates, which allows a better homogenization when mixed with the polyol and better control of the rheological properties when trying to lose fluidity.
- Allows better temperature control because the resulting heat bond formation is released in two stages (145).

#### 5.4 Synthesis of polyurethanes from carbohydrates

Kennedy et al, 1986 describe preparing polyurethanes from carbohydrates such as pectin and sucrose, one amine was employing as a catalyst. The syntheses were developed from polyisocyanates at temperatures above 60 °C, yielding highly crystalline polymers (146).

Polyurethanes from prepolymers were obtained using different amounts of milliequivalents sucrose, glucose, and fructose which reacted with MDI and PEG. In the polyurethanes obtained was observed that the increasing of the content of saccharides influence in values of glass transition temperature (Tg), Young's modulus and tension stress. The synthesis of the prepolymer and polyurethane were developed at 25 °C without solvent (147).

They have been reported polyurethanes employing glycosylamines and glucosamines modifications. Only modified near the anomeric hydroxyl group, being the most reactive. Hexamethylene diisocyanate (HDI) and 2,5 dianhydro -2,5 -dideoxy - L- iditol - diisocyanate is used. The polymers were soluble in dimethylformamide, and their molecular weights were between 53 655-75 300, (148).

In 2001, were proposed two polyurethanes obtained from partially protected carbohydrates. They developed reactions of HDI with methyl 2,6-di- O- pyranosyl -  $\alpha$  - D - glucopyranose and methyl 4,6-O- benzylene -  $\alpha$  -D - glucopyranose, in the ratio 1: 1, using 1,4- diazabicyclo catalyst (2,2,2) octane. Tetrahydrofuran was used as a solvent in the reaction, obtaining polyurethanes with values of Tg between 147-150°C (149).

According to polyaddition catalytic process, polyurethanes using monomers D- Sorbitol, L - iditol and D - mannitol were synthesized. The method was developed at 80 °C, with a stream of nitrogen (143).

In 2005 was synthesized a polyurethane from sucrose and PEG 600 and 1000. The polymer was not toxic (151). According to acute oral toxicity test, the administration of the polyurethane did not present any clinical signs in any of the animals treated or damages in the organs analyzed, which suggest that the polyurethane was a safe product (150).

In 2013 Aurelie Boyer and collaborates, synthesise a linear polyurethane from transesterification of sucrose and  $\alpha$ -d glucopyranoside. In the research was employing dibutyl tin dilaurate as catalyst (151).

The synthesis of the linear polymer has many applications in research of Vicent Besse et al, the aim of the work was obtaining a polyurethane with higher chemical and hydrolysis

resistance. The polyhydroxyurethane was obtained by reaction of isosorbide, hydroxylated polybutadiene and methylene diphenyl-4,4 diisocyanate (152).

Another example of the synthesis of polyurethanes from carbohydrate was the polyurethane synthesized from the reaction of hexamethylene diisocyanate and various ratios of isosorbide to poly(tetra methylene glycol) by one-shot bulk polymerization without a catalyst. The rigid diols impart biocompatible and bioactive properties to thermoplastic polyurethane elastomers. The degradation test showed loss of mass in the polyurethane from 4–9% after 8 weeks. In the case of polymers with lowest isosorbide content, the weight loss was in a short time compared with polyurethane that present highest isosorbide content (153).

The L-lactide is another carbohydrate to permit synthesized biodegradable crosslinked polyurethane using polyethylene glycol and hexamethylene diisocyanate (HDI). In the reaction, the iron acetylacetonate was using as catalyst (154).

### **5.5 Application of polyurethane in biomedical industry**

The polyurethanes are copolymers which have been used for biomedical applications for over three decades.

These desirable properties attract the attention of developers of biomedical devices. In 1958, polyurethane materials were first introduced in biomedical applications; Pangman described a composite breast prosthesis covered with a polyester-urethane foam (155). In the same year, Mandrino and Salvatore also used a rigid polyester-urethane foam called Ostamer™ for in situ bone fixation (156).

Three years later, the application of polyester-urethane Polyurethane Estane® VC was proposed by Dreyer *et al* to be used as components for heart valves and chambers, and aortic grafts (157). In the mid-1960s, Cordis Corp. started to commercialize polyester-urethane diagnostic catheters (137).

In 1954, textile chemistry at DuPont developed Lycra® spandex as a high-performance alternative to natural rubber in elastic thread. It was first introduced as a biomaterial in 1967 by Boretos and Pierce who obtained the polymer in solution directly from the DuPont spinning line that produced Lycra spandex yarn. This material was first used as the elastomeric components of a cardiac assist pump and its arterial cannula (156).

The years 1970-1972, were a time of designed of polyurethane specifically commercialized for medical use; Avcothane®-51™, a polyurethane/silicone hybrid, Biomer®™, a version

of Lycra® T-126. Avcothane® and Biomer® were regarded as the first ‘real’ biomedical polyurethanes, where some of them (156). Avcothane® was used clinically in the first intra-aortic balloon pump (IAB), starting in about 1971, and is still in clinical use today in IABs(90). Biomer®TM components were used in the ‘Jarvik Heart’ in 1982, the first artificial heart used for implantation (137).

In the Figure 1.8 showed the application of polyurethanes in biomedical. These polymers have been applied in some biomedical tissue engineering areas such as pacemaker lead insulators, heart valves, vascular prostheses, breast implants, gastric bubbles, drug release carriers, etc.

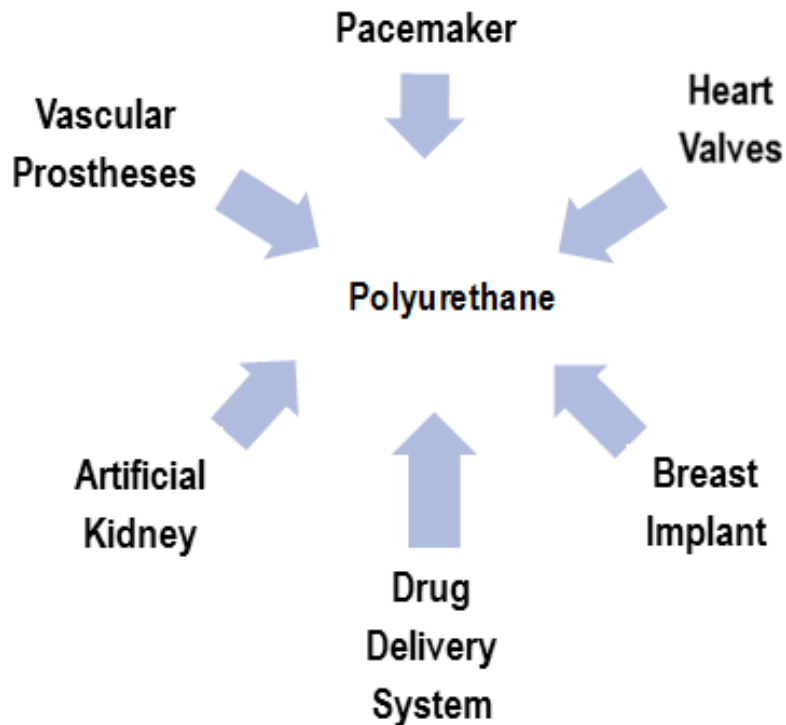


Figure 1. 8. Biomedical application of polyurethanes.

### 5.6 Application of polyurethane in drug delivery system.

The polyurethane system is being used for sustained and controlled delivery of various dosage forms. These systems are based on a physical combination of the drug with polymers and kinetics of drug release is generally controlled by the diffusion phenomena through the

polymer (159). Some examples of polyurethane with application for controlled release, are described below:

Controlled delivery System employing polyurethane and nystatin was development in 2001 by Michaela Mandru, *et al* (160). Sustained release of nystatin from polyurethane membrane for biomedical application. The system was prepared by a mixture of a different amount of polyurethane and nystatin. The final system consists of a membrane of polymers with nystatin obtained by phase inversion methods. The mechanism for release of nystatin was according to fickian diffusion.

Lijuan Zhou *et, al* in 2011, synthesized a pH-sensitive polyurethanes. For the synthesis of polymers was used LDI, PCL-Hyd-PEG- Hyd-PCL, and tripeptide chain extender. The reaction took place in two step. The pH-sensitive polymers were employing for anticancer drug delivery. The polyurethane was degrading at pH 5-6, and release the antitumoral drug in tumor site (161).

In other hand systems consisting of albumin nanoparticles were dispersed into a carboxylated polyurethane. The release of drug was by diffusion phenomen, which observed in Figure 1.9, (162).

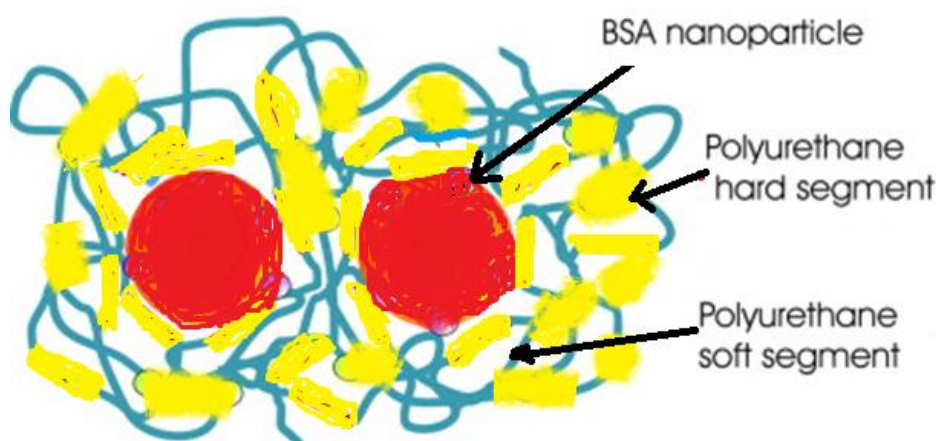


Figure 1. 9. Release of nanoparticles from polyurethane matrix. Adapted from (162)

In 2006 the polyurethane was evaluated as theophylline delivery matrices. The polymers were synthesized from aliphatic diisocyanate (Lysine methyl ester diisocyanate), poly  $\epsilon$  (caprolactone) and 1,4 butanediamine. The release of drug from the polyurethane matrix was according to fickian diffusion model. The release of theophylline was faster with the increase of the hydrophilicity of the polyurethane (163).

In 2008 Andrea Hafeman *et al*, showed a polyurethane for release a growing factor (I-PDGF) for tissue repair and regeneration. The polyurethane was prepared by the one-shot foaming process. The controlled release system formulated, described a two-stage release profile, characterized by a 75% burst release within the first 24h and slower release thereafter. By 21 days 89% of the (I-PPGF) has eluted from the matrix of polyurethane (159).

Chlorhexidine diacetate polyurethane controlled delivery system with the employ of polyurethane. In this work, the drug loaded to the film of polyurethane was released for 11 days. The kinetic of the system was the zero-order (164).

The polyurethane was used in the blend of chitosan microspheres. The system obtained permitted to release two cardiovascular drugs: isoxuprine hydrochloride and calcium dobesilate. The microsphere with chitosan and polyurethane were prepared by emulsion cross-linking method. The drug release from the microsphere followed the fickian to non fickian diffusion mechanism (165).

The matrix of poly (ester ether urethane)s with rifampicim were prepared to employ different concentration of urethane groups. The release of drugs was higher than the minimum inhibitory concentration of rifampicim for gram-positive bacteria (166).

Another example of the release of drug from polyurethane was the heparin. In this work, the heparin was blended with the polymer. The quantitative of heparin released from the system was controlled by the thickness of polyurethane films (167).

The polyurethane was synthesized with vancomycin. The medical device permits inhibition of infection of the bone wound in a rat femoral segmental defect model. The antibiotic quantitative released after 8 weeks exceeding the minimal concentration for bactericide action. The system was promisor for the treatment of osteomyelitis (168).

In 2008, the 7-ter-butyldimethylsilyl-10-hydroxyl-camptothecin was employed in a formulation with polyurethane. This drug formulation was studied for the treatment of cancer. The drug was covalently incorporated into the delivery system and released 0,1% of the total drug load to the polymer in 65 days (169).

Polyurethanes have a great application for controlled release of the drug. The use of such compounds for the release of antifungal has not been explored so far. Thus, the use of polyurethane for the active principle release against onychomycosis is still a challenge.

## 6. References

1. Lecha M, Effendy, Feuilhade de Chauvin M, Di Chiacchio D, Baran R. Treatment options development of consensus guidelines. *Journal European Academy of Dermatology and Venerology*. 2005; 19(1): 876–90.
2. Singal A, Khanna D. Onychomycosis: Diagnosis and management. *Indian Journal of Dermatology Venereology and leprology*. 2011;77(6):659-672.
3. Grover C, Khurana A. An update on treatment of onychomycosis. *Mycoses*. 2012;55(6):541–51.
4. Thomas J, Jacobson G, Narkowicz CK, Peterson GM, Burnet H, Sharpe C. Toenail onychomycosis: An important global disease burden. *Journal of Clinical Pharmacy Therapeutic*. 2010;35(5):497–519.
5. Tchernev G, Penev PK, Nenoff P, Zisova LG, Cardoso JC, Taneva T, et al. Onychomycosis: Modern diagnostic and treatment approaches. *Wiener Medizinische Wochenschrift*. 2013;163(1-2):1–12.
6. Pierard GE, Pierard-Franchimont C, Arrese JE. The boosted antifungal topical treatment (BATT) for onychomycosis. *Medical Mycology*. 2000; 38: 391–3923
7. Tan EST, Chong W-S, Tey HL. Nail psoriasis: a review. *American Journal of Clinical Dermatology*. 2012 Dec;13(6):375–88.
8. Parisi R, Symmons DPM, Griffiths CEM, Ashcroft DM. Global Epidemiology of Psoriasis: A Systematic Review of Incidence and Prevalence. *Journal of Investigative Dermatology*. 2012;133(2):377–85.
9. Shi Y, Hu FB. The global implications of diabetes and cancer. *Lancet [Internet]*. Elsevier; 2014;383:1947–8.
10. Loo DS. Onychomycosis in the elderly: drug treatment options. *Drugs & Aging*. 2007 Jan;24(4):293–302.
11. Ghannoum M, Isham N. Fungal Nail Infections (Onychomycosis): A Never-Ending Story? *PLoS Pathogens*. 2014;10(6):1-5.
12. Tosti A, Hay R, Arenas-Guzmán R. Patients at risk of onychomycosis-risk factor identification and active prevention. *Journal of European Academy of Dermatology and Venereology*. 2005;19(1):13–6.
13. Stone N, Dawber R. Crinkly toenails. Toenail onychomycosis can cause serious problems.

- British Medical Journal. 2000;320(7232):448.
14. Gupta AK, Sibbald RG, Lynde CW, Hull PR, Prussick R, Shear NH, et al. Onychomycosis in children: Prevalence and treatment strategies. *Journal of the American Academy of Dermatology*. 1997 Mar;36(3):395–402.
  15. Elewski BE. Onychomycosis: pathogenesis, diagnosis, and management. *Clinical Microbiology. Reviews*. 1998;11(3):415–29.
  16. Feldstein S, Totri C, Friedlander SF. Antifungal therapy for onychomycosis in children. *Clinics in Dermatology*. 2015;33(3):333–339.
  17. Gupta AK, Gupta M a., Summerbell RC, Cooper E a., Konnikov N, Albreski D, et al. The epidemiology of onychomycosis: Possible role of smoking and peripheral arterial disease. *Journal of the European Academy of Dermatology and Venereology*. 2000;14(6):466–469.
  18. Clemons K V, Schar G, Stover EP, Feldman D, Stevens DA. Dermatophyte-hormone relationships: characterization of progesterone-binding specificity and growth inhibition in the genera *Trichophyton* and *Microsporum*. *Journal of Clinical Microbiology*. 1988:2110–2115.
  19. Faergemann J, Correia O, Nowicki R, Ro B-I. Genetic predisposition--understanding underlying mechanisms of onychomycosis. *Journal of European Academy of Dermatology and Venereology*. 2005;19(1):17–9.
  20. Faergemann J, Baran R. Epidemiology, clinical presentation and diagnosis of onychomycosis. *British Journal Dermatology*. 2003 Sep;(149) :1–4.
  21. Iorizzo M, Piraccini B, Tosti A. Today's treatments options for onychomycosis. *Journal of the German Society of Dermatology*. 2010. 8:875–879.
  22. Zaias N, Tosti A, Rebell G, Morelli R, Bardazzi F, Bieleley H, et al. Autosomal dominant pattern of distal subungual onychomycosis caused by *Trichophyton rubrum*. *Journal of the American Academy of Dermatology*. 1996 Feb;34(2):302–4.
  23. Eisman S, Sinclair R. Fungal nail infection: diagnosis and management. *British Medical Journal*. 2014; 1800:1–11.
  24. Seebacher C, Brasch J, Abeck D, Cornely O, Effendy I, Ginter-Hanselmayer G, et al. Onychomycosis. *Mycoses*. 2007;50(4):321–7.
  25. Grover C, Khurana A. Onychomycosis: Newer insights in pathogenesis and diagnosis. *Indian Journal of Dermatology, Venereology Leprology*. 2012;78(3):263.

26. Baran R, Kaoukhov A. Topical antifungal drugs for the treatment of onychomycosis: an overview of current strategies for monotherapy and combination therapy. *Journal of the European Academy of Dermatology and Venereology: JEADV*. 2005;21–29.
27. Baran R, Hay RJ, Garduno JI. Review of antifungal therapy and the severity index for assessing onychomycosis: part I. *Journal of Dermatological Treatment*. 2008;19(2):72–81.
28. Repka M A., Mididoddi PK, Stodghill SP. Influence of human nail etching for the assessment of topical onychomycosis therapies. *International Journal of Pharmaceutics*. 2004; 282:95–106.
29. Baran R, Hay RJ, Garduno JI. Review of antifungal therapy, part II: treatment rationale, including specific patient populations. *Journal of Dermatological Treatment*. 2008: 168–75.
30. Özcan D, Şekin D, Demirbilek M. In vitro antifungal susceptibility of dermatophyte strains causing tinea pedis and onychomycosis in patients with non-insulin-dependent diabetes mellitus: A case-control study. *Journal of the European Academy of Dermatology and Venereology*. 2010: 1442–1446.
31. Baran R, Hay R-J. Nouvelle classification Clinique des onychomycoses. *Journal of Medical Mycology*. 2014;24(4):247–60.
32. Hay RJ, Baran R. Onychomycosis: A proposed revision of the clinical classification. *Journal of the American Academy of Dermatology*. 2011;65(6):1219–1227.
33. Zaias N, Escovar SX, Rebell G. Opportunistic toenail onychomycosis. the fungal colonization of an available nail unit space by non-dermatophytes is produced by the trauma of the closed shoe by an asymmetric gait or other trauma. A plausible theory. *Journal of the European Academy of Dermatology and Venereology*. 2014:1002–1006.
34. Klaassen G, Dulak MG, van de Kerkhof PCM, Pasch MC. The prevalence of onychomycosis in psoriatic patients: a systematic review. *Journal of the European Academy of Dermatology and Venereology*. 2014;28(5):533–41.
35. Saner M V, Kulkarni AD, Pardeshi C V. Insights into drug delivery across the nail plate barrier. *Journal of Drug Targeting*. 2014;2330(9):1–21.
36. Täuber A, Müller-Goymann CC. In vitro permeation and penetration of ciclopirox olamine from poloxamer 407-based formulations-comparison of isolated human stratum corneum, bovine hoof plates and keratin films. *International Journal Pharmaceutics*. 2015 Jul;489(1-2):73–82.

37. Elsayed MM a. Development of topical therapeutics for management of onychomycosis and other nail disorders: A pharmaceutical perspective. *Journal of controlled release: official journal of the Controlled Release Society*. 2014. p. 132–44.
38. Murdan S. Enhancing the nail permeability. *Expert Opinion Drug Delivery*. 2008;5(11):1267–1282.
39. Murdan S. Drug delivery to the nail following topical application. *International Journal of Pharmaceutics*. 2002;236(1-2):1–26.
40. Sugiura K, Sugimoto N, Hosaka S, Katafuchi-Nagashima M, Arakawa Y, Tatsumi Y, et al. The low keratin affinity of efinaconazole contributes to its nail penetration and fungicidal activity in topical onychomycosis treatment. *Antimicrobial Agents and Chemotherapy*. 2014. p. 3837–42.
41. Czaika VA, Phi-Anh L. Trichophyton mentagrophytes cause underestimated contagious zoophilic fungal infection. *Mycoses*. 2013; 56 (1): 33–37.
42. Esteves JA, Baptista AP, Rodrigo FG, Gomes MAM. *Dermatologia*. 3ª Edição ed. Lisboa: Fundação Calouste Gulbenkian; 2005. 1643l.
43. Miron D, Cornelio R, Troleis J, Mariath J, Zimmer a R, Mayorga P, et al. Influence of penetration enhancers and molecular weight in antifungals permeation through bovine hoof membranes and prediction of efficacy in human nails. *European journal of pharmaceutical sciences : official journal of the European Federation for Pharmaceutical Sciences*. 2014: 20–25.
44. Kobayashi Y, Komatsu T, Sumi M, Numajiri S, Miyamoto M, Kobayashi D, et al. In vitro permeation of several drugs through the human nail plate: Relationship between physicochemical properties and nail permeability of drugs. *European Journal of Pharmaceutical Sciences*. 2000:471–7.
45. Lusiana, Reichl S, Müller-Goymann CC. Keratin film made of human hair as a nail plate model for studying drug permeation. *European Journal of Pharmaceutics and Biopharmaceutics*. 2011:432–40.
46. Saner M V, Kulkarni AD, Pardeshi C V. Insights into drug delivery across the nail plate barrier. *Journal of Drug Target*. 2014;2330(9):769–789.
47. Gupta AK, Paquet M. Improved efficacy in onychomycosis therapy. *Clinics Dermatology*. 2013;31(5):555–63.
48. Cribier BJ, Paul C. Long-term efficacy of antifungals in toenail onychomycosis: A critical

- review. *British Journal Dermatology*. 2001;145(3):446–52.
49. Gupta AK, Paquet M, Simpson FC. Therapies for the treatment of onychomycosis. *Clinics Dermatology*. 2013;31(5):544–54.
50. Pajaziti L, Vasili E. Treatment of Onychomycosis - a Clinical Study. *Medical Archives*]. 2015;69(3):173.
51. Gupta AK, Paquet M. Systemic antifungals to treat onychomycosis in children: A systematic review. *Pediatric Dermatology*. 2013;30(3):294–302.
52. Thatai P, Sapra B. Transungual delivery: deliberations and creeds. *International Journal of Cosmetic Science*. 2014;36(5):398–411.
53. Kerai LV, Hilton S, Murdan S. UV-curable gel formulations: Potential drug carriers for the topical treatment of nail diseases. *International Journal of Pharmaceutics*. 2015 Aug; 492: 177-190
54. Van Duyn Graham L, Elewski BE. Recent updates in oral terbinafine: Its use in onychomycosis and tinea capitis in the US. *Mycoses*. 2011;54(6):679–85.
55. Schaller M, Borelli C, Berger U, Walker B, Schmidt S, Weindl G, et al. Susceptibility testing of amorolfine, bifonazole and ciclopiroxamine against *Trichophyton rubrum* in an in vitro model of dermatophyte nail infection. *Medical mycology*. 2009: 753–738.
56. Monti D, Herranz U, Dal Bo L, Subissi a. Nail penetration and predicted mycological efficacy of an innovative hydrosoluble ciclopirox nail lacquer vs. a standard amorolfine lacquer in healthy subjects. *Journal of the European Academy of Dermatology and Venereology: JEADV*. 2013:153–158.
57. Chouhan P, Saini TR. Hydroxypropyl-  $\beta$  -cyclodextrin: A Novel Transungual Permeation Enhancer for Development of Topical Drug Delivery System for Onychomycosis. *Journal Drug Delivery*. 2014 Jan:1-7.
58. Evans EG V. Drug synergies and the potential for combination therapy in onychomycosis. *British Journal of Dermatology*. 2003;149 :11–3.
59. Rosenson RS. The rationale for combination therapy. *American Journal of Cardiology*. 2002;90(10B):2K – 7K.
60. Malhotra GG, Zatz JL. Investigation of nail permeation enhancement by chemical modification using water as a probe. *Journal of Pharmaceutical Sciences*. 2002;91(2):312–23.
61. Mohorčič M, Torkar a., Friedrich J, Kristl J, Murdan S. An investigation into

- keratinolytic enzymes to enhance unguinal drug delivery. *International Journal Pharmaceutical*. 2007;332(1-2):196–201.
62. Khengar RH, Jones SA, Turner RB, Forbes B, Brown MB. Nail swelling as a pre-formulation screen for the selection and optimisation of unguinal penetration enhancers. *Pharmaceutical Research*. 2007 Dec;24(12):2207–12.
63. Shivakumar HN, Repka M a., Narasimha Murthy S. Transungual drug delivery: an update. *Journal of Drug Delivery Science and Technology*. 2014;24(3):301–10.
64. Gunt HB, Kasting GB. Effect of hydration on the permeation of ketoconazole through human nail plate in vitro. *European Journal Pharmaceutical Sciences*. 2007;32(4-5):254–60.
65. Stüttgen G, Bauer E. Bioavailability, skin- and nailpenetration of topically applied antimycotics. *Mykosen*. 1982;25(2):74–80.
66. Lahfa M, Bulai-Livideanu C, Baran R, Ortonne JP, Richert B, Tosti a., et al. Efficacy, safety and tolerability of an optimized avulsion technique with Onyster® (40% urea ointment with plastic dressing) ointment compared to bifonazole-urea ointment for removal of the clinically infected nail in toenail onychomycosis: A randomized e. *Dermatology*. 2013. 5–12.
67. Tietz HJ, Hay R, Querner S, Delcker A, Kurka P, Merk HF. Efficacy of 4weeks topical bifonazole treatment for onychomycosis after nail ablation with 40% urea: A double-blind, randomized, placebo-controlled multicenter study. *Mycoses*. 2013: 414–21.
68. Baran R, Coquard F. Combination of fluconazole and urea in a nail lacquer for treating onychomycosis. *Journal Dermatology Treatment*. 2005;16(1):52–5.
69. Hui X, Chan TCK, Barbadillo S, Lee C, Maibach HI, Wester RC. Enhanced econazole penetration into human nail by 2-n-nonyl-1,3-dioxolane. *Journal of Pharmaceutical Sciences*. 2003;92(1):142–8.
70. Vejnovic I, Huonder C, Betz G. Permeation studies of novel terbinafine formulations containing hydrophobins through human nails in vitro. *International Journal of Pharmaceutics*. 2010: 67–76.
71. Vejnovic I, Simmler L, Betz G. Investigation of different formulations for drug delivery through the nail plate. *International Journal Pharmaceutics*. 2010 Feb;386(1-2):185–94.
72. Pal P, Thakur RS, Ray S, Mazumder B. Design and development of a safer non-invasive transungual drug delivery system for topical treatment of onychomycosis. *Drug*

- Development and Industrial Pharmacy. 2014:1–5.
73. Repka M a., O’Haver J, See CH, Gutta K, Munjal M. Nail morphology studies as assessments for onychomycosis treatment modalities. *International Journal of Pharmaceutics*. 2002; 245:25–36.
74. Andrews JM. Determination of minimum inhibitory concentrations. *Journal of Antimicrobial Chemotherapy*. 2001;48 (1):5–16.
75. Fothergill AW. Interaction of yeasts, moulds and antifungal agents: How to detect resistance. Cap 2 Antifungal Susceptibility Testing: Clinical (CLSI) Methods. Hall G S (ed). XIV. 2012 :65–75.
76. Murdan S, Hinsu D, Guimier M. A few aspects of transonychia water loss (TOWL): Inter-individual, and intra-individual inter-finger, inter-hand and inter-day variabilities, and the influence of nail plate hydration, filing and varnish. *European Journal Pharmaceutics and Biopharmaceutics*. 2008;70(2):684–9.
77. Elewski BE, Tosti A. Tavaborole for the treatment of onychomycosis. *Expert Opinion*. 2014;15(10):1439–48.
78. Hui X, Baker SJ, Wester RC, Barbadillo S, Cashmore AK, Sanders V, et al. In Vitro penetration of a novel oxaborole antifungal (AN2690) into the human nail plate. *Journal of Pharmaceutical Science*. 2007 Oct;96(10):2622–31.
79. Tamura T, Asahara M, Yamamoto M, Yamaura M, Matsumura M, Goto K, et al. In vitro susceptibility of dermatomycoses agents to six antifungal drugs and evaluation by fractional inhibitory concentration index of combined effects of amorolfine and itraconazole in dermatophytes. *Microbiology and Immunology*. 2014: 1–8.
80. Jo Siu WJ, Tatsumi Y, Senda H, Pillai R, Nakamura T, Sone D, et al. Comparison of in vitro antifungal activities of efinaconazole and currently available antifungal agents against a variety of pathogenic fungi associated with onychomycosis. *Antimicrobial agents and chemotherapy*. 2013:1610–6.
81. Santos D a, Hamdan JS. In vitro antifungal oral drug and drug-combination activity against onychomycosis causative dermatophytes. *Medical mycology*. 2006: 357–62.
82. Carrillo-Muñoz A-J, Giusiano G, Cárdenes D, Hernández-Molina J-M, Eraso E, Quindós G, et al. Terbinafine susceptibility patterns for onychomycosis-causative dermatophytes and *Scopulariopsis brevicaulis*. *International Journal of Antimicrobial Agents*. 2008 Jun;31(6):540–543.

83. Ameen M, Lear JT, Madan V, Mohd Mustapa MF, Richardson M. British Association of Dermatologists' guidelines for the management of onychomycosis 2014. *British Journal of Dermatology*. 2014;1200–1214.
84. Flagothier C, Piérard-Franchimont C, Piérard GE. New insights into the effect of amorolfine nail lacquer. *Mycoses*. 2005;48(2):91–94.
85. Zaug M, Bergstraesser M. Amorolfine in the treatment of onychomycosis and dermatomycoses (an overview). *Clinical and Experimental Dermatology*. 1992;17 (1):61–70.
86. Crawford F, Hollis S. Topical treatments for fungal infections of the skin and nails of the foot. *Cochrane Database Syst Rev*. 2007;(3):2-90.
87. Gupta AK, Daigle D, Foley KA. Topical therapy for toenail onychomycosis: an evidence-based review. *American Journal of Clinical Dermatology*. 2014 Dec;15(6):489–502.
88. INFARMED. Governo Portugal. [11 July 2015]. <https://www.infarmed.pt/infomed/inicio.php>
89. FDA. FDA - U.S. Food and Drug Administration. USA. [12 September 2015] <http://www.fda.gov/Drugs/default.htm>
90. EMA - European Medicines Agency. European Union. European Union. [2 September 2015]. <http://www.ema.europa.eu/ema/index.j>.
91. Tabara K, Szewczyk AE, Bienias W, Wojciechowska A, Pastuszka M, Oszukowska M, et al. Amorolfine vs. ciclopirox - lacquers for the treatment of onychomycosis. *Postępy dermatologii i Alergol*. 2015;32(1):40–5.
92. Bohn M, Kraemer KT. Dermatopharmacology of ciclopirox nail lacquer topical solution 8% in the treatment of onychomycosis. *Journal of the American Academy of Dermatology*. 2000: 57–69.
93. Shemer A, Nathansohn N, Trau H, Amichai B, Grunwald MH. Ciclopirox nail lacquer for the treatment of onychomycosis: an open non-comparative study. *Journal of Dermatology*. 2010;37(2):137–139.
94. Gupta a K, Fleckman P, Baran R. Ciclopirox nail lacquer topical solution 8% in the treatment of toenail onychomycosis. *Journal of the American Academy Dermatology*. 2000;43(4):S70–80.
95. Elewski BE, Rich P, Pollak R, Pariser DM, Watanabe S, Senda H, et al. Efinaconazole 10% solution in the treatment of toenail onychomycosis: Two phase III multicenter,

- randomized, double-blind studies. *Journal of the American Academy of Dermatology*. 2013;600–8.
96. Del Rosso JQ, Plattner JJ. From the test tube to the treatment room: Fundamentals of boron-containing compounds and their relevance to dermatology. *Journal of Clinical and Aesthetic Dermatology*. 2014;13–21.
97. Elewski BE, Aly R, Baldwin SL, González Soto RF, Rich P, Weisfeld M, et al. Efficacy and safety of tavaborole topical solution, 5%, a novel boron-based antifungal agent, for the treatment of toenail onychomycosis: Results from 2 randomized phase-III studies. *Journal of the American Academy Dermatology*. 2015 Jul;73(1):62–9.
98. Hay RJ, Mackie RM, Clayton YM. Tioconazole nail solution--an open study of its efficacy in onychomycosis. *Clinical Experimental Dermatology*. 1985;10(2):111–5.
99. Commission BP. British Pharmacopoeia 2009. UK [4 July 2015]. <https://www.pharmacopoeia.com>
100. Chang R, Raw A, Lionberger R, Yu L. Generic Development of Topical Dermatologic Products: Formulation Development, Process Development, and Testing of Topical Dermatologic Products. *AAPS Journal*. 2013 Jan; 15(1): 41–52.
101. Gregorí BS. Estructura y actividad de los antifúngicos. *Revista Cubana Farmacia*. 2005;39(2):1-5
102. Bayer Portugal SA, Resumo das características do medicamento - Canespor. *Infarmed Portugal*. [4 July 2015]. <http://www.infarmed.pt/>
103. Santos DA, Hamdan JS. In vitro antifungal oral drug and drug-combination activity against onychomycosis causative dermatophytes. *Medical Mycology*. Oxford University Press. 2006 Jun ;44(4):357–62.
104. Lipner SR, Scher RK. Efinaconazole in the treatment of onychomycosis. *Journal of Infection and Drug Resistance*. 2015 Jan; 8:163–72.
105. Tamura T, Asahara M, Yamamoto M, Yamaura M, Matsumura M, Goto K, et al. In vitro susceptibility of dermatomycoses agents to six antifungal drugs and evaluation by fractional inhibitory concentration index of combined effects of amorolfine and itraconazole in dermatophytes. *Microbiol Immunol*. 2014;58(1):1–8.
106. Bhatt V, Pillai R. Efinaconazole Topical Solution, 10%: Formulation Development Program of a New Topical Treatment of Toenail Onychomycosis. *Journal of Pharmaceutical Sciences*. 2015;104(7):2177–2182.

107. Del Rosso JQ. The role of topical antifungal therapy for onychomycosis and the emergence of newer agents. *Journal of Clinical and Aesthetic Dermatology*. 2014;7(7):10–8.
108. Bahn C a. What is new in fungal pharmacotherapeutics? *Journal of Drug in Dermatology*. 2014;101(4):161–165.
109. Gupta AK, Simpson FC. Efinaconazole: A New Topical Treatment for Onychomycosis. *Skin Therapy Letter*. 2014; 19(1).
110. Laboratórios Pfizer. Resumo das Características do Medicamento Trosyd. [3 Janeiro 2015] <http://www.medicamentos.com.mx/DocHTML/22353.htm>.
111. Naumann S, Meyer JP, Kiesow A, Mrestani Y, Wohlrab J, Neubert RHH. Controlled nail delivery of a novel lipophilic antifungal agent using various modern drug carrier systems as well as in vitro and ex vivo model systems. *Journal of Controlled Release*. 2014: 60–70.
112. Pradhan M, Singh D, Singh MR. Novel colloidal carriers for psoriasis: Current issues, mechanistic insight and novel delivery approaches. *Journal of Controlled Release*. 2013:380–395.
113. Yang Y, Ou R, Guan S, Ye X, Hu B, Zhang Y, et al. A novel drug delivery gel of terbinafine hydrochloride with high penetration for external use. *Drug Delivery*. 2014; 7544:1–8.
114. Hamouda T, Flack M, Jr JRB, Mic C. Development of a novel antiviral drug (NB-001) for topical application in humans. *Journal American Academic Dermatology*. 2008;58(2):95-96.
115. Nogueiras-Nieto L, Begoña Delgado-Charro M, Otero-Espinar FJ. Thermogelling hydrogels of cyclodextrin/poloxamer polypseudorotaxanes as aqueous-based nail lacquers: Application to the delivery of triamcinolone acetonide and ciclopirox olamine. *European Journal of Pharmaceutics and Biopharmaceutics*. 2013: 370–7.
116. Vaghasiya H, Kumar A, Sawant K. Development of solid lipid nanoparticles based controlled release system for topical delivery of terbinafine hydrochloride. *European journal of pharmaceutical sciences: official journal of the European Federation for Pharmaceutical Sciences*. 2013:311–322.
117. Ghannoum M, Isham N, Herbert J, Henry W, Yurdakul S. Activity of TDT 067 (terbinafine in transfersome) against agents of onychomycosis, as determined by

- minimum inhibitory and fungicidal concentrations. *Journal of Clinical Microbiology*. 2011: 1716–20.
118. Dominicus R, Weidner C, Tate H, Kroon Ha. Open-label study of the efficacy and safety of topical treatment with TDT 067 (terbinafine in Transfersome®) in patients with onychomycosis. *British Journal of Dermatology*. 2012:1360–2.
119. Tanrıverdi ST, Özer Ö. Novel topical formulations of Terbinafine-HCl for treatment of onychomycosis. *European Journal Pharmaceutical Science*. 2013;48(4-5):628–36.
120. Barot BS, Parejiya PB, Patel HK, Gohel MC, Shelat PK. Microemulsion-Based Gel of Terbinafine for the Treatment of Onychomycosis: Optimization of Formulation Using D-Optimal Design. *AAPS PharmSciTech*. 2012: 184–92.
121. Barot BS, Parejiya PB, Patel HK, Mehta DM, Shelat PK. Microemulsion-based antifungal gel delivery to nail for the treatment of onychomycosis: Formulation, optimization, and efficacy studies. *Drug Delivery and Translation Research*. 2012;2(6):463–476.
122. Angamuthu M, Nanjappa SH, Raman V, Jo S, Cegu P, Murthy SN. Controlled-release injectable containing terbinafine/PLGA microspheres for onychomycosis treatment. *Journal Pharmaceutical Science*. 2014;103(4):1178–1183.
123. Kumar KJR, Muralidharan S, Dhanaraj SA. Antifungal activity of microemulsion based fluconazole gel for onychomycosis against *Aspergillus niger*. *International Journal of Pharmacy and Pharmaceutical Sciences* 2012;5(1):3–9.
124. Murdan S, Kerai L, Hossin B. To what extent do in vitro tests correctly predict the in vivo residence of nail lacquers on the nail plate? *Journal of Drug Delivery Science and Technology*. 2015: 23–8.
125. Joshi M, Sharma V, Pathak K. Matrix based system of isotretinoin as nail lacquer to enhance transungual delivery across human nail plate. *International Journal of Pharmaceutics*. 2014:268–77.
126. Monti D, Saccomani L, Chetoni P, Burgalassi S, Senesi S, Ghelardi E, et al. Hydrosoluble medicated nail lacquers: In vitro drug permeation and corresponding antimycotic activity. *British Journal of Dermatology*. 2010;162(2):311–7.
127. Monti D, Saccomani L, Chetoni P, Burgalassi S, Tampucci S, Mailland F. Validation of bovine hoof slices as a model for infected human toenails: In vitro ciclopirox transungual permeation. *British Journal of Dermatology*. 2011. p. 99–105.

128. Baraldi a., Jones S a., Guesné S, Traynor MJ, McAuley WJ, Brown MB, et al. Human Nail Plate Modifications Induced by Onychomycosis: Implications for Topical Therapy. *Pharaceutical Research*. 2014;1626–1633.
129. Sigurgeirsson B, Olafsson J, Steinsson J, Kerrouche N, Sidou F. Efficacy of amorolfine nail lacquer for the prophylaxis of onychomycosis over 3 years. *Journal of the European Academy of Dermatology and Venereology*. 2009;24(8):910–5.
130. Fiddaman PJ, Rossall S. The production of antifungal volatiles by *Bacillus subtilis*. *Journal Applied Bacteriology*. 1993 Feb;74(2):119-126.
131. Monti D, Saccomani L, Chetoni P, Buralassi S, Saettone MF, Mailland F. In Vitro Transungual Permeation of Ciclopirox from a Hydroxypropyl Chitosan-Based, Water-Soluble Nail Lacquer. *Drug Development and Industrial Pharmacy*. 2005: 11–7.
132. Shivakumar HN, Vaka SRK, Madhav NVS, Chandra H, Murthy SN. Bilayered nail lacquer of terbinafine hydrochloride for treatment of onychomycosis. *Journal Pharmaceutical Science*. 2010 Oct;99(10):4267–4276.
133. Kiran S, Shekar C. Ungual Drug Delivery System of Ketoconazole Nail Lacquer. In *Vitro*. *International Journal of Applied Pharmaceutics*. 2010;2(4):1–3.
134. Hafeez F, Hui X, Chiang A, Hornby S, Maibach H. Transungual delivery of ketoconazole using novel lacquer formulation. *International Journal Pharmaceutics*. 2013;456(2):357–361.
135. Vipin K V, Chandran SC, Augusthy AR, Premaletha K, Kuriakose MR. Formulation and Evaluation of an Antifungal Nail Lacquer for Onychomycosis. *British Biomedical Bulletin*. 2014; 1(2):242-248.
136. Baran R, Tosti a, Hartmane I, Altmeyer P, Hercogova J, Koudelkova V, et al. An innovative water-soluble biopolymer improves efficacy of ciclopirox nail lacquer in the management of onychomycosis. *Journal of the European Academy of Dermatology and Venereology: JEADV*. 2009: 773–81.
137. Szycher M. Szycher's Handbook of Polyurethanes, Second Edition [Internet]. Szycher's Handbook of Polyurethanes, Second Edition. 2013. 1112 p. Available from: [http://books.google.fr/books/about/Szycher\\_s\\_Handbook\\_of\\_Polyurethanes\\_Seco.html?id=e-ecDSA58rYC&redir\\_esc=y](http://books.google.fr/books/about/Szycher_s_Handbook_of_Polyurethanes_Seco.html?id=e-ecDSA58rYC&redir_esc=y)
138. Tramontano VJ, Thomas ME, Coughlin RD. Synthesis and coating properties of novel waterborne polyurethane dispersions. *Technol Waterborne Coatings* [Internet]. 1997;

- 663:164–82. Available from: <Go to ISI>://WOS: A1997BH71T00009
139. Howard GT. Biodegradation of polyurethane: A review. In: International Biodeterioration and Biodegradation. 2002. p. 245–52.
140. Kiran S, James NR, Jayakrishnan A, Joseph R. Polyurethane thermoplastic elastomers with inherent radiopacity for biomedical applications. *J Biomed Mater Res - Part A*. 2012;100 A (12):3472–9.
141. Kreye O, Mutlu H, Meier M a. R. Sustainable routes to polyurethane precursors. *Green Chem* [Internet]. 2013;15(6):1431–55. Available from: <http://xlink.rsc.org/?DOI=c3gc40440d>
142. Petrović ZS, Ferguson J. Polyurethane elastomers. *Progress in Polymer Science*. 1991. p. 695–836.
143. Bachmann F, Reimer J, Ruppenstein M, Thiem J. Synthesis of novel polyurethanes and polyureas by polyaddition reactions of dianhydrohexitol configured diisocyanates. *Macromol Chem Phys*. 2001;202(17):3410–9.
144. Król P. Synthesis methods, chemical structures and phase structures of linear polyurethanes. Properties and applications of linear polyurethanes in polyurethane elastomers, copolymers and ionomers. *Progress in Materials Science*. 2007. p. 915–1015.
145. Cardoso G, Claro Neto S, Vecchia F. Rigid foam polyurethane (PU) derived from castor oil (*Ricinus communis*) for thermal insulation in roof systems. *Front Archit Res*. 2012;1(4):348–56.
146. Stokes KB, Church TR. Ten-year experience with implanted polyurethane lead insulation. *Pacing Clin Electrophysiol*. 1986;9(6 Pt 2):1160–5.
147. Abdel Hakim AA, Nassar M, Emam A, Sultan M. Preparation and characterization of rigid polyurethane foam prepared from sugar-cane bagasse polyol. *Mater Chem Phys*. 2011;129(1-2):301–7.
148. Chen TK, Tien YI, Wei KH. Synthesis and characterization of novel segmented polyurethane clay nanocomposite via poly(epsilon-caprolactone)/clay. *J Polym Sci Part a-Polymer Chem* [Internet]. 1999;37(13):2225–33. Available from: <Go to ISI>://WOS:000080878600037\nhttp://onlinelibrary.wiley.com/store/10.1002/(SICI)1099-0518(19990701)37:13<2225:AID-POLA37>3.0.CO;2-Z/asset/37 ftp.pdf?v=1&t=hujm5kga&s=39343b071b38c1b6cfd341e670ca9879afc829bf
149. Li G, Li P, Qiu H, Li D, Su M, Xu K. Synthesis, characterizations and

- biocompatibility of alternating block polyurethanes based on P3/4HB and PPG-PEG-PPG. *J Biomed Mater Res Part A* [Internet]. 2011 Jul;98A(1):88–99. Available from: <http://doi.wiley.com/10.1002/jbm.a.33100>
150. Brown A, Gregori B, Garcia G, Alba L GC. Caracterización del poliuretano modificado con sacarosa (PSU). *ICIDCA Sobre los Deriv la caña azúcar* [Internet]. 2005;xxxix:3–7. Available from: Disponible en: <http://www.redalyc.org/articulo.oa?id=78430207>
151. Boyer A, Lingome CE, Condassamy O, Schappacher M, Moebs-Sanchez S, Queneau Y, et al. Glycolipids as a source of polyols for the design of original linear and cross-linked polyurethanes. *Polym Chem*. 2013;4(2):296–306.
152. Besse V, Auvergne R, Carlotti S, Boutevin G, Otazaghine B, Caillol S, et al. Synthesis of isosorbide based polyurethanes: An isocyanate free method. *React Funct Polym* [Internet]. 2013;73(3):588. Available from: <http://dx.doi.org/10.1016/j.reactfunctpolym.2013.01.002>
153. Kim H-J, Kang M-S, Knowles JC, Gong M-S. Synthesis of highly elastic biocompatible polyurethanes based on bio-based isosorbide and poly (tetramethylene glycol) and their properties. *J Biomater Appl* [Internet]. 2014;29(3):454–64. Available from: <http://www.pubmedcentral.nih.gov/articlerender.fcgi?artid=4230967&tool=pmcentrez&rendertype=abstract>
154. Shen Z, Lu D, Li Q, Zhang Z, Zhu Y. Synthesis and characterization of biodegradable polyurethane for hypopharyngeal tissue engineering. *Biomed Res Int*. 2015;2015.
155. Pangman WJ. United States Patent Office. 1958. p. 15–7.
156. Boretos JW, Pierson WS. Segmented Polyurethane: A New Elastomer for Biomedical Applications. *Science*. 1967; 158:1481–2.
157. Griesser HJ. Degradation of polyurethanes in biomedical applications-A review. *Polym Degrad Stab*. 1991;33(3):329–54.
158. Ghista DN, Reul H. Optimal prosthetic aortic leaflet valve: Design parametric and longevity analyses: Development of the avcothane-51 leaflet valve based on the optimum design analysis. *J Biomech*. 1977;10(5-6):313–24.
159. Li B, Yoshii T, Hafeman AE, Nyman JS, Wenke JC, Guelcher SA. The effects of rhBMP-2 released from biodegradable polyurethane/microsphere composite scaffolds on

- new bone formation in rat femora. *Biomaterials*. 2009;30(35):6768–79.
160. Mandru M, Ciobanu C, Ignat ME, Popa M, Verestiuc L, Vlad S. Sustained release of nystatin from polyurethane membranes for biomedical applications. *Dig J Nanomater Biostructures*. 2011;6(3):1227–38.
161. Zhou L, Yu L, Ding M, Li J, Tan H, Wang Z, et al. Synthesis and characterization of pH-sensitive biodegradable polyurethane for potential drug delivery applications. *Macromolecules*. 2011;44(4):857–64.
162. Martinelli A, D’Ilario L, Francolini I, Piozzi A. Water state effect on drug release from an antibiotic loaded polyurethane matrix containing albumin nanoparticles. *Int J Pharm*. 2011;407(1-2):197–206.
163. Ready TT, Hadano M, Takahara A. Controlled release of model drug from biodegradable segmented polyurethane ureas: Morphological and structural features. *Macromol Symp*. 2006; 242:241–9.
164. Huynh TTN, Padois K, Sonvico F, Rossi A, Zani F, Pirot F, et al. Characterization of a polyurethane-based controlled release system for local delivery of chlorhexidine diacetate. *Eur J Pharm Biopharm*. 2010;74(2):255–64.
165. Sullad AG, Manjeshwar LS, Aminabhavi TM. Blend microspheres of chitosan and polyurethane for controlled release of water-soluble antihypertensive drugs. *Polym Bull*. 2014;72(2):265–80.
166. Mândru M, Ciobanu C, Vlad S, Butnaru M, Lebrun L, Popa M. Characteristics of polyurethane-based sustained release membranes for drug delivery. *Cent Eur J Chem [Internet]*. 2013;11(4):542. Available from: <http://www.springerlink.com/index/10.2478/s11532-012-0187-y>
167. Liu X-Y, Zhang C-C, Xu W-L, Ouyang C. Controlled release of heparin from blended polyurethane and silk fibroin film. *Mater Lett [Internet]*. 2009 Jan;63(2):263–5. Available from: <http://linkinghub.elsevier.com/retrieve/pii/S0167577X08008501>.
168. Li B, Brown K V., Wenke JC, Guelcher SA. Sustained release of vancomycin from polyurethane scaffolds inhibits infection of bone wounds in a rat femoral segmental defect model. *J Control Release*. 2010;145(3):221–30.
169. Sivak WN, Pollack IF, Petoud S, Zamboni WC, Zhang J, Beckman EJ. LDI-glycerol polyurethane implants exhibit controlled release of DB-67 and anti-tumor activity in vitro against malignant gliomas. *Acta Biomater*. 2008;4(4):852–62.



**Chapter 2: Synthesis and Characterization of Polyurethanes  
employing Carbohydrates**



## 1. Introduction

The covering of drugs with biodegradable polymers is one of the processes for producing sustained and controllable drug release systems, also preventing the degradation of the drugs (1). Film coating has been successfully utilized to control the release of active ingredients, prevent interaction between ingredients and external medium and increase the strength of the dosage form by maintaining the product integrity during storage (2).

Biomaterials in drug delivery systems have an enormous impact on human health care (3). During the last years, the synthesis of new polymers for this application has increased markedly (4). One of the polymers that have recognized application for coatings in the pharmaceutical industry is the polyurethane (1). Polyurethanes have generated large interest among the research community because they offer the greatest versatility in compositions and properties of any other family of polymers. The use of elastomeric polyurethanes as implantable medical devices have demonstrated a combination of toughness, durability, biocompatibility and biostability not achieved by any other available material (3).

The PUs are composed of repeating units of monomers bonded by the urethane group (4,5). Their versatility arises from the possibility of producing tailored PU and PUU. These materials are obtained by the addition of different chain extenders or by varying the pre-polymers' composition using different polyol structure and functionality, and also changing the NCO content (6). The polyurethane has been applied in the medical and pharmaceutical industries since 1970 as a biomaterial in a variety of situations, e.g. prosthesis (7,8), microspheres (9), apposite (10,11), patches (12) and others (13–15). The PUs are conventionally prepared by a so-called one-shot process (16,17) or by a prepolymer mixing process (18–23). In these processes, the ionic centers are incorporated as chain extenders and located among the hard segments. Consequently, the mobility of the ionic segments is very much limited by the rigidity of the hard segments, and the ionic groups are not well exposed to the particle surfaces, requiring more ionic groups to produce a stable dispersion (15,24).

The biocompatibility of the polyurethanes becomes an attractive alternative for application in the pharmaceutical industry in therapeutic nail lacquer formulation (25).

In this study, we synthesized, five different quasi-prepolymer polyurethanes using PEG (Mw1500) and pMDI. The quasi prepolymers were characterized by viscosity test, the content of NCO and FTIR. Later was select one quasi pre-polymer to synthesize different

polyurethanes employing carbohydrates as extensor monomers. Finally, the polyurethanes were characterized by FTIR, ( $^1\text{H}$  and  $^{13}\text{C}$ ) NMR spectroscopy, DSC and cytotoxicity test.

## 2. Materials and methods

### 2.1 Materials

Polyethylene glycol (PEG) 1500, were purchased from Basf (Germany), sucrose, glucose, fructose, isopropyl myristate, 2-methyl-2,4-pentanediol, triethanolamine were obtained from Merck (Germany), DMSO, THF, polyethylene glycol 300, glycerin was obtained from Sigma-Aldrich (Germany), ethanol was purchased from Across (France), Transcutol<sup>®</sup>GC and Labrasol<sup>®</sup> were obtained from Gattefossé (France). The acetone was acquired from Panreac (Spain). Polymeric 4,4-methylene diphenyl diisocyanate (pMDI) (Desmodur<sup>®</sup> 44V20L) was supplied by Bayer Material Science. The molecular sieves 4 Å was acquired from Merck (Germany).

### 2.2 Methods

#### 2.2.1 Synthesis of the polyurethane quasi-prepolymers

The synthesis of quasi-prepolymers was carried out using the quasi-prepolymer method. The quasi-prepolymers were prepared by reacting pMDI and PEG 1500 (purchased from Basf, Germany) in a 50% w/v solution with DMSO and dried over molecular sieves 4 Å) in a glass flask of 500 mL, under a dry nitrogen atmosphere. An inert atmosphere was used to avoid the ingress of moisture and the consequent formation of urea linkages during synthesis. The reaction was developed with mechanical stirring (400 rpm) at 40°C and with drop-by-drop addition of polyol for 8h. The syntheses of polyurethane quasi-prepolymers were done in triplicate. Further syntheses were carried out under identical conditions in the presence of 0.5 mL of the catalyst triethanolamine, which was added to each polyol solution that later reacted with the isocyanate (8,23). The ratios of monomers employing for obtained the quasi-prepolymer polyurethanes were presented in Table 2.1.

Table 2. 1. Relation of monomers for synthesis of quasi-prepolymers.

	<b>Pre-6</b>	<b>Pre -8</b>	<b>Pre-10</b>	<b>Pre-12</b>	<b>Pre-14</b>
m (pMDI) (g)	100	100	100	100	100
m(PEG 1500)(g)	96	69	55	46	39
NCO/OH	1.1	1.4	1.8	2.2	2.6

### 2.2.2 Synthesis of polyurethanes

The synthesis of polyurethane was carried out in a reactor of 250 mL with a quasi-prepolymer polyurethane selected. Later amount of carbohydrate (glucose, fructose or sucrose) dissolved in 10 mL of DMSO was added by dropping according to the relation presented in Table 2.2. The mixture was maintained under 400 rpm agitation for 1 hour, with a nitrogen stream. PUS was the polyurethane obtained employing sucrose as extender, PUF was the polyurethane obtained employing fructose as extender and PUG was the polyurethane obtained employing glucose as extender.

Table 2. 2. Relation of monomers for synthesis of polyurethane.

<b>PU</b>	<b>NCO/OH</b>	<b>Carbohydrate</b>
PUS 14/4	1	Sucrose
PUS 14/6	0.75	Sucrose
PUS 14/8	0.5	Sucrose
PUF 14/4	1	Fructose
PUF 14/6	0.75	Fructose
PUF 14/8	0.5	Fructose
PUG 14/4	1	Glucose
PUG 14/6	0.75	Glucose
PUG 14/8	0.5	Glucose

## 2.3 Characterization of polyurethane quasi-prepolymers

### 2.3.1 Determination of viscosity

The viscosity of the quasi-prepolymer polyurethanes was determined by parallel plate rheometer in a shear stress-controlled ICI, London, LTD rheometer, using parallel plates (upper plate diameter  $\frac{1}{4}$  20 mm); the gap selected was 0.4 mm. The viscosity was measured at 25 °C and a frequency of 20 Hz.

### 2.3.2 Free isocyanate content

The NCO content in the quasi-prepolymer polyurethanes was determined by back titration of excess N,N-dibutylamine with standard HCl, described in research of Daniela da Silva *et al* 2008 (12).

### 2.3.3 FTIR

The FTIR spectra were obtained with a Nexus Thermo Nicolet spectrometer equipped with attenuated total reflectance (ATR) device. 128 scans with a spectral resolution of 4 cm<sup>-1</sup> were averaged to give the specimen spectrum from 4000 cm<sup>-1</sup> to 600 cm<sup>-1</sup>. All FTIR spectra were recorded at room temperature.

## 2.4 Polyurethane characterization

### 2.4.1 Solubility studies for polyurethanes

Polyurethane was added to different vehicles such as water, water-ethanol (1:1), ethanol, Transcutol®GC, isopropyl myristate, 2-methyl-2,4-pentanediol, glycerin, PEG 300, acetone, Labrasol® and DMSO.

### 2.4.2 FTIR

The FTIR spectra were obtained according description in section 2.3.3 in the present chapter.

### 2.4.3 NMR

<sup>1</sup>H NMR and <sup>13</sup>C NMR spectra in the liquid state were obtained using a BRUKER 300 MHz spectrometer. Samples were dissolved in CDCl<sub>3</sub>, at room temperature (the spectra were

referred internally using HDMSO,  $\delta_H$  0.058 and  $\delta_C$  1.9 relative to TMS. The measurement was done using  $\approx 10$  mg samples of samples.

#### 2.4.4 Thermoanalytical measurements

Thermoanalytical measurements were performed with a Mettler DSC system (Mettler, Switzerland) with a sample robot TS0801RO (Mettler, Switzerland). The sample and the reference (air) were placed in hermetically sealed pans. A scan speed of 10 °C/ min was used, from -100°C to 250°C. The weight of each sample were 5-6 mg. These values gave the best compromise between resolution, temperature accuracy and attenuation.

#### 2.4.5 Cytotoxicity assay

##### 2.4.5.1 Preparation of sample

For this study, 350 mg of polyurethane in solid stated with a dimension of 0.5x 0.5cm was tested.

##### 2.4.5.2 Direct contact assay

The biocompatibility of the polymer was evaluated *in vitro* by direct contact with cells, following the ISO 10993-5:2009 recommendation guidelines(26). Each material was added to a 0.5 mL of HaCaT cell suspension [a spontaneously immortalized human keratinocyte cell line (CLS, Germany)], in fresh culture medium [RPMI-1640<sup>®</sup> (Gibco, UK) medium supplemented with 10% fetal bovine serum (FCS, Life Technologies, Inc., UK), penicillin (100 IU/mL), and streptomycin (100  $\mu$ g/mL)] ( $2.5 \times 10^4$  cells/mL), in sterile 24-well plates. Glass slides without any formulation were used as control. The plates were incubated for 72 h in a humidified atmosphere of 5% CO<sub>2</sub> at 37 °C, without refreshing the culture medium. For cell proliferation quantification, the general cell viability endpoint MTT reduction (3-(4,5-dimethyl-2-thiazolyl)-2,5-diphenyl-2H-tetrazolium bromide) was used (27,28). Accordingly, the previous culture medium was removed and replaced with a fresh medium containing 0.5 mg/mL of MTT. The cells were further incubated for 3 h. In the plates containing the reduced MTT, the medium was removed and the intracellular formazan crystals were solubilized and extracted with dimethylsulfoxide. After 15 min, at room temperature, the absorbance was

measured at 570 nm in a Microplate Reader (FLUOstar Omega, BMGLabtech, Germany). The relative cell viability (%) compared to control cells was calculated using Equation 1:

$$\% \text{ Cell viability} = 100 \times \left( \frac{OD_{\text{samples}}}{OD_{\text{Control}}} \right) \quad (1)$$

The OD, is the optical density measurement. The data are expressed as the mean and the respective standard deviation (mean  $\pm$  SD) of 6 experiments. The statistical evaluation of data was performed using one-way analysis of variance (ANOVA). The Tukey–Kramer multiple comparison tests (GraphPad PRISM 5 software, USA), were used to compare the significance of the difference between the groups; a  $p < 0.05$  was accepted as statistically significant.

### 3. Results and discussion

#### 3.1 Syntheses of polyurethane quasi-prepolymers

The chemical structures proposed for the polyurethane quasi-prepolymers are given in Figure 2.1. All the quasi-prepolymers were obtained in the liquid phase and presented an amber color.

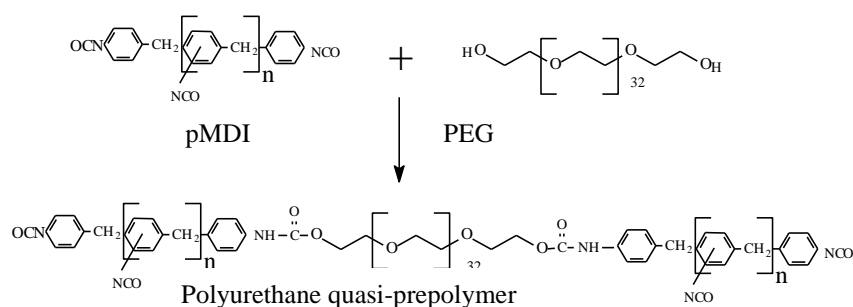


Figure 2. 1. Scheme of the quasi-prepolymer reaction.

#### 3.2 Viscosity and NCO content of polyurethane quasi-prepolymers

The NCO content and viscosity of all polyurethane quasi-prepolymers synthesized are presented in Table 2.3. The viscosity values of the samples decreased when the NCO content increased. These results are in good agreement with the results of other authors. A.L. Daniel

*et al.* 2007 (10), who comment that the decreasing of the NCO/OH molar ratio produced an increase in the average molecular weight and viscosity of the quasi-prepolymers. Almost all the quasi-prepolymers remained liquids for five months after the synthesis, maintaining constant viscosity values. Hardening was only observed for the Pre-6 sample on the seventh day after the synthesis. Table 2.3 shows a viscosity of 24 Pa.s for this quasi pre-polymer, which might indicate that it possesses the highest molecular weight and the highest degree of crosslinking than the rest of the quasi-prepolymers. The quasi-prepolymer 14 was the polymers with the highest percent of isocyanate free.

Table 2. 3. Formulation, isocyanate content and viscosity of the polyurethane quasi pre-polymers. (mean $\pm$ SD, n=3).

Polyurethane quasi-prepolymer	m(pMDI) g	m(PEG) g	NCO/OH m/m	% NCO free	Viscosity (Pa.s)
Pre – 6	100	92	1.1	9 $\pm$ 0.3	24 $\pm$ 0.1
Pre – 8	100	69	1.4	10 $\pm$ 0.3	11 $\pm$ 0.1
Pre – 10	100	55	1.8	13 $\pm$ 0.6	10 $\pm$ 0.1
Pre – 12	100	46	2.2	14 $\pm$ 0.2	8 $\pm$ 0.2
Pre – 14	100	39	2.6	15 $\pm$ 0.4	5 $\pm$ 0.1

### 3.3 FTIR analysis of polyurethane quasi pre-polymers

All quasi polyurethane pre-polymers show a similar FTIR spectrum. In Figure 2.2 and Figure 2.3 were presented the spectrum of quasi pre-polymers and the monomers employing in the syntheses. The weak band to NH around 3000  $\text{cm}^{-1}$  was not observed. The bands between 2980-2976  $\text{cm}^{-1}$  corresponding to  $\text{CH}_2$  groups of PEG were observed. The strong band at 2265–2260  $\text{cm}^{-1}$  confirms the existence of free NCO groups in the quasi-prepolymer polyurethane (10,15). The band from 1716 to 1712  $\text{cm}^{-1}$  was attributed to the stretching vibration of C=O bond (13,15) characteristic of urethane group, due to the deformation of the NH bond and C–N stretching vibration. The peak about 1600-1595  $\text{cm}^{-1}$  corresponds to C=C

stretching in the aromatic ring (6,8). Two peaks at 1012 and 1510  $\text{cm}^{-1}$  arise from symmetric and asymmetric stretching vibrations of N–C–N, respectively, corresponding to the reactions of the NCO groups with the OH groups (22). This behavior has been reported previously for polyurethane (10). The DMSO did not influence in the synthesis process of the quasi-prepolymers.

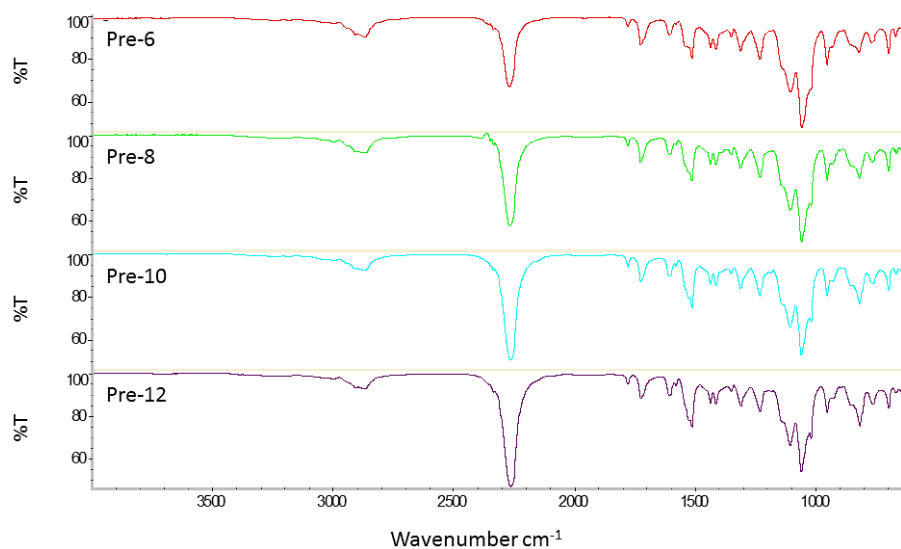


Figure 2. 2. FTIR in ATR mode spectra of the Pre-6, Pre-8, Pre10 and Pre-12.

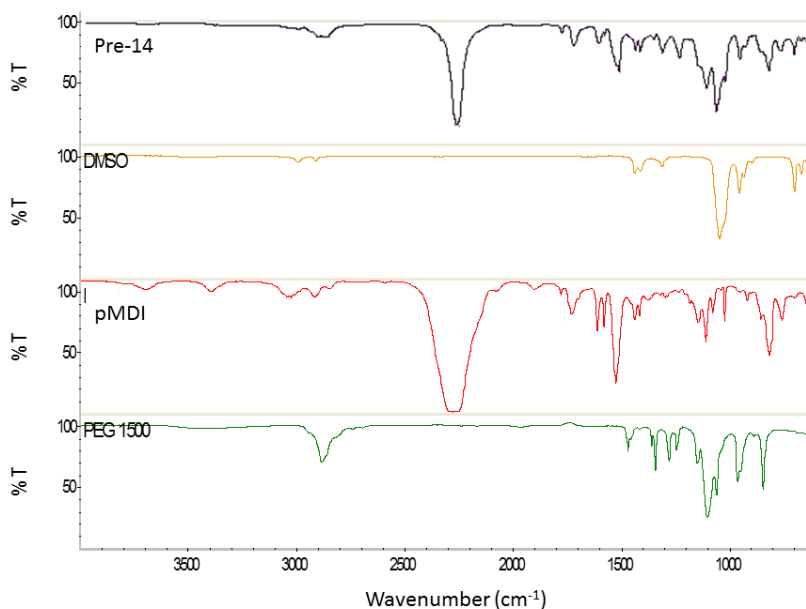


Figure 2. 3. FTIR in ATR mode spectra of the Pre-14, PEG 1500, DMSO and pMDI.

### 3.4 Synthesis and characterization of polyurethanes

The polyurethane quasi-prepolymers hardening in contact with the chain extender in the few minutes of the beginning of the syntheses, except in the synthesis were Pre-14 was employed. These results were due to the high viscosity of the quasi-prepolymers and a low content of free NCO, which causes immediate crosslinking.

The quasi-prepolymer 14 presents the highest content of isocyanate free (see Table 2.3), it was selected for the syntheses of polyurethanes. Different content of sucrose, fructose or glucose were incorporated, leading to ratios NCO/OH 1, 0.75 and 0.50.

#### 3.4.1 Solubility of PU

The solubility of PUs was studied in different solvents. Only the PUS 14/4 present solubility in DMSO, in the rest of solvent, the polymers not present solubility. The polymers: PUS 14/6, PUS 14/8, PUG 14/4, PUG 14/6, PUG 14/8, PUF 14/4, PUF 14/6 and PUF 14/8, not present solubility in the solvent study. In the literature is mentioned that the amount of primary alcohol reacts first that the second alcohol in the same molecular (29). According this, one hypothetical and ideal structured for these polyurethanes are presented in Figure 2.4.

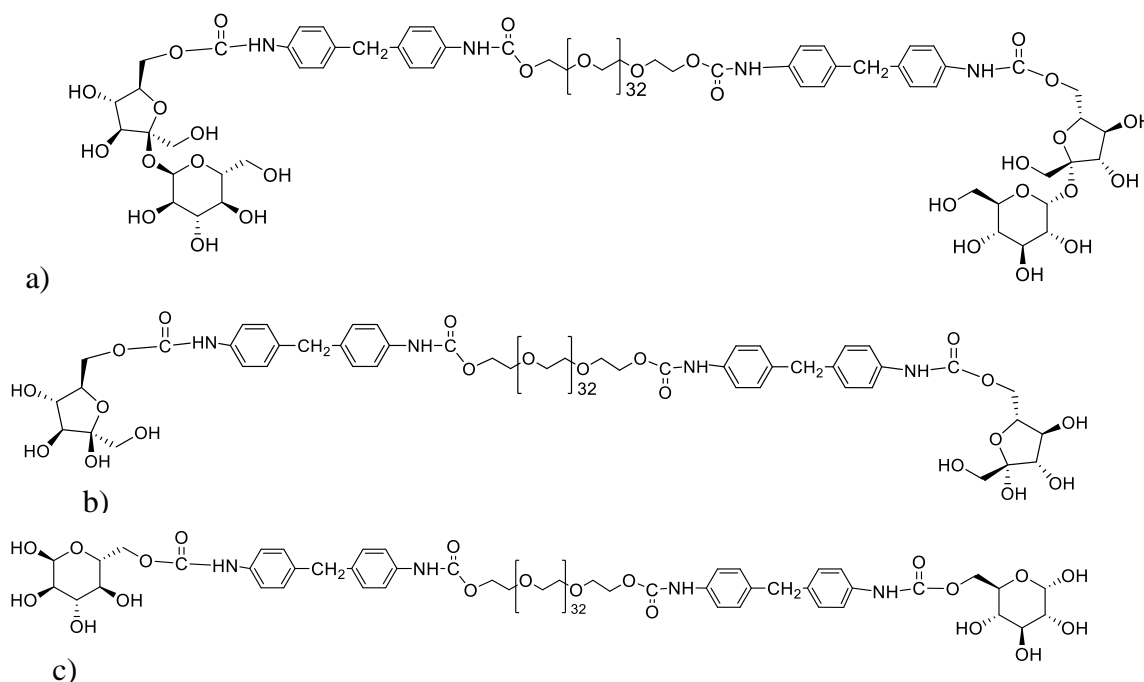
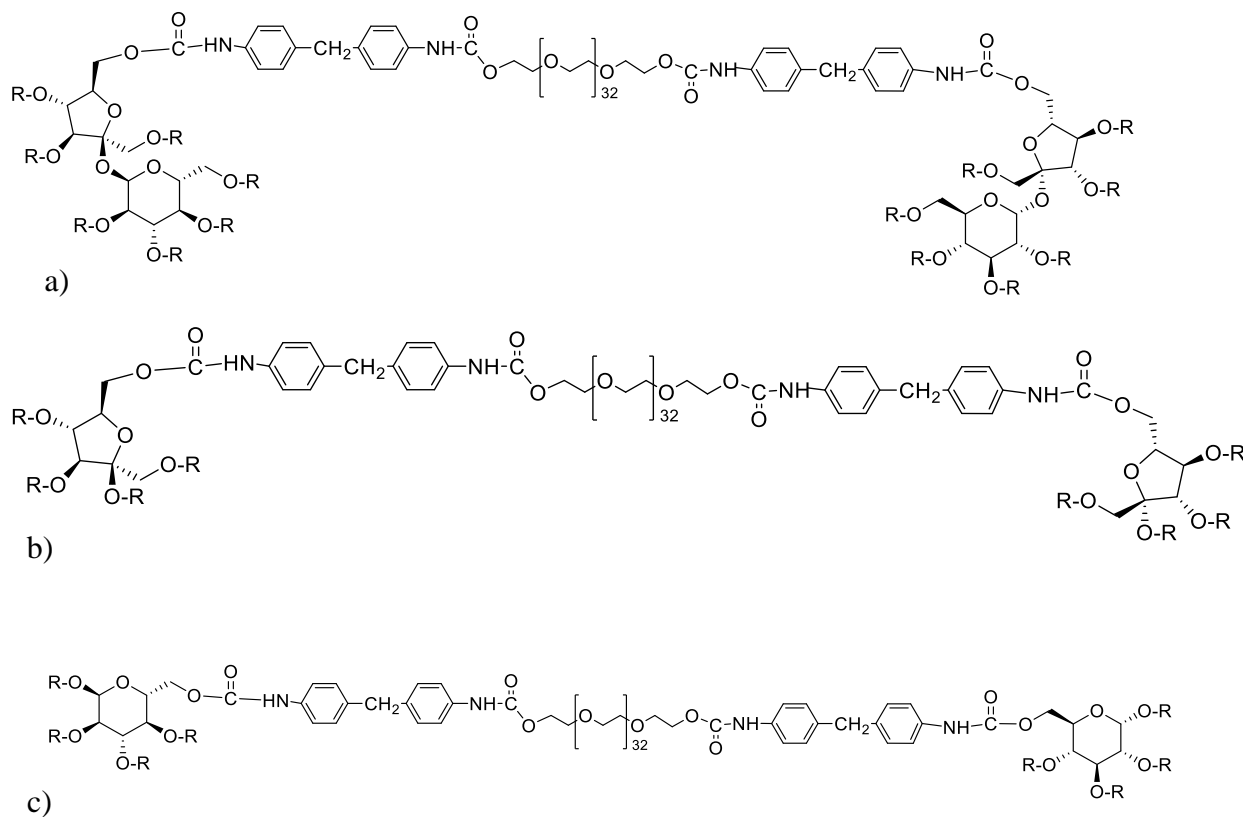


Figure 2. 4. Ideal structure for polyurethanes: a) PUS, b) PUF, c) PUG.

However, the results obtained indicated that not only one hydroxyl group reacted with the quasi-prepolymer polyurethane. In the real structure of polyurethane, all the hydroxyl groups from sucrose, fructose and glucose reacted with the quasi-prepolymer and formed a hydrophobic, non-linear polyurethane, as presented in Figure 2.5. These types of polymers do not present the usual solubility properties in the solvents employed in the pharmaceutical industry, such as ethanol (30).



R: quasi- prepolymer polyurethane

Figure 2. 5. Structure of polyurethanes obtained, a) PUS, b) PUF, c) PUG.

### 3.4.2 FTIR analysis of polyurethanes

The characterization by FTIR was performed only for the PU obtained from sucrose. Comparative analysis of the full spectra (Figure 2.6) shows a similarity between the polyurethanes obtained. This evidence indicates that it is possible to achieve the polyurethane in all cases.

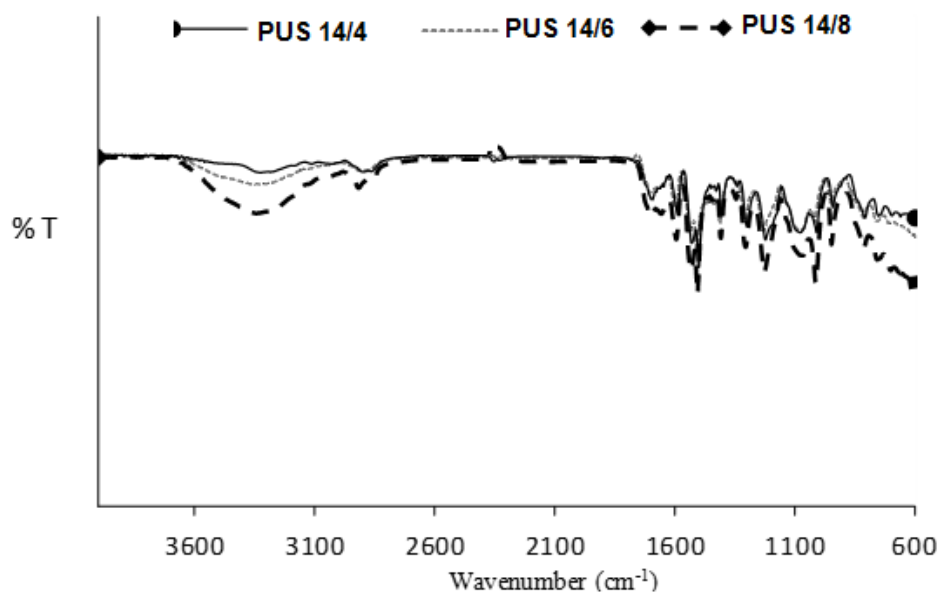


Figure 2. 6. FTIR in ATR mode spectra of polyurethanes prepared with Pre-14.

The presence of a weak band to  $3326\text{ cm}^{-1}$ , corresponding to the stretching vibrations of NH groups is observed in all the polyurethanes synthesized. The confirmation of the complete polymerization and formation of all urethane groups is obtained by the disappearance of the band to  $2265 - 2260\text{ cm}^{-1}$  in the spectrum and the formation the band from  $1716$  to  $1712\text{ cm}^{-1}$  attributed to the stretching vibration of C=O bond (24,31,32) characteristic of urethane group.

### 3.4.3 NMR analysis of polyurethane

#### 3.4.3.1 $^1\text{H-NMR}$ of polyurethane

The analysis by NMR only will be obtained for PU14/4 because the rest of polyurethanes don't present solubility in the deuterated solvents used.

For the interpretation of polyurethanes spectra, the signal corresponding to PEG 1500, pMDI and sucrose were studied

The structure of PEG 1500 presented in Figure 2.7, shows four chemically different protons, its  $^1\text{H-NMR}$  spectrum is presented in Annex 1. In the Table 2.4 are observed the chemical shifts obtained for PEG 1500, as well as those found in the literature. However, in the presented spectra due to the chemical environmental those chemical shifts which should

present distinguished peaks appeared very closed to each other, this effect was corroborated by some studies found in literature.

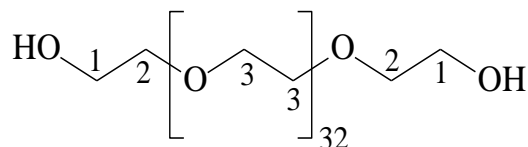


Figure 2. 7. Structure of PEG.

Table 2. 4. Chemical shifts of PEG 1500.

Type of H	Experimental chemical shifts CDCl <sub>3</sub> (ppm)	Chemical shifts of reference* CDCl <sub>3</sub> (ppm)
1	3.38	3.4
2	3.83	3.6
3	3.62	3.6
* (33)		

Furthermore, (see Annex 1) were observed the sign of hydrogen corresponding to hydrophilic group. These results are similar to report for PEG in the literature (34).

Similarly, to previous compound, the structure of pMDI (see Figure 2.8) presented three types of chemically different protons, observed in Table 2.5. The <sup>1</sup>H-NMR spectrum of pMDI was presented in Annex 2.

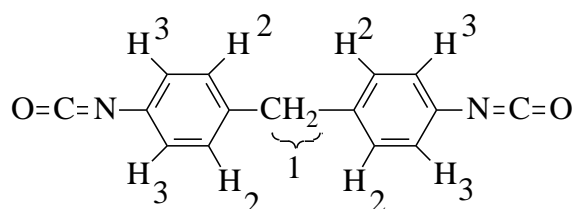


Figure 2. 8. Structure of pMDI.

The detected signals are summarized in Table 2.5. There is complete correspondence with shifts reported in the scientific literature consulted.

Table 2. 5. Chemical shifts of pMDI.

Type of H	Chemical shifts CDCL <sub>3</sub> (ppm)	Chemical shifts reference* CDCL <sub>3</sub> (ppm)
1	3.87	3.9
2	7.08	7.1
3	6.87	7.0
* (10)		

The sucrose was another monomer for analyses, the <sup>1</sup>H NMR spectrum of sucrose was presented in Annex 2. The structure of disaccharide was presented in Figure 2.9 and in the Table 2.6 are showed the chemical shifts.

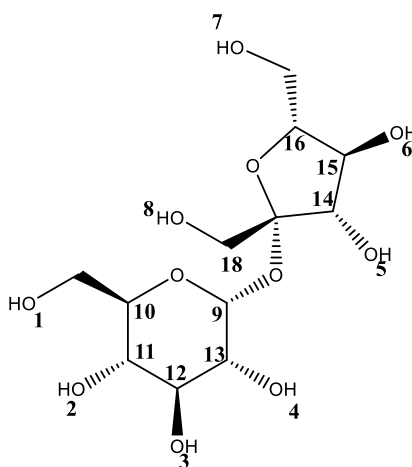


Figure 2. 9. Structure of Sucrose.

Table 2. 6. Chemical shifts of Sucrose.

Type of H	Chemical shifts CDCL <sub>3</sub> (ppm)	Chemical shifts reference* CDCL <sub>3</sub> (ppm)
1,7,8	3.94	3.8-3.9
2,3,4,5,6	4.37-4.88	4.37-4.9
9	5.40	5.3
10,11,12,13	3.6-3.9	2.4-4
14,15,16	4.05-4.51	4.1-4.5
17,18,19	3.57-3.90	3.5-3-85
*(32,35)		

All the spectroscopy information obtained from the monomers employ in the synthesis of polyurethane, permitted confirm the structure of the final polymer. The <sup>1</sup>H-NMR spectrum of PUS 14/4 is presented in Figure 2.10.

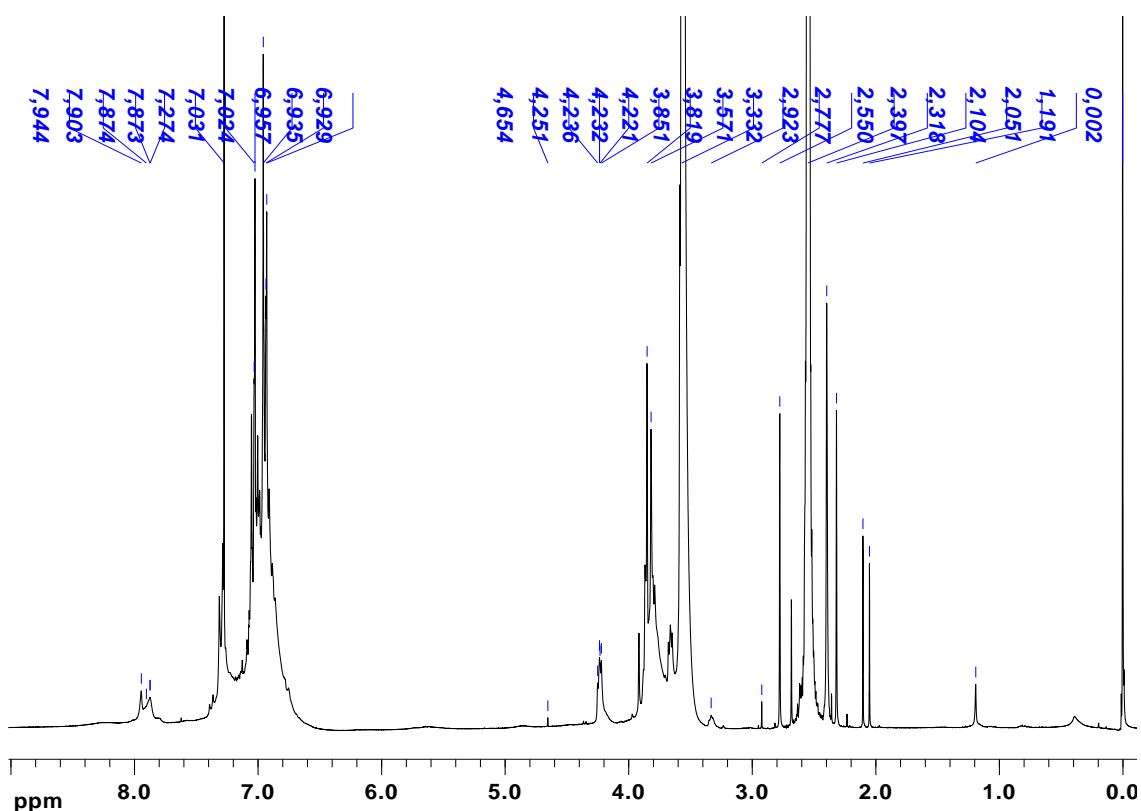


Figure 2. 10. Spectrum <sup>1</sup>H-NMR of PUS 14/4.

The signals presented in the spectrum corroborated the structure of polyurethane. Considering the small amounts of sucrose employed for the synthesis of the macromolecule, most signals of sugar are lost in the spectrum. However, in the spectrum appear signs between 2-4 ppm that indicated the presence of sucrose in the polyurethane.

In the aromatic polyurethane section (6.9-7.3 ppm) observed increased complexity due to the loss of symmetry of the aromatic protons compared with pMDI. In this case, it was not possible to assign the signals of each one of the hydrogens. The sign corresponded CH<sub>2</sub> to aromatic isocyanate, was identified at 3.85 ppm, agree with the identified in other research (10). On the other hand, signals between 3.3 to 3.5 ppm helped to identify the presence of PEG 1500 in the structure of the polyurethane.

The characteristic signals of the protons bonded to heteroatoms, between 7.9 – 8.0 ppm correspond to the amine groups present in the compound (10,32). These signals are imperative because it confirms the proposed reaction between hydroxyl groups (PEG 1500) and isocyanate groups (pMDI) (Figure 2.10).

### 3.4.3.2 $^{13}\text{C}$ NMR of polyurethanes

To support the above results, another experiment was done,  $^{13}\text{C}$ -NMR. The  $^{13}\text{C}$ -NMR spectrum is presented in Figure 2.11, the signals which are in line with the proposed structure of the polyurethane.

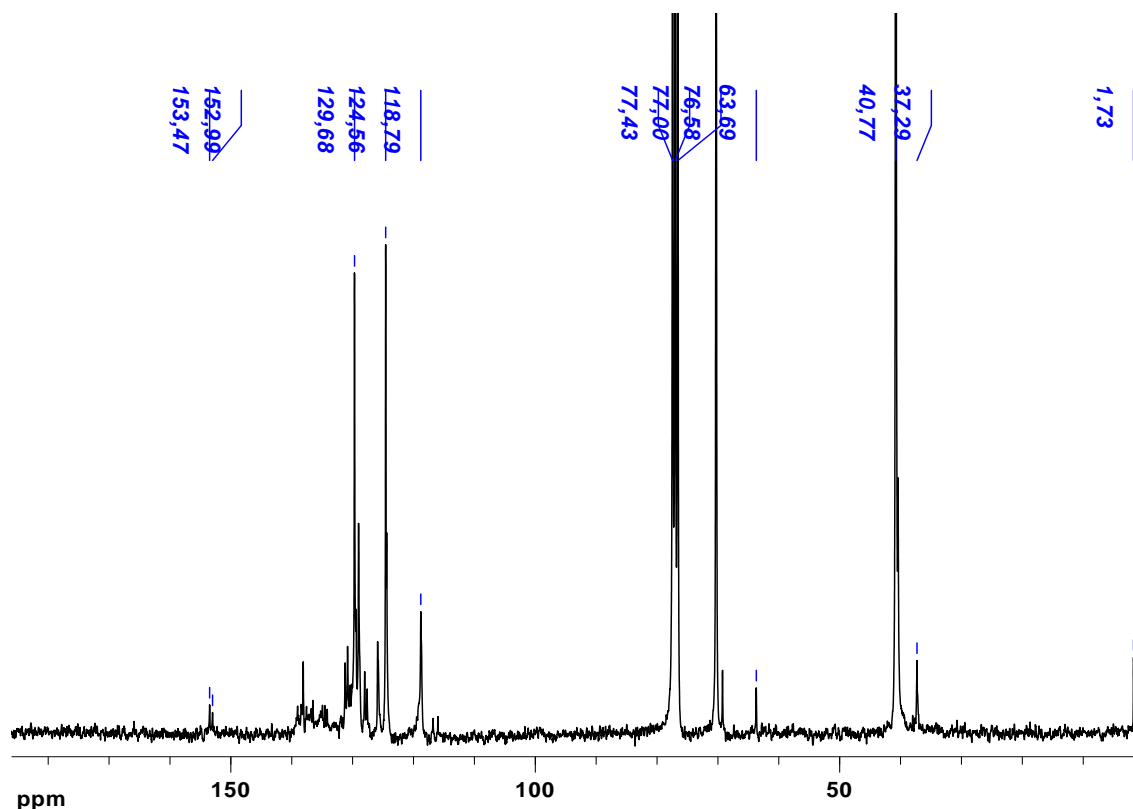


Figure 2. 11. Spectrum  $^{13}\text{C}$ -NMR of PUS 14/4

The signals corresponding to sucrose lost in the  $^{13}\text{C}$ -NMR spectrum of polyurethane situation previously detected in the assay of  $^1\text{H}$ -NMR. The sign of 40.6–41.6 ppm corresponded to  $\text{CH}_2$  of pMDI (32). The signs of carbons corresponding to PEG were found in 65 ppm. The aromatic area of pMDI were observed at 70.4 ppm and 80 ppm. The signs detected between 118-154 ppm corresponding to carbonyl of polyurethane (36).

### 3.5 DSC analysis of polyurethanes

The study by DSC of polyurethanes synthesized employing sucrose showed different values of  $T_g$ . This behavior is entirely logical considering that small variations in the formulation of a polymer can lead to substantial changes in its structure(37).

As a result of the analysis of polyurethanes PUS 14/4, PUS14/6 and PUS14/8, the values of the respective  $T_g$  are shown in Figure 2.12. It was found temperatures in the range between 24.00 to 34.49 °C for the three studied cases, that correspond with  $T_g$ .

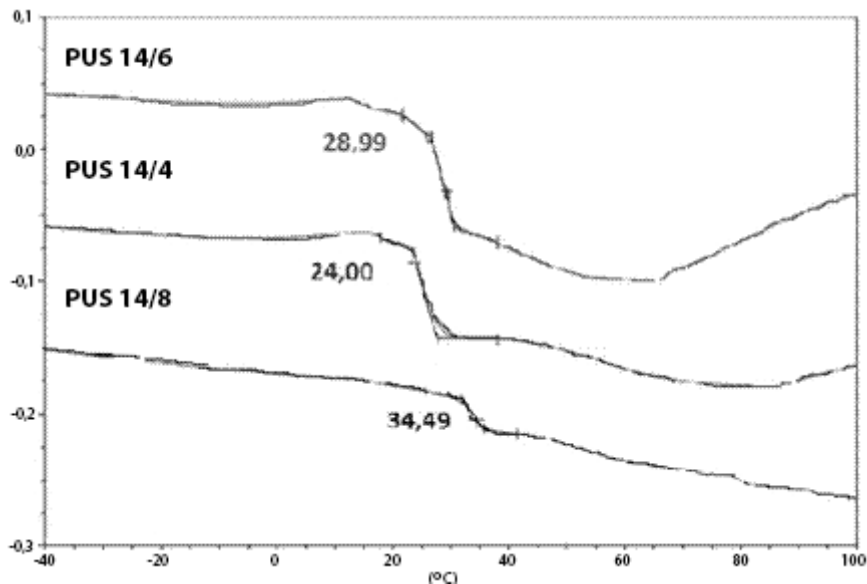


Figure 2. 12. DSC thermograms of polyurethane PUS 14/4, PUS 14/6, PUS 14/8.

$T_g$  values in this study are less than those reported by Ganta (38), which means that the structure of the polyurethane contains predominant soft segments conferring flexibility to the polymer, explaining thus why the developed materials have the characteristics of elastomers.

### 3.6 Results of cytotoxicity assay

This test was carried out for PUS14/4 and control slide glass (Figure. 2.13). Significant morphologic change was observed in the cells in contact with the polyurethane, in the studied time periods, the cells studied present different appearance compared with the structure of HaCaT.

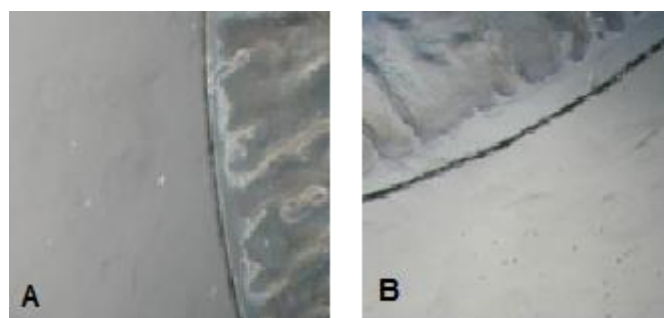


Figure 2. 13. HaCaT cells after 72h of proliferation under contact with polyurethane. A glass slide (control), B PUS 14/4.

The cell viability of PUS 14/4 was  $21 \pm 2\%$  ( $p < 0.001$ ) thus this polymer is not biocompatible and thus not allow cell growth.

The incompatibility of the polyurethane probably present relation to the concentration of DMSO residual.(39)

## 4. Conclusions

Five quasi-prepolymers with free isocyanate between 9-15% and viscosity between 24-5 Pa.s were synthesized. All the polyurethane quasi-prepolymers were characterized by FTIR. From the quasi-prepolymer 14, three polyurethanes with different content of sucrose were obtained with high cross-linking bonds density. The polyurethanes were characterized by Spectroscopic techniques (FTIR and NMR). The glass transition temperature of the polyurethanes obtained was between 24-34 °C, similar to elastomers. However the biocompatibility of the polyurethanes obtained was affected probably by the structure of pMDI and the DMSO residual. These preliminary results in the synthesis of polyurethane from carbohydrate led the study of another isocyanate that permit to obtain polyurethanes with better solubility and biocompatible with HaCaT cells.

## 5. References

1. Lee Y-H, Mei F, Bai M-Y, Zhao S, Chen D-R. Release profile characteristics of biodegradable-polymer-coated drug particles fabricated by dual-capillary electrospray. *J Control Release*. 2010 Jul 1;145(1):58–65.
2. McGinity JW. Aqueous polymeric coatings for pharmaceutical dosage forms. *Drugs and the pharmaceutical sciences*; v. 79. 1997. xi, 582 p.
3. Manzano M, Vallet-Regí M. Revisiting bioceramics: Bone regenerative and local drug delivery systems. *Progress in Solid State Chemistry*. 2012. p. 17–30.
4. Xu LC, Runt J, Siedlecki CA. Dynamics of hydrated polyurethane biomaterials: Surface microphase restructuring, protein activity and platelet adhesion. *Acta Biomater*. 2010;6(6):1938–47.
5. Grzesiak J, Marycz K, Szarek D, Bednarz P, Laska J. Polyurethane/polylactide-based biomaterials combined with rat olfactory bulb-derived glial cells and adipose-derived mesenchymal stromal cells for neural regenerative medicine applications. *Mater Sci Eng C*. 2015;52:163–70.
6. Guelcher SA, Gallagher KM, Didier JE, Klinedinst DB, Doctor JS, Goldstein AS, et al. Synthesis of biocompatible segmented polyurethanes from aliphatic diisocyanates and diurea diol chain extenders. *Acta Biomater*. 2005 Jul;1(4):471–84.
7. Zhao P, Hua X, Wang Y, Zhu J, Wen Q. Structure and properties of polyurethane elastomer cured in graded temperature field. *Mater Sci Eng A*. 2007;457(1–2):231–5.
8. Adhikari R, Gunatillake PA, Griffiths I, Tatai L, Wickramaratna M, Houshyar S, et al. Biodegradable injectable polyurethanes: Synthesis and evaluation for orthopaedic applications. *Biomaterials*. 2008;29(28):3762–70.
9. Sharma V, Kundu PP. Condensation polymers from natural oils. *Progress in Polymer Science (Oxford)*. 2008. p. 1199–215.
10. Daniel Da Silva ALL, Martín-Martínez JM, Bordado JCMJCM, Martín-Martínez JM, Bordado JCMJCM. Influence of the free isocyanate content in the adhesive properties of reactive trifunctional polyether urethane quasi-prepolymers. *Int J Adhes Adhes*. 2006;26(5):355–62.
11. Zia KM, Zuber M, Barikani M, Hussain R, Jamil T, Anjum S. Cytotoxicity and mechanical behavior of chitin-bentonite clay based polyurethane bio-nanocomposites.

- Int J Biol Macromol. 2011;49(5):1131–6.
12. Daniel-da-Silva AL, Bordado JCM, Martín-Martínez JM. Moisture curing kinetics of isocyanate ended urethane quasi-prepolymers monitored by IR spectroscopy and DSC. *J Appl Polym Sci.* 2008;107(2):700–9.
  13. John KR St. The use of polyurethane materials in the surgery of the spine: a review. *Spine J.* 2014;14:3038–3047.
  14. Simmons A, Padsalgikar AD, Ferris LM, Poole-Warren LA. Biostability and biological performance of a PDMS-based polyurethane for controlled drug release. *Biomaterials.* 2008;29(20):2987–95.
  15. Deka H, Karak N, Kalita RD, Buragohain AK. Bio-based thermostable, biodegradable and biocompatible hyperbranched polyurethane/Ag nanocomposites with antimicrobial activity. *Polym Degrad Stab.* 2010;95(9):1509–17.
  16. Laschke MW, Strohe A, Scheuer C, Eglin D, Verrier S, Alini M, et al. In vivo biocompatibility and vascularization of biodegradable porous polyurethane scaffolds for tissue engineering. *Acta Biomater.* 2009;5(6):1991–2001.
  17. Jabbari E, Khakpour M. Morphology of and release behavior from porous polyurethane microspheres. *Biomaterials.* 2000;21(20):2073–9.
  18. Li B, Yoshii T, Hafeman AE, Nyman JS, Wenke JC, Guelcher SA. The effects of rhBMP-2 released from biodegradable polyurethane/microsphere composite scaffolds on new bone formation in rat femora. *Biomaterials.* 2009;30(35):6768–79.
  19. Encalada-Diaz I, Cole BJ, MacGillivray JD, Ruiz-Suarez M, Kercher JS, Friel NA, et al. Rotator cuff repair augmentation using a novel polycarbonate polyurethane patch: Preliminary results at 12 months' follow-up. *J Shoulder Elb Surg.* 2011;20(5):788–94.
  20. Hashizume R, Fujimoto KL, Hong Y, Guan J, Toma C, Tobita K, et al. Biodegradable elastic patch plasty ameliorates left ventricular adverse remodeling after ischemia-reperfusion injury: A preclinical study of a porous polyurethane material in a porcine model. *J Thorac Cardiovasc Surg.* 2013;146(2):391–9.
  21. Zia KM, Zia F, Zuber M, Rehman S, Ahmad MN. Alginate based polyurethanes: A review of recent advances and perspective. *International Journal of Biological Macromolecules.* 2015. p. 377–87.
  22. Zia KM, Bhatti IA, Barikani M, Zuber M, Bhatti HN. XRD studies of polyurethane elastomers based on chitin/1,4-butane diol blends. *Carbohydr Polym.* 2009;76(2):183–

- 7.
23. Gunatillake PA, Martin DJ, Meijs GF, McCarthy SJ, Adhikari R. Designing biostable polyurethane elastomers for biomedical implants. *Aust J Chem.* 2003;56(6):545–57.
24. Bachmann F, Reimer J, Ruppenstein M, Thiem J. Synthesis of novel polyurethanes and polyureas by polyaddition reactions of dianhydrohexitol configured diisocyanates. *Macromol Chem Phys.* 2001;202(17):3410–9.
25. Vejnovic I, Simmler L, Betz G. Investigation of different formulations for drug delivery through the nail plate. *Int J Pharm.* 2010 Feb;386(1–2):185–94.
26. International Organization for Standardization. Biological Evaluation of Medical Devices Part 5: Tests for In Vitro Cytotoxicity. *Iso 10993–5.* 2009;5:1–52.
27. Fernández-D’Arlas B, Alonso-Varona A, Palomares T, Corcuera MA, Eceiza A. Studies on the morphology, properties and biocompatibility of aliphatic diisocyanate-polycarbonate polyurethanes. *Polym Degrad Stab.* 2015;122:153–60.
28. Pyun DG, Choi HJ, Yoon HS, Thambi T, Lee DS. Polyurethane foam containing rhEGF as a dressing material for healing diabetic wounds: Synthesis, characterization, in vitro and in vivo studies. *Colloids Surfaces B Biointerfaces.* Elsevier B.V.; 2015;135:699–706.
29. Ritter FO. Differentiation between primary, secondary and tertiary alcohols. *J Chem Edu.* 1953;38:395.
30. Hofer R, Clark J, Kraus G, Saling P. Sustainable solutions for modern economies. *Book.* 2009;
31. Pereira IHL, Ayres E, Patrício PS, Góes AM, Gomide VS, Junior EP, et al. Photopolymerizable and injectable polyurethanes for biomedical applications: Synthesis and biocompatibility. *Acta Biomater.* 2010;6(8):3056–66.
32. Kizuka K, Inoue S. Synthesis and Properties of Polyurethane Elastomers Containing Sucrose as a. 2015;(October):103–12.
33. Wacker BK, Scott EA, Kaneda MM, Alford SK, Elbert DL. Delivery of Sphingosine 1-phosphate from poly(ethylene glycol) hydrogels. *Biomacromolecules.* 2006;7(4):1335–43.
34. Garcia-Fuentes M, Torres D, Martín-Pastor M, Alonso MJ. Application of NMR Spectroscopy to the Characterization of PEG-Stabilized Lipid Nanoparticles. *Langmuir.* 2004;20(20):8839–45.

35. Peris M. Sucrose: Properties and Determination. *Encyclopedia of Food and Health*. 2016. 205-210 p.
36. Yilgör I, Yilgör E, Wilkes GL. Critical parameters in designing segmented polyurethanes and their effect on morphology and properties: A comprehensive review. *Polymer (United Kingdom)*. 2015. p. A1–36.
37. Hsu SH, Kao YC, Lin ZC. Enhanced biocompatibility in biostable poly(carbonate)urethane. *Macromol Biosci*. 2004;4(4):464–70.
38. Ganta SR, Piesco NP, Long P, Gassner R, Motta LF, Papworth GD, et al. Vascularization and tissue infiltration of a biodegradable polyurethane matrix. *J Biomed Mater Res A*. 2003;64(2):242–8.
39. Da Violante G, Zerrouk N, Richard I, Provot G, Chaumeil JC, Arnaud P, et al. Evaluation of the cytotoxicity effect of dimethyl sulfoxide (DMSO) on Caco2/TC7 colon tumor cell cultures. *Biol Pharm Bull*. 2002;25(12):1600–3.



**Chapter 3: Synthesis of biocompatible polyurethanes.  
Characterization by Techniques Spectroscopy, GPC and MALDI-  
TOF**



## 1. Introduction

The synthesis of polyurethanes has been extensively studied by several groups with the aim of investigating the novel combination of monomers that allow obtaining polyurethanes with greater versatility of properties (1–6).

The choice of monomers used to synthesize PUs are dependent on the final applications of the material (7). For example, monomers that offer good durability will be selected for polymers to be used for prostheses (8), those that increase the compatibility of PU with tissues will be applied for pacemakers (9) and monomers that offer thermal stability will be carefully chosen for catheters that required sterilization process (7,10). The properties of PUs are remarkably affected by the content, type, and molecular weight of the soft segments (7).

We are interested in the synthesis of linear polyurethanes from carbohydrates suitable functionalized for application in pharmaceutical industry. Recent work has shown that the use of disaccharides such as sucrose increase the crosslinked of the polymer. This result is a consequence of the number of OH in the structure of glycol. A monomer with 2 OH groups permits obtained linear polyurethane.

Isosorbide is a monomer already used in the synthesis of biocompatible polymers(3,7,11,12). This glycol is a chiral and relatively thermostable diol. It is technically produced from glucose, as showed in Figure 3.1.

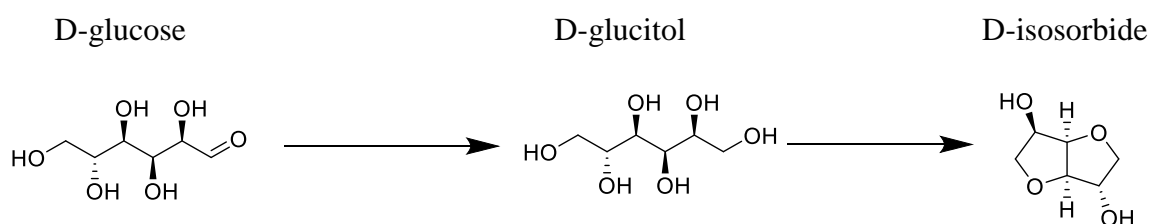


Figure 3. 1. Two step procedure for the synthesis of isosorbide from D-glucose adapted from (13).

On the other hand, the PPG is a biocompatible polyether which has been extensively investigated for application as a biomedical material that confers elastomeric properties to polyurethanes(14–16). This monomer was then chosen as a second glycol in outlined synthesis.

To avoid the use of monomers that, probably yield toxic compounds, the IPDI and HMDI are envisaged as option to access to non toxic formulation since those isocyanates have been already used in the synthesis of several biocompatible polyurethane (15,17,18).

Our work aims is to synthesize new polyurethanes from D-isosorbide by polyaddition. The novelty of this work consists not only in the synthesis of this type of polymer but also in the production of innovative building block to synthesize a biocompatible polyurethane. Moreover, we established a methodology for the study of the chemical structure of this type of PUs by FTIR,  $^1\text{H}$  NMR,  $^{13}\text{C}$  NMR, their molecular weight being determined by GPC/SEC and MALDI-TOF.

## 2. Material and Methods

### 2.1 Materials

The D-isosorbide was provided by Acrös (Belgium). The HMDI was acquired from Bayer Material Science (Germany). IPDI and DMDEE were supplied from Aldrich (Germany) and PPG (VORANOL 1010L) from Dow Chemical (Germany). Anhydrous ethanol was acquired by Carlo Erba (France). The DMSO- $d_6$ ,  $\text{CDCl}_3$ , TMS (99.9% purity), THF, Polystyrene standards (TSK Tosoh Co),  $\text{NaBF}_4$  and DHB for MALDI-MS were purchased from Sigma-Aldrich (Germany). The methanol (HPLC) was provided by Panreac (Spain).

### 2.2 Methods

#### 2.2.1 Synthesis of quasi-prepolymers

The quasi-prepolymers were synthesized using the pre-polymerization method. As a first step, a quasi-prepolymer was prepared by reacting of IPDI or HMDI and PPG in a 250 mL glass flask, under a dry nitrogen atmosphere, to avoid the presence of moisture and subsequently the formation of urea bonds during the synthesis. The reaction took place with the dropwise addition of PPG under mechanical stirring (400 rpm), at 80 °C and in the presence of 0.5 mL of the catalyst (DMDEE). This reaction practically completed in 3 h. The ratios for the syntheses are presented in Table 3.1.

Table 3. 1. Molar ratios employed in the synthesis of the quasi-prepolymers.

	Pre 1	Pre 2	Pre 3
IPDI	6	6	-
HMDI	-	-	6
PPG	1	2	1

### 2.2.2 Synthesis of polyurethanes

The synthesis of polyurethanes was carried out in a 250 mL reactor starting from a selected quasi-prepolymer polyurethane. The D-isosorbide was then added to the quasi-prepolymer. The reaction took place in 1 h. The molar ratio of the monomer is presented in Table 3.2.

Table 3. 2. Molar ratios employed in the synthesis of the PU.

PU	PU19	PU20	PU21	PU22
IPDI	6	6	6	-
HMDI	-	-	-	6
PPG	1	2	1	1
D-isosorbide	5	5	6	5

### 2.2.3 Determination of viscosity

The viscosity of the quasi-prepolymer polyurethanes was determined according to section 2.3.1, Chapter 2.

### 2.2.4 Determination of free isocyanate

The NCO content in the quasi-prepolymer polyurethanes was determined according to section 2.3.2, Chapter 2.

### 2.2.5 FTIR Characterization

The FTIR spectra were obtained for the quasi-prepolymer, according to section 2.2.3, in Chapter 2. The solid samples of polyurethane were finely divided, (approximately of 1 mg) and dispersed in a KBr matrix (200 mg). A pellet was then formed by compressing the sample

at 784 MPa. For the sample of the liquid monomers, attenuated total reflectance (ATR-FTIR) spectra were obtained using the same spectrometer equipped with an ATR accessory. The FTIR spectra were obtained at room temperature, in the range of 4000  $\text{cm}^{-1}$  to 600  $\text{cm}^{-1}$ , during 128 scans with 4 $\text{cm}^{-1}$  resolution.

### 2.2.6 NMR Characterization

$^1\text{H}$ -NMR and  $^{13}\text{C}$ -NMR spectra were obtained using a Bruker Avance III 500 MHz spectrometer. The monomers employed in the synthesis of polyurethanes were analyzed by  $^1\text{H}$  NMR, in chloroform- $d_3$  ( $\text{CDCl}_3$ ). However, the samples of polyurethane (PU19, PU20, PU21, and PU22) were dissolved in DMSO- $d_6$ . All the spectra were obtained at room temperature employing one referred internally TMS. The measurements were performed using between 20-53 mg of samples of polyurethane. The chemical shifts are given in ppm relative to TMS.

### 2.2.7 DOSY

The DOSY experiment, which is a non-invasive analytic technique, enables the determination of diffusion coefficients, being based on the method of spin echoes with pulsed-field gradients (PGSE) (19).

The molecular diffusion is based on the random translational movements (Brownian) of molecules, due to their thermal energy (20). Experimentally, it appears that the probability  $P(x,t)$  of the mass center of a molecule which diffuses from a position  $x$  to a position  $x+\delta x$ , after a time  $t$ , is given by this Equation 1:

$$P(x,t) = \frac{e^{-\frac{(x-x_0)^2}{4Dt}}}{(4\pi Dt)^{3/2}} \quad (1)$$

where  $D$  is the diffusion coefficient of the analyzed molecule ( $\text{m}^2\text{s}^{-1}$ ). Typical values of diffusion coefficients, at room temperature, are around  $10^{-9}$ - $10^{-12}$   $\text{m}^2\text{s}^{-1}$  (respectively for little molecules in less viscous solutions or for molecules with high molecular weight).

This technique permits to make a 2D spectrum, similar to spectrum represented in Figure 3.2, whose represented dimensions are the chemical shift ( $\delta$ ) and  $D$  of the species of the sample.

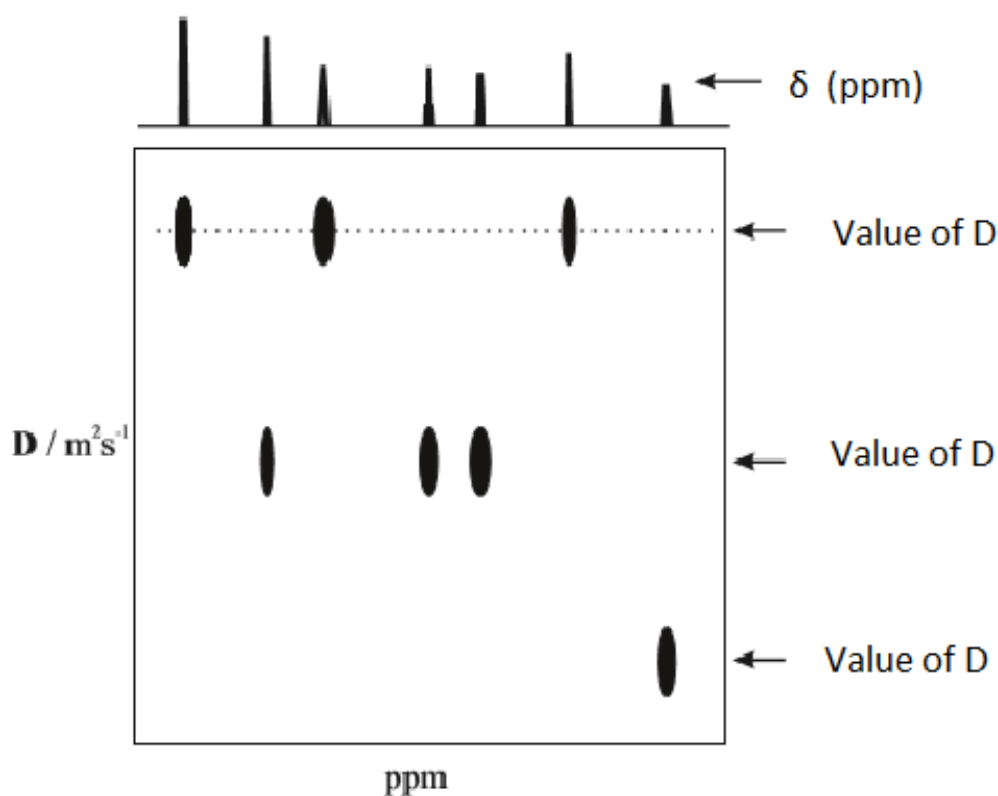


Figure 3. 2. Typical spectrum DOSY ( $D$  ( $\text{m}^2\text{s}^{-1}$ ) vs  $\delta$  (ppm)).

To determine the diffusion coefficients, several experiences are performed, usually varying the strength of the gradient(21,22). In our study, the diffusion coefficients ( $D$ ) were determined at infinite dilution of the polymers. The value of  $D$  was obtained from plots of  $D$  versus concentration. For this purpose, a series of five solutions was prepared with concentrations  $0.34 \times 10^{-3} \text{ g.mL}^{-1}$ ,  $0.74 \times 10^{-3} \text{ g.mL}^{-1}$ ,  $1.74 \times 10^{-3} \text{ g.mL}^{-1}$ ,  $3.42 \times 10^{-3} \text{ g.mL}^{-1}$  and  $11.4 \times 10^{-3} \text{ g.mL}^{-1}$  in  $\text{DMSO-}d_6$  and the diffusion coefficients  $D$  were measured using the PGSE method in a NMR Bruker Avance III 500 MHz spectrometer with a 3 mm BBO probe with a z-gradient shielded coil. The solutions of the polymers were poured in 3mm NMR tubes to a total volume of 0.3mL. To guarantee reproducibility of the results this volume was kept in all the samples. The temperature was controlled at  $30^\circ\text{C}$  by a BCU05 Bruker unit with an air flow of  $521 \text{ L.h}^{-1}$ .

The use of the exponential regression of the data allowed the determination of the diffusion coefficient.

The final processing and visualization of spectra was performed employing the software Topspin, version 3.2, of the Bruker spectrometer.

### 2.2.8 Hydrodynamic radii ( $r_h$ )

The  $r_h$  for each polyurethane were determined by the Stokes-Einstein equation (Equation 2) in which diffusion coefficient and radius are in inverse proportionality(22).

$$D = \frac{k_B T}{f} = \frac{k_B T}{6\pi\eta r} \quad (2)$$

In the Equation 2,

$k_B$ : Constant of Boltzmann ( $1.38066 \times 10^{-23} \text{ kg.m}^2.\text{k}^{-1}.\text{s}^{-2}$ )

T: Temperature

$\eta$ : viscosity of the solution ( $\text{N.s.m}^{-2} = \text{kg.s}^{-1}.\text{m}^{-1}$ ),

The Stokes-Einstein equation was originally developed for spherical colloidal particles, which are well defined the Brownian motion. However, it is also an approach for small non-spherical particles. The use of the equation to predict the diffusion can be improved by replacing the radius of the molecules ( $r$ ), for their effective radius  $r_f$ , also called hydrodynamic radius ( $r_h$ ). The value of  $r_h$  can be used to compensate the factors like non-spherical molecules and spheres of solvation.

The viscosity of DMSO- $d_6$  at 30°C,  $\eta = 1.951 \times 10^{-3} \text{ Pa.s}$ , was estimated from that of the non-deuterated solvent taking into account the isotopic effects of the viscosity(23).

### 2.2.9 Gel Permeation Chromatographic

The analyses were made in an HPLC Waters chromatograph containing a Waters 515 isocratic pump and a Waters 2414 refractive index detector. In this apparatus, the oven was stabilized at 35 °C, and the elution of samples was carried out through two PolyPore columns, protected by a PolyPore Guard column (Polymer Labs). The software Empower® performed the acquisition and data processing.

THF was used as eluent, at a flow rate of 1.0 mL.min<sup>-1</sup>. Before use, the solvent was filtrated through 0.45 µm PTFE membranes Fluoropore (Millipore or Pall Corporation) and degassed in an ultrasound bath for 45 min. The oligomer/polymer samples were also filtered across 0.20 µm PTFE filters Durapore (Millipore). Molecular weights were calibrated relative to polystyrene standards (TSK Tosoh Co.). As a result, it should be taken into account that small deviations could occur when the present polymer samples were analyzed.

### 2.2.10 MALDI-TOF

The polyurethane samples were analyzed in a MALDI-TOF mass spectrometry Voyager-DETM PRO Workstation, equipped with a nitrogen laser operating at a wavelength of 337 nm.

A solution of polyurethane 4×10<sup>-4</sup> mg.mL<sup>-1</sup> in methanol was prepared (Solution 1). A second solution of NaBF<sub>4</sub> 10 mg.mL<sup>-1</sup> in miliQ water (Solution 2). Finally, DHB was dissolved in Solution 2 at a concentration of 10 mg.mL<sup>-1</sup> (Solution 3). The Solution 1 was mixed with Solution 3 (matrix) in a ratio of 1:10 (sample:matrix), later 1 µL of the whole solution was applied in the sample holder and allowed to dry. The resulting homogeneous solid mixture, which ideally consists of a thin layer of microcrystals, was then introduced into the ion source of the mass spectrometer. The time of flight mass spectrometer was in reflector and/or linear mode. All spectra were obtained in the positive ion mode. Ionization was performed with a 337nm pulsed nitrogen UV laser. All data were processed using the Data Explorer software package (Applied Biosystems). The spectra were averaged over 500 laser shots over the complete sample area.

The equation of step-growth polymerization, with the name: Carothers (Equation 3) gives the degree of polymerization. (24,25) :

$$DP = \frac{1+r}{2r(1-p)+1-r} \quad (3)$$

Where  $r$  is the stoichiometric ratio of monomers, the excess of monomers is conventionally the denominator so that  $r < 1$  and,  $p$  is the extent of reaction (or conversion to polymer), defined by Equation 4:

$$p = \frac{N_0 - N}{N_0} \quad (4)$$

Where  $N_0$  is the number of molecules present initially and  $N$  is the number of unreacted molecules at the time ( $t$ ). If neither monomer is in excess, then  $r = 1$  and the equation reduces to the equimolar. In the limit of complete conversion of the limiting reagent monomer,  $p \rightarrow 1$ . The  $M_w$  (weight average molecular weight) of the polyurethanes were calculated according to the Equation 5, and the  $M_n$  (number average molecular weight) were calculated according to the Equation 6, (26)

$$M_n = \frac{\sum_i N_i M_i}{\sum_i N_i} = \frac{\sum_i w_i}{\sum_i (w_i / M_i)} \quad (5)$$

$$M_w = \frac{\sum_i N_i M_i^2}{\sum_i N_i M_i} = \frac{\sum_i w_i M_i}{\sum_i w_i} \quad (6)$$

A convenient measure of the molecular weight distribution is the ratio  $M_w/M_n$ , called polydispersity index (26).

## 2.2.11 *In vitro* cytotoxicity assay

### 2.2.11.1 Preparation of samples

The polyurethanes were solubilized completely in ethanol, under stirring (200 rpm), at 250 mg/mL. Later one side of the 0.5 mm diameter glass sheet was exposed with this solution and dried for 30 min.

### 2.2.11.2 Direct contact assay

The morphological characterization of the cell behavior in the presence of the tested materials was performed according section 2.4.5.2, chapter 2.

### 3. Results and discussion

A family of aliphatic biocompatible PU based on D-isorbide and PPG were synthesized in order to design several polymers to convey the active principle. The segmented PUs were composed of various ratios of soft segments and hard segments. Polymerization of IPDI with various ratios of D-isorbide and PPG was carried out by poly-condensation at 80 °C for 4h catalyzed by DMDEE, as shown in Figure 3.3. On the other hand, correspondingly, the PU 22 was obtained from the reaction of HMDI, PPG and D-isorbide, with the same catalyst (Figure 3.3).

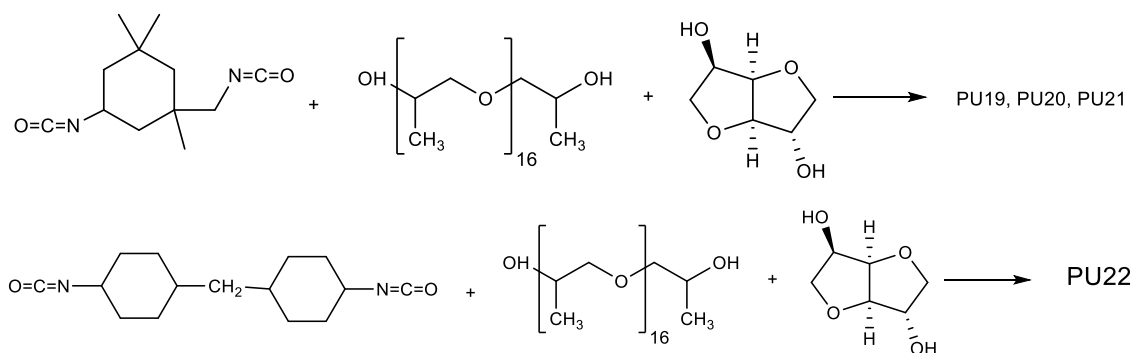


Figure 3. 3. Synthetic route of polyurethane PU19, PU20, PU21, and PU22.

#### 3.1 Viscosity and free isocyanate of quasi-prepolymers

In the Table 3.3 the values of free isocyanate and the viscosity of the prepolymers are presented.

Table 3. 3. Values of viscosity and free isocyanate of quasi-prepolymers, (n=3).

Quasi-prepolymer polyurethanes	NCO/OH	% NCO-free $\pm$ SD	Viscosity (Pa.s) $\pm$ SD
Pre – 1	6/1	12 $\pm$ 0.3	10 $\pm$ 0.1
Pre – 2	6/2	9 $\pm$ 0.3	21 $\pm$ 0.1
Pre – 3	6/1	11 $\pm$ 0.6	10 $\pm$ 0.1

### 3.2 FTIR Characterization

#### 3.2.1 Characterization of quasi-prepolymers polyurethanes

In the Figure 3.4 the FTIR of the quasi-prepolymer synthesized are presented, which correspond to the molar ratio of Table 3.1.

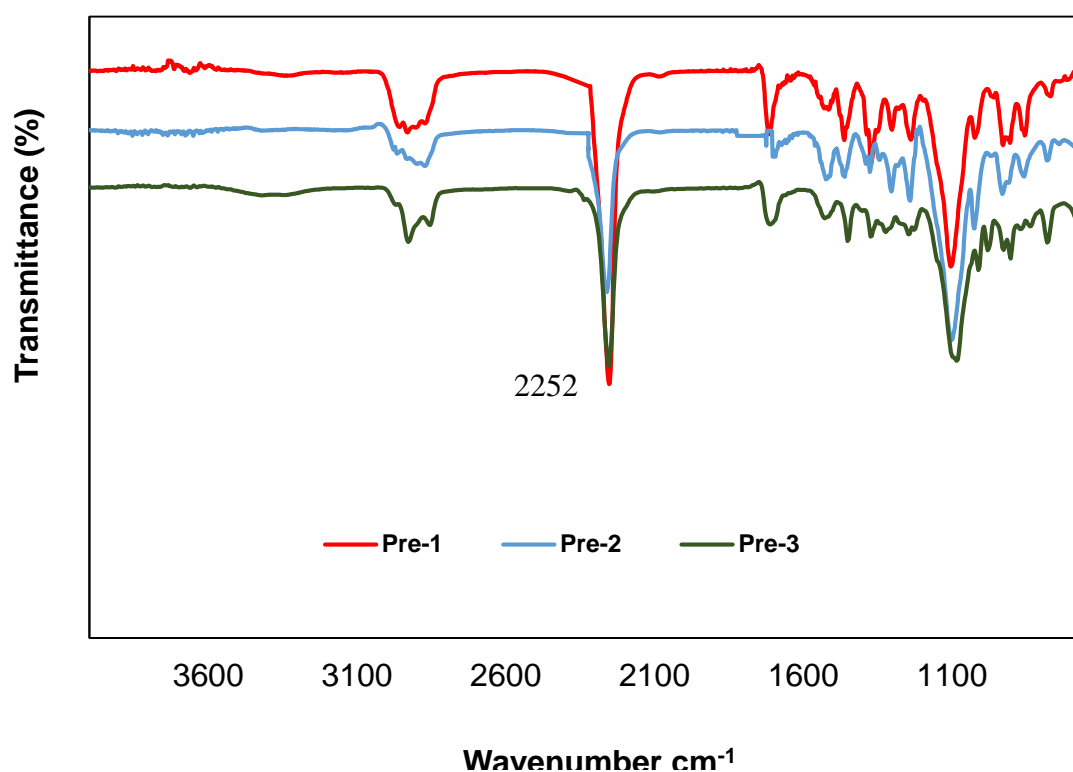


Figure 3. 4. Spectra of quasi-prepolymer polyurethanes.

In all the quasi-prepolymers a band at  $2252\text{ cm}^{-1}$  is observed, indicating the presence of isocyanate groups ( $\text{-NCO-}$ ) corresponding to the monomers IPDI and HMDI, which is in agreement with the reports of the literature ( $2270$  to  $2250\text{ cm}^{-1}$  for the  $\text{N=C=O}$  stretching vibration)(30–32). The spectra of quasi-prepolymers also showed bands at  $2927\text{ cm}^{-1}$ , corresponding to  $\text{-CH}_2\text{-}$  groups, and the peak of the ether group at  $1527\text{ cm}^{-1}$ . These bands correspond to PPG segments; (pure PPG presents a  $\text{-CH}_2\text{-}$  band between  $2970\text{-}2850\text{ cm}^{-1}$  and another one corresponding to the ether group at  $1526\text{ cm}^{-1}$  (33). The band corresponding to the carbonyl groups is observed between  $1677\text{-}1708\text{ cm}^{-1}$ , which is indicative of the condensation reaction between the  $\text{-OH}$  group of PPG and the  $\text{-NCO-}$  group of HMDI and IPDI (34–36).

### 3.2.2 Characterization of Polyurethanes

#### Polyurethanes from IDPI

The FTIR spectra of the PUs and monomers are showed in Figure 3.5.

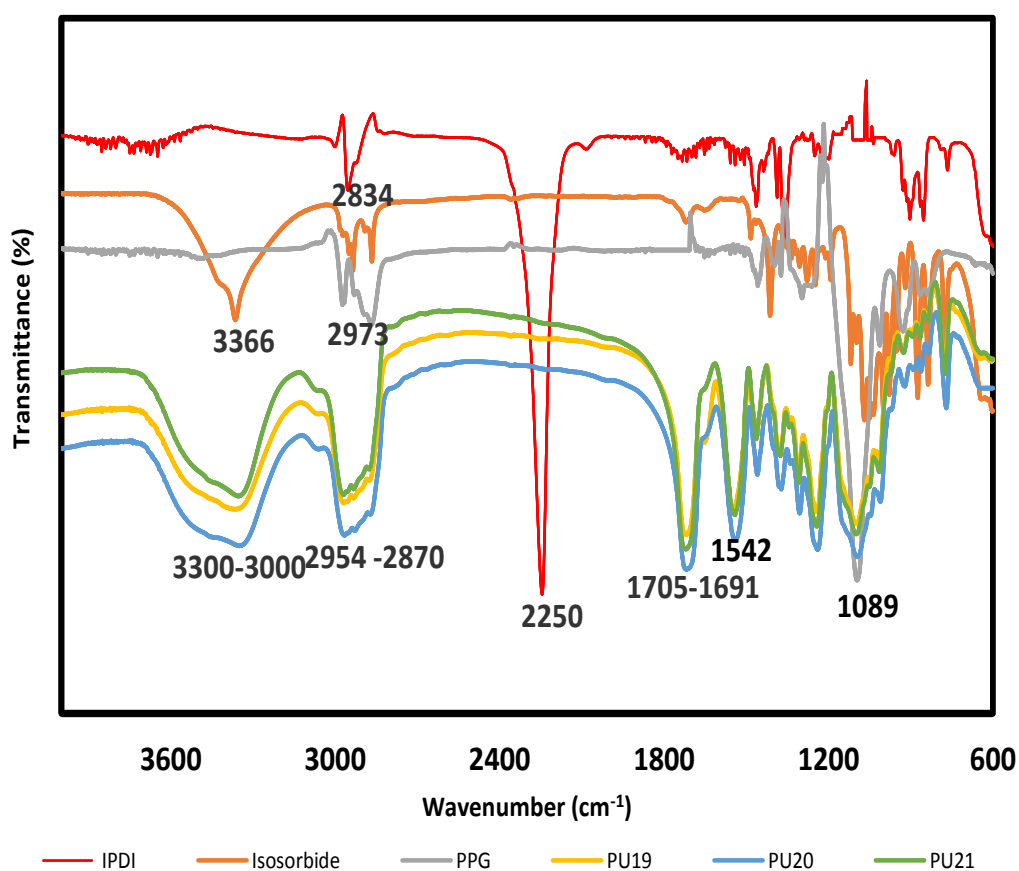


Figure 3. 5. FTIR spectra of Isosorbide, PPG, IPDI and PUs.

In Figure 3.5 is observed the characteristic band of -OH- at 3366, this band correspond to the presence of isosorbide (37). The -CH<sub>2</sub>- is observed at 2973 cm<sup>-1</sup> corresponding to the position mention for other authors then identified the band of methylene (37). The band OH disappears in the spectra of PUs. The -CH<sub>2</sub>- identified in isosorbide and PPG, are detected in the spectra of PUs between 2954-2870cm<sup>-1</sup>. The hard segment of polyurethanes present bands characteristics, the stretching vibrations of -NH- and C=O group. The -NH- bands are detected around 3300-3000 cm<sup>-1</sup> and the carbonyl bands can be observed between 1705-1691cm<sup>-1</sup>(34,38). These structures can interact and form intermolecular hydrogen bonding. The disappearance of -N=C=O stretching vibration around 2250cm<sup>-1</sup> in the spectra of polyurethanes synthesized (Figure 3.4) suggested that there was no unreacted isocyanate group (18) and meaning that all the isocyanate groups had reacted with the OH group (39). On the other hand, NH bending bands of the PUs synthesized in our work were identified at 1542 cm<sup>-1</sup>(Figure 3.5) (31). The position of this bands was observed in the reaction between polycaprolactone and 2-isocyanate ethyl methacrylate (40). The NH bending from urethane group was detected too by Daniel da Silva, *et al*, at the same position (41). Furthermore, the C-O-C stretching was observed at 1089 cm<sup>-1</sup> (38).

In Figure 3.6, the intensity of some peaks in the PUs synthesized is observed.

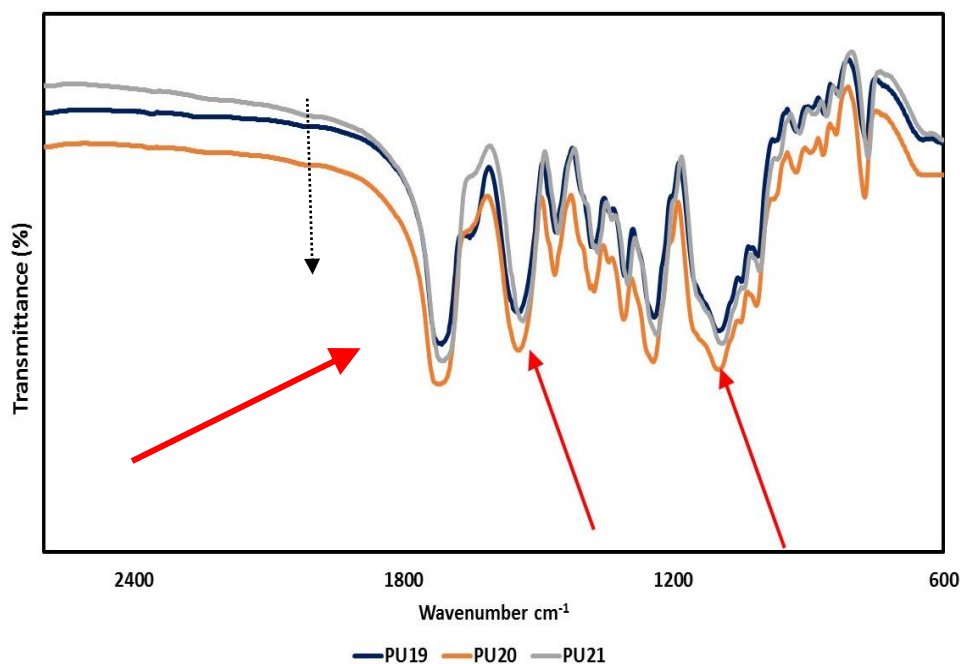


Figure 3. 6. FTIR of PU, C=O, C-H and C-O- C stretching bands of PUs.

The FTIR spectra of PU19, PU20 and PU21 showed differences between the intensity of group amine  $\text{-NH-}$ , ethylene  $\text{C-H}$  stretching and ether combination absorption, band around  $3344\text{ cm}^{-1}$ ,  $2967\text{ cm}^{-1}$ ,  $2875\text{ cm}^{-1}$ , represented in Figure 3.5 and bands at  $1718\text{ cm}^{-1}$ ,  $1542\text{ cm}^{-1}$  and  $1108\text{ cm}^{-1}$  presented in Figure 3.6, indicating that the molar ratio of isosorbide and PPG influenced the spectrum intensities, that corresponding with report in the literature(7).

### Polyurethanes from HMDI

In Figure 3.7 presents the FTIR of the PU22.

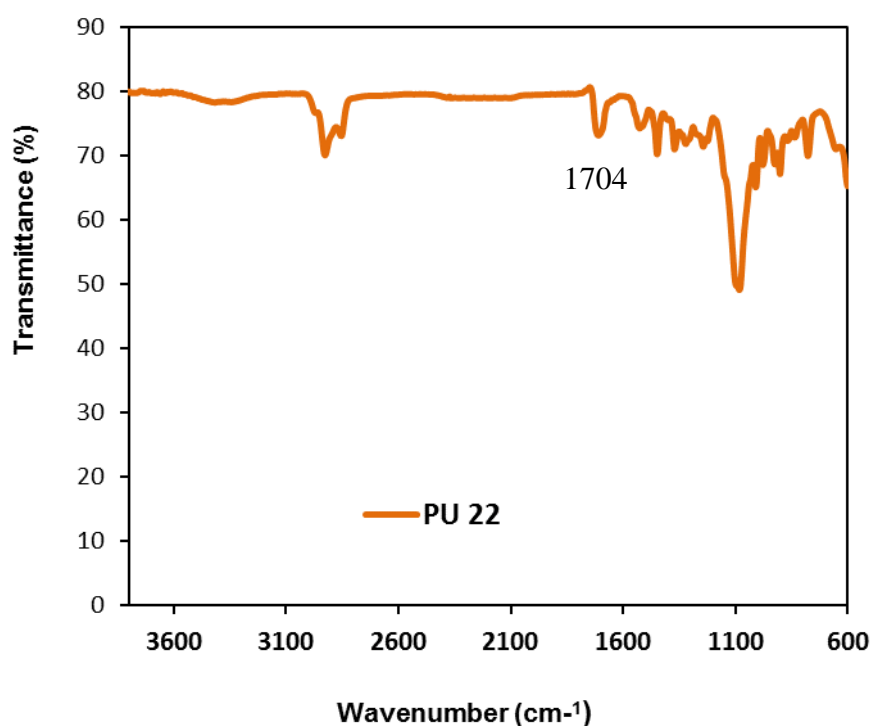


Figure 3. 7. FTIR spectrum of PU22.

In Figure 3.7, the peaks of CH<sub>2</sub> stretching (from PPG) are observed between 2927 and 2854 cm<sup>-1</sup>, the band of carbonyl of urethane is detected at 1704 cm<sup>-1</sup>. The bands typically of C-N stretching, combined with N-H in plane bending are observed at 1523 cm<sup>-1</sup> and 1446 cm<sup>-1</sup>, these signs demonstrating the occurrence of the reaction between the hydroxyl and the isocyanate group (42). The C-O-C characteristic band was identified at 1079 cm<sup>-1</sup>.

### 3.3 <sup>1</sup>H NMR Characterization

#### 3.3.1 Characterization of some monomer by <sup>1</sup>H NMR spectroscopy

##### 3.3.1. 1 Characterization of IPDI

The structure observed in Figure 3.8, show different chemical environment for all the protons of IPDI.

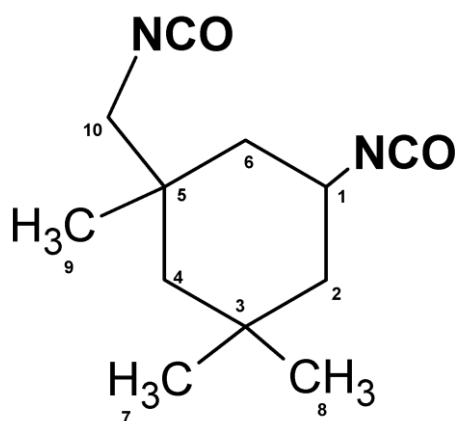


Figure 3. 8. The structure of IPDI.

The spectrum of this aliphatic diisocyanate (Figure 3.8), are observed in the Figure 3.9.

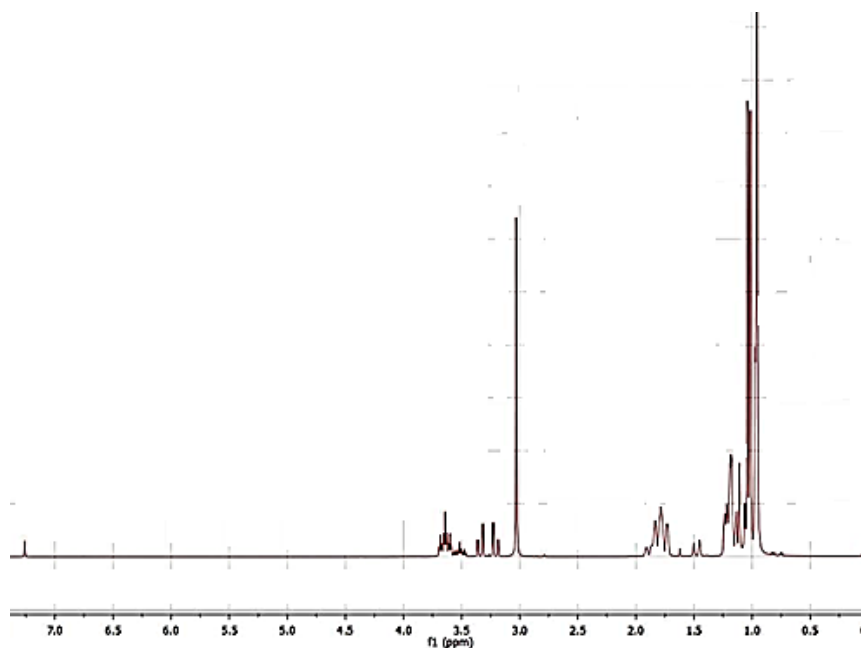


Figure 3. 9.  $^1\text{H}$  NMR spectrum of the IPDI (500 MHz, in  $\text{CDCl}_3$  at room temperature).

In the Table 3.4 was represented, the chemical shifts obtained for the IPDI as well as those found in the literature.

Table 3. 4. Assignments of  $^1\text{H}$  NMR and chemical shifts of IPDI

Assignments	Chemical shifts $\text{CDCl}_3$ (ppm)	Reference of chemical shifts* $\text{CDCl}_3$ (ppm)
1H	3.45-3.70	3.2-3.8
2H - 4H	1.45	1.4-1.9
6H	1.65-1.95	1.24-1.82
7H-8H-9H	0.85-1.25	0.9-1.3
10H	3.02	3.1-3.4
*(16,43,44)		

Usually, the IPDI consists in a mixture of cis and trans isomer, Z to E isomers in a 3:1 ratio. The two isocyanate groups presented in the asymmetric molecule are chemically different; one is bonded directly to a primary carbon (NCO-C10) and the other is bonded to the cycloaliphatic ring to a secondary carbon (NCO-C1) (16). According to the spectrum of this isocyanate, the assign a chemical shift of each proton is complicated.

### 3.3.1. 2 Characterization of PPG by $^1\text{H}$ NMR

The structure developed for PPG (Figure 3.10) shows three chemically different protons.

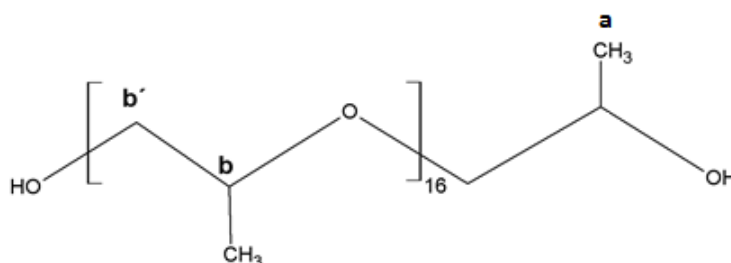


Figure 3. 10. The structure of PPG.

However, when considering the chemical environment can be observed very close to each of these types of hydrogens chemical shifts (Figure 3.10).

In Figure 3.11 is presented the  $^1\text{H}$ -NMR spectrum of PPG.

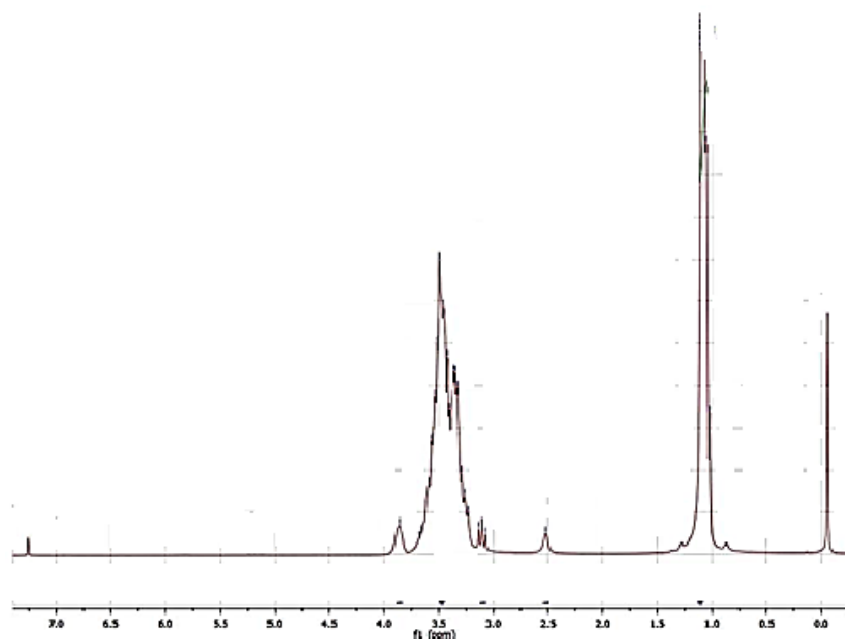


Figure 3. 11.  $^1\text{H}$  NMR spectrum of the PPG (500 MHz, in  $\text{CDCl}_3$  at room temperature).

The chemical shifts of the PPG observed are described in Table 3.5, as well as those found in the literature.

Table 3. 5. Assignments of  $^1\text{H}$ -NMR and chemical shifts of PPG.

Assignments	Chemical shifts $\text{CDCl}_3$ (ppm)	Reference of chemical shifts* $\text{CDCl}_3$ (ppm)
Ha	1.2	1.12-1.37
Hb - H b'	3.2-3.5	3.4-4.0
OH	3.9	3.1-3.9
* (16,45,46)		

### 3.3.1. 3 Characterization of Isosorbide by $^1\text{H}$ -NMR

In Figure 3.12 the structure of isosorbide and the identification of the different protons found in the molecule is presented.

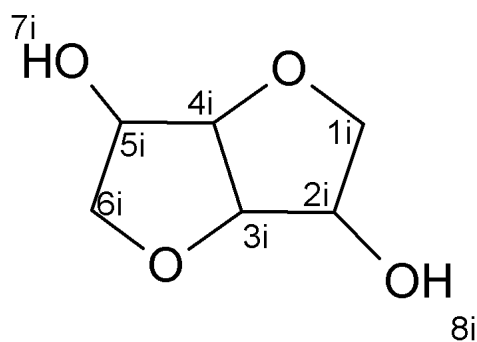


Figure 3. 12. The structure of Isosorbide.

In the Figure 3.13 was observed the  $^1\text{H}$ -NMR spectrum of the Isosorbide

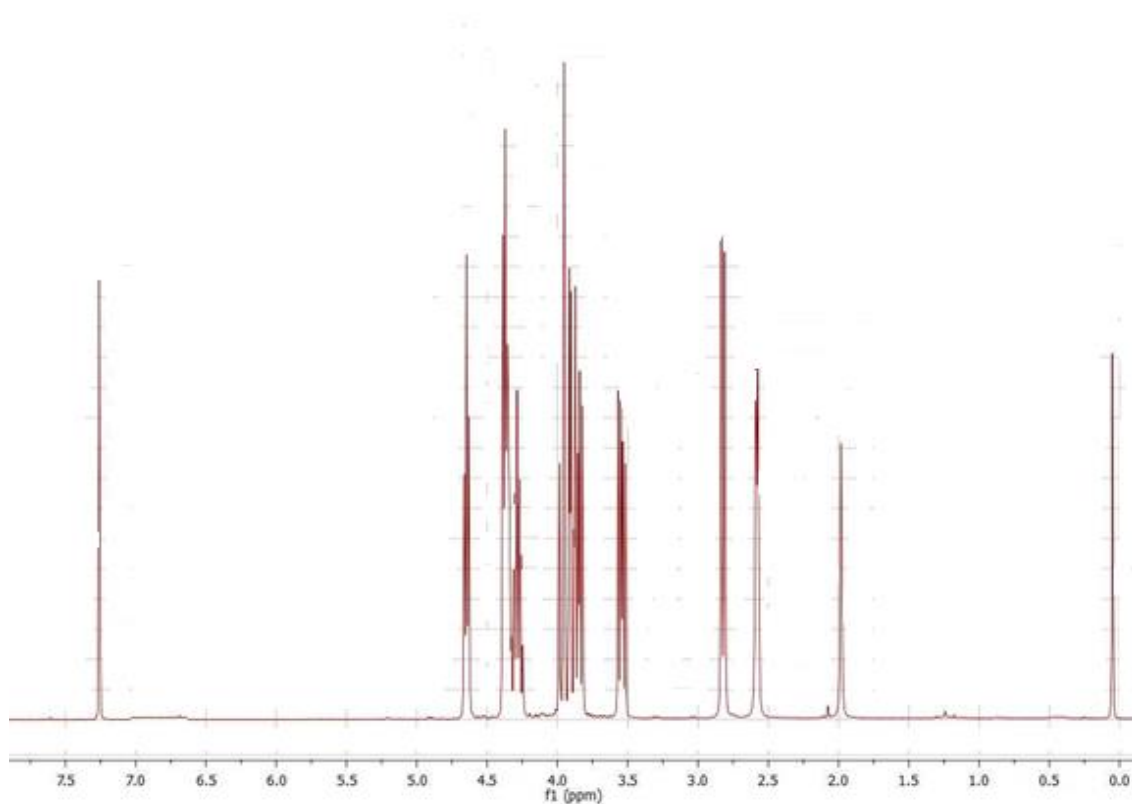


Figure 3. 13.  $^1\text{H}$  NMR spectrum of the Isosorbide (500 MHz, in  $\text{CDCl}_3$  at room temperature).

The hydroxyl of isosorbide appears at 2.2 ppm (7). Table 3.6 are presents the chemical shifts corresponding to the structure of Figure 3.12. The peaks identified are in accordance with isosorbide signals observed in other works for the characterization by  $^1\text{H}$ -NMR (37,47).

Table 3. 6. Assignments of  $^1\text{H}$  NMR and chemical shifts of Isosorbide.

Assignments	Chemical shifts $\text{CDCl}_3$ (ppm)	Reference of chemical shifts* $\text{CDCl}_3$ (ppm)
1H,6H	3.8-4	3.9-4
3H,4H	3.5	3.7-4.4
2H	4.25	4.7
5H	4.6	5.0
OH	2.1	2.2
* (7,37,48,47)		

### 3.3.2 Analysis of PUs synthesized of by NMR spectroscopy

The analysis by  $^1\text{H}$ -NMR and  $^{13}\text{C}$ -NMR of the PUs presented in this study disclosed four structures.

The structure that represents the fraction of IPDI- PPG-IPDI is presented in Figure 3.14A and the fraction of the structure corresponding to IPDI-(D-isosorbide)-IPDI is represented in Figure 3.14B.

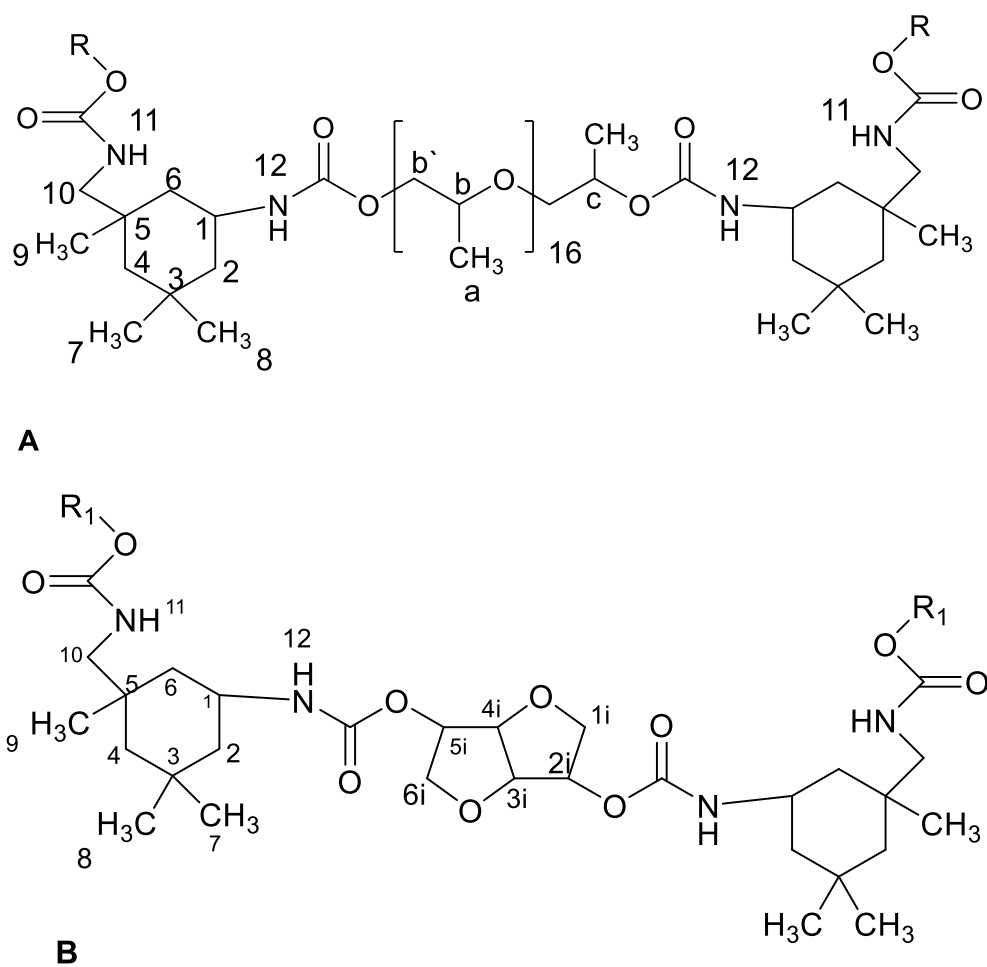


Figure 3. 14. Segment of polyurethane with monomers IPDI and PPG (A). Segment of a chain of polyurethane with monomers IPDI and D-isosorbide (B).

The structure resulting from HMDI-PPG-HMDI is showed in Figure 3.15A and the fraction HMDI-Isosorbide-HMDI in Figure 3.15B.

The  $^1\text{H-NMR}$  were performed in  $\text{DMSO-}d_6$  since it presented a better resolution regarding the  $-\text{NH}-$  proton. The identification of NH indicated reaction between diols and the isocyanate group (16).

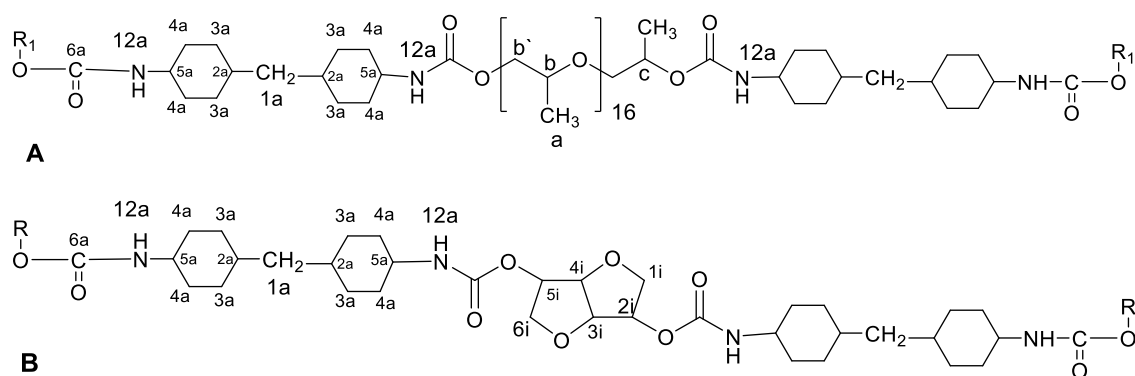


Figure 3. 15. Segment of a chain of polyurethane with monomers HMDI and PPG (A).

Segment of a chain of polyurethane with monomers HMDI and D-isosorbide (B).

### 3.3.2.1 Analysis of polyurethanes by $^1\text{H-NMR}$ spectroscopy

The  $^1\text{H NMR}$  spectra of polyurethanes PU19, PU 20, PU21 are depicted in Figure 3.16.

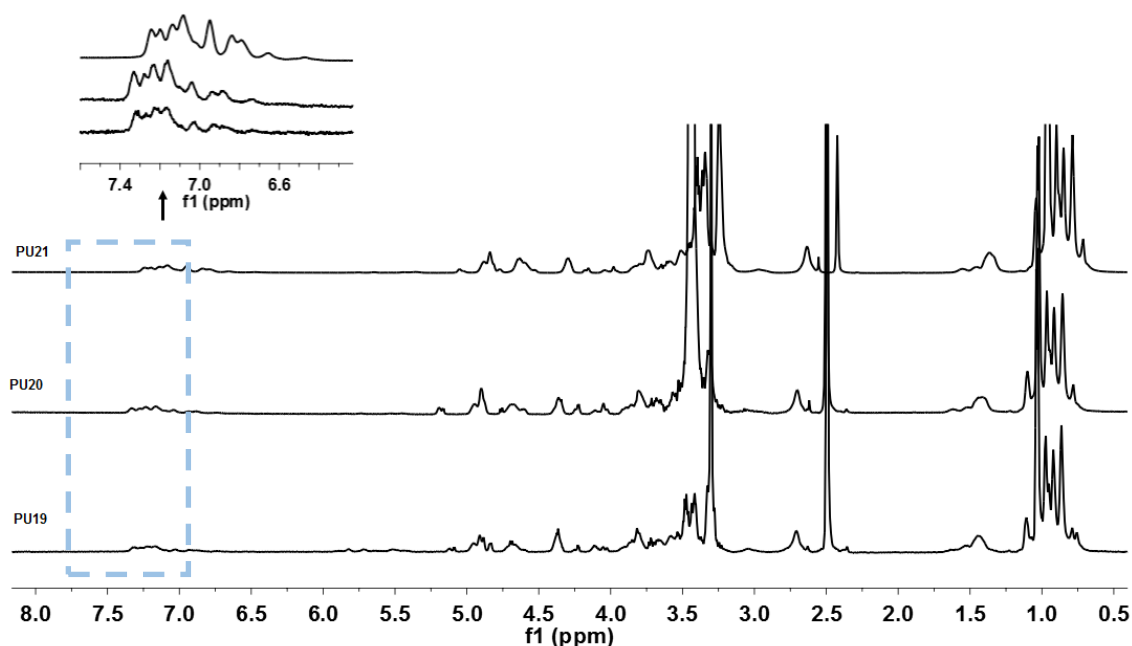


Figure 3. 16.  $^1\text{H}$  NMR spectra of PUs (500 MHz, in  $\text{DMSO-}d_6$  at room temperature).

The principal signals of polyurethanes identified by  $^1\text{H}$ -NMR are summarized in Table 3.7. The  $^1\text{H}$ -NMR spectra of the synthesized PUs synthesized are confirmed the presence of the urethane group by the identifications of resonances of  $-\text{HN}-$ , near to 7.0 ppm. These results are agreement with those reported by Bessel *et al*, where the characteristic  $\text{NH}-$  of the urethane group, was identified at 7.1 ppm as a result of the synthesis of polyhydroxy-urethanes by an isosorbide dicyclocarbonates from isosorbide with four commercial diamines (3). Other authors mention that the proton from the group  $-\text{NHCOO}-$ , obtained for the reaction between IPDI and polyester can also be observed at 6.8, 6.82 and 7.2 ppm(43). In the literature the resonance of  $-\text{NH}-$  is described at 8.07 ppm in polyurethanes synthesized from isosorbide, HDI, and PTMG (7).

Table 3. 7. Assignments of <sup>1</sup>H-NMR and chemical shifts of PU 19, PU 20 and PU21.

Assignment	Chemical Shifts	Chemical Shifts	Chemical Shifts	Reference of Chemical shifts (ppm) *
	PU19 (ppm)	PU20 (ppm)	PU21 (ppm)	
1	3.80	3.90	3.75	3.20-3.80
2,4,6	1.40-1.60	1.25-1.75	1.30-1.60	1.24-1.9
7,8,9	0.70-1.10	0.60-1.20	0.80-1.20	0.90-1.30
10	2.60	2.60	2.70	3.10-3.40
11,12	7.1	7.2	7.1	7.1-8.02
13	7.30	7.00-7.25	7.00-7.50	7.00-8.07
1i	3.50	3.50	3.50	3.90-4.00
2i	4.75	4.50	4.00	4.00-4.70
3i	4.30-4.40	4.25-4.30	4.50	3.70-4.40
4i	4.40	4.60	5.00	3.70-4.40
5i	4.75	4.90	5.00	5.00
6i	4.00	3.80	4.10	3.90-4.00
a	1.20	1.00	1.20	1.12-1.37
b	3.00	3.20	3.50	3.40-4.00
b'	3.50	3.50	3.50	3.40-4.00
c	4.90	4.80	5.00	4.70-5.00

\*(7,16,43)

The spectrum of PU 22 is presented in Figure 3.17.

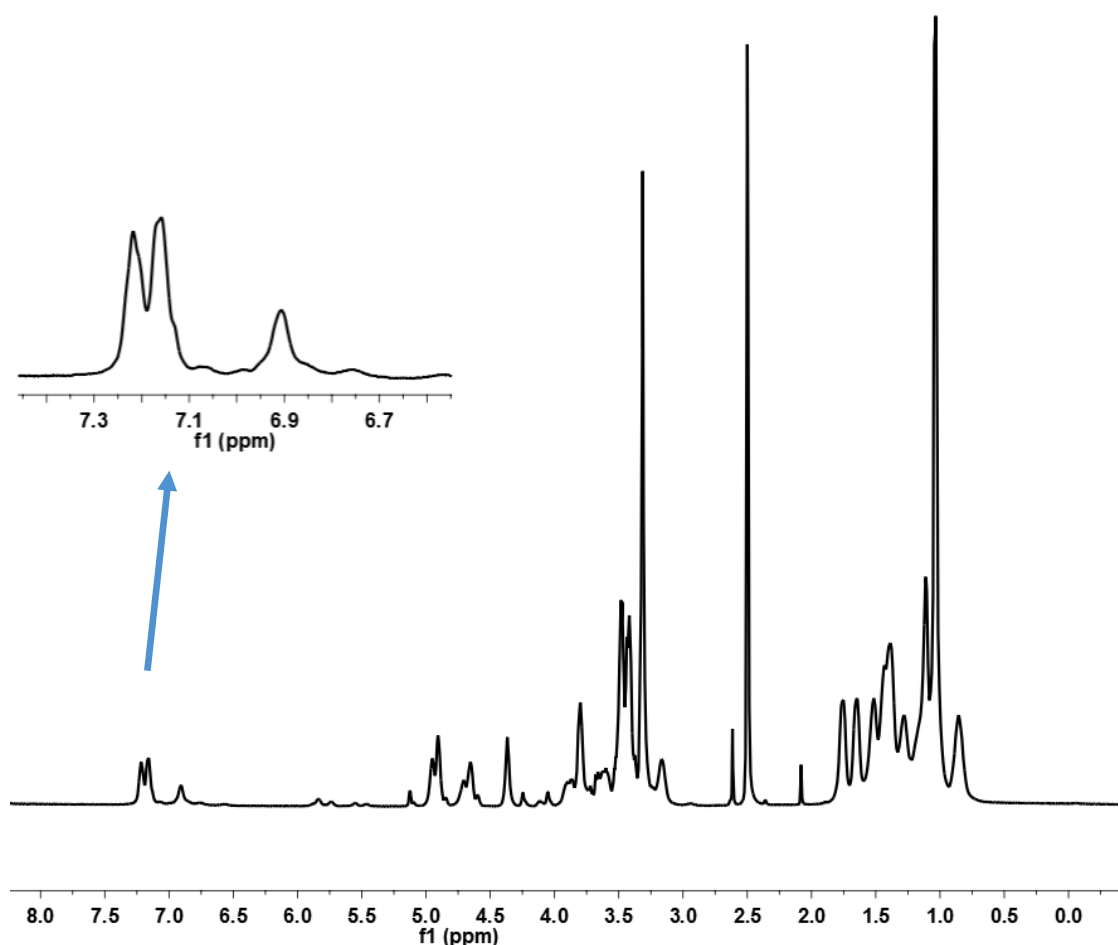


Figure 3. 17.  $^1\text{H}$  NMR spectrum of PU22 in  $\text{DMSO-}d_6$ . Bruker 500 MHz spectrometer.

NMR spectroscopy provided more conclusive evidence of the structure of PU 22. The corresponding chemical shifts for  $^1\text{H}$  NMR assignment are listed in Table 3.8. The peak at 6.9 and 7.2 ppm corresponds to urethane group. The signals between 4.0-5.2 ppm are evidence of the presence of isosorbide, in the structure of the polyurethane. The intense resonance at 1.2 ppm and 3.5 ppm shows to the presence of  $-\text{CH}_2$  from PPG, being the peaks of HMDI identified in the range 0.75-0.9 ppm.

In the work of M Rahman *et al*, polyurethanes were prepared using siloxane polyol poly(dimethyl siloxane), poly(propylene oxide glycol), poly (tetramethylene adipate glycol) and HMDI. In the  $^1\text{H}$ -NMR spectra of these polyurethanes were identified the protons of the

cycle of HMDI between 0.3-0.65ppm. On the other hand the -NH- of the urethane was identified at 7.18 ppm(35,49).

In synthesis of polyether poly(urethane urea), composed of poly(ethylene glycol) as the soft segment and 4,4'-methylenebis(cyclohexyl isocyanate) extended with ethylenediamine as the hard segment, the urethane group was identified in <sup>1</sup>H-NMR spectra at 7.09 and the proton corresponds to HMDI between 0.87-1.75 ppm(50).

Table 3. 8. Assignments of <sup>1</sup>H-NMR and chemical shifts of PU 22.

Assignment	Chemical Shifts PU22 (ppm)	Reference of Chemical shifts (ppm) *
1a, 2a,3a,4a,5a	0.75-0.80	0.3-0.65
12a	6.90-7.20	7.1-7.2
1i	4.10	3.90-4.00
2i	4.40	4.00-4.70
3i	3.60-3.90	3.70-4.40
4i	4.75	3.70-4.40
5i	5.00	5.00
6i	3.90	3.90-4.00
a	1.20	1.12-1.37
b	3.50	3.40-4.00
b'	3.60	3.40-4.00
c	4.80	4.70-5.00
*(7,16,35,49,50)		

### 3.3.2.2 Analysis of polyurethanes by <sup>13</sup>C-NMR spectroscopy

<sup>13</sup>C NMR is a powerful tool to identify monomer groups, photopolymers and copolymers molecules of a very well defined composition.

The study of the <sup>13</sup>C NMR spectra of the polyurethanes synthesized depicted in Figure 3.18 were relatively complex because the IPDI and the isosorbide employed in this work were used as mixture of isomers (cis/trans). Nevertheless, the experimental chemical shifts assigned are

according to the reference in the literature. The same phenomenon occurs in the interpretation of PU22, synthesized from HMDI (mixture of cis–trans isomers), the spectrum of this polymer is showed in Figure 3.19.

The structure presented in Figure 3.14 and Figure 3.15 were useful in the interpretation the  $^{13}\text{C}$  NMR spectra.

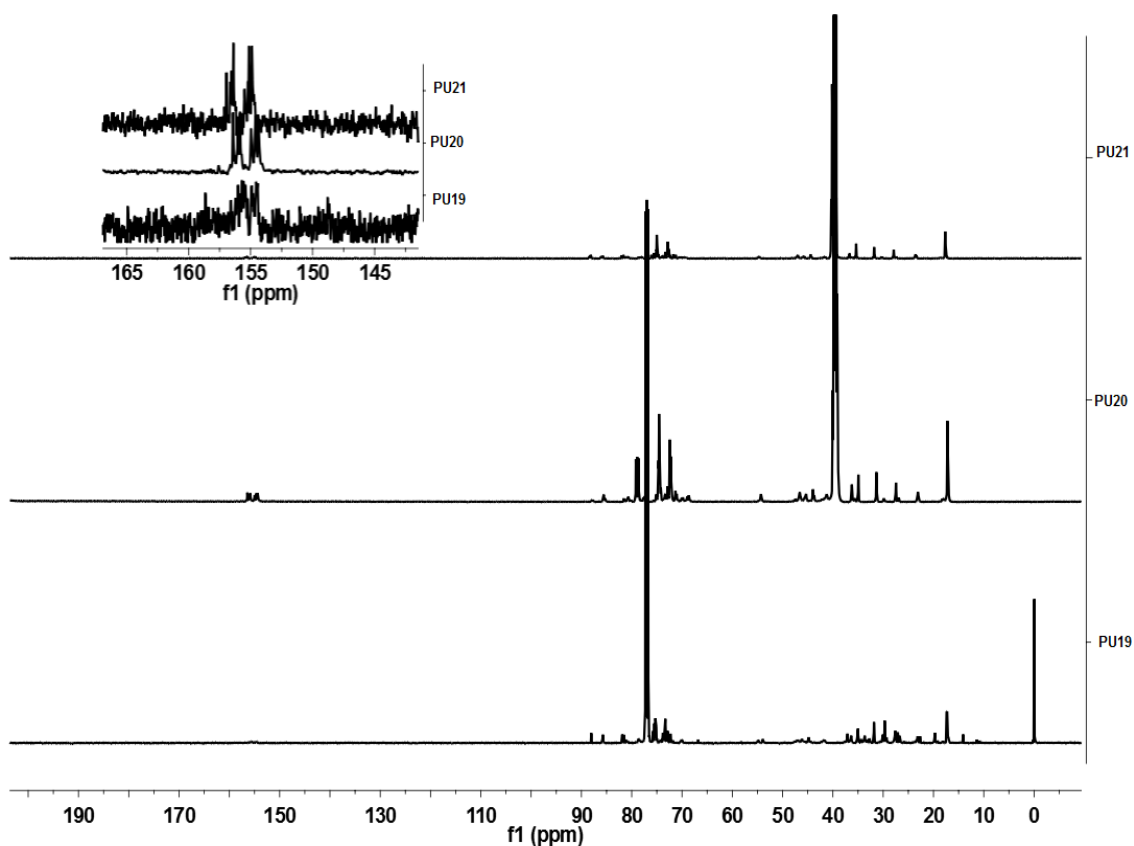


Figure 3. 18.  $^{13}\text{C}$  NMR spectra of the polyurethanes (500 MHz, in  $\text{DMSO-}d_6$  at room temperature).

In Table 3.9 summarizes the principal chemical shifts determined for the polyurethanes (44). The PU19, PU20, and PU21 displayed resonances of carbonyl group between 153–157 ppm. (16).

On the other hand, the peaks of a primary isocyanate at 121.7 ppm and the secondary -NCO- at 122.6 ppm, disappear in the  $^{13}\text{C}$  NMR spectra (44). These results indicate that the PUs are free of residual IPDI.

Table 3. 9. Assignments of  $^{13}\text{C}$  NMR chemical shifts for PU19, PU20 and PU21.

Assignment	Chemical Shifts PU19 (ppm)	Chemical Shifts PU20 (ppm)	Chemical Shifts PU21 (ppm)	Reference of Chemical shifts (ppm) *
Ca	16.5	16.7	16.5	17.12-18.24
C9	23.00	22.5	22.5	23.33-29.95
C7	27.9	26.8	26.7	27.19-27.71
C3	31.9	32.0	32.3	32.11-32.24
C8	34.5	34.3	34	34.92-34.97
C5	36.0	36	36	36.87-36.92
C6	-	41.5	41.5	43.63-44.13
C1	44	44	44	48.97-49.25
C4	45	45	45	46.40-46.64
C2	46	45.8	46	48.20-48.44
C10	54	54	54	51.18-57.24
Cb	68	68.7	68	72-78
C6i	70	70	70.5	70-75
C1i	71	71	71.5	70-71
Cc	72.5	72	72.5	72-78
C5i	73	73	75.5	70-80
Cb	74	74	75	72-78
C2i	75	75	75.5	70-75
C4i	81	80.5	81	80-81
C3i	85.5	85.5	86	79-81
C=O	154.3-157.5	154.3-157.5	153.3-157.5	153-157

\*(16,43,44,51)

$^{13}\text{C}$  NMR PU22

In Figure 3.19 is presented the  $^{13}\text{C}$  NMR spectrum of PU22. The urethane carbonyl resonance are identified between 154 ppm and 155.5 ppm. This result is similar to the findings observed in the characterization of the polyether urethane urea, prepared by reaction between HMDI and polyethylene glycol and ethylenediamine, where the carbonyls were detected at 155 ppm and 157 ppm (50).

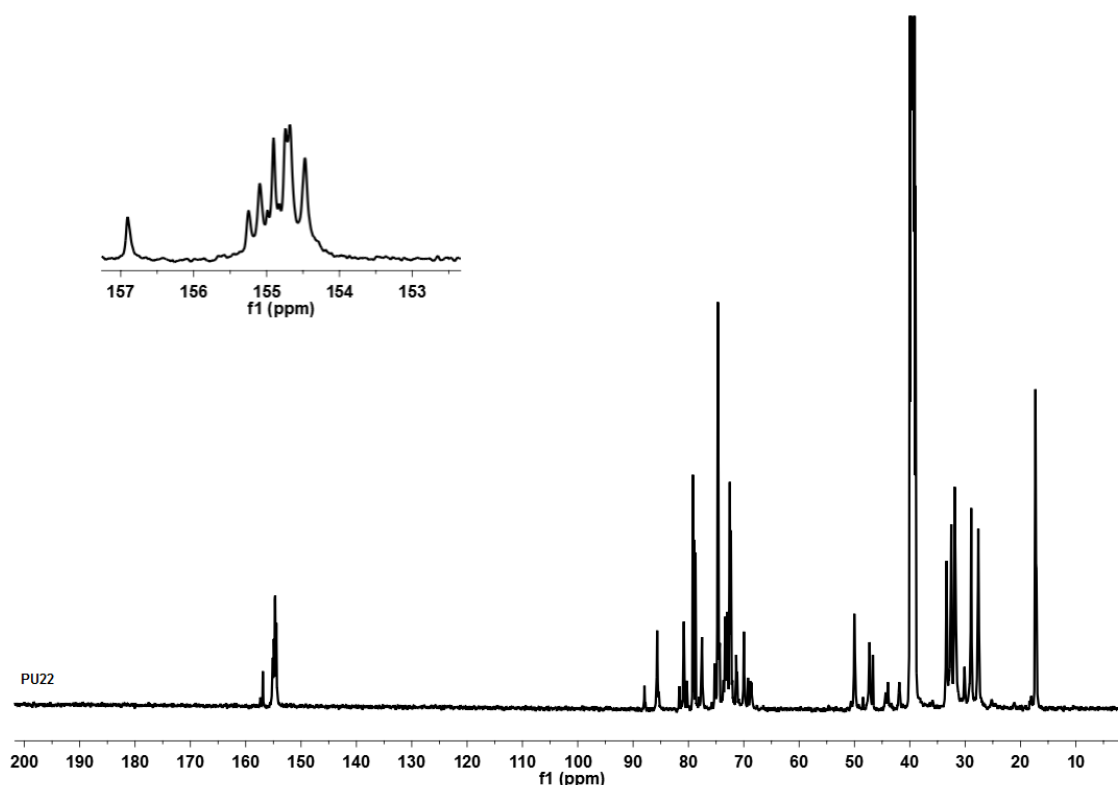


Figure 3. 19.  $^{13}\text{C}$  NMR spectrum of the PU 22 (500 MHz, in  $\text{DMSO-}d_6$  at room temperature).

In the spectrum displayed in Figure 3.19 the resonance at 124ppm, which is characteristic of isocyanate group, carbon atom is absent. These means that all the diisocyanate reacted (35) which was also confirmed by the FTIR analysis (Figure 3.7).

Two strong and sharp peaks centered at 27.2 and 71.1ppm were observed in the spectrum corresponding to the PPG structure. The signal at 51 ppm, confirmed the HMDI backbone (35). Table 3.10 summarizes all the chemical shift from  $^{13}\text{C}$  NMR spectrum of the PU 22.

Table 3. 10. Assignments of  $^{13}\text{C}$  NMR and chemical shifts for PU22.

Assignment	Chemical Shifts PU22 (ppm)	Reference of Chemical shifts (ppm) *
Ca	28.00	27.00
C2a	33.00	33.00
C3a	30.00	31.00
C4a	38.00	36.0
C1a	45.00	44.00
C5a	36.0	54.00
Cb	72	71.1-72
C6i	70	70-75
C1i	71	70-71
Cc	72.5	72-78
C5i	73	70-80
Cb	74	72-78
C2i	75	70-75
C4i	81	80-81
C3i	85.5	79-81
C6a	154.0-155.5	155-157
*(16,35,43,50)		

### 3.5 DOSY of Polyurethanes

The diffusion coefficient (D) represents the movement of a solute in a solvent. The D basically dependent on four factors: the size and shape of the solute, the temperature, and viscosity of the solvent(52). In the Figure 3.20 are presented the D corresponding to PUs.

The values of D measurement at different concentration are represented in Figure 3.21.

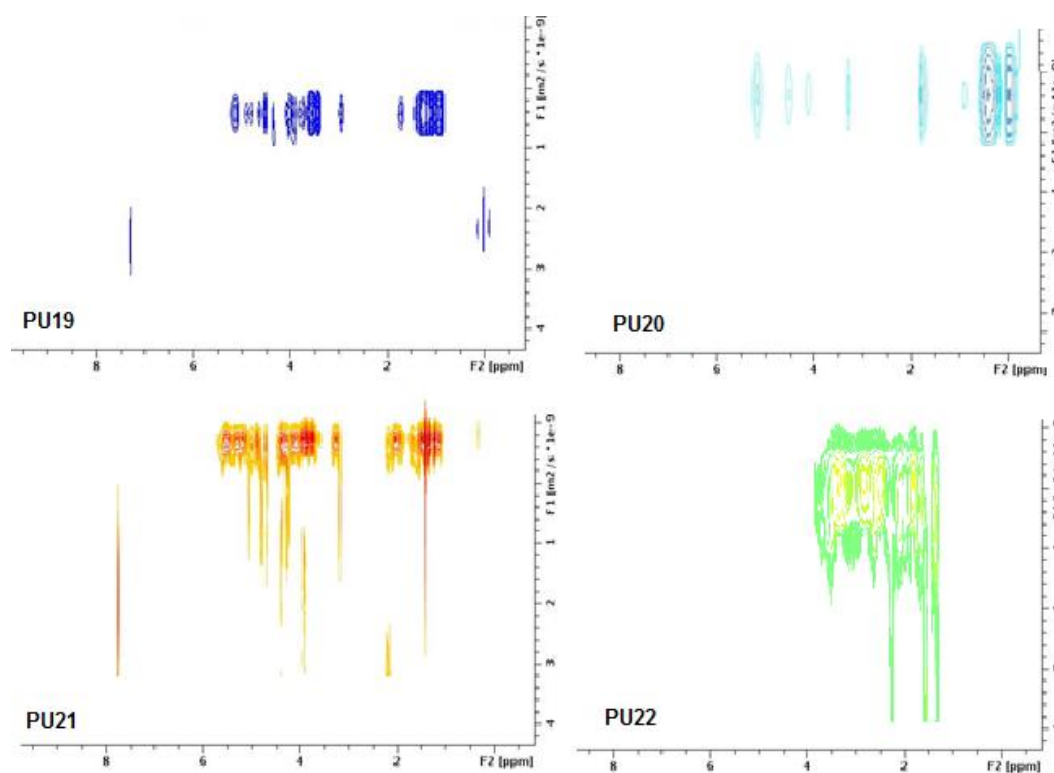


Figure 3. 20. DOSY spectra of polyurethanes ( $^1\text{H}$  500 MHz, in  $\text{DMSO-}d_6$  at room temperature, 0.348 mg/mL).

From different concentration of polyurethanes were determined the value of  $D$  for each polyurethane. The different measurement is observed in Figure 3.21.

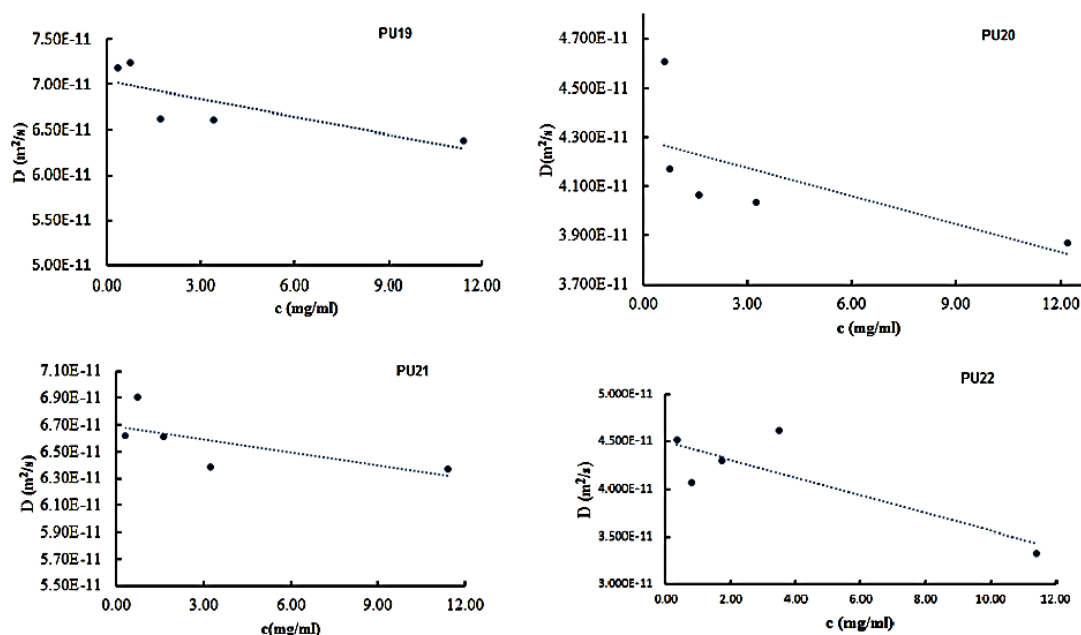


Figure 3. 21. Diffusion coefficient vs concentration for PU19–PU22 in DMSO- $d_6$ , measured at  $T = 30$  °C.

In the Table 3.11, the values obtained for the  $D$  of the corresponding PUs are presented.

Table 3. 11. Values of  $D$  for PU19- PU22, measured at  $T=30^\circ\text{C}$ , DMSO- $d_6$ .

Polyurethane	$D \cdot 10^{-11}$ ( $\text{m}^2/\text{s}^{-1}$ )
PU19	7.04
PU20	4.49
PU21	6.74
PU22	4.52

The values obtained for  $D$  indicate that PU19 and PU21 presented high mobility in DMSO at a temperature of the study. However according to expected the PU 20 showed slowly diffusion in the solvent at the condition of the test. PU 22 also presented slow mobility, according to the low diffusion coefficient. This result should be analyzed together with the results of the molecular weight measurement. However, because the temperature and viscosity of the solvent are the same in the measurements,  $D$  values depend only of: the size and shape of the polyuretane, probably the PU 20 and PU22, present higher size and shape that the other polyuretanes, in this condition of the study.

### 3.6 Hydrodynamic radii

The values of  $r_h$  for the polyurethanes are presented in Table 3.12.

Table 3. 12. Values of  $r_h$  for PU19-PU22, measured at T=30 °C, DMSO- $d_6$

Polyurethane	$r_h$ 10 <sup>-9</sup> (m)	$\Delta r_h$ 10 <sup>-9</sup> (m)
PU19	1.62	0.04
PU20	2.65	0.15
PU21	1.69	0.04
PU22	2.52	0.19

The  $r_h$  according to Stokes-Einstein equation are inversely proportional to the value of D. The  $r_h$  of PU20 and PU22 are higher than the PU19 and PU21, probably they present higher size and shape.

### 3.7 Result of the analysis of polyurethanes by GPC

Table 3. 13. Average Molecular weight by GPC.

Polyurethane	Mw (Dalton)	Mn (Dalton)	Dispersity ( $D=M_w/M_n$ )
PU19	15600	10300	1.50
PU20	19200	12800	1.48
PU21	9200	7200	1.27
PU22	23500	15140	1.55

The higher number average molecular weight was obtained for the PU22, because the polyurethane presented  $D = 4.52 \cdot 10^{-11} \text{ m}^2/\text{s}^{-1}$ . The lower number average molecular weight was to PU21 because present higher diffusion coefficient and lower  $r_h$ .

The polyurethane synthesized presented similar polydispersity index and the values are closed to 1.

### 3.8 MALDI-TOF

The objectives of the use of the MALDI-TOF technique are related to the determination of the molecular weight of the polyurethane without fragmentation.

The MALDI-TOF mass spectra of polyurethanes were obtained using DHB matrix and sodium iodide salt as the cationization reagent, showed in Figure 3.22, Annexes 4-7 and Table 3.14. The MALDI-TOF spectra contains one mass distributions in the range 400-4200 Da with mass intervals corresponding to the molar mass of the repeating unit (368 Mw and 408 Mw).

The PU 19 present one distribution, at  $m/z = 368n + 22.99(\text{Na}^+)$  that corresponds to the D-isosorbide and IPDI groups. This distribution allows calculated a Mw of 948.57 Dalton.

The PU 20 presents one distribution at  $m/z = 58N$  corresponding to fragment of PPG and another at  $m/z = 368n + 22.99(\text{Na}^+)$  corresponding to IPDI+ D-isosorbide. This last allows the calculation Mw of 756.6 Dalton.

PU 21 present one distribution of chain at  $m/z = 368n + 22.99(\text{Na}^+)$ , that allows calculation Mw of 975.94 Dalton.

Finally, the PU 22 present one distribution at  $m/z = 408n + 22.99(\text{Na}^+)$  corresponding to fragment of PPG, HMDI + D-isosorbide, that allow calculated a Mw of 921.1 Dalton.

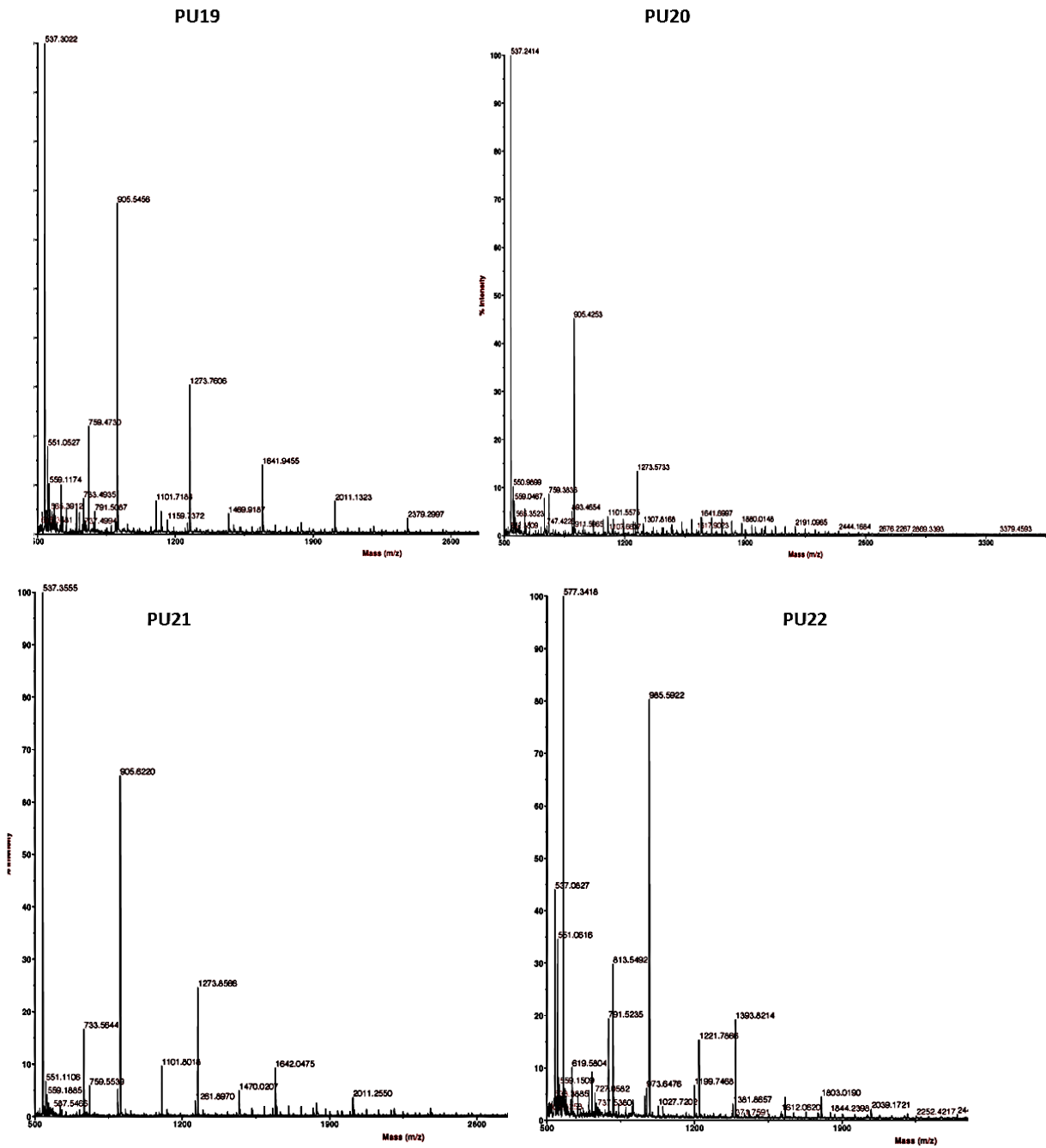


Figure 3. 22. MALDI-TOF mass spectra of polyurethane after deisotoping procedure.

Table 3. 14. Higher mass identified by MALDI -TOF and mass calculated according to molar ratios.

	<b>Maldi-TOF MS</b>	<b>Calculated Mass</b>
PU19	2379	3013.67
PU20	3379	4036.80
PU21	2378	3195.14
PU22	3691	3280.30

The values showed in Table 3.14 indicated that the polymer with higher molecular weight, correspond to PU22, this agrees with the molecular weight measurement by GPC. Nevertheless, the values of Mw for each polymer obtained by MALDI-TOF are different compared with the determination done by GPC. The difference is justified by the hydrodynamic volume of the polymers. The measurement of Mw obtained by GPC was performed using polystyrene as a standard reference. The hydrodynamic volume of polystyrene is different from the polyurethane; however, this polymer is the available reference in GPC for polyurethane analysis.

The MALDI-TOF and GPC demonstrated, the relation between the molecular weight expected according to the molar ratios employed in the synthesis of the polymer.

The GPC didn't present any accuracy in the values of Mw when compared with molecular weight determined according to molar ratios of PU19, PU21, and PU22. However, the MALDI- TOF revealed some correspondence between the molecular weight determined and the molecular weight calculated according the molar ratios used in the synthesis.

### 3.9 Cytotoxicity assay

The direct contact tests were carried out for PU19, PU20, PU21, PU22 and control slide glass. As shown in Figure 3.23, the HaCaT shows proliferation in contact with PU19.

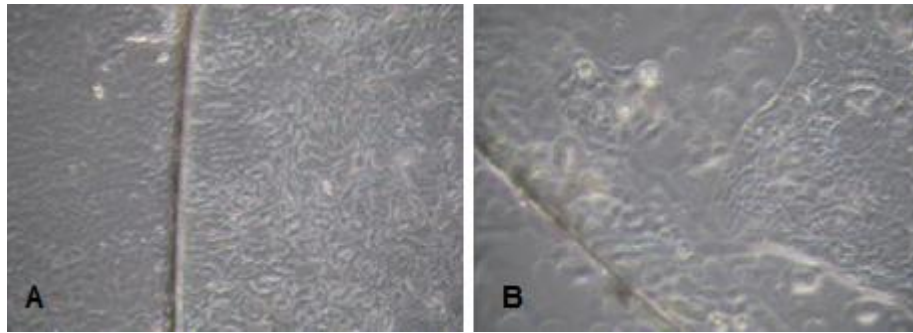
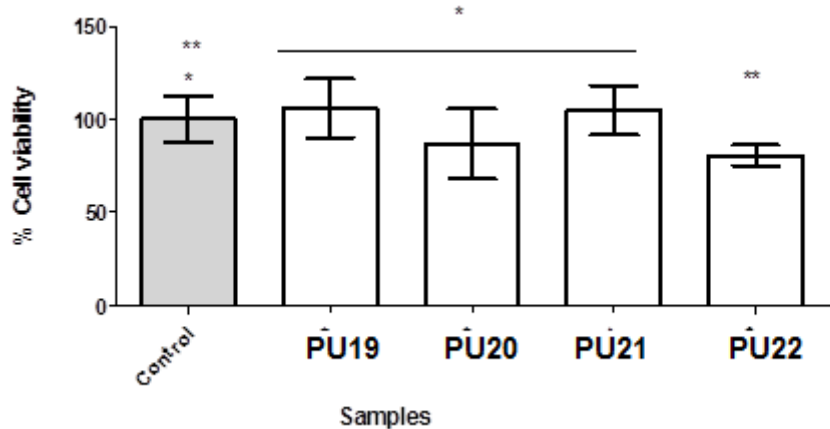


Figure 3. 23. HaCaT cells after 72h of proliferation a) glass slide (control) , b) PU19.

The image obtained in Figure 3.23 show a monolayer of HaCaT in contact with the PU19 after 72h and demonstrated the compatibility of the polymer with keratinocyte cells.

From Figure 3.24 it can be observed that polymers PU19, PU20 and PU 21 presents a cell viability (measured by the MTT reduction) that did not differ significantly from the control (glass slide) whereas the PU22 polymer the cell viability is  $80\% \pm 5\%$  (significantly different from control for  $p < 0.05$ )



\* Not significantly difference ( $p < 0.05$ ), \*\* significantly different ( $p < 0,05$ ).

Figure 3. 24. HaCaT cell viability by MTT after proliferation under different polymers material. Control (glass slide), (mean  $\pm$  SD, n = 6).

## 4. Conclusions

The structure of polyurethanes was confirmed by FTIR,  $^1\text{H}$  and  $^{13}\text{C}$  NMR spectroscopy in all the samples. This observation confirms the higher reactivity of the secondary NCO group of IPDI compared to the primary group.

The NMR spectroscopy showed the properties of the polyurethane, behind the elucidation of D and the hydrodynamic radii from DOSY. The polyurethanes with highest D, present lowest hydrodynamic radius, in the conditions of the study.

The GPC, allowed the determination of the distribution of molecular weight according to a standard reference. The MALDI-TOF confirms that the molecular weights determined is according to the molar ration employed in the polyurethanes synthesized.

## 5. References

1. Sarkar D, Yang JC, Sen Gupta A, Lopina ST. Synthesis and characterization of L-tyrosine based polyurethanes for biomaterial applications. *J Biomed Mater Res - Part A*. 2009;90(1):263–71.
2. Han J, Chen B, Ye L, Zhang AY, Zhang J, Feng ZG. Synthesis and characterization of biodegradable polyurethane based on poly( $\epsilon$ -caprolactone) and L-lysine ethyl ester diisocyanate. *Front Mater Sci China*. 2009;3(1):25–32.
3. Besse V, Auvergne R, Carlotti S, Boutevin G, Otazaghine B, Caillol S, et al. Synthesis of isosorbide based polyurethanes: An isocyanate free method. *React Funct Polym*. 2013;73(3):588–94.
4. Chen TK, Tien YI, Wei KH. Synthesis and characterization of novel segmented polyurethane clay nanocomposite via poly( $\epsilon$ -caprolactone)/clay. *J Polym Sci Part a-Polymer Chem*. 1999;37(13):2225–33.
5. Bachmann F, Reimer J, Ruppenstein M, Thiem J. Synthesis of novel polyurethanes and polyureas by polyaddition reactions of dianhydrohexitol configured diisocyanates. *Macromol Chem Phys*. 2001;202(17):3410–9.
6. Guelcher SA, Gallagher KM, Didier JE, Klindedinst DB, Doctor JS, Goldstein AS, et al. Synthesis of biocompatible segmented polyurethanes from aliphatic diisocyanates and diurea diol chain extenders. *Acta Biomater*. 2005 Jul;1(4):471–84.
7. Kim H-J, Kang M-S, C; K s J, Myoung-Seon G. Synthesis of highly elastic biocompatible polyurethanes based on bio-based isosorbide and poly(tetramethylene glycol) and their properties. *J Biomater Appl*. 2014;29(3):454–64.
8. Abraham GA, Marcos-Fernández A, San Román J. Bioresorbable poly(ester-ether urethane)s from L-lysine diisocyanate and triblock copolymers with different hydrophilic character. *J Biomed Mater Res - Part A*. 2006;76(4):729–36.
9. Zhang C, Zhang N, Wen X. Synthesis and characterization of biocompatible, degradable, light-curable, polyurethane-based elastic hydrogels. *J Biomed Mater Res Part A*. 2007;Volume 82A(3):521–776.
10. Spiridon I, Popa VI. Monomers, Polymers and Composites from Renewable Resources. *Monomers, Polymers and Composites from Renewable Resources*. 2008. 289-304 p.
11. Gogolewski S, Gorna K, Zaczynska E, Czarny A. Structure-property relations and

- cytotoxicity of isosorbide-based biodegradable polyurethane scaffolds for tissue repair and regeneration. *J Biomed Mater Res - Part A*. 2008;85(2):456–65.
12. Fenouillot F, Rousseau A, Colomines G, Saint-Loup R, Pascault JP. Polymers from renewable 1,4:3,6-dianhydrohexitols (isosorbide, isomannide and isoidide): A review. *Prog Polym Sci*. Elsevier Ltd; 2010;35(5):578–622.
  13. Stoss Peter; Hemmer Reinhard. 1,4:3,6-Dianhydrohexitols. *Adv Carbohydr Chem Biochem*. 1991;49:93–173.
  14. Marques MFF, Gordo PM, De Lima AP, Queiroz DP, De Pinho MN, Major P, et al. Free-volume studies in polycaprolactone/poly(propylene oxide) urethane/urea membranes by positron lifetime spectroscopy. In: *Acta Physica Polonica A*. 2008. p. 1359–64.
  15. Chattopadhyay DK, Raju NP, Vairamani M, Raju KVS. Structural investigations of polypropylene glycol (PPG) and isophorone diisocyanate (IPDI) based polyurethane prepolymer by matrix-assisted laser desorption/ionization time-of-flight (MALDI-TOF)-mass spectrometry. *Prog Org Coatings*. 2008;62(2):117–22.
  16. Prabhakar A, Chattopadhyay DK, Jagadeesh B, Raju KVS. Structural investigations of polypropylene glycol (PPG) and isophorone diisocyanate (IPDI)-based polyurethane prepolymer by 1D and 2D NMR spectroscopy. *J Polym Sci Part A Polym Chem*. 2005;43(6):1196–209.
  17. Wen TC, Wang YJ, Cheng TT, Yang CH. The effect of DMPA units on ionic conductivity of PEG-DMPA-IPDI waterborne polyurethane as single-ion electrolytes. *Polymer (Guildf)*. 1999;40(14):3979–88.
  18. Boyer A, Lingome CE, Condassamy O, Schappacher M, Moebs-Sanchez S, Queneau Y, et al. Glycolipids as a source of polyols for the design of original linear and cross-linked polyurethanes. *Polym Chem*. 2013;4(2):296–306.
  19. Price WS. Pulsed-Field Gradient Nuclear Magnetic Resonance as a Tool for Studying Translational Diffusion. Part 1. Basic Theory. *Concepts Magn Reson*. 1997;9(5):no-no.
  20. Price WS. ChemInform Abstract: Pulsed-Field Gradient Nuclear Magnetic Resonance as a Tool for Studying Translational Diffusion. Part 1. Basic Theory. *ChemInform*. 2010;28(50):no-no.
  21. Geil B. Measurement of translational molecular diffusion using ultrahigh magnetic field gradient NMR. *Concepts Magn Reson*. 1998;10(5):299–321.

22. Mondiot F, Loudet JC, Mondain-Monval O, Snabre P, Vilquin A, Würger A. Stokes-Einstein diffusion of colloids in nematics. *Phys Rev E - Stat Nonlinear, Soft Matter Phys.* 2012;86(1).
23. Holz M, Mao XA, Seiferling D, Sacco A. Experimental study of dynamic isotope effects in molecular liquids: Detection of translation-rotation coupling. *J Chem Phys.* 1996;104(2):669–79.
24. Allcock HR, Lampe FW. *Contemporary Polymer Chemistry*,. Prentice Hall: New Jersey, 3rd Ed.,. 2003.
25. Barmar M, Barikani M, Kaffashi B. Synthesis of Ethoxylated Urethane and Modification with Cetyl Alcohol as Thickener. *Iran Polym J.* 2001;10(5):331–5.
26. Sperling LH. *Introduction to Physical Polymer Science*. Polymer. 2005. 845 p.
27. International Organization for Standardization. *Biological Evaluation of Medical Devices Part 5: Tests for In Vitro Cytotoxicity*. Iso 10993–5. 2009;5:1–52.
28. Cadete A, Figueiredo L, Lopes R, Calado CCR, Almeida AJ, Gonçalves LMD. Development and characterization of a new plasmid delivery system based on chitosan-sodium deoxycholate nanoparticles. In: *European Journal of Pharmaceutical Sciences*. 2012. p. 451–8.
29. Lopes R, Eleutério C V., Gonçalves LMD, Cruz MEM, Almeida AJ. Lipid nanoparticles containing oryzalin for the treatment of leishmaniasis. In: *European Journal of Pharmaceutical Sciences*. 2012. p. 442–50.
30. MCHEN-CHI KH-CCW-P; M. Synthesis and characterization of a clay/waterborne polyurethane nanocomposite. *J Mater Sci.* 2005;40:179–185.
31. Ferreira P, Pereira R, Coelho JFJ, Silva AFM, Gil MH. Modification of the biopolymer castor oil with free isocyanate groups to be applied as bioadhesive. *Int J Biol Macromol.* 2007;40(2):144–52.
32. Ferreira P, Silva AFM, Pinto MI, Gil MH. Development of a biodegradable bioadhesive containing urethane groups. *J Mater Sci Mater Med.* 2008;19(1):111–20.
33. Li G, Li P, Qiu H, Li D, Su M, Xu K. Synthesis, characterizations and biocompatibility of alternating block polyurethanes based on P3/4HB and PPG-PEG-PPG. *J Biomed Mater Res Part A.* 2011 Jul;98A(1):88–99.
34. Alves P, Coelho JFJ, Haack J, Rota A, Bruinink A, Gil MH. Surface modification and characterization of thermoplastic polyurethane. *Eur Polym J.* 2009;45(5):1412–9.

35. Rahman MM, Hasneen A, Chung I, Kim H, Lee W-K, Chun JH. Synthesis and properties of polyurethane coatings: the effect of different types of soft segments and their ratios. *Compos Interfaces*. 2013;20(1):15–26.
36. Caracciolo PC, Buffa F, Abraham GA. Effect of the hard segment chemistry and structure on the thermal and mechanical properties of novel biomedical segmented poly(esterurethanes). *J Mater Sci Mater Med*. 2009;20(1):145–55.
37. Kricheldorf HR, Chatti S, Schwarz G, Krüger RP. Macrocycles 27: Cyclic Aliphatic Polyesters of Isosorbide. *J Polym Sci Part A Polym Chem*. 2003;41(21):3414–24.
38. Ferreira P, Coelho JFJ, Pereira R, Silva AFM, Gil MH. Synthesis and characterization of a poly(ethylene glycol) prepolymer to be applied as a bioadhesive. *J Appl Polym Sci*. 2007 Jul 15;105(2):593–601.
39. Vieira A, Ferreira P, Coelho J GM. Photocrosslinkable Polymers for Biomedical Applications. *Int J Biol Macromol*. 2008;43:325–32.
40. Ferreira P, Coelho J GM. Developmet of a new photocrosslinkable biodegradable bioadhesive. *Int J Pharm*. 2008;352:172–81.
41. Daniela da Silva A, Martinez J BJ. Influence of the storage of reactive urethane quasi-prepolymers in their compositions and adhesion properties. *Int J Adhes Adhes*. 2007;28:29–37.
42. Zhu R, Wang Y, Zhang Z, Ma D, Wang X. Synthesis of polycarbonate urethane elastomers and effects of the chemical structures on their thermal, mechanical and biocompatibility properties. *Heliyon*. Elsevier Ltd; 2016;2(6).
43. Zhang S, Cheng L, Hu J. NMR studies of water-borne polyurethanes. *J Appl Polym Sci*. 2003;90(1):257–60.
44. Götz H, Beginn U, Bartelink CF, Grünbauer HJM, Möller M. Preparation of isophorone diisocyanate terminated star polyethers. *Macromol Mater Eng*. 2002;287(4):223–30.
45. Asha SK, Thirumal M, Kavitha A, Pillai CKS. Synthesis and curing studies of PPG based telechelic urethane methacrylic macromonomers. *Eur Polym J*. 2005;41(1):23–33.
46. Woo; CI, Mamoru;Nomura, Hyun; KJ. Synthesis and aqueous solution behavior of water-soluble polyurethane (IPDI-PPG-DMPA) resin. 2000;201(17 November):2221–

- 2227.
47. Gunther H. NMR spectroscopy. John Wiley. 1980. 342-343 p.
  48. He X, Zhai Z, Wang Y, Wu G, Zheng Z, Wang Q, et al. New method for coupling collagen on biodegradable polyurethane for biomedical application. *J Appl Polym Sci.* 2012;126(SUPPL. 1).
  49. Rahman MM, Hasneen A, Jo NJ, Kim HI, Lee WK. Properties of Waterborne Polyurethane Adhesives with Aliphatic and Aromatic Diisocyanates. *J Adhes Sci Technol.* 2011;25(16):2051–62.
  50. Wang H, Kao H, Digar M, Wen T. FTIR and Solid State  $^{13}\text{C}$  NMR Studies on the Interaction of Lithium Cations with Polyether Poly(urethane urea). *Macromolecules.* 2001;34(3):529–37.
  51. Corcuera MA, Rueda L, Fernandez D'Arlas B, Arbelaiz A, Marieta C, Mondragon I, et al. Microstructure and properties of polyurethanes derived from castor oil. In: *Polymer Degradation and Stability.* 2010. p. 2175–84.
  52. Holz M, Heil SR, Sacco A. Temperature-dependent self-diffusion coefficients of water and six selected molecular liquids for calibration in accurate  $^1\text{H}$  NMR PFG measurements. *Phys Chem Chem Phys.* 2000;2(20):4740–2.

**Chapter 4: New polyurethane nail lacquers for the delivery  
terbinafine – formulation and antifungal activity evaluation**



---

This chapter was adapted from the published paper *in press*:

Barbara S. Gregorí Valdes, Ana Paula Serro, Paulo M. Gordo, Alexandra Silva, Lídia Gonçalves, Ana Salgado, Joana Marto, Diogo Baltazar, Rui Galhano dos Santos, João Moura Bordado, Helena Margarida Ribeiro. New polyurethane nail lacquers for the delivery of terbinafine – formulation and antifungal activity evaluation. *Journal of Pharmaceutical Sciences*. 2017 Jun; 106(6): 1570-1577.



## 1.Introduction

Tinea unguium, a fungal nondermatophytic nail infection is commonly referred as onychomycosis. This disease is often underestimated, being considered as “only” a simple cosmetic problem. As such, the solutions for its treatment and the investment made in developing new ones are limited. However, this disease causes, in patients suffering from such infection, pernicious effects on its interaction with society as well as emotional and psychological damage (1).

One of the solutions to treat such condition is the use of nail lacquer formulations, which emerged in the pharmaceutical market in the late 1990's (2). Generally, they comprise the drug dispersed in a polymer solution, which, after solvent evaporation, leaves a film on the nail plate. Upon solvent evaporation, a polymeric water resistant film is formed that acts as a drug reservoir, allowing the drug to permeate through the nail plate continuously (3). There are many drugs active against *Tricophyton rubrum*, the dermatophytic fungus responsible for onychomycosis (4,5). One of those drugs is terbinafine, an active antifungal drug with a minimum inhibitory concentration (MIC) against *Tricophyton rubrum* of 0.004-0.06 µg/mL (6). Nail lacquers are being considered as a solution to deliver relevant drugs to infected nails, although there is no formulation containing terbinafine yet. The cause of this oversight is related to difficulties in formulating vehicles using currently available polymer excipients. The polymeric formulation must be carefully chosen since it may influence the therapeutic nail lacquer efficacy. Chitosan-based water soluble polymers allow an excellent drug permeation and adhesion to the nail plate, having a soft, flexible and matte finish, which may improve patient compliance (7,8). However, this excipient leads to a faster drug release when in contact with water, which occurs during the patient daily hygiene routines. Hydrophobic polymers, possessing a poor solubility in water, produce more durable and harder films with a glossier finish (9). Therefore, the development of new polymeric materials that adhere to the nail plate and allow a continuous transungual drug delivery is still a challenge. Polyurethane (PU) has been applied in the medical and pharmaceutical industries since 1970 in prosthesis (3), microspheres for bone regeneration (11) and patches (12). However, the use of PU as a vehicle for transungual drug delivery has never been explored. Aliphatic PUs are biocompatible and present an excellent nail plate adhesion, depending on the monomers used for their synthesis. Bachmann et al. have proven that the presence of carbohydrate monomers

like fructose, glucose, and isosorbide as chain extenders of PUs, increases the biodegradability of their polymers (13). Furthermore, a PU based on PEG 400 has been synthesized by the reaction of PEG hydroxyl groups with isophorone diisocyanate, presenting good bioadhesive properties (14). Another study disclosed a biomedical PU obtained through the reaction of hexamethylene diisocyanate, poly( $\epsilon$ -caprolactone) and isosorbide. Such synthesis leads to a biodegradable and biocompatible elastomeric PU with an enhanced affinity for cells and tissues (15).

The manuscript presented herein describes a new nail lacquer employing novel PUs formulations. The biocompatibility, as well as the wettability and the free volume of the holes found in the film formulations, were evaluated. Additionally, the nail lacquers' morphology, bioadhesion and viscosity were assessed and *in vitro* release tests were performed. Finally, the *in vitro* antifungal activity was screened for the formulation which presented the best properties.

## 2. Materials and methods

### 2.1 Materials

D-isosorbide was provided by Acros (Portugal). IPDI, Desmodur<sup>®</sup> I, was purchased from Bayer Material Science (Germany) and PPG, VORANOL<sup>®</sup> 1010L, from Dow Chemical (Germany). The DMDEE was provided by Aldrich (Germany). Anhydrous ethanol, butyl acetate and ethyl acetate were acquired from Carlo Erba (France). Terbinafine hydrochloride (TH) manufactured by Uquifa México S.A. was kindly offered by Generis (Portugal). Tagat<sup>®</sup> CH 60 (PEG-60 Hydrogenated Castor Oil) was purchased from Evonik (Germany). Methanol HPLC grade was purchased from Panreac (Spain). Triethanolamine was provided by Merck (Germany).

### 2.2 Methods

#### 2.2.1 Preparation of the PU based nail lacquers

Three PU were synthesized using the quasi-pre-polymerization method. They were prepared by reacting IPDI and PPG in the presence of the catalyst DMDEE. D-isosorbide was added

afterwards. The mole ratios used for each synthesis were: PU 19 (6:1:5), PU 20 (6:2:5), PU 21 (6:1:6), of IPDI, PPG and D-isosorbide, respectively as previously was described in chapter 3. Three PU-based nail lacquer formulations containing terbinafine were prepared according the formulas described in Table 4.1. Firstly, PUs were fully solubilized in ethanol under stirring (200 rpm). Butyl acetate, ethyl acetate and terbinafine were added afterwards, one by one, until their complete dissolution.

Table 4. 1. PU, terbinafine based nail lacquers composition.

	<b>Formulation A PU19 -10%</b>	<b>Formulation B PU 20-10%</b>	<b>Formulation C PU 21-10%</b>
	<b>TH</b>	<b>TH</b>	<b>TH</b>
PU 19	10.0	--	--
PU 20	--	10.0	--
PU 21	--	--	10.0
Terbinafine HCl	1.0	1.0	1.0
Ethyl acetate	7.8	7.8	7.8
Butyl acetate	10.0	10.0	10.0
Ethanol	71.2	71.2	71.2

### 2.2.2 *In vitro* cytotoxicity assay

The biocompatibility of the PU based nail lacquers was evaluated *in vitro* by direct contact with cells, following the ISO 10993-5:2009 recommendation guidelines (16). Each nail lacquer formulation material was added to a 0.5 mL of HaCaT cell suspension [a spontaneously immortalized human keratinocyte cell line (CLS, Germany)], in fresh culture medium [RPMI-1640<sup>®</sup> (Gibco, UK) medium supplemented with 10% fetal bovine serum (FCS, Life Technologies, Inc., UK), penicillin (100 IU/mL), and streptomycin (100 µg/mL)] ( $2.5 \times 10^4$  cells/mL), in sterile 24-well plates. Glass slides without any formulation were used as control. The plates were incubated for 72 h in a humidified atmosphere of 5% CO<sub>2</sub> at 37 °C, without refreshing the culture medium. For cell proliferation quantification, the general cell viability endpoint MTT reduction (3-(4,5-dimethyl-2-thiazolyl)-2,5-diphenyl-2H-tetrazolium bromide) was used (17,18). Accordingly, the previous culture medium was removed and replaced with a fresh medium containing 0.5 mg/mL of MTT. The cells were further incubated for 3 h. In the plates containing the reduced MTT, the medium was removed

and the intracellular formazan crystals were solubilized and extracted with dimethylsulfoxide. After 15 min, at room temperature, the absorbance was measured at 570 nm in a Microplate Reader (FLUOstar Omega, BMGLabtech, Germany).

The data are expressed as the mean and the respective standard deviation (mean  $\pm$  SD) of 6 experiments. The statistical evaluation of data was performed using one-way analysis of variance (ANOVA). The Tukey–Kramer multiple comparison tests (GraphPad PRISM 5 software, USA), were used to compare the significance of the difference between the groups; a  $p < 0.05$  was accepted as statistically significant.

### 2.2.3 Determination of wettability by measurement of contact angle

The measurement of the static contact angle of water with the therapeutic nail lacquer samples was carried out by the sessile drop method (19).

Drops (2 – 4  $\mu$ L) were generated with a micrometric syringe and deposited on the substrate surface, inside a temperature-controlled chamber (25 °C), which had previously been saturated with water to avoid the drops' evaporation. A sequence of images, obtained with a video camera (JVC Colour) mounted on a microscope (Wild M3Z) and connected to a frame grabber (Data Translation DT3155), was recorded during 60 s, starting from the moment of the drop deposition. Images were analyzed using the axisymmetric drop shape analysis-profile (ADSA-P) program. At least 6 drops were analyzed on the air-facing surfaces of each film.

### 2.2.4 PALS

The PALSs of the nail lacquer formulations films were determined by detecting the prompt  $\gamma$ -ray (1.28 MeV) from the nuclear decay that accompanies the emission of a positron from the  $^{22}\text{Na}$  radioisotope and the annihilation  $\gamma$ -ray (0.511 MeV). A fast-fast coincidence circuit of the PALS setup (featuring Pilot-U scintillators and XP2020 photomultipliers), with a time resolution of approximately 260 ps (FWHM), was used to record the positron lifetime spectra. The positron  $^{22}\text{Na}$  source (ca.  $\sim 10\mu\text{Ci}$ , closed between Kapton  $\gamma$  foils) was sandwiched by two identical samples. Several spectra were collected at room temperature. The lifetime spectra had a total number of ca.  $4 \times 10^6$  integral counts and were evaluated using the LT (version 9) software (20,21).

### 2.2.5 SEM

The SEM Field Emission Gun (FEG) SEM JEOL JSM-7001F was used to obtain images of the surface of each therapeutic nail lacquer formulation film. Human nails were obtained with nail clippers from the fingers of a healthy Caucasian female of 24 years of age, after ethical approval and informed consent. The nail plates were cut 24 h before each test. The nail plates were stored in a glass jar with paper moistened with distilled water to avoid dehydration. First, the formulations were applied on the nails, by using a thin rectangular plastic rod (3 x 0,5 mm). The nails were dried at room temperature. The samples were gold sputter coated (10 nm) in a chromium deposition equipment (Q150T ES, Quorum Technologies).

### 2.2.6 Adhesion test

The assessment of the adhesion of therapeutic nail lacquers was developed as an adaptation of ISO 2409:2013(22). This manual measurement of film adhesion is used to measure the resistance of paint coatings with a Kit Elcometer<sup>®</sup> 107. A quantity of  $0.25 \pm 0.02$  g of the therapeutic nail lacquers were weighed and spread in cow horn samples, to create a homogeneous film. Cow horn samples were cut in cylinders 35 mm in diameter, 1.5 mm thick. The samples were polished with a 600 mesh SiC paper under flowing water for lubrication, and then rinsed with water. Afterwards, the samples were dried with absorbing paper and stored at room temperature. The nail lacquer formulations were applied on the cow horn samples and dried at room temperature for 15 min. Subsequently, the samples with nail lacquer films were cut in a lattice pattern with a cutting blade (Kit Elcometer<sup>®</sup> 107, France). The first cut was made at 45° angle to the direction of the grain and the second cut was repeated at 90° angle to the first. Afterwards, the sample was brushed (Kit Elcometer<sup>®</sup> 107, France). Then, an adhesive tape (ISO 2409 Elcometer<sup>®</sup> 107, France) with the size of the cow horn samples, was placed over the lattice pattern. The adhesive tape was removed at an angle of 60° with the surface, and the latter was examined and evaluated according to the classification of the ISO 2409:2013 guideline, where 5 refers to ‘very damaged’, meaning the lattice pattern and the sample have bad adhesion, and 1 refers to a value for good adhesion, corresponding to the integrity of the lattice pattern. The test was repeated 5 times for each therapeutic nail lacquer.

### 2.2.7 Viscosity measurement

The determination of viscosity was performed in a cone-plate Brookfield® viscometer, model DV-II + Pro coupled with a constant temperature bath, previously gauged with a CPE-40 spindle. The temperature of the measurement was  $32 \pm 0.2$  °C, shear rate  $375 \text{ s}^{-1}$  and shear stress  $0.8\text{-}1 \text{ N/cm}^2$ . A volume of 500  $\mu\text{L}$  of therapeutic nail lacquer was used for this test.

### 2.2.8 *In vitro* release of terbinafine hydrochloride from therapeutic nail lacquers

For the *in vitro* release studies of terbinafine release from the therapeutic nail lacquers, 200-300 mg of each formulation (equivalent to 2-3 mg of terbinafine hydrochloride) was weighed in glass slides, dried and suspended in 15 mL of a 0.5% Tagat® CH 60 aqueous solution. Containers were placed in an incubator-shaker at  $32 \pm 0.5$  °C for 24 h. Samples of 1000  $\mu\text{L}$  were collected at predefined times (1, 2, 3, 4, 8 and 24 h) and the same volume was replaced with fresh receptor solution maintained at the same temperature.

The samples of terbinafine were analyzed by HPLC-UV in a Hitachi Elite Lachrom System (VWR, USA) equipped with four L-2130 pumps, an autosampler L-2200, a column Lichrospher 100 RP18 (150 mm x 4 mm, 5  $\mu\text{m}$ , Merck), a UV Detector L-2400 and a signal processing software EZ Chrom Elite Version 3.2.1. The method used an isocratic gradient mobile phase containing 0.5% (v/v) triethanolamine, 84.5% (v/v) methanol and 15% (v/v) water. A flow rate of 1.0 mL/min was used with a 10  $\mu\text{L}$  injection volume. The auto sampler chamber was maintained at room temperature and the eluted peaks were monitored at a wavelength of 283 nm. The run time was 5 min. All chromatographic separations were carried out at 25 °C. A calibration curve was performed using 19.8  $\mu\text{g/mL}$ , 39.7  $\mu\text{g/mL}$ , 79.4  $\mu\text{g/mL}$ , 99.2  $\mu\text{g/mL}$  and 119  $\mu\text{g/mL}$  of terbinafine hydrochloride in methanol. Three replicates per formulation were analyzed.

The data obtained from the *in vitro* release studies was computed using a DDSolver (23), which is an Excel-plugin module, and the obtained data were fitted to four different kinetic models: zero order, first order, Higuchi and Korsmeyer-Peppas<sup>24</sup>. For all models, the adjusted coefficient of determination ( $R^2_{\text{adjusted}}$ ) was estimated, fitted and used as the model ability to describe a given dataset.

Statistical analysis was performed on the release profiles obtained using an ANOVA two factor with replication, assuming p values  $\leq 0.05$  as statistically significant.

### 2.2.9 *In vitro* antifungal activity

*Candida albicans* ATCC 10240, *Aspergillus brasiliensis* ATCC 16404 and *Trichophyton rubrum* ATCC 28188 were used for the determination of *in vitro* antifungal inhibitory activity of a terbinafine nail lacquer formulation. The test was performed according to the standard disc diffusion method (DDM) in accordance with the Clinical and Laboratory Standards Institute (CLSI) guidelines (25). The Mueller-Hinton agar (BioKar, Spain) microbiologic medium was used.

The test took place over 2 days for *Candida albicans* and 7 days for *Aspergillus brasiliensis*. For *Trichophyton rubrum* the study took place over 20 days under  $22.5 \pm 2.5$  °C and humidity  $\geq 85\%$ . The positive or negative activity of the formulation was assessed according to the presence or absence of growth around the disks and is an indirect measure of the ability of the formulation to inhibit those microorganisms. Fungal inoculum: stock inoculum fungi suspensions were prepared from 5–7 days old cultures grown on Mueller-Hinton agar. The suspensions obtained were diluted with distilled water to obtain a turbidity equivalent to a McFarland 0.5 turbidity standard (25), containing  $1.5 \times 10^8$  cfu/mL of microorganisms. 20 mL of the Mueller-Hinton agar mediums were poured into petri dishes (90 mm diameter) and inoculated with 100  $\mu$ L of the suspension containing  $1.5 \times 10^8$  cfu/mL of each microorganism. Sterile paper discs (6 mm, Sigma-Aldrich, UK), were loaded with 15  $\mu$ L of Formulation A PU 19 with a concentration of 10 mg/mL. Placebo formulations were used to compare the inhibition zones. The antifungal activity of the formulations was compared to the antifungal activity of a commercial terbinafine cream, Lamisil® 1%. All the results were recorded by measuring the zone of growth inhibition surrounding the discs. All determinations were made in triplicate.

## 3. Results and Discussion

### 3.1 *In vitro* cytotoxicity

The direct contact assay tests were carried out for the nail lacquer formulations and control glass slide. No significant morphologic changes were observed in the HaCaT cells in contact with any of the tested materials for all the studied time periods (results not shown). All nail

lacquer formulations presented values superior to 70% cell viability (Figure. 4.1), thus it can be concluded that these materials are biocompatible according to this viability assay.

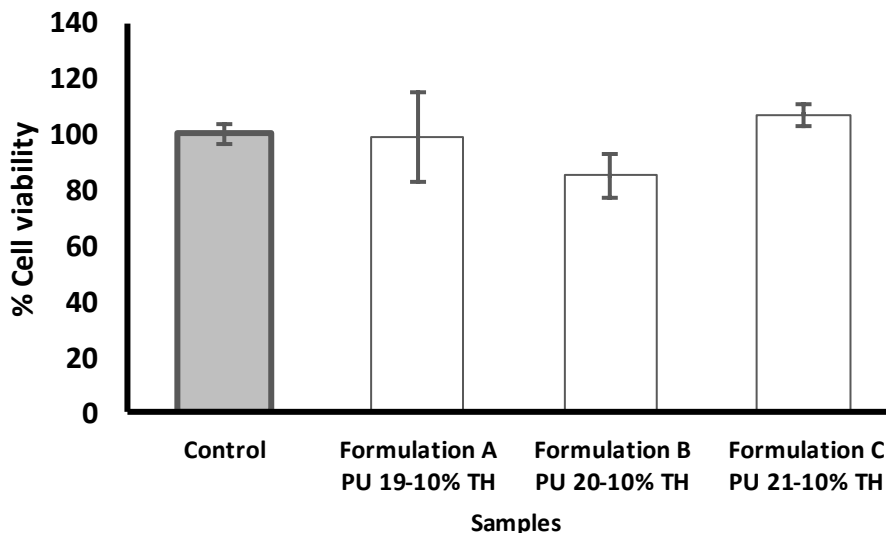


Figure 4. 1. HaCaT cell viability by MTT after proliferation under different nail lacquer formulations. Control (glass slide) (mean $\pm$ SD, n = 6).

The evaluation of the formulations' toxicity over cells surrounding the application site according to the ISO 10993-5:2009(16), is an essential test for the regulatory authorities of the pharmaceutical industry. Nail lacquer formulations are not in contact only with the keratin of the nail plate, but also come into contact with the skin.

The keratinocyte cell line was selected to evaluate the cytotoxicity of the nail lacquer formulations containing terbinafine, since these cells are the predominant cell type in the epidermis, the outermost layer of the skin, comprising 90% of the epidermic cells, thus presenting an adequate *in vitro* cell model that better mimic *in vivo* conditions (9). After analyzing the nail lacquer formulations by direct contact, a monolayer of HaCaT cells was observed, hence the conclusion that the formulations are biocompatible. These results are in agreement with other applications of PU polymers that demonstrated their biocompatibility in HaCaT cell line for proteins delivery (34) and in L929 cell line for other applications (35).

### 3.2 Wettability

The presence of water in the nail is related to the diffusion of drug through the nail (9) and for this reason it is important to measure the wettability of nail formulations.

A water contact angle lower than  $90^\circ$  indicates that wetting of the surface is favorable and that the fluid will spread over a large area on the surface. On the other hand, contact angles greater than  $90^\circ$  mean that wetting of the surface is unfavorable; the fluid will minimize its contact with the surface and form a compact liquid droplet (26).

The average values of the angles obtained were: Formulation A PU 19-10% TH,  $\theta = 45 \pm 6^\circ$ , Formulation B PU 20-10% TH,  $\theta = 77 \pm 4^\circ$  and Formulation C PU 21-10% TH,  $\theta = 61 \pm 4^\circ$ . The nail presented a contact angle of  $\theta = 94 \pm 8^\circ$ . The one-way ANOVA statistical test highlighted a significant difference between the mean values of the different PUs and the nail.

The wettability test results showed water contact angles lower than those observed for the nail surface alone, which presented a reference value of  $94^\circ$ . In the work of Mândru *et al.*, the polymers synthesized with poly (ethylene glycol), poly (butylene adipate), methylene diphenyl-diisocyanate and 1,4-butane-diol, presented contact angle values of  $73^\circ$  and  $87^\circ$ . This result explained the hydrophilic properties of the nail lacquer preparations, which contained PU with polyester and derivatives of carbohydrates in their chain structures (36).

### 3.3 PALS determination of free volume in films

This technique is the most efficient method for studying subnanometer size distributions and free volume fractions, which has been used to explain the free electron property, structural relaxation, mechanic deformation, permeability and physical aging of polymers (27,28,29,30). PALS was used to assess the free volume of the formulations. This non-destructive technique probes local free volumes between molecular chains in polymeric structures. In this technique, the anti-electron, i.e. the positron, is employed as a probe and monitors the lifetime of the positron and Positronium, Ps (a bound atom which consists of an electron and the positron), in the polymeric materials under study (31). Due to the positron's positive charge, itself and the Ps are repelled by the polymers core electrons and trapped in open spaces, i.e. the free volume. The trapped Ps could appear either as a para-Positronium (p-Ps, spin singlet state) or as an ortho-Positronium (o-Ps, triplet spin state), with a relative abundance of 1:3,

respectively. The annihilation photons come from these open spaces mainly, and the results of the positron annihilation lifetime (PAL) measurements give evidence that the positron and the Ps are located in these preexisting free volumes in polymers. In PAL measurements, the observed lifetime ( $\tau$ ) is the reciprocal of the integral of the positron and the electron densities at the site where the annihilation takes place (31). A larger hole, which has a lower average electron density, is expected to have a longer Ps lifetime. A correlation between the free volumes in molecular systems and the observed *o*-Ps has been postulated (32,33). This correlation is expressed in a semi-empirical equation (Equation 1) (33) between the *o*-Ps lifetime ( $\tau_{o-Ps}$ ) and the mean radius of holes ( $R$ ):

$$\tau_{o-Ps} = 0,5 \left[ 1 - \frac{R}{R+\Delta R} + \frac{1}{2\pi} \sin \left( \frac{2\pi R}{R+\Delta R} \right) \right]^{-1} \quad (ns) \quad (1)$$

where  $\tau_{o-Ps}$  and  $R$  are in the units of nanosecond and angstroms, respectively, and  $\Delta R$  ( $= 1,66 \text{ \AA}$ ) is the best fitting parameter between observed *o*-Ps lifetimes and known mean hole radii in porous materials. With equation 2, the mean free volume hole size in a polymeric material can be determined, by measuring the *o*-Ps lifetime. As the holes are assumed to have a spherical shape, this lifetime is related to a mean radius  $R$ . With this assumption, the correspondent free-volume cavity was calculated with the equation  $V = (4/3)\pi R^3$ . The intensity of the *o*-Ps lifetime component,  $I_{o-Ps}$ , is often treated as a measure of the density of the holes<sup>31</sup>. The free volume fraction ( $F_v$ ), Equation 3, is directly related to  $I_{o-Ps}$  and  $\tau_{o-Ps}$  through the following expression (31):

$$F_v = C \frac{4}{3} \pi R^3 I_{o-Ps} \quad (3)$$

Where  $C$  is an empirical scaling constant that reflects the probability of *o*-Ps formation. In the systematic PAL analysis it was observed that all spectra were well fitted with the components showed in Table 4.2; two short-lifetime components of around 200 ps and 420-470 ps, which could be assigned to the annihilation of free and trapped positrons, respectively, and the longest lifetime component ( $>2100$  ps) was due, of course, to the pick-off annihilation of *o*-Ps in the free volume holes. The values of the lifetime components and the intensities of the positron and *o*-Ps annihilation are presented in Table 4.2.

Table 4. 2. PALS parameters (lifetime and intensity components), hole radius (R) and free volume cavity associated with the *o*-Ps lifetime for PU, terbinafine based nail lacquers.

Samples	$\tau_1$ (ps)	I1 (%)	$\tau_2$ (ps)	I2 (%)	$\tau_{o-Ps}$ (ps)	I <sub>o-Ps</sub> (%)	Volume (Å <sup>3</sup> )
Formulation A PU19-10% TH	196.8±7.6	27.2±2.4	436.2±9.8	46.0 ±2.4	2190.0±1.0	26.8±0.1	114.2±1.1
Formulation B PU20-10%TH	212.8±6.6	32.2±1.8	470.5±9.4	39.5±1.9	2490.0±7.0	28.3±0.3	145.1±1.3
Formulation C PU21-10%TH	192.0±3.1	26.5±1.0	420.7±4.2	46.5±1.0	2153.0±5.0	26.9±0.2	110.8±1.1

The free volume concept is extensively adopted in polymer science to explain the change of microscopic structure and to relate it to macroscopic properties. In the last decades, PALS measurements have revealed that a strong correlation exists between the free volume of polymers and the possibility of charging them for sustained release or for selection permeability (38).

The free volume of the tested formulations was determined using PALS: the lifetime of *o*-Ps was used to define the size of free volume in the molecular system (holes) of the films and the intensity of the *o*-Ps lifetime  $I_{o-Ps}$ , to quantify the density of holes. The PALS results are summarized in Table 4.2. The two short-lifetime components of around 200 ps and 420-470 ps are assigned to the annihilation of free and trapped positrons, respectively. The longest lifetime component (>2100 ps) was due to the pick-off annihilation of *o*-Ps in the free volume holes. The *o*-Ps lifetime component and its intensity are the only parameters significantly sensitive to the change in the free volume and all attention must be given to the variation of these parameters. The values of the lifetime component and the intensity of the *o*-Ps for these formulations revealed that Formulation A PU19-10%TH and Formulation C PU21-10%TH had a similar free volume; indeed, both the radius of the holes ( $R$ ) and the density of holes ( $I_{o-Ps}$ ) were similar. On the other hand, Formulation B PU20-10%TH showed, simultaneously, higher values for  $\tau_{o-Ps}$  and  $I_{o-Ps}$ , which were considered to be associated with an increase of the free volume fraction of this polymer, compared to Formulation A PU 19-10% TH and Formulation C PU 21-10%TH. The PU19 and PU21 had identical molar ratios of PPG in the process of synthesis, while the PU20 had a higher molar ratio of PPG. The observed amorphous characteristic of PU20 was corroborated with the increase in the free volume fraction of Formulation B PU 20. The mean radius of the cavities of this formulation

was higher than Formulation A PU 19-10% TH and Formulation C PU 21-10%TH. Additionally, the value of  $I_{O-PS}$  was also higher, revealing an increase of the number of cavities in these films.

### 3.4 SEM

Images of a nail without varnish (A) and three nails containing the three developed formulations were obtained by scanning electron microscopy (SEM) (Figure. 4.2). It was observed that the nail lacquers leave a homogenous film covering the entire nail, making the surface of the nails uniform.

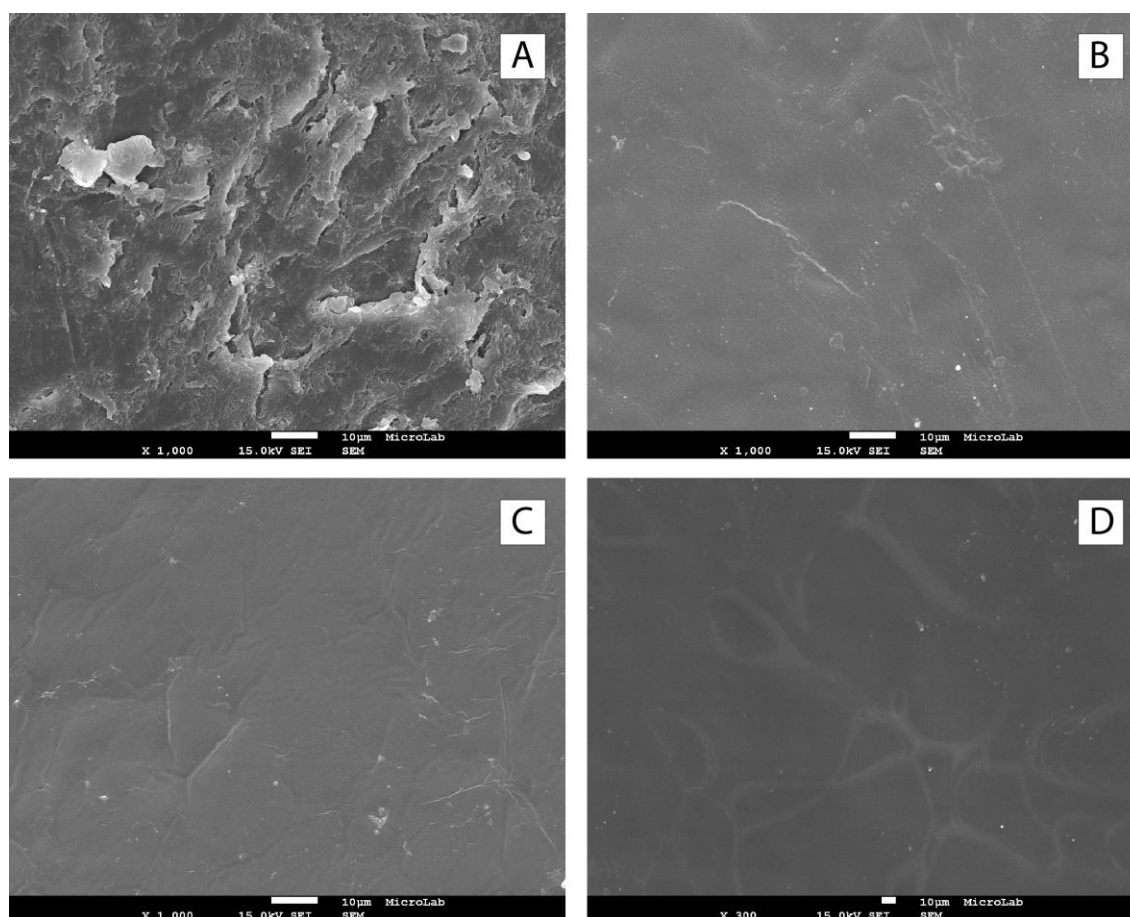


Figure 4. 2. Scan Electron Micrograph with 1000x magnification. A) dorsal surface of nail plate B) film of Formulation A PU 19-10%, C) film of Formulation B PU20-10%, D) film of Formulation C PU21-10%.

The nail lacquer films' elucidated morphology, by SEM, revealed them to be homogeneous and smooth. The application of the nail lacquers improved the homogeneity of the nail surface, making it smooth and uniform. The nail lacquer film homogeneity, porosity and distribution were similar for the three nail lacquers. Nevertheless, Formulation A PU 19-10%TH and Formulation C PU 21-10%TH presented a thinner film with almost no pores, while Formulation B PU 20-10% TH showed visible pores and cracks, on the surface (Figure 4.2 C). This was related to the amorphous characteristics of PU20, presented in formulation B. The presence of terbinafine hydrochloride had no influence in the homogeneity of the films obtained after the formulation had been applied on the nails.

### 3.5 *In vitro* adhesion test

All the PU terbinafine nail lacquers adhered to the keratin of cow horn. The values of flaking in the lattice pattern for Formulation A PU 19-10% was  $1.8 \pm 0.5$  and for Formulation C PU 21-10% TH the value was  $0.7 \pm 0.5$ , which means that both formulations presented good adhesion to the keratin of cow horn. On the surface of the cross-cut area some detachment of small flakes of the coating could be observed where the cuts were intersected. In the case of Formulation B PU 20-10%TH, the value was greater than  $5.0 \pm 0.5$ , corresponding to a appearance of surface of cross-cut greater than 65 %.

The nail lacquer film must adhere to the nail plate. The adhesion test procedure examines the cut area and the results obtained are compared to a six-step classification. The first three steps classification are satisfactory for general purposes and are used when a pass/fail assessment is required.

Regarding Formulation A PU 19-10%TH and Formulation C PU 21-10%TH, the obtained adhesion values showed some detachment of small flakes of the coating at the intersections of the cuts, on the surface of the cross-cut area. These results are promising when compared to previous studies that assessed the adhesion of a UV-curable gel formulation with methacrylates; in this study, the coating flaked along the edges of the cuts partly in large ribbons and some squares detached partly or wholly, corresponding to higher mean cross-cut score values (3 and 4) (38).

In the case of Formulation B PU 20-10%TH, the value corresponded to a classification of 5, which means the coating flaked along the edges and at the intersections of the cuts. The PU

terbinafine nail lacquer that presented the higher flaking in the lattice pattern was Formulation B PU 20-10%. This means it is not effective in adhering to the keratin of cow horn. On the other hand, the formulation with better adhesion to cow horn was the Formulation C PU 21-10%TH, with a degree of flaking in the lattice pattern of 0.7. The increased values of adhesion are thought to be related to the proportional increase of isosorbide in the PU chain, due to the formation of hydrogen bonds between the NH groups of the cow horn's keratin and the oxygen of the isosorbide sub-structure in the polymer.

### 3.6 Viscosity values

The viscosity values for the therapeutic PU terbinafine nail lacquers at 32 °C were:  $2.62 \pm 0.04$  mPa.s for Formulation A PU 19-10%;  $2.67 \pm 0.98$  mPa.s for Formulation B PU 20-10%; and  $3.42 \pm 0.07$  mPa.s for Formulation C PU 21-10%. There are no significant differences among the formulations, probably due to the fact that viscosity was determined at the same temperature used for the study of drug release ( $32 \pm 0.5$  °C); the aim was to mimic nail lacquer application.

### 3.7 *In vitro* release of terbinafine from Formulations A PU 19-10%, B PU 20-10% and C PU 21-10%

Figure 4.3 shows the release profiles of terbinafine hydrochloride from the PU based nail lacquers for 24 h.

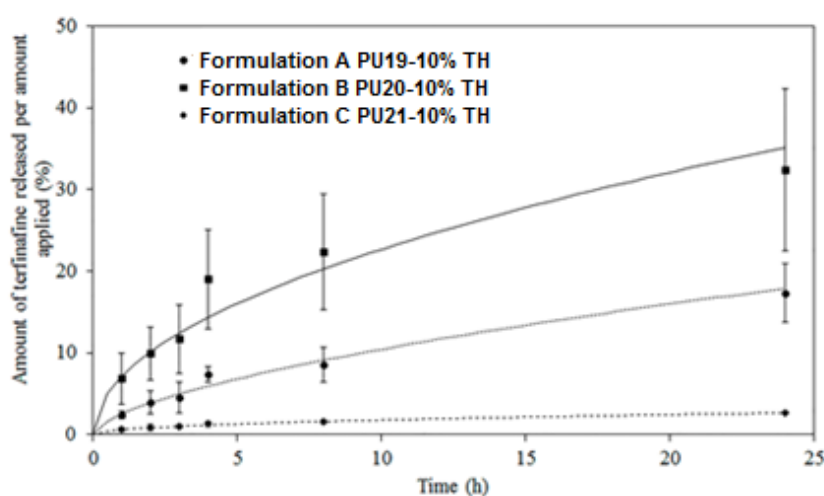


Figure 4. 3. Release profile of terbinafine from PU based nail lacquer for 24 h in aqueous solution of 0.5% Tagat® CH 60 at 32°C (mean  $\pm$ SD, n = 3).

All the formulations released the drug from the matrix. Additionally, the release data were fitted to different mathematical models to describe the release profile. The best-fit was obtained with the Korsmeyer-Peppas function for Formulation A PU 19-10%TH and Formulation C PU 21-10% TH and Higuchi function for Formulation B PU 20-10%TH; as confirmed by the highest values for  $R^2_{\text{adjusted}}$  and model selection criterion (MSC) and the lowest values for Akaike Information Criterion (AIC), they statistically described the best drug release mechanism (23,24).

Concerning the release results, Formulation B PU 20-10%TH released the highest amount of drug (32.4%) in 24 h, followed by Formulation A PU 19-10%TH (17.3 %) and Formulation C PU 21-10%TH (2.6%). Once again, the polymer composition is an important factor, because it influences the diffusion of the drug from the nail lacquers. Formulation B PU 20-10% TH contained PU with a high PPG content, which permitted the incorporation of the drug in an amorphous state. The degree of solvent permeability of Formulation B PU 20-10%TH, determined by PALS, resulted an increase of released terbinafine due to a higher water permeability (39). Formulations A PU19-10% and C PU21-10%TH, showed a delayed release of terbinafine in the tested time range. Therefore, the contact with the receptor solution was lower and the holes' radii in these formulations reduced the permeation of solvents, leading to a lower diffusion of the drug through the nail plate. All release profiles suggested a diffusion-controlled release over the tested time period. According to the kinetic models, the diffusion-controlled release behavior was due to the dispersion of terbinafine in a homogeneous and uniform matrix, which acted as the diffusional medium, indicating a uniform drug distribution over the PU matrix (40,41).

However, as formulation C PU 21-10%TH has more hydrophilic groups, leading to a more reticulated network (a gel) which does not allow the drug to be released.

### 3.8 Antifungal activity

The antifungal activity of the drug against *Trycophyton rubrum*, *Candida albicans* and *Aspergillus brasiliensis* was determined in terms of the mean diameter of zone inhibition. The results obtained are shown in Table 4.3. Formulation A PU 19-10% was proved to be more effective (higher inhibition halos) for the *Trycophyton rubrum* and *Candida albicans* when compared to the commercial cream.

Table 4. 3 Antifungal activity of different formulations with terbinafine against *Tricophyton rubrum*, *Candida albicans* and *Aspergillus brasiliensis*.

	Inhibition zone (mm)				
	Formulation A PU19-10%TH	Formulation B PU20-10%TH	Formulation C PU21-10%TH	Solution of terbinafine 1%	Commercial Cream
<i>Candida albicans</i> ATCC 10240	38.4±3.6	26.7±0.5	27.3±2.6	21.4±1.8	< 6
<i>Aspergillus brasiliensis</i> ATCC 16404	25.0±0.4	26.8±1.7	24.4±0.6	32.0±0.8	27.0±0.1
<i>Tricophyton rubrum</i> ATCC 2818	90.0±0.3	n.d.	n.d.	n.d.	26.6±0.1

n.d: not determined.

The Minimum Inhibitory Concentration (MIC) is the lowest drug concentration that prevents microbial growth. A lower MIC value indicates that less drug is required for inhibiting the growth of a microorganism. Therefore, drugs with lower MIC scores are more effective. The reference terbinafine MIC values vary from 0.004 to 1 µg/mL against *Tricophyton rubrum* (6), *Candida albicans* and *Aspergillus brasiliensis* (42). All formulations presented antifungal activity (Table 4.3). The controls presented inhibition zone < 6 mm.

The antifungal activity results demonstrated that Formulation A PU 19-10%TH showed activity against dermatophytes and non-dermatophytes. In addition, Formulation B PU20-10%TH, Formulation C PU21-10%TH showed lower inhibitory effects against *Candida albicans* in compared to Formulation A PU 19-10%TH.

Although the activity substance concentration is the same in all preparations, the commercial reference (Lamisil® 1% cream) is a formulation with higher viscosity values which may influence the release of terbinafine and consequently the microbiological efficacy.

The Formulation B PU 20-10%TH showed the higher antifungal activity against *Aspergillus brasiliensis*. However, Formulation A PU 19-10%TH presented higher antifungal activity against *Candida albicans*, probably by the influence of -NH- of polyurethane in the pH of the medium that potential the antifungal activity of the drug. The *in vitro* activity of terbinafine is pH dependent and rises with increasing pH value (43).

## 4. Conclusions

In the present work, three nail lacquer formulations employing polyurethanes for the release of terbinafine were characterized. Relevant properties for the intended application were studied, namely cell viability, wettability and free-volume. All the formulations were biocompatible with keratinocytes and presented hydrophilic properties. The PALS study indicated that the nail lacquer formulations have an unusually high free-volume. The nail lacquers showed potential to adhere to the nail plate, and the formulation film (after application) formed a homogeneous layer of terbinafine hydrochloride, according to images obtained by SEM and the mechanical test.

These studies contributed to the development of new nail lacquer formulations with adequate properties for controlled drug release, nail adhesion and biocompatibility for the treatment of onychomycosis. The antifungal activity of the nail lacquer formulations were demonstrated.

The Formulation A PU 19-10%TH allow more effective action against *Trycophyton rubrum*, *Candida albicans* and *Aspergillus brasiliensis*.

Furthermore, it contributed to the fine-tuning of a novel controlled drug release system: PU based nail lacquers, containing terbinafine hydrochloride as a model drug.

The novel system showed potential to be further developed as a topical polyurethane based nail lacquer for the treatment of onychomycosis. It is expected that this novel system may be used to release many other lower molecular weight, ionic drugs to keratinous surfaces.

According the results obtained new formulations must be performed studing the content of PU19.

## 5. References

1. Boni E, Elewski. Onychomycosis: Pathogenesis, Diagnosis, and management. *Clin. Microbiol. Rev.* 1998; 11(3):415-429.
2. Gupta AK, Paquet M, Simpson F, Tavakkol A. Terbinafine in the treatment of dermatophyte toenail onychomycosis: a meta-analysis of efficacy for continuous and intermittent regimens. *J Eur Acad Dermatol Venereol* 2013;27(3):267–272.
3. Murdan S, Kerai L, Hossin B. To what extent do *in vitro* tests correctly predict the *in vivo* residence of nail lacquers on the nail plate? *J Drug Deliv Sci Technol.* 2015;25:23–28.
4. Tamura T, Asahara M, Yamamoto M, Yamaura M, Matsumura M, Goto K, et al. *In vitro* susceptibility of dermatomycoses agents to six antifungal drugs and evaluation by fractional inhibitory concentration index of combined effects of amorolfine and itraconazole in dermatophytes. *Microbiol Immunol* 2014;58(1):1–8.
5. Yang Y, Ou R, Guan S, Ye X, Hu B, Zhang Y, et al. A novel drug delivery gel of terbinafine hydrochloride with high penetration for external use. *Drug Deliv* 2014;7544:1–8.
6. Carrillo-Muñoz AJ, Giusiano G, Cárdenes D, Hernández-Molina JM, Eraso E, Quindós G, et al.. Terbinafine susceptibility patterns for onychomycosis-causative dermatophytes and *Scopulariopsis brevicaulis*. *Int J Antimicrob Agents* 2008;31(6):540–543.
7. Monti D, Saccomani L, Chetoni P, Burgalassi S, Senesi S, Ghelardi E, et al.. Hydrosoluble medicated nail lacquers: *In vitro* drug permeation and corresponding antimycotic activity. *Br J Dermatol.* 2010;162(2):311–317.
8. Monti D, Saccomani L, Chetoni P, Burgalassi S, Saettone MF, Mailland F. *In vitro* transungual permeation of ciclopirox from a hydroxypropyl chitosan-based, water-soluble nail lacquer. *Drug Dev Ind Pharm.* 2005;31(1):11–17.
9. Thatai P, Sapra B. Transungual delivery: deliberations and creeds. *Int J Cosmet Sci.* 2014;36(5):398–411.
10. Guelcher SA, Gallagher KM, Didier JE, Klinedinst DB, Doctor JS, Goldstein AS, et al. Synthesis of biocompatible segmented polyurethanes from aliphatic diisocyanates and diurea diol chain extenders. *Acta Biomater* 2005;1(4):471–484.
11. Jabbari E, Khakpour M. Morphology of and release behavior from porous polyurethane microspheres. *Biomaterials* 2000;21(20):2073–2079.

12. Li B, Yoshii T, Hafeman AE, Nyman JS, Wenke JC, Guelcher SA. The effects of rhBMP-2 released from biodegradable polyurethane/microsphere composite scaffolds on new bone formation in rat femora. *Biomaterials* 2009;30(35):6768–6779.
13. Bachmann F, Reimer J, Ruppenstein M, Thiem J. Synthesis of novel polyurethanes and polyureas by polyaddition reactions of dianhydrohexitol configured diisocyanates. *Macromol Chem Phys* 2001;202(17):3410–3419.
14. Ferreira P, Coelho JFJ, Pereira R, Silva AFM, Gil MH. Synthesis and characterization of a poly(ethylene glycol) prepolymer to be applied as a bioadhesive. *J Appl Polym Sci* 2007;105(2):593–601.
15. Gorna K, Gogolewski S. Biodegradable porous polyurethane scaffolds for tissue repair and regeneration. *J Biomed Mater Res - Part A* 2006;79(1):128–138.
16. International Organization for Standardization. ISO 10993-5:2009 Biological evaluation of medical devices – Part 5: Tests for *in vitro* cytotoxicity. 2009 (Available at:[http://www.iso.org/iso/home/store/catalogue\\_tc/catalogue\\_detail.htm?csnumber=36406](http://www.iso.org/iso/home/store/catalogue_tc/catalogue_detail.htm?csnumber=36406)).
17. Marto J, Ascenso A, Gonçalves LM, Gouveia LF, Manteigas P, Pinto P, et al. Melatonin-based Pickering emulsion for skin's photoprotection. *Drug Deliv.* 2016; 23(5):1594-607.
18. Lopes R, Eleutério CV, Gonçalves LMD, Cruz MEM, Almeida AJ. Lipid nanoparticles containing oryzalin for the treatment of leishmaniasis. *Eur J Pharm Sci.* 2012;45(4):442–550.
19. Hejda F, Solař P, Kousal J. Surface free energy determination by contact angle measurements a comparison of various approaches. *WDS'10 Proc Contrib Pap* 2010;2010(3):25–30.
20. Kansy J. Microcomputer program for analysis of positron annihilation lifetime spectra. *Nucl Instruments Methods Phys Res Sect A Accel Spectrometers, Detect Assoc Equip* 1996;374(2):235–244.
21. Owens DK, Wendt RC. Estimation of the surface free energy of polymers. *J Appl Polym Sci.* 1969;13(8):1741–1747.
22. International Organization for Standardization. ISO 2409:2013 Paints and varnishes – Cross-cut test. 2013 (Available at: [http://www.iso.org/iso/home/store/catalogue\\_tc/catalogue\\_detail.htm?csnumber=51923](http://www.iso.org/iso/home/store/catalogue_tc/catalogue_detail.htm?csnumber=51923)).

23. Zhang Y, Huo M, Zhou J, Zou A, Li W, Yao C, et al. DDSolver: an add-in program for modeling and comparison of drug dissolution profiles. *AAPS J* 2010;12(3):263–271.
24. Costa FO, Sousa JJS, Pais AACC, Formosinho SJ. Comparison of dissolution profiles of Ibuprofen pellets. *J Control Release* 2003;89(2):199–212.
25. Clinical and Laboratory Standards Institute. M02-A12: Performance Standards for Antimicrobial Disk Susceptibility Tests, 12th Ed. 2015.
26. Darmanin T, Guittard F. Wettability of conducting polymers: From superhydrophilicity to superoleophobicity. *Prog Polym Sci* 2014;39(4):656–682.
27. Jean YC, David Van Horn J, Wei-Song Hung, Kuier-Rarn Lee. Perspective of Positron Annihilation Spectroscopy in Polymers. *Macromolecules* 2013; 46, 7133–7145.
28. Gong W, Mai Y, Zhou Y, et al. Effect of the degree of branching on atomic scale free volume in hyperbranched poly[3-ethyl-3-(hydroxymethyl)oxetane]: positron study. *Macromolecules* 2005, 38, 9644–9649.
29. Monge MA, Diaz JA, Pareja, R. Strain-induced changes of free volume measured by positron lifetime spectroscopy in ultrahigh molecule weight polyethylene. *Macromolecules* 2004, 37, 7223–7230.
30. Merkel TC, Freeman BD, Spontak RJ, et al. Ultrapermeable, reverse-selective nanocomposite membranes. *Science*, 2002, 296, 519–522.
31. Kobayashi Y, Ito K, Oka T, Hirata K. Positronium chemistry in porous materials. *Radiat Phys Chem* 2007;76(2):224–230.
32. Tao SJ. Positronium annihilation in molecular substances. *J Chem Phys* 1972;56:5499.
33. Pyun DG, Choi HJ, Yoon HS, Thambi T, Lee DS. Polyurethane foam containing rhEGF as a dressing material for healing diabetic wounds: Synthesis, characterization, *in vitro* and *in vivo* studies. *Colloids Surf B* 2015;135(1): 699-706.
34. Fernández-d’Arlas B, Alonso-Varona A, Palomares T, Corcuera MA, Eceiza A. Studies on the morphology, properties and biocompatibility of aliphatic diisocyanate-polycarbonate polyurethanes. *Polym Degrad Stab* 2015;122: 153-160.
35. Mândru M, Ciobanu C, Vlad S, Butnaru M, Lebrun L, Popa M. Characteristics of polyurethane-based sustained release membranes for drug delivery. *Cent Eur J Chem* 2013;11(4):542–553.

36. M.F. Ferreira Marques, P.M. Gordo, C. Lopes Gil, Zs. Zsolt, M.H. Gil, M.J. Mariz, A.P. de Lima. Positron lifetime studies in vinyl polymers of medical importance. *Radiation Physics and Chemistry* 2003; 68 (3-4), 485-488
37. M.F. Ferreira Marques, P.M. Gordo, Zs. Zsolt, C. Lopes Gil, A.P. de Lima, D.P. Queiroz, M.N. de Pinho. Positron studies on the temperature-dependence of free volumes in polydimethylsiloxane/poly(propylene oxide) urethane/urea membranes. *Radiation Physics and Chemistry* 2007; 76 (2), 129-133.
38. Kerai LV, Hilton S, Murdan S. UV-curable gel formulations: Potential drug carriers for the topical treatment of nail diseases. *Int J Pharm* 2015;492(1-2):177–190.
39. Cheong LWS, Heng PWS, Wong LF. Relationship between polymer viscosity and drug release from a matrix system. *Pharm Res* 1992;9(11):1510–1514.
40. Arifin DY, Lee LY, Wang CH. Mathematical modeling and simulation of drug release from microspheres: Implications to drug delivery systems. *Adv Drug Deliv Rev* 2006;58(12-13):1274–1325.
41. Arun Raj C, Senthil Kumar P, Sathish Kumar K. Kinetics and drug release studies of isoniazid encapsulated with PLA-co-PEG/ gold nanoparticles. *Int J Pharm Pharm Sci* 2012;4(4):398–404.
42. Jo Siu WJ, Tatsumi Y, Senda H, Pillai R, Nakamura T, Sone D, et al. Comparison of in vitro antifungal activities of efinaconazole and currently available antifungal agents against a variety of pathogenic fungi associated with onychomycosis. *Antimicrobial agents and chemotherapy*. 2013: 1610–6.
43. Petranyi G, Meingassner JG, Mieth H. Antifungal activity of the allylamine derivative terbinafine in vitro. *Antimicrob Agents Chemother*. 1987;31(9):1365–1368.



**Chapter 5: Formulation optimization of PU based Nail Lacquers  
containing Terbinafine hydrochloride and Ciclopirox Olamine**



## 1. Introduction

Onychomycosis is a nail fungal infection caused by dermatophytes, non-dermatophytes and yeast species(1).

*Candida* species have a high incidence in fingernail infection, present in as many incidence of as 75% of cases, and are more prevalent than dermatophytes(2). In contrast, the incidence of yeasts in toenail infections is much lower; approximately 2-10% cases. Infection attributed to non-dermatophytes are estimated to be 2-65% of cases although higher rates, 15% have been reported(3).

The untreated onychomycosis may worsen, spread to other uninfected locations (other nails or to the surrounding skin) or infect other patient (4).

Nail keratin is impermeable structure thus restricting drug access to the organisms causing onychomycosis(5). The development of therapeutic transungual drug delivery is an urgency for patients that are affected by such infection.

Topical treatment would be of special interest for immunosuppressed, diabetic and elderly patients who suffers from chronic pathologies and follow long-term drug therapies and among whom the prevalence of onychomycosis is higher(5,6). Despite an active interest in method aimed at improving the efficacy of such formulations and the permeation study is testified by recent research report (7–10).

Many antifungal formulations have been developed. Some of them are related with ciclopirox olamine and terbinafine hydrochloride.

The ciclopirox olamine (CPX) is used in nail topical formulations have been marketed worldwide for about 25 years and it is available in different pharmaceutical preparations: creams (Selergo<sup>®</sup>, MycoSter<sup>®</sup>, 1%), lotion (MycoSter<sup>®</sup>, 10mg/L) (11), gel (Loprox<sup>®</sup>, 0.77%) (12) and solutions, such as Penlac<sup>®</sup>, Batrafen<sup>®</sup>, MycoSter<sup>®</sup>, Ciclopoli<sup>®</sup>, Ony-Tec<sup>®</sup> and RejuveNail<sup>®</sup> containing 8% of active substance. They present butyl monoester of poly methyl vinyl ether/maleic acid (5) or hydroxy propyl chitosan as film formers (13). The CPX present a minimum inhibitory concentration value for *Candida albicans* and *Aspergillus* species between 0.13-4 µg/mL (14,15).

On the other hand, terbinafine hydrochloride (TH) is used in systemic and topical formulations (Lamisil<sup>®</sup> cream, 1%, Mycova<sup>®</sup> nail coat, 10%, TDT 067 liquid spray, 15 mg/mL and P-3058, hydroxypropyl chitosan based, 5%) (5,16). These nail formulations uses

dodecyl 2-(N,N dimethylamino)-propionate hydrochloride, soybean phosphatidylcholine and hydroxypropyl chitosan, respectively (5). TH, an allylamine derivative, represents the most effective antimycotic drug, presenting a minimum inhibitory concentration against dermatophytes of 0.004-0.06  $\mu\text{g/mL}$ (17), non-dermatophytes of 0.063-2.5  $\mu\text{g/mL}$ (18) and yeast of 0.06-8  $\mu\text{g/mL}$ (18)

All of them have proved to be effective presenting transungual permeation. However, there is a need to improve the patient compliance with less repeat applications meaning that topical nail' formulations needs to be improved. Nail lacquers, formulated with polymers that act as film former agents, could be an alternative to be used as of new drug carriers(9).

In this study, the influence of polyurethanes (polymer) concentration on the properties of nail lacquer formulations is assessed and compared with a commercial formulation. The incorporation of two drugs (TH and CPX) validated the use of PU as versatile polymers in nail lacquer formulations. Direct contact cytotoxicity, wettability, SEM, adhesion, drying time, viscosity measurement, permeation studies and antifungal activity were performed in order to achieve these aims.

## 2. Material and methods

### 2.1 Materials

Ethanol anhydrous, butyl acetate and ethyl acetate were acquired from Carlo Erba (France). The terbinafine hydrochloride manufactured by Uquifa México S.A. was kindly offered by Generis. Tagat® CH 60 (PEG-60 Hydrogenated Castor Oil) was a kind gift from Evonik (Germany). PU 19 was synthesized in laboratory of IST according to described in the chapter 3. Ciclopirox was obtained from Fagron Iberica (Spain), Ony-Tec® was kindly offered by Laboratorio Medea, Reig Jofre (Spain).

### 2.2 Methods

#### 2.2.1 Preparation of Nail lacquers

The PU 19 was the polymer selected for preparing 5 different nail lacquers formulations containing 1% of drug (TH and CPX). Different polymer concentrations (10%, 15%, 20% and 25%) were employed. The formulations were prepared according to component described in

Table 5.1. Firstly, polyurethanes have been fully solubilized in ethanol under stirring (200 rpm). Afterward, the solvents and the drugs (TH and CPX) were added, separately, until its complete dissolution. Placebos, formulations with no drug, were also prepared.

A commercial formulation containing 8% (w/v) of CPX was also used as a control: Ony-Tec<sup>®</sup>. It's qualitative composition is ethanol, water, ethyl acetate, hydroxipropyl chitosan and cetylstearyl alcohol.

Table 5. 1. Nail lacquers composition.

	Formulation A PU19-10% TH	Formulation D PU 19-15% TH	Formulation E PU 19-20% TH	Formulation F PU 19-25% TH	Formulation G PU19-10% CPX
PU 19	10	15	20	25	10
Terbinafine HCl (TH)	1.0	1.0	1.0	1.0	-
Ciclopirox (CPX)	-	-	-	-	1.0
Ethyl acetate	7.8	7.2	6.8	6.3	17.8
Butyl acetate	10	9.6	9.0	8.5	-
Ethanol	71.2	67.2	63.2	59.2	71.2

### 2.2.2 Direct contact cytotoxicity assay for Nail lacquer

The cytotoxicity test are described in chapter 3, section 2.2.11.

### 2.2.3 Determination of wettability by contact angle measurement

The contact angle measurement is described in chapter 4, section 2.2.3

### 2.2.4 SEM

The nail morphology study before and after nail lacquer formulations were applied are described in chapter 4, section 2.2.6.

### 2.2.5 Adhesion test

The adhesion of nail lacquers test is described in chapter 4, section 2.2.7

### 2.2.6 Drying time for nail lacquer therapeutics

The nail lacquer must dry. A quantity of  $0.25 \pm 0.02$ g of the nail lacquers were weighed and spread into a glass, to create a homogeneous film. The drying time was measurement with a chronometer. This methodology was adapted from ISO 2409:2013(19).

### 2.2.7 Viscosity determination

The viscosity determination is described in chapter 4, section 2.2.7.

### 2.2.8 *In vitro* release of terbinafine from nail lacquers containing different concentrations of PU

*In vitro* release studies were performed using Franz diffusion cell apparatus through a hydrophilic membrane (Tuffryn® Membrane) (Pall corporation 79579I), with a diffusion area of  $1\text{cm}^2$  for 6 hours (20). The receptor phase was solution Tagat® CH 60 in water 0.5% established based on a preliminary solubility study of terbinafine. The system was maintained at  $37 \pm 0.5^\circ\text{C}$  for approximately 30 minutes before starting the experiment and during the course of the same. The receptor medium was homogenized by small magnetic bar stirring. The amount applied was 200-300 mg for either formulation (equivalent to 2000-3000  $\mu\text{g}$  of terbinafine). Samples of 200  $\mu\text{L}$  were collected at predefined times (0, 1, 2, 3, 4, 5 and 6 hours) and the same volume was replaced with fresh receptor solution maintained at the same temperature.

The samples of terbinafine were analysed by HPLC-UV in a Hitachi Elite Lachrom System (VWR, USA) equipped with four Pumps L-2130, an autosampler L-2200, a column Lichrospher 100 RP18, (150mm x 4mm,  $5\mu\text{m}$ , Merck), an UV Detector L-2400 and signal processing by software EZ Chrom Elite Version 3.2.1. The method used an isocratic gradient mobile phase containing, 85% (v/v) methanol and 15% (v/v) solution of water 0.5% triethanolamine. A flow rate of 1.0 mL/min was used with a 10  $\mu\text{L}$  injection volume. The auto sampler chamber was maintained at room temperature and the eluted peaks were monitored at wavelength of 283 nm. The run time was 5 min. All chromatographic separations were carried

out at 25°C. A calibration curve was performed using 19.8 µg/mL; 39.7µg/mL; 79.4 µg/mL; 99.2 µg/mL and 119 µg/mL of terbinafine hydrochloride in methanol. Six replicate containers for each formulation were analyzed.

### 2.2.9. *In vitro* antifungal activity

*Candida albicans* ATCC 10240 and *Aspergillus brasiliensis* ATCC 16404 were used for the determination of *in vitro* antifungal inhibitory activity of a terbinafine and ciclopirox nail lacquer formulations. The test was performed according to the standard disc diffusion method (DDM) in accordance with the Clinical and Laboratory Standards Institute (CLSI) guidelines<sup>25</sup>. The potato dextrose agar (PDA) (BioKar, Spain) and sabouraud dextrose agar (SDA) (BioKar, Spain) microbiologic media were used for *A. brasiliensis* and for *C. albicans*, respectively.

The test took place over 2 days under  $37 \pm 2$  °C for *C. albicans* and 7 days under  $22.5 \pm 2.5$  °C for *A. brasiliensis*. The positive or negative activity of the formulation was assessed according to the presence or absence of growth around the disks and is an indirect measure of the ability of the formulation to inhibit those microorganisms. *A. brasiliensis* inoculum was prepared from 5–7 days old cultures grown on Mueller-Hinton agar (BioKar, Spain). The suspensions obtained were diluted with distilled water to obtain a turbidity equivalent to a McFarland 0.5 turbidity standard<sup>25</sup>, containing  $3.4 \times 10^8$  cfu/mL of microorganisms. *C. albicans* inoculum was prepared from 1 day cultures grown on Mueller-Hinton agar. The suspensions obtained were diluted with distilled water to obtain a turbidity equivalent to a McFarland 0.5 turbidity standard<sup>25</sup>, containing  $7.2 \times 10^8$  cfu/mL of microorganisms. Sterile paper discs (6 mm, Sigma-Aldrich, UK), were loaded with 15 µL of each formulation. Placebo formulations were used to compare the inhibition zones. All the results were recorded by measuring the zone of growth inhibition surrounding the discs. All determinations were made in duplicate.

### 2.2.10. Final formulations - Permeation studies

The nail tips were obtained by cutting the free edge of the nail plate of healthy volunteer (female 25 years old) after ethical approval and informed consent. The samples had a minimum length of 5 mm. The nail tips were hydrated in 10 mL receptor solution (some in

aqueous solution of 0.5% Tagat® CH 60 and the other in phosphate buffer saline to which sodium azide) for 1 h. Ony-Tec® was used as control. The nail tip samples were sandwiched between two cylindrical adapters made of polytetrafluoroethylene (PTFE) (Mecanizados del noroeste, Santiago de compostela, Spain) with an o-shaped ring providing an effective diffusional area of 0.049 cm<sup>2</sup>. The set was placed between the donor and receptor chambers of vertical Franz-type diffusion cell (Vidrafoc, Barcelona, Spain) of the dorsal and ventral layers of the nails faced the donor and the receptor compartments, respectively. The donor chamber contained either 2 ml of one of the nail lacquer (Formulation A PU19-10% TH, Formulation G PU19 10% CPX) and was covered with parafilm®. The receptor medium, 5.5 mL receptor volume, was aqueous solution of 0.5% Tagat® CH 60 for Formulation A PU19-10% TH and phosphate buffer saline which sodium azide (30 mg/L) pH 7.4 (9) for Formulation G PU19-10% CPX and Ony-Tec®. The receptor compartments were at constant temperature by use of thermostated (32± 0.5 °C) water. The sink conditions were assumed. Samples of 1000 µL were collected at predefined times (each day at same time) and the same volume was replaced with fresh receptor solution maintained at the same temperature. The experiments were performed for 11 days and three replicates were made for each condition (9).

The amount of TH and CPX present in the nail plate at the end of penetration experiment was also determined by UV spectrophotometry (spectrophotometer diode array Hewlett Packard 8452A). The wavenumber for terbinafine was 283 nm (21) and for ciclopirox 308 nm (9) after the drug extraction. The section of the nail exposed to the formulation was cut, weighed and cut in small fragments that were transferred into a vial containing either 5 ml of receptor solution at 5% in methanol. Later, the prepared solutions were incubated and shaken for 4 days at room temperature to facilitate drug extraction. The CPX extraction method was adapted and validated from the literature (9,21) while the TH extraction method was validated for sensitivity, linearity and precision in the concentration range of 6.32 µg/mL-31.6 µg/mL ( $r^2=0.9884$ , calibration curve standards were assayed together with every sample batch to account for inter day variability).

Standard and blank solutions were made up using PBS buffer (pH 7.4) containing 30 mg/L of sodium azide and aqueous solution of 0.5% Tagat® CH 60.

The data were normalized to account for thickness of the nails.

### 2.2.11 Porosity measurement

Untreated and treated nail samples were analyzed using a Micromeritics 9305 pore sizer (Norcross GA, USA) fitted with a 3-mL powder penetrometer and working pressures in a 0.004–172.4 MPa range. Nail tips were used as described in chapter 5, section 2.2.10.

The nails were soaked in 10 mL of either water Ony-Tec and Formulation A PU19-10% TH. Later the samples were stored at room temperature for 24h. After the time, the nails were removed from the solution tested, dried and determined the porosity. The amount of nail tip for test was approximately 0.6 g. The pore size data were used for modeling the porous structure of the samples as simulated porous networks using poreXpert™ 1.3 software (Environmental and Fluid Modelling Group, University of Plymouth, UK)(22).

## 3. Results and discussion

### 3.1 Direct contact assay

The cell viability test was carried out for nail lacquer containing different percentages of polymers and control slide glass. Phase contrast micrographs were taken at the interface of the cell layer with outer contact areas of the different matrices.

In the Figure 5.1, were observed the color of HaCaT cells in contact with MTT. The purple color was detected in the almost every samples, confirming the viability of cell in contact with all the formulations. These results corresponding to the measurement of PU19 section 3.9, chapter 3.

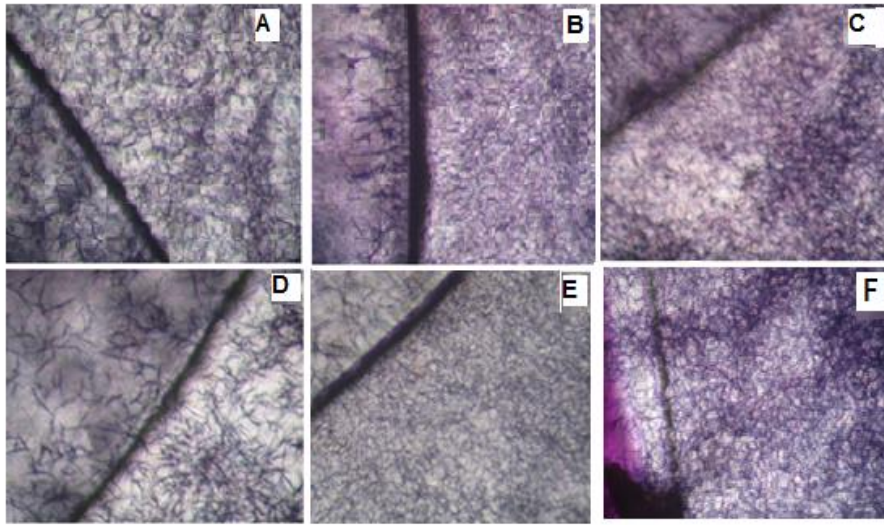


Figure 5.1. Micrograph with 400x magnification of HaCaT cells after 72h of proliferation under contact with different therapeutic nail lacquer: A) glass slide, B) Formulation A PU19-10% TH, C) Formulation D PU19-15% TH, D) Formulation E PU19-20% TH, E) Formulation F PU19-25% TH and F) PU19.

Figure 5.2 represents the percent of cell viability measured by the MTT reduction for the nail lacquer formulations.

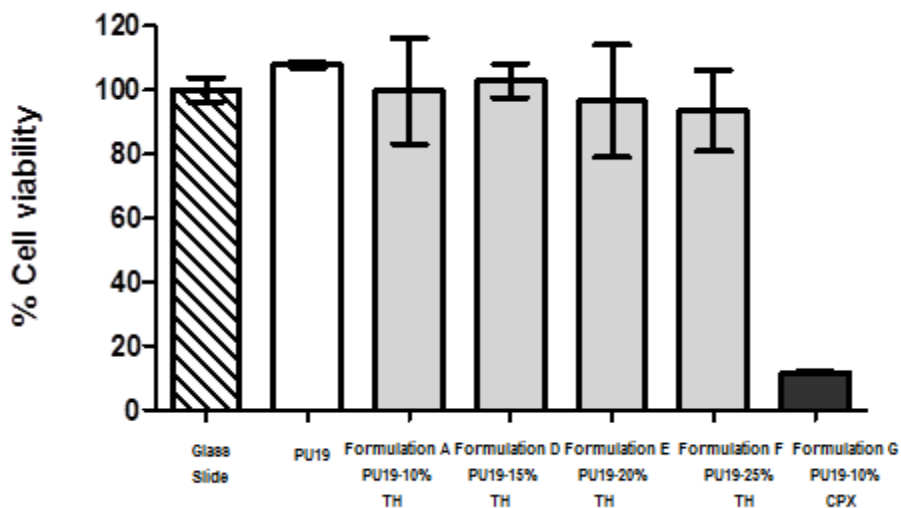


Figure 5. 2. HaCaT cell viability by MTT after proliferation under different nail lacquers. Control (glass slide), (mean  $\pm$  SD, n = 6).

From Figure 5.2 it can be observed that PU 19, Formulation A PU19-10% TH, Formulation D PU19-15% TH, Formulation E PU19-20% TH and Formulation F PU19-25% TH presents a cell viability (measured by the MTT reduction) that did not differ significantly from the control (glass slide) and PU19 (section 3.9, chapter 3). The polymer concentration did not influence the cell viability.

The Formulation G PU19-10% CPX cell viability is 12% (significantly different from control for  $p < 0.05$ ). This formulation is not biocompatible and not allow cell growth.

The results of cell viability of PU19-10% CPX probably present relation to the proportion of ethyl acetate and the ciclopirox. Ethyl acetate is used as a solvent for chemical reactions and it is often used in cosmetics as nail polishes because is not toxic but in short-term exposure to high levels of ethyl acetate results in irritation of different tissues (23)

All the samples tested with TH allow the cell proliferation under the surface covered by the polymers that was confirmed by the presence of a monolayer of viable cells.

The Formulation G PU19-10% CPX, will be study in the rest of the chapter only with comparative objective.

### 3.2 Wettability

As referred previously (section 3.2, chapter 4), the wettability tests show that the water contact angle of PU19 based nail lacquer is lower than the one observed for the nail surface alone, which presented an average value of  $94^\circ$ , indicating that the nail lacquer favors the wetting of the surface. However, different concentrations of the polymer in the solutions that were used to prepare the films led to variations in the water contact angle. An increase in the content of PU19 origins higher contact angles: while for 10% of PU19 a water contact angle of  $45^\circ \pm 4^\circ$  is obtained, for 20% of PU19 it increased to  $66^\circ \pm 4^\circ$  and for 25% to  $68^\circ \pm 11^\circ$  (Figure 5.3). This fact shall be related with the surface morphology of the films, since the chemical composition is the same after the evaporation of the solvent. As it can be observed in SEM images (see below, Figure 5.4), the surfaces of Formulation A PU19-10% TH are more irregular than those produced from solutions with higher contents of polymer. This behavior may be explained by the Wenzel theory(24). According to this author, the equilibrium contact angle in a rough surface ( $\theta_w$ , apparent Wenzel angle) is related with the real contact angle ( $\theta$ ) trough Equation 1:

$$\cos \theta_w = r \cos \theta \quad (1)$$

where  $r$  is a roughness factor, defined as the reason between the real surface area and the corresponding projected area. This approach implies that an increase of roughness leads to a decrease of the observed contact angle when  $\theta_w$  is lower than  $90^\circ$ , as is the case.

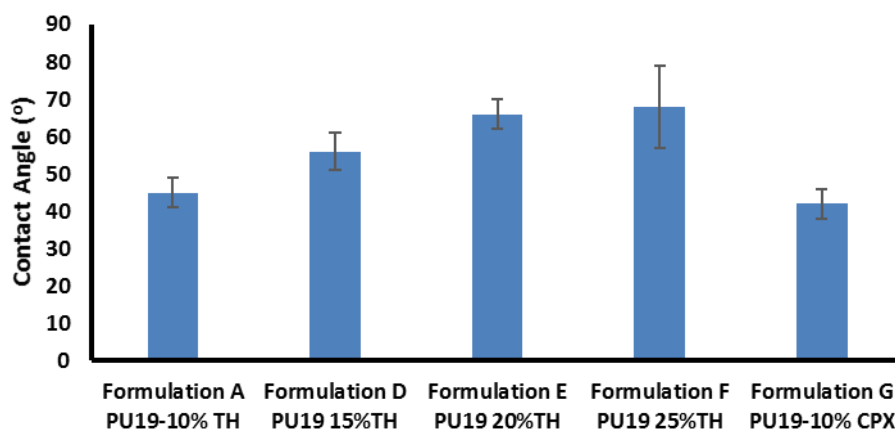


Figure 5.3. Water contact angle of PU terbinafine nail lacquers (mean  $\pm$  SD,  $n=3$ ).

Wettability measurements were also carried out with samples PU19-10% loaded with CPX, instead of TH. The water contact angle was similar in both cases ( $45^\circ \pm 4^\circ$  and  $42^\circ \pm 4^\circ$ , respectively), being visible that the surface morphologies are similar (Figure 5.4 below). This means that the nature of the drug does not affect the wettability of the surfaces.

Overall, these results allow to select Formulations A PU19-10% and G PU 19-10% CPX as those which present better wettability properties.

### 3.3 SEM

The images obtained by SEM of nail lacquers show homogeneous films, which cover the surface to the nail as observed in Figure 5.4.

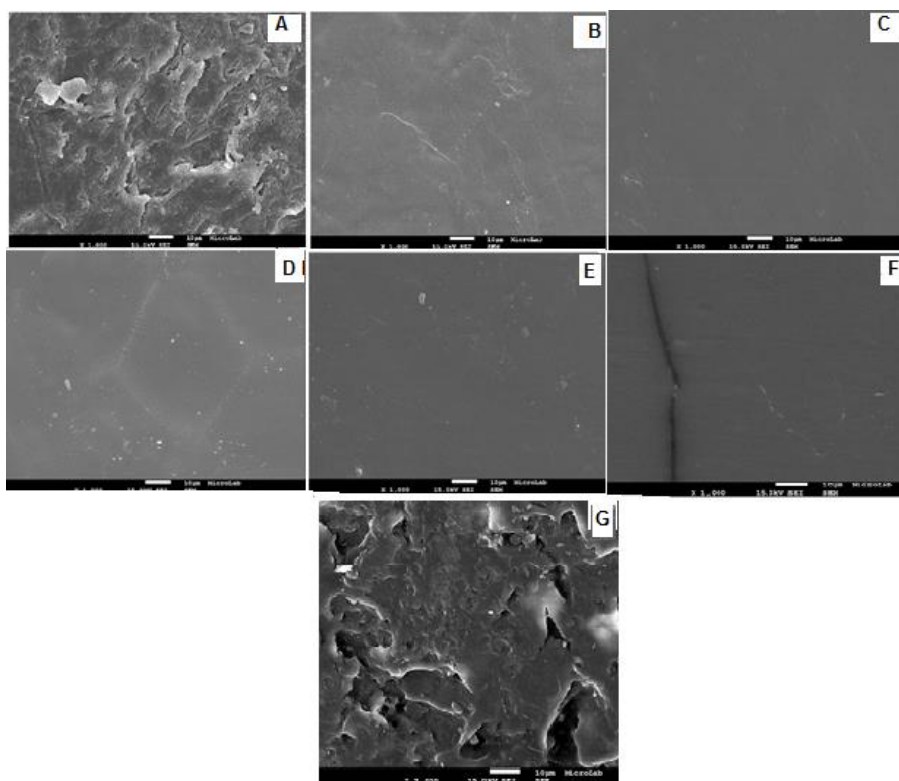


Figure 5.4. Scan Electron Micrograph with 1000x magnification. A) dorsal surface of nail plate B) film of Formulation A PU 19-10% TH, C) film of Formulation D PU19-15% TH, D) film of Formulation E PU19-20% TH, E) film of Formulation F PU19-25% TH, F) film of Formulation G PU19-10% CPX and G) Ony-Tec<sup>®</sup>.

The inclusion of the drug (TH or CPX) had no influence on film thickness and on the film thickness and on the microstructure of PU based nail lacquers. However, Ony-Tec<sup>®</sup> did not form a homogenous film in the surface of the nail. These measurements indicated that the application of the PU nail lacquers coated the roughness of the nail surface, making it smooth and uniform, while chitosan film from (9) was similar to the untreated nail with visible pores and cracks on the surface.

### 3.4 Adhesion test results

The nail lacquer must to adhere to nail. The duration of residence of the film on the nail plate is therefore critically important, because the film of nail lacquer acts as a drug depot, from which the drug can be continuously released and permeate into the nail. A film with a long residence time would need less frequent lacquer application, which could in turn lead to

increased patient compliance, improved treatment efficacy and reduced cost of treatment (25). In the Figure 5.5 are presented the evaluation of adhesion test.

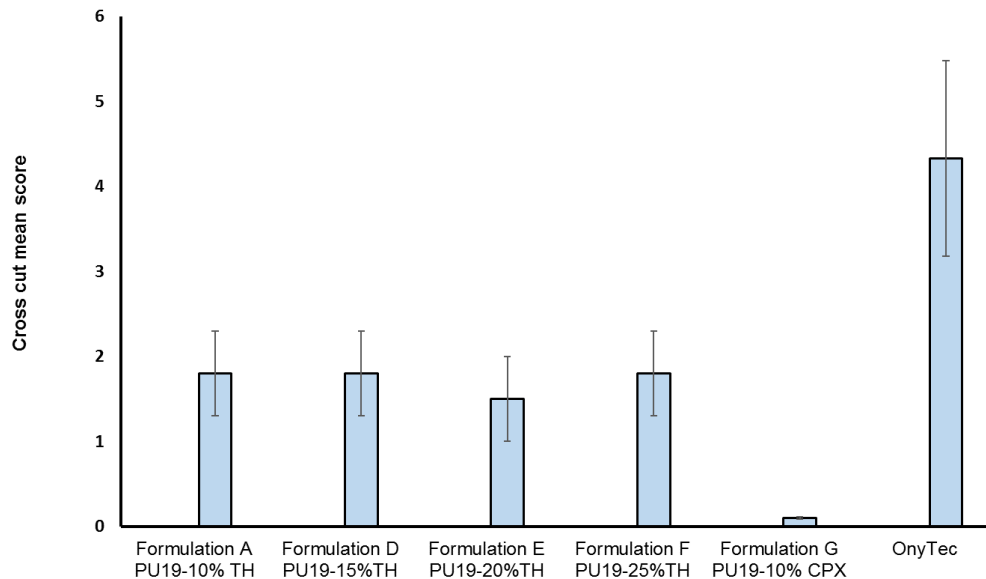


Figure 5.5. Nail lacquer adhesion test to keratin of cow horn.

All the formulations presented adhesion to keratin of cow horn, as observed in Figure 5.5. The adhesion values in cow horn corresponding to better results in compared with the result of adhesion from nail lacquer formulated with methacrylates, where the cross cut mean score were between 4 and 5 (10).

On the other hand, the nail lacquer that presents the higher flaking in the lattice pattern was formulation Ony-Tec<sup>®</sup>. The formulation Ony-Tec<sup>®</sup> is a chitosan derivative' hydrogel. Previously study by SEM showed a film with pores and cracks on the surface of nail, furthermore hidroypropyl chitosan is a water soluble film former with affinity to keratin(26). The results obtained permit to concluded that the polyurethanes films present more affinity to keratin that Ony-Tec<sup>®</sup>.

The formulation with more adhesion to cow horn was the Formulation G PU 19-10% CPX, with a degree of flaking in the lattice pattern of 0.1, probably, because the formulation G PU19-10% presented highest value ethyl acetate as solvent and permit more exposition of the hydrophilic group of polyurethane to keratin of cow horn (27).

### 3.5 Nail lacquer's drying time

For complaint of patient the formulation must dry in the nail (29–32). In table 5.2 is observed the value of drying time of formulation.

Table 5. 2. Nail lacquer's drying time (mean±SD, n= 3).

Formulation	Time (min)
Formulation A PU19-10% TH	9±0.1
Formulation D PU19-15% TH	10±0.3
Formulation E PU 19-20% TH	15±0.1
Formulation F PU19-25% TH	16±0.2
Formulation G PU19-10% CPX	7±0.1
Ony-Tec <sup>®</sup>	13±0.1

The PU formulations present drying times from 9 to 16 min. In fact, the higher the concentration of the polymer, the longer the drying time of the nail lacquer. These results are in agreement with the solvent contents because the higher the concentration of ethyl and butyl acetate the shorter the drying time.

The Ony-Tec<sup>®</sup> presents a drying time of 13 minutes, which is related to its composition. Ethanol is main solvent of this formulation. According to these results, Formulation A PU19-10% TH, Formulation D PU19-15% TH and the Formulation G PU19-10% CPX should be selected.

### 3.6 Viscosity values

The values of viscosity for the PU terbinafine nail lacquers at 32°C in order to mimic nail lacquer application are shown in Table 5.3. It observed that the higher the concentration of polymer increased the viscosity.

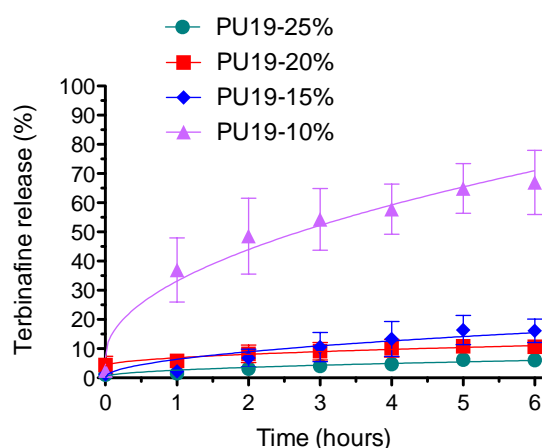
Table 5. 3. Viscosity values of therapeutic nail lacquers (mean $\pm$ SD, n= 3).

Formulation	Viscosity (mPa.s)
Formulation A PU19-10% TH	2.62 $\pm$ 0.04
Formulation D PU19-15% TH	4.70 $\pm$ 0.06
Formulation E PU19-20% TH	8.80 $\pm$ 0.11
Formulation F PU19-25% TH	17.03 $\pm$ 0.07
Formulation G PU19-10% CPX	2.24 $\pm$ 0.04
Ony-Tec <sup>®</sup>	5.47 $\pm$ 0.06

As already explained in chapter 4, formulations that presents more reticulated network (a gel) do not allow a high release of the drug. Thus, and using Ony-Tec<sup>®</sup> as a reference with regard to viscosity values, Formulation A PU19-10% TH, Formulation D PU19-15% TH and Formulation G PU19-10% CPX are the ones that, probably should release the amount of drug needed to be effective (35).

### 3.7 Preliminary test for select formulation with better condition to release the terbinafine

In order to confirm that the polymer concentration affect the drug release an *in vitro* preliminary test was assessed just using the TH formulations. The results confirm that the highest the polymer concentration the less amount of drug is released (Figure 5.6).

Figure 5.6. Release of TH from different formulations at 32 °C (mean  $\pm$  SD, n = 6).

The Formulation A PU19-10%TH release 66.96%, after 6h, while the rest of formulation retain the terbinafine in the matrix for the same time of study. The Formulation D PU19-15%TH release 16%, the Formulation E PU19-20%TH release 10.6% and the Formulation F PU19-25%TH release 6%. These results indicated that the increase of amount of polymer, decreases the release of terbinafine from the formulations.

In another study with the aim of investigate the role of hydrophilic polymers in sustaining the release of drugs in tablets dosages form, was find that the higher viscosity, have relation with resistance of matrix to dissolution and erosion. It was study that matrix prepared with hydroxy propyl methyl cellulose, present more viscosity of hydroxyethyl cellulose, this increase of viscosity could explain the release retardation property of the hydroxy ethyl cellulose (36). Furthermore, the movement of the drug solute through the matrix system is diffusion controlled, it may be expected that the dissolution process will be slower in the more viscous medium (35).

### 3.8 Antifungal activity

The antifungal activity of the drugs against *Candida albicans* ATCC 10240 and *Aspergillus brasiliensis* ATCC 16404 were performed. The results are shown on Table 5.4.

The terbinafine present antifungal activity against *Candida albicans*(37) however the CPX is more effective against this yeast(18).

On the other hand the CPX present lower activity against *Aspergillus brasiliensis*(18).

Table 5. 4. Inhibition zone (mm) of all formulations in plate dish for *Candida albicans*, and *Aspergillus brasiliensis* (mean±SD, n=2).

	Inhibition zone (mm)							
	Formulation A PU19 10% TH	Formulation D PU19 15% TH	Formulation E PU19 20% TH	Formulation F PU19 25% TH	Formulation G PU19 10% CPX	Solution TH(1%)	Solution CPX(1%)	Ony-Tec®
<i>Candida albicans</i> ATCC 10240	38.4±3.6	29.7±0.4	29.0±0.6	26.2±1.0	32.3±1.3	21.4±1.8	29.0±1.1	43.9±2.0
<i>Aspergillus brasiliensis</i> ATCC 16404	25.0±0.4	23.7±0.6	23.2±0.1	21.1±1.7	26.7±0.3	32.0±0.8	31.4±0.4	33.3±0.4

All the nail lacquer formulation presents antifungal activity against the fungi of the study. The results obtained demonstrated the nail lacquer formulations with higher antifungal activity, are the ones that have the lower polymer concentration probably, because they allow a higher release of the drug. All the control formulation presented inhibition zone < 6mm. The solution TH formulation presented higher inhibition zone against *Candida albicans* probably for the influence of -NH- of polyurethane in the pH of the medium that potential the antifungal activity of the drug. The *in vitro* activity of terbinafine is pH dependent and rises with increasing pH value (38). The Formulation G PU19-10% CPX present one interesting value of antifungal activity in comparison with Ony-Tec®.

### 3.9 Permeation Test

Know the amount of drug that permeates the nail in an animal model similar to that of man, for purposes of pre-clinical studies is still under study and to date has not been established. The optional solution to be able to study the passage of the drug is the use of healthy human nails (4,39,40).

Permeation profiles of drugs into the nail are shown in Table 5.5. As it was observed, in release experiments (section 3.6), the presence of polyurethane allows the diffusion of terbinafine trough hydrophilic membrane and as expected the results of this study was similar.

Table 5. 5. Permeation profiles of formulations and Ony-Tec<sup>®</sup> through the nail. (mean $\pm$ SD, n=3).

Time (h)	Amount of Drug Diffusion ( $\mu\text{g}/\text{cm}^3$ )		
	Formulation A PU 19 10% TH	Formulation G PU19 10% CPX	Ony-Tec
24	1542.24 $\pm$ 896.73	561.31 $\pm$ 482.34	282.53 $\pm$ 53.70
48	4030.43 $\pm$ 3934.95	3502.19 $\pm$ 2639.37	290.53 $\pm$ 43.50
72	3809.94 $\pm$ 3435.92	3695.06 $\pm$ 2829.67	342.53 $\pm$ 43.80
96	3899.71 $\pm$ 3386.31	3850.59 $\pm$ 2938.92	582.53 $\pm$ 43.70
120	4273.13 $\pm$ 3659.95	3992.68 $\pm$ 2929.31	540.53 $\pm$ 33.60
168	4405.92 $\pm$ 3714.03	3691.65 $\pm$ 2627.53	560.53 $\pm$ 23.70
192	4236.98 $\pm$ 3488.06	3723.40 $\pm$ 2640.22	550.53 $\pm$ 43.80
216	4214.38 $\pm$ 3343.91	3810.57 $\pm$ 2671.87	586.53 $\pm$ 53.20
240	4389.38 $\pm$ 3454.15	3910.11 $\pm$ 2785.01	593.53 $\pm$ 67.20
264	4435.47 $\pm$ 3391.68	3909.61 $\pm$ 2769.71	598.53 $\pm$ 33.20

The values of drugs permeated through the nail from Formulation A PU19-10% TH after 11 days was 4435.47  $\mu\text{g}/\text{cm}^3$  and from Formulation G PU19-10% CPX was 2649  $\mu\text{g}/\text{cm}^3$ . The results showed that the total amount of TH permeated through the nail was higher than the CPX and Ony-Tec<sup>®</sup>.

The permeation profiles of both drugs indicate that the higher concentrations in receptor solution are obtained in the first 120 hours after application, probably attributed to the presence of ethanol in the tested formulation. The ethanol increased the drug solubility in the vehicle and has action as enhancer (41). Furthermore, the small molecular size of both drugs allows the permeation through the nail (TH-291.43 g/mol and CPX-207.3g/mol)(5).

Regarding to standard deviation found in all the formulation testing is possible to conclude that in the permeation process influence: the thickness of nail that is different from one individual to another and the composition of nail (percent of water, lipid, mineral)(42) and drug-keratin interactions(43).

In another research where were testing the diffusion coefficient of amorolfine, terbinafine and caffeine, the standard deviation was significant. The author explains that the data which were not corrected in terms of nail thickness, however the number of replicated were n=5-7 for caffeine, n=11-13 for the amorolfine and n=13-15 for terbinafine did not prevent the finding of equal and superior deviations from the determination(4).

Then the quantities of each drug were determined in the nail plate. Results are shown in Figure 5.7.

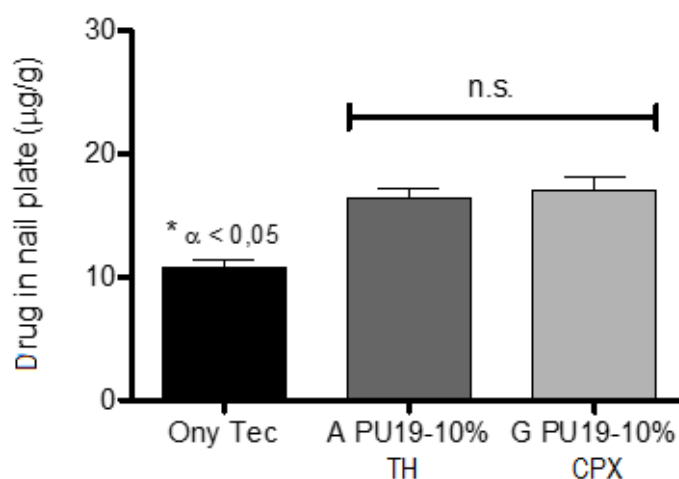


Figure 5.7. Amount of drug determined in nail plate after 11 days of experiments. One-way ANOVA and Tukey's multiple comparison tests indicates significant differences between Ony-Tec® and PU based nail lacquer formulations.

The amount of CPX and TH determined in nail plate, showed similar values, furthermore the formulations based polyurethane retain more drug in keratin structure that Ony-Tec®, probably to the concentration of ethanol as vehicle in the formulation.

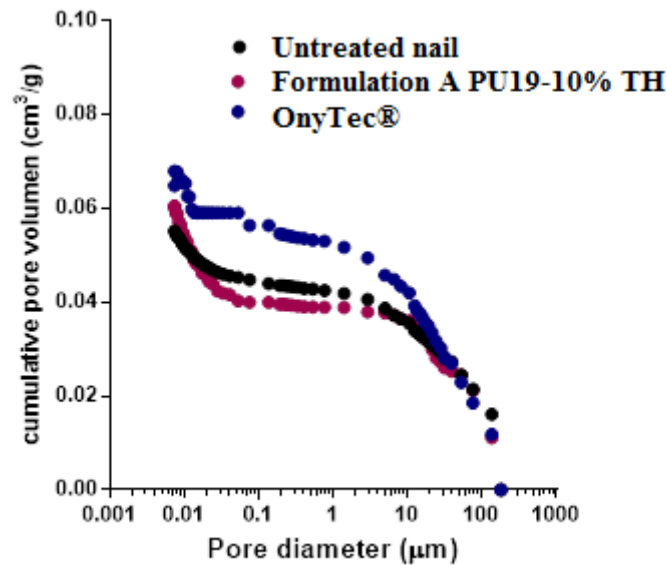
The amount of TH determined in nail presented higher values ( $>0.004 - 1 \mu\text{g/mL}$ ), value of minimum inhibitory concentration of TH against *Candida albicans* and *Aspergillus species*(18).

On the other hand the values of CPX determined in nail are superior to the range  $0.015 - 4 \mu\text{g/mL}$  corresponding to minimum inhibitory concentration of drug, against *Candida albicans* and *Aspergillus species* respectively (18).

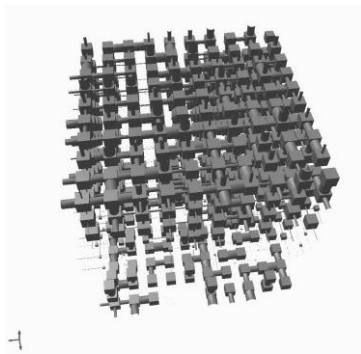
### 3.10 Porosity study

The porosity of the nail is another parameter to take in count for explain changes in the diffusion of drug due to modification on hydration of nail plate. This hydration allows drug flux from certain vehicles (22). Indeed, an increase in nail plate hydration was found to increase the permeation ketoconazole by three-fold and the diffusivity of water by more than 400-fold, when relative humidity was increased from 15 to 100% (36). One method useful to

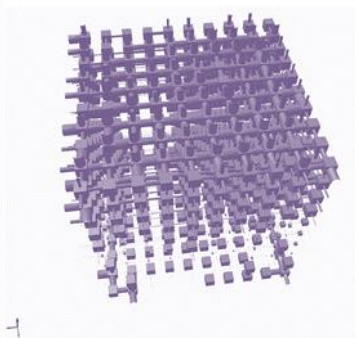
characterize the internal microstructure of the nail is mercury intrusion porosimetry (MIP) in combination with PoreXpert™ software. The combination of these techniques allow to obtain models useful to characterize the permeability properties of the nails (22). In the figure 5.8 are presented the values of porosity of nail obtained by MIP before and after different treatment.



a)



b)



c)

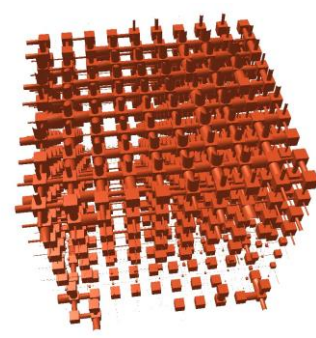


Figure 5.8. Cumulative curves of porosity obtained by MIP for treated and untreated nail and PoreXpert models of the microstructure of a) untreated nail, b) Ony-Tec® treated nails and c) Formulation A PU19-10% TH treated nails. Cubes represent the pores and cylinders the connection between pores.

No significant changes on the microstructure of the nail were observed after the application of nail lacquers. The cumulative pore distribution curve of Ony-Tec® seems to be relatively higher for lower pore diameter but the model and the parameters characteristic of the model

obtained by PoreXpert™ (table 5.6) indicates similar porosity and connectivity regardless the formulation. The values of correlation of the models, near the unity, obtained in treated and untreated nail indicates structures with high level order caused by the well delimited areas with high porosity at the top and bottom of the model and the low porosity structure in the middle of the model. Similar results were obtained by Nogueiras et al (9) for healthy untreated nail using MIP plus PoreCore™ software.

These results indicates that Formulation A PU19-10% TH and Ony-Tec® did not produce microstructural changes in the nail plate probably due to the presence of organic solvents and PU19-10% or the low proportion of water (Ony-Tec®) used in the elaboration of these nail lacquers.

Table 5. 6. Main parameters of the models obtained from porosity data using PoreXpert.

	<b>Porosity (%)</b>	<b>Correlation</b>	<b>Conectivity</b>	<b>Water permeability (mD)</b>
Untreated nails	6.83 %	0.795	5.02	1.5775x10 <sup>-6</sup>
Ony-Tec®	6.75 %	0.796	5.02	1.5417x10 <sup>-6</sup>
Formulation A PU19-10%TH	6.75 %	0.795	5.02	1.5775 x10 <sup>-6</sup>

## 4. Conclusions

This study reports the physic-chemical characterization of TH and CPX nail lacquer formulations based polyurethane. The TH nail lacquers obtained were compatible with keratinocytes cell and presented hydrophilic properties, however the CPX nail lacquer presented incompatible with skin cell.

While the homogenous films obtained from the nail lacquer presented adhesion to nail. The viscosity studied demonstrated that the Formulation A PU19-10% TH and Formulation G PU19-10% CPX presented low viscosity compared to Ony-Tec®.

*In vitro* release studies reveal that the amount of PU19 used had influence on the release profiles of drug, which was in agree with the antifungal activity of the formulations.

All the nail lacquer formulations showed antifungal activity against *Candida albicans* and *Aspergillus brasiliensis*. The permeation profiled of antifungal formulation through the nail were higher than Ony-Tec®.

The result obtained of permeation and determination of CPX in nail allow to prepare another formulation with used of PU19 with the aims to improve the compatibility with keratinocytes cells.

The use of polyurethane in nail formulation can be a promising strategy for the release of lipophilic drug.

## 5. References

1. Souza LKH, Fernandes OFL, Passos XS, Costa CR, Lemos JA, Silva MRR. Epidemiological and mycological data of onychomycosis in Goiania, Brazil. *Mycoses*. 2010;53(1):68–71.
2. Foster KW, Ghannoum MA, Elewski BE. Epidemiologic surveillance of cutaneous fungal infection in the United States from 1999 to 2002. *J Am Acad Dermatol*. 2004;50(5):748–52.
3. Garcia-Martos P, Dominguez I, Marin P, Linares M, Mira J, Calap J. [Onychomycoses caused by non-dermatophytic filamentous fungi in Cadiz]. *Enferm Infecc Microbiol Clin*. 2000;18(7):319–24.
4. McAuley WJ, Jones SA, Traynor MJ, Guesn?? S, Murdan S, Brown MB. An investigation of how fungal infection influences drug penetration through onychomycosis patient's nail plates. *Eur J Pharm Biopharm*. 2016;102:178–84.
5. Elsayed MMA a. Development of topical therapeutics for management of onychomycosis and other nail disorders: A pharmaceutical perspective. *J Control Release*. Elsevier B.V.; 2014;199C:132–44.
6. Barot BS, Parejiya PB, Patel HK, Mehta DM, Shelat PK. Drug delivery to the nail: Therapeutic options and challenges for onychomycosis. *Crit Rev Ther Drug Carrier Syst*. 2014;31(6):459–94.
7. Monti D, Herranz U, Dal Bo L, Subissi a. Nail penetration and predicted mycological efficacy of an innovative hydrosoluble ciclopirox nail lacquer vs. a standard amorolfine lacquer in healthy subjects. *Journal of the European Academy of Dermatology and Venereology : JEADV*. 2013. p. e153-8.
8. Monti D, Saccomani L, Chetoni P, Burgalassi S, Senesi S, Ghelardi E, et al. Hydrosoluble medicated nail lacquers: In vitro drug permeation and corresponding antimycotic activity. *Br J Dermatol*. 2010;162(2):311–7.
9. Nogueiras-Nieto L, Begoña Delgado-Charro M, Otero-Espinar FJ. Thermogelling hydrogels of cyclodextrin/poloxamer polypseudorotaxanes as aqueous-based nail lacquers: Application to the delivery of triamcinolone acetonide and ciclopirox olamine. *European Journal of Pharmaceutics and Biopharmaceutics*. 2013. p. 370–7.
10. Kerai LV, Hilton S, Murdan S. UV-curable gel formulations: Potential drug carriers for

- the topical treatment of nail diseases. *Int J Pharm.* 2015 Aug;492(1–2):177–90.
11. Thatai P, Tiwary AK, Sapra B. Progressive Development in Experimental Models of Transungual Drug Delivery of Antifungal Agents. *International journal of cosmetic science.* 2015.
  12. MCHEN-CHI KH-CCW-P; M. Synthesis and characterization of a clay/waterborne polyurethane nanocomposite. *J Mater Sci.* 2005;40:179–185.
  13. Täuber A, Müller-Goymann CC. In vitro permeation and penetration of ciclopirox olamine from poloxamer 407-based formulations--comparison of isolated human stratum co.pdf. *International journal of pharmaceutics* 2015 p. 73–82.
  14. Bohn M, Kraemer KT. Dermatopharmacology of ciclopirox nail lacquer topical solution 8% in the treatment of onychomycosis. *J Am Acad Dermatol.* 2000;43(4):S57–69.
  15. Lass-Flör C, Mayr A, Perkhofer S, Hinterberger G, Hausdorfer J, Speth C, et al. Activities of antifungal agents against yeasts and filamentous fungi: Assessment according to the methodology of the European Committee on Antimicrobial Susceptibility Testing. *Antimicrob Agents Chemother.* 2008;52(10):3637–41.
  16. I. H, A. D, F. M, I. M, L. F. Evaluation of safety profile, pharmacokinetics, and clinical benefit of an innovative terbinafine transungual solution (P-3058): A phase i study in patients with mild-to-moderate distal subungual onychomycosis. *Journal of the American Academy of Dermatology.* 2013. p. AB105-AB105.
  17. Tanrıverdi ST, Özer Ö. Novel topical formulations of Terbinafine-HCl for treatment of onychomycosis. *Eur J Pharm Sci.* 2013;48(4–5):628–36.
  18. Jo Siu WJ, Tatsumi Y, Senda H, Pillai R, Nakamura T, Sone D, et al. Comparison of in vitro antifungal activities of efinaconazole and currently available antifungal agents against a variety of pathogenic fungi associated with onychomycosis. *Antimicrobial agents and chemotherapy.* 2013. p. 1610–6.
  19. EN ISO 2409. Paints and varnishes, cross-cut test. 2013;3:4–13.
  20. Salgado A, Raposo S, Marto J, Silva AN, Simões S, Ribeiro HM. Mometasone furoate hydrogel for scalp use: *in vitro* and *in vivo* evaluation. *Pharm Dev Technol.* 2014;19(5):618–22.
  21. Arunprasad K, Narayanan N, Rajalakshmi G. Preparation and Evaluation of Solid Dispersion of. 2010;3(1):130–4.

22. Nogueiras-Nieto L, Gómez-Amoza JL, Delgado-Charro MB, Otero-Espinar FJ. Hydration and N-acetyl-L-cysteine alter the microstructure of human nail and bovine hoof: Implications for drug delivery. *Journal of Controlled Release*. 2011. p. 337–44.
23. Kleinbeck S, Juran SA, Kiesswetter E, Schäper M, Blaszkewicz M, Brüning T, et al. Evaluation of ethyl acetate on three dimensions: Investigation of behavioral, physiological and psychological indicators of adverse chemosensory effects. *Toxicol Lett*. 2008;182(1–3):102–9.
24. Wenzel RN. Resistance of solid surfaces to wetting by water. *J Ind Eng Chem (Washington, D C)*. 1936;28:988–94.
25. Murdan S, Kerai L, Hossin B. To what extent do in vitro tests correctly predict the in vivo residence of nail lacquers on the nail plate? *J Drug Deliv Sci Technol*. Elsevier Ltd; 2015;25:23–8.
26. Baran R, Tosti a, Hartmane I, Altmeyer P, Hercogova J, Koudelkova V, et al. An innovative water-soluble biopolymer improves efficacy of ciclopirox nail lacquer in the management of onychomycosis. *Journal of the European Academy of Dermatology and Venereology : JEADV*. 2009. p. 773–81.
27. Shivakumar HN, Vaka SRK, Madhav NVS, Chandra H, Murthy SN. Bilayered nail lacquer of terbinafine hydrochloride for treatment of onychomycosis. *J Pharm Sci*. 2010 Oct;99(10):4267–76.
28. Stanley W RMLJMWRPH-YW. Antifungal nail coat and method of use. EP 1635770B1. 2009.
29. Babapour R. Treatment of onychomycosis and related compositions. US P201002616A1. 2009.
30. Gyurik R. Pharmaceutical composition. US 20030049307A1. 2003.
31. Federico Mailland, Michela Legora, Daniela Ceriani GI. Method of treating onychomycosis. US 8697753 B1. 2013.
32. Otero-Espinar, Francisco J; Nieto-Nogueiras,Luis; Igea Anguiano F. Aqueous pharmaceutical system for the administration of drug to the nails. WO 2011138484A1. 2011.
33. Jones D. *Pharmaceutical Applications of Polymers for Drug Delivery*. Polysaccharides for Drug Delivery and Pharmaceutical Applications. 2004. 136 p.
34. Khattab IS, Bandarkar F, Fakhree MAA, Jouyban A. Density, viscosity, and surface

- tension of water+ethanol mixtures from 293 to 323K. *Korean J Chem Eng.* 2012;29(6):812–7.
35. Cheong LWS, Heng PWS, Wong LF. Relationship between polymer viscosity and drug release from a matrix system. *Pharm Res.* 1992;9(11):1510–4.
  36. Saeio K, Pongpaibul Y, Viernstein H, Okonogi S. Factors influencing drug dissolution characteristics from hydrophilic polymer matrix tablet. *Sci Pharm.* 2007;75:147–63.
  37. Ryder NS, Wagner S, Leitner I. In vitro activities of terbinafine against cutaneous isolates of *Candida albicans* and other pathogenic yeasts. *Antimicrob Agents Chemother.* 1998;42(5):1057–61.
  38. Petranyi G, Meingassner JG, Mieth H. Antifungal activity of the allylamine derivative terbinafine in vitro. *Antimicrob Agents Chemother.* 1987;31(9):1365–8.
  39. Chouhan P, Saini TR. Hydration of nail plate: A novel screening model for transungual drug permeation enhancers. *Int J Pharm. Elsevier B.V.*; 2012;436(1–2):179–82.
  40. Khengar RH, Jones SA, Turner RB, Forbes B, Brown MB. Nail swelling as a pre-formulation screen for the selection and optimisation of unguinal penetration enhancers. *Pharm Res.* 2007;24(12):2207–12.
  41. Murdan S, Milcovich G, Goriparthi GS. An assessment of the human nail plate pH. *Skin Pharmacol Physiol.* 2011;24(4):175–81.
  42. Murdan S. Enhancing the nail permeability of topically applied drugs. *Expert Opin.* 2008;5:1267–82.
  43. Sugiura K, Sugimoto N, Hosaka S, Katafuchi-Nagashima M, Arakawa Y, Tatsumi Y, et al. The low keratin affinity of efinaconazole contributes to its nail penetration and fungicidal activity in topical onychomycosis treatment. *Antimicrobial Agents and Chemotherapy.* 2014. p. 3837–42.



## **Chapter 6: Conclusions and Final Remarks**



## Conclusions and Near-Future Research

**Synthesis of polyurethanes employing isosorbide and aliphatic diisocyanate.** Four polyurethanes (PU) obtained from isosorbide, PPG and aliphatic diisocyanate were synthesized and characterized. The soft segment segmentation (PPG) increased the molecular weight and the hydrodynamic radius of PU but decreased the diffusion coefficient of the macromolecules. On the other hand, increasing the extender of chain (isosorbide) the PU adhesion to keratin gave better results. The polyurethane presented adequate solubility properties.

According to these properties and diffusion coefficient, determined by NMR, polyurethane 19 (PU19), synthesized from 1 mol PPG, 6 mol IPDI and 5 mol of isosorbide, was selected for the final formulations.

*Further investigation may include:*

Experimental design using other molar relation and different temperatures should be assessed with this monomer.

Determination of polymers' molecular weight in different solvents according to hydrodynamic volume should also be performed.

### **PU based nail lacquers: formulation and antifungal activity evaluation.**

PU-terbinafine based nail lacquers prepared with four PU selected showed keratinocyte compatibility, good wettability properties and adequate free volume. They formed a homogenous film after application, with suitable adhesion to the nail plate. Furthermore, the antifungal test results demonstrated that the terbinafine released from the nail lacquer Formulation A PU 19 showed activity against dermatophytes namely, *Tricophyton rubrum*.

*Further investigation may include:*

Structural studies using Wide- Angle X-ray Scattering (WAXS), Atomic Force Microscopy (AFM) and Differential Scanning Calorimetry (DSC) techniques would complement the physicochemical characterization of the PU based nail lacquers.

Transungueal permeation studies

**Preparation of 19 PU based nail lacquer.**

PU 19 was the polymer selected to prepared four nail lacquers with different amounts of polymer, 10%, 15%, 20% and 25%. The concentration of 10% permitted a nail lacquer with better adhesion properties, release and antifungal results.

*Further investigation may include:*

Study of the effect of lower quantities of polyurethane in order to determine the best nail lacquer formulation with drug effectiveness.

**Formulation optimization of PU based Nail Lacquers containing Terbinafine hydrochloride and Ciclopirox Olamine.**

The incorporation of two drugs (TH and CPX) validated the use of PU as versatile polymers in nail lacquer formulations. Direct contact cytotoxicity, wettability, SEM, adhesion, drying time, viscosity measurement, permeation studies and antifungal activity were performed.

The results indicates that the total quantity of terbinafine hydrochloride permeated through the nail was higher than the ciclopirox from the same matrix. The developed nail lacquers permitted better diffusion of antifungal drugs through the nail than reference one (Ony-Tec®). The amount of terbinafine hydrochloride and ciclopirox olamine determined in nail were higher than the minimum inhibitory concentration of these drugs against *Candida Albicans* and *Aspergillus brasiliensis*. However, CPX formulation was incompatible to keratinocytes cells. The antifungal activity of the terbinafine hydrochloride and ciclopirox olamine PU based nail lacquer against *Candida albicans* and *Aspergillus brasiliensis* was determined. The results obtained demonstrated that the amount of drug release from the nail lacquer formulations presented antifungal activity. The influence of -NH- of polyurethane in the pH of the medium, potential the antifungal activity of the terbinafine hydrochloride against *Candida albicans*

*Further investigation may include:*

Diffusion and permeation studies in keratin should be performed with TOWL determination in each nail. The development of new safe and biocompatible formulations with CPX effectiveness must be performed.

Stability test should be done.

Antifungal activity against dermatophytes and non dermatophytes.

Clinic trials should be assessed.

The research work presented in this thesis, led to the development of a new nail lacquer with adhesive, biocompatible and improved the antifungal activity.

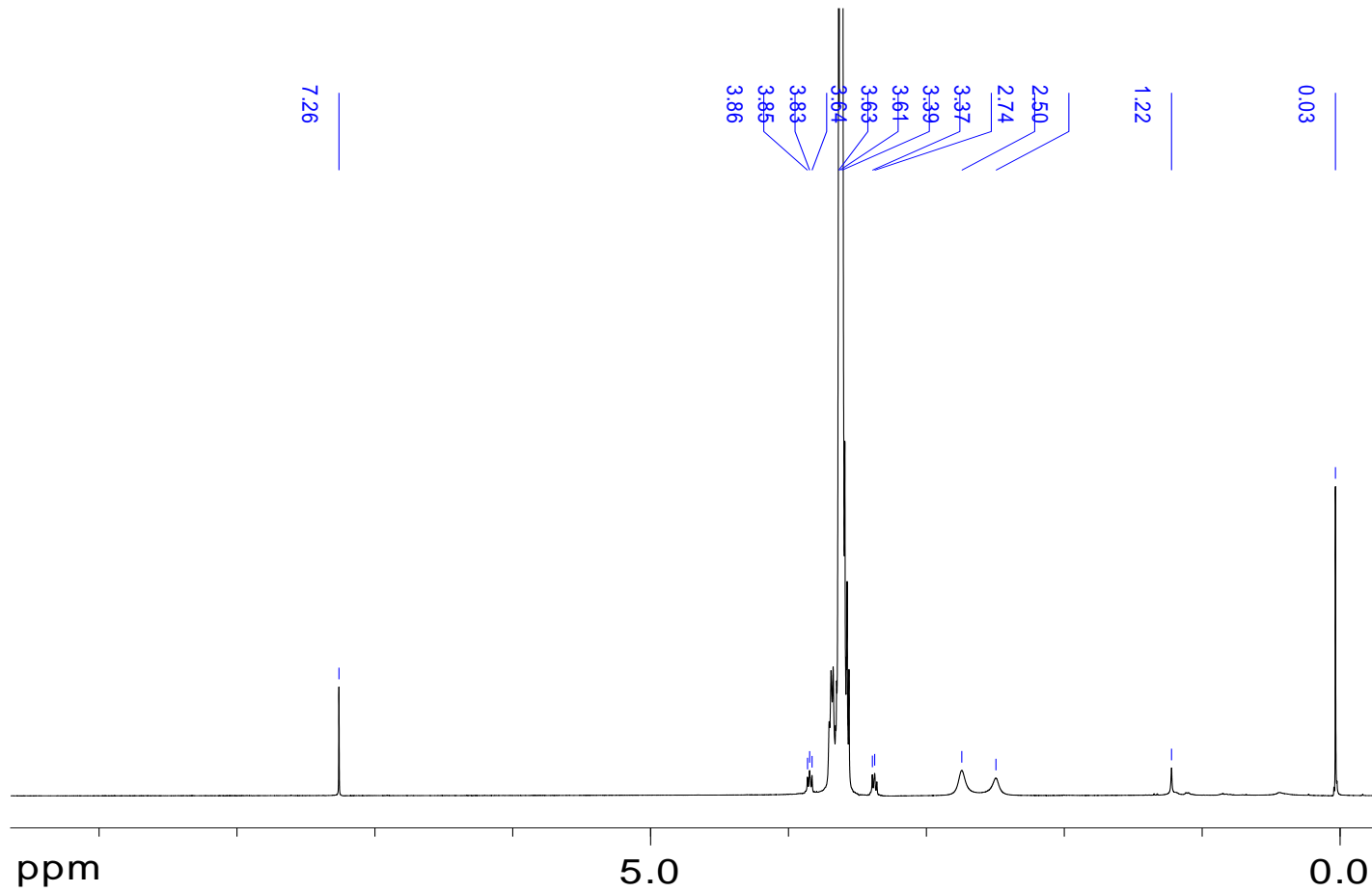
Nevertheless, this new nail lacquers (polyurethane-antifungal drugs) and taking into account the challenge of treating nail infections, need further studies such as structural and clinical studies.



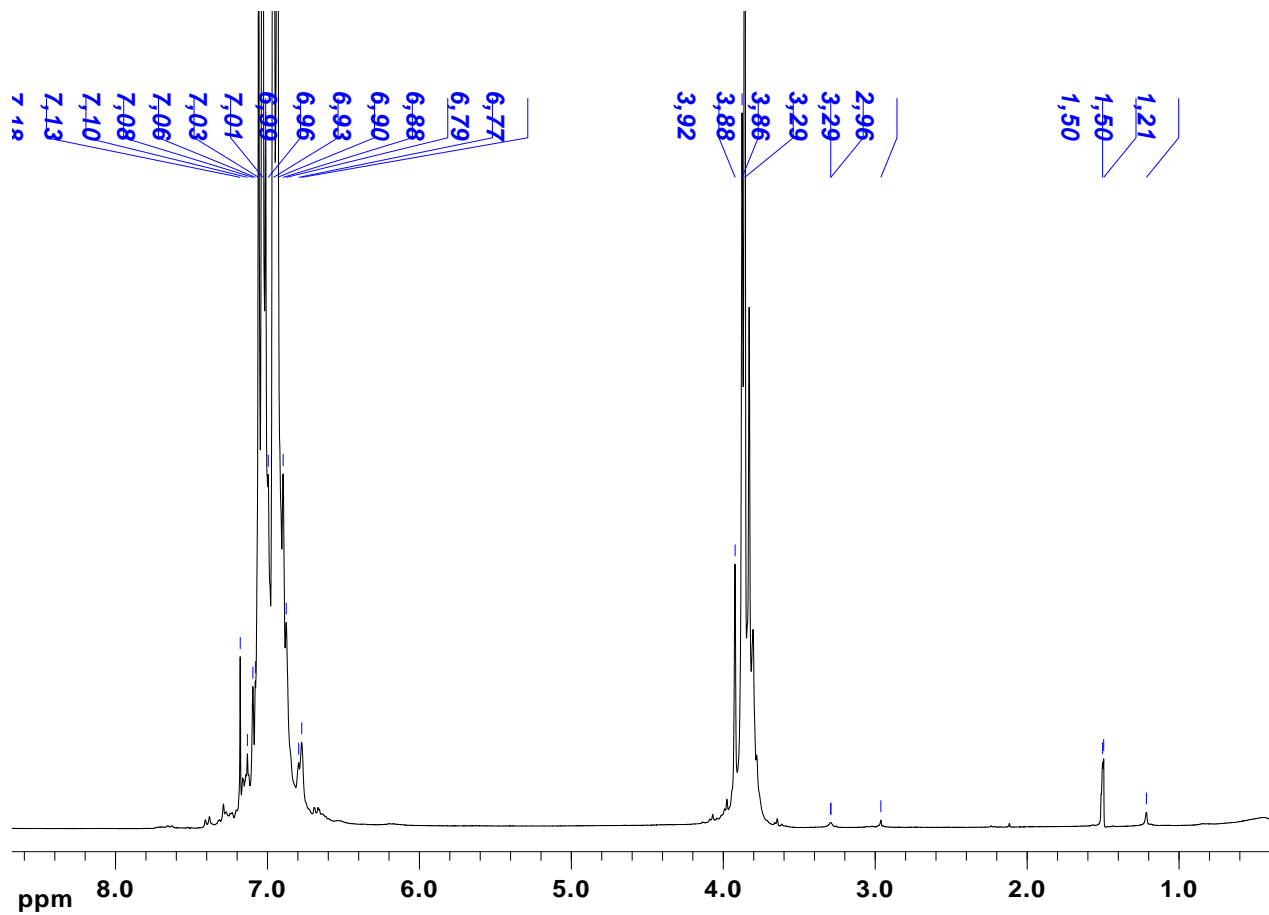
## **Annexes**



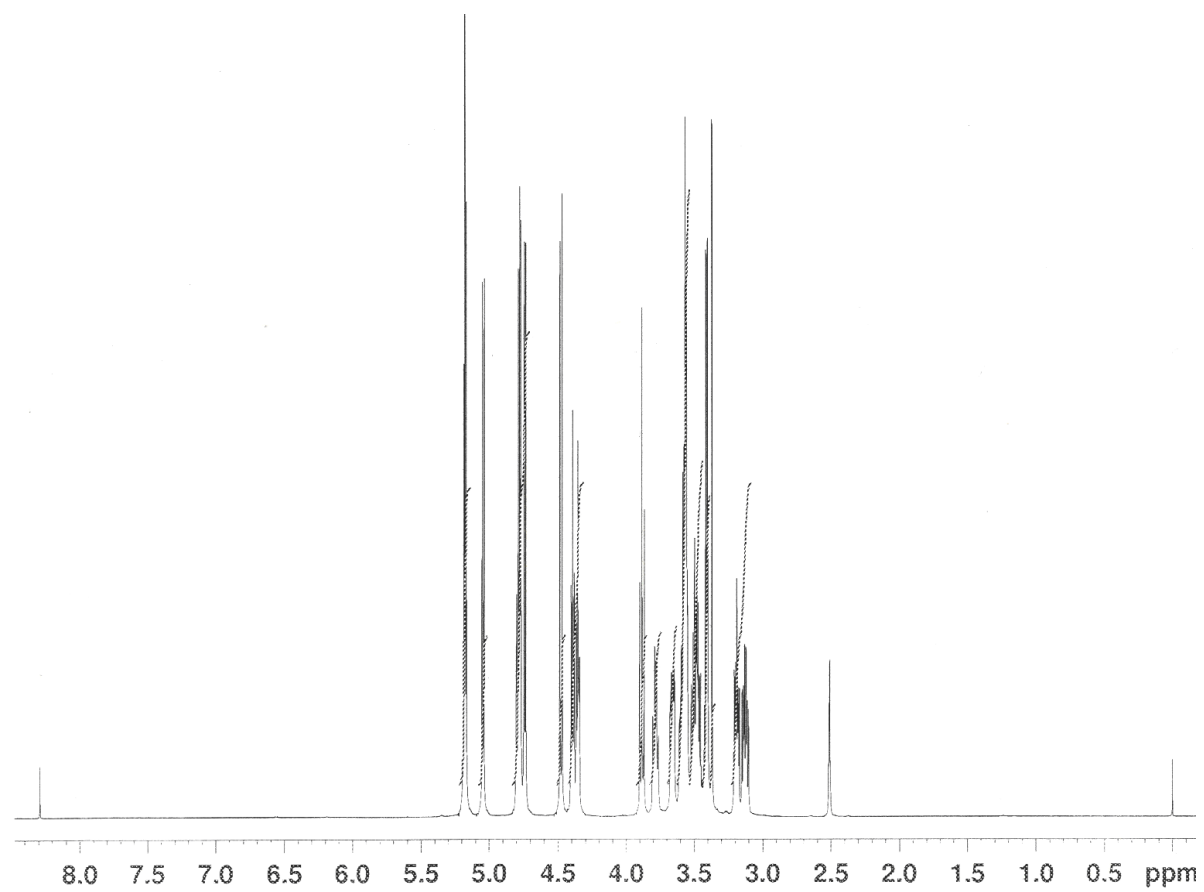
**Annex 1. Spectrum  $^1\text{H}$  NMR PEG 1 500**



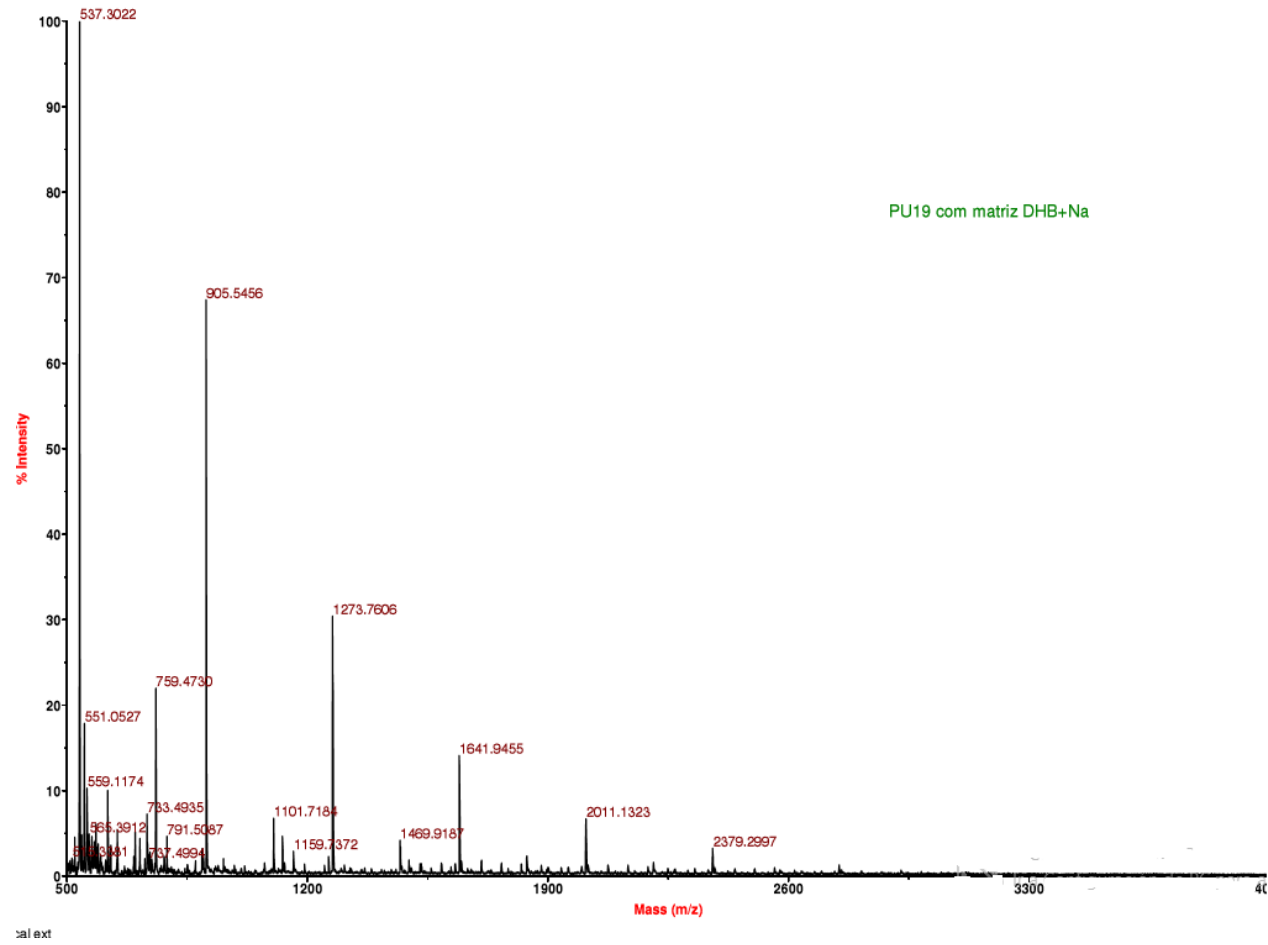
**Annex 2. Spectrum  $^1\text{H}$  NMR pMDI**



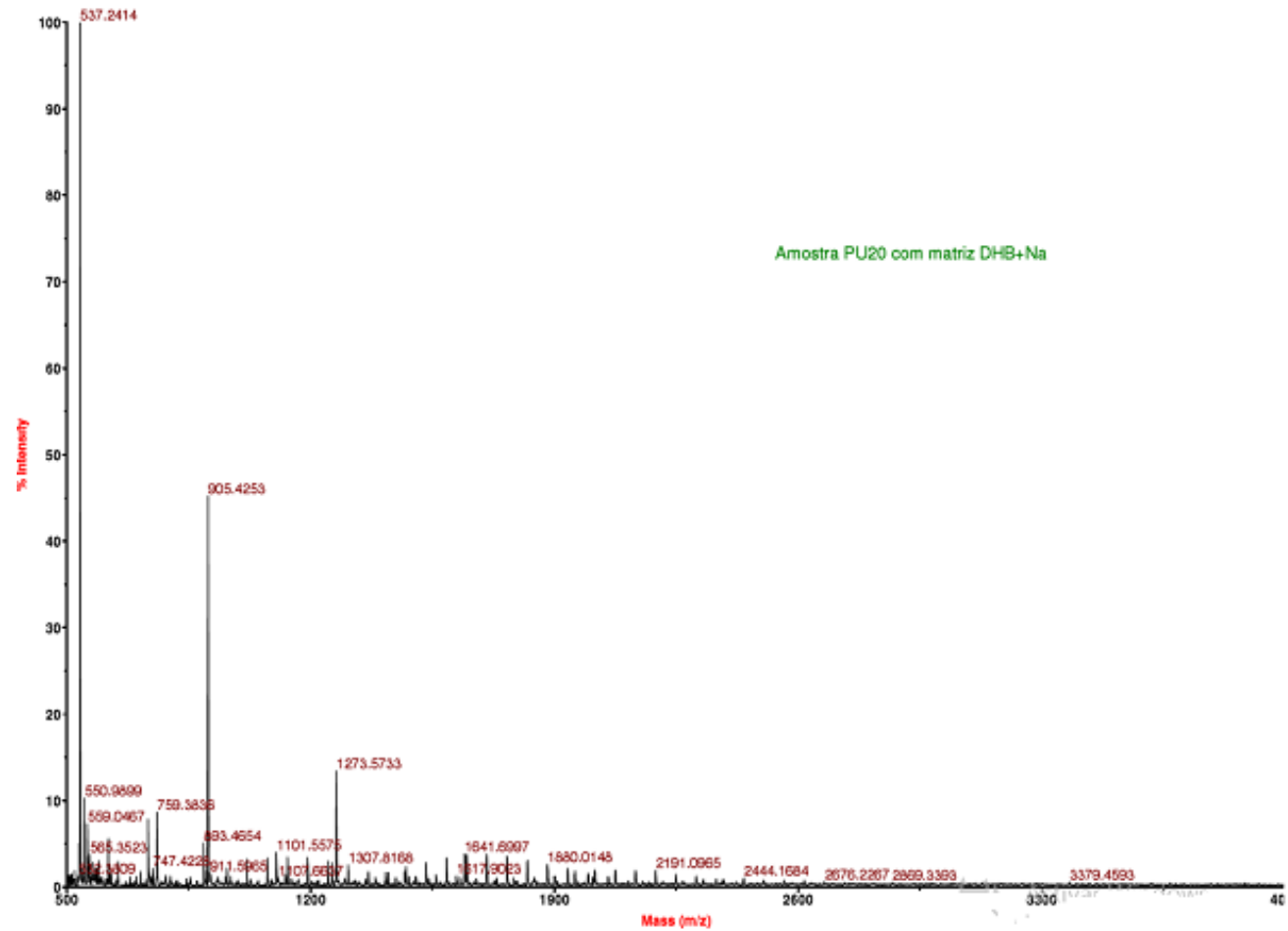
Annex 3. Spectrum  $^1\text{H}$  NMR Sucrose



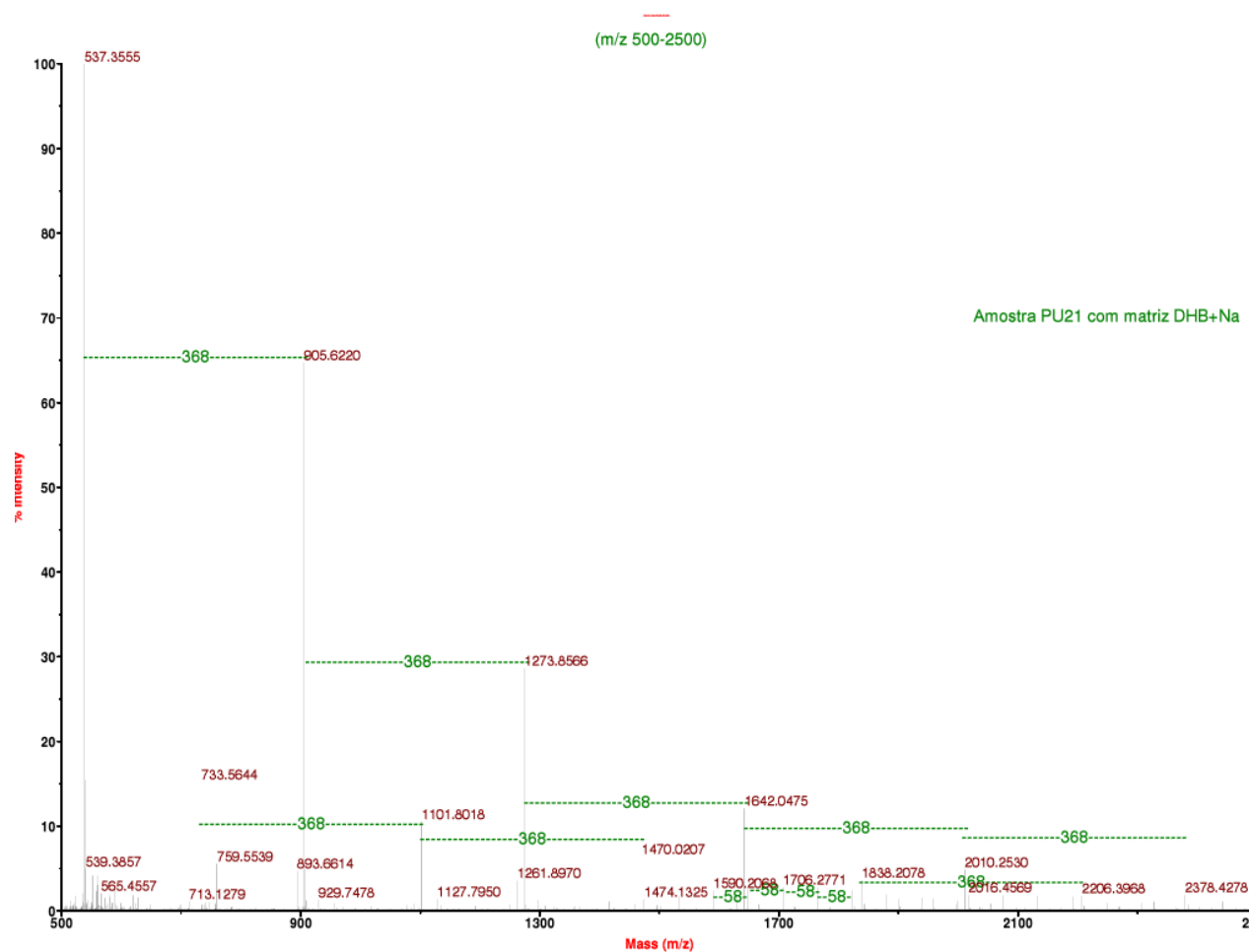
**Annex 4. MALDI-TOF mass spectra of PU19**



**Annex 5. MALDI-TOF mass spectra of PU20**



**Annex 6. MALDI-TOF mass spectra of PU21**



**Annex 7. MALDI-TOF mass spectra of PU22**

